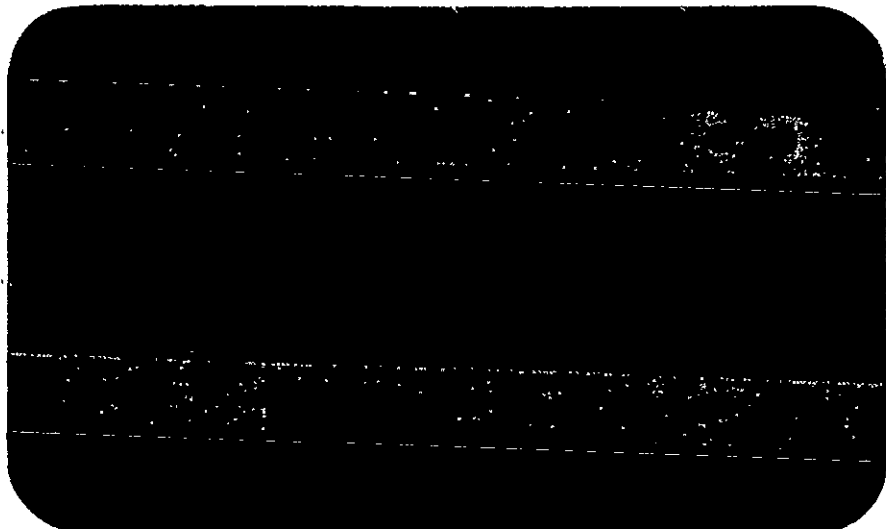


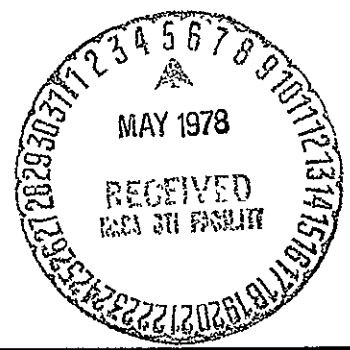
Princeton University



(NASA-CR-152135)	OPTIMAL CONTROL THEORY	N78-21161
(OWEM) APPLIED TO A HELICOPTER IN THE HOVER		
AND APPROACH PHASE (Princeton Univ., N. J.)		
289 p HC A13/MF A01	CSCL 01C	Unclas
		G3/08 15627



Department of
Aerospace and
Mechanical Sciences



OPTIMAL CONTROL THEORY (OWEM)
APPLIED TO A HELICOPTER IN THE
HOVER AND APPROACH PHASE

By

Gerard J. Born and Tadao Kai

Department of Aerospace & Mechanical Sciences
Instrumentation and Control Laboratory
Princeton University

Report No. 1205
January, 1975

ABSTRACT

A major difficulty in the practical application of linear-quadratic regulator theory is how to choose the weighting matrices in quadratic cost functions. In this work, the control system design with optimal weighting matrices is applied to a helicopter in the hover and approach phase. The weighting matrices are calculated to extremize the closed loop "Total System Damping" subject to constraints on the determinants. The extremization is really a minimization of the effects of disturbances, and interpreted as a compromise between the generalized system accuracy and the generalized system response speed. The trade-off between the accuracy and the response speed is adjusted by a single parameter--the ratio of determinants, which is the only arbitrariness left for designer's choice.

By this approach an objective measure can be obtained for the design of a control system. The measure is to be determined by the system requirements.

ACKNOWLEDGEMENT

This work reported was supported by the National Aeronautics and Space Administration under Contract No. NAS2-7187, RFP 2 18306(DD-40).

The Instrumentation and Control Laboratory of Princeton University acknowledges the understanding encouragement and constructive criticism provided by members of Ames Research Center, Moffett Field; in particular the most valuable contributions of Mr. Terrence Gossett.

Among the contributors to this research, special acknowledgements are expressed to Mr. Theodor A. Dukes, for his active, fruitful discussions, and advice.

It is hoped the results of the research pursued under this program will provide the basis for further development by the Ames Research Center.

TABLE OF CONTENTS

	Page
Abstract	ii
Acknowledgements	iii
List of Figures	vi
List of Symbols	xiii
Chapter 1 Introduction	1
2 Review of the Application of Linear Optimal Control Theory	4
3 Controller Design for a Helicopter (OWEM)	21
A. Helicopter System and Control Equations	21
B. Controller Design for Vertical and Yaw Control	27
C. Controller Design for Longitudinal Equation	41
D. Controller Design for Lateral Equation	51
4 Conclusions and Recommendations	58
Appendix A1 Review of Helicopter Dynamics	136
B1 Decoupling Method (Least Squares)	159
B2 Decoupling of Helicopter Dynamics	162
C1 Sensitivity Analysis	176
D1 Review of Linear Optimal Regulator	198
D2 Optimal Linear Controller Design Applied to a Second Order System	207
E1 Review of OWEM Design Method	213
E2 The OWEM Method Applied to a Second Order System	230
F1 The Root Square Locus	236

TABLE OF CONTENTS (CON'T.)

	Page
F2 Root Square Locus Method Applied to a Helicopter (Hover)	241
G1 Review of Model Following by Linear Optimal Control	253

LIST OF FIGURES

<u>Figure No.</u>		<u>Page</u>
1	System Description	64
2	Roots Configuration for Basic, Decoupled and Un- coupled Helicopter Dynamics	65
3	General Construction for Decoupling Helicopter Dynamics	66
4	Construction of Decoupling for Helicopter (Hover) Dynamics	67
5	Power Spectrum Density and Transient Analogue of Assumed Gust Model with Different Bandwidths Under Constant Intensity	68
6	Root Square Locus with Varying r , some q_{22} 's, and $q_{11} =$ 1.0 and by the OWEM Method for Vertical Equation	69
7	Root Square Locus with Varying r , some q_{22} 's, and $q_{11} =$ 1.0 and by the OWEM Method for Yawing Equation	70
8	Vertical Optimal Feedback Gains	71
9	Yawing Optimal Feedback Gains	72
10	ISE of Second Order Rate Constant System vs the Closed Loop System Damping Ratio ζ , Undamped Natural Frequency ω_n	73
11	ISE Values of Z and θ_o for Command Input (unit step) in the Optimal Control Systems	74

LIST OF FIGURES (CON'T)

<u>Figure No.</u>		<u>Page</u>
12	ISE Values of ϕ and δ_r for Command Input (unit step) in the Optimal Yawing Control System	75
13	RMS Values of Z and δ_c for Vertical Gust in the Optimal Height Control Systems ($\sigma_g = 10$ ft/sec. ω)	76
14	RMS Values of ϕ and δ_r for Sideway Gust in the Optimal Yawing Control Systems ($\sigma = 10$ ft/sec., $\omega = .314$ rad/sec.)	77
15	RMS Values of Z and δ_c for Different Vertical Gust Break Frequencies in the Optimal Height Control Systems ($\sigma = 10$ ft/sec.)	78
16	RMS Values of ϕ and δ_r for Different Sideway Gust Break Frequencies in the Optimal Yawing Control Systems ($\sigma = 10$ ft/sec.)	79
17a	Frequency Response of $\omega_g \rightarrow Z$ Transfer Function	80
17b	Frequency Response of $\omega_g \rightarrow \delta_c$ Transfer Function (straight line approximation)	80
18	Desirable Roots Location for the Second Order System to Satisfy No Overshoot, ISE, ISU and rms Gust Response Requirements	81
19	Root Square Locus with Varying r, $q_{11} = 1.0$ and by OWEM Method for Longitudinal Equation	82

LIST OF FIGURES (CON'T.)

<u>Figure No.</u>		<u>Page</u>
20	Root Square Locus with Varying r , $q_{11} = 1.0$, $q_{33} = 820$ for Longitudinal Equation	83
21	Root Square Locus with Varying r , $q_{11} = 1.0$, $q_{33} = 3283$ for Longitudinal Equation	84
22	Root Square Locus with Varying r , $q_{11} = 0.1$, $q_{33} = 3283$ for Longitudinal Equation	85
23	Root Square Locus with Varying r , $q_{11} = 0.01$, $q_{33} = 3283$ for Longitudinal Equation	86
24	Root Square Locus with Varying r , $q_{11} = 1.0$, $q_{33} = q_{44} = 3280$ for Longitudinal Equation	87
25	Root Square Locus with Varying r , $q_{11} = 1.0$, $q_{33} = 1.0$, $q_{33} = 3283$, $q_{44} = 3283$ for Longitudinal Equation	88
26	Root Square Locus with Varying r , $q_{11} = q_{22} = 0.1$, $q_{33} = q_{44} = 3283$ for Longitudinal Equation	89
27	Root Square Locus with Varying r , $q_{11} = 0.1$, $q_{22} = 0.4$, $q_{33} = 3283$, $q_{44} = 13132$ for Longitudinal Equation	90
28	Longitudinal Optimal Feedback Gains for the OWEM Method	91
29	Longitudinal Optimal Feedback Gains for $q_{11} = 1.0$	92
30	Longitudinal Optimal Feedback Gains for $q_{11} = 1.0$, $q_{33} = 820$	93

LIST OF FIGURES (CON'T.)

<u>Figure No.</u>		<u>Page</u>
31	Longitudinal Optimal Feedback Gains for $q_{11} = 1.0$, $q_{33} = 3283$	94
32	Longitudinal Optimal Feedback Gains for $q_{11} = 0.1$, $q_{33} = 3283$	95
33	Longitudinal Optimal Feedback Gains for $q_{11} = 0.01$, $q_{33} = 3283$	96
34	Longitudinal Optimal Feedback Gains for $q_{11} = 1.0$, $q_{33} = q_{44} = 3283$	97
35	Longitudinal Optimal Feedback Gains for $q_{11} = q_{22} = 1.0$, $q_{33} = q_{44} = 3283$	98
36	Longitudinal Optimal Feedback Gains for $q_{11} = q_{22} = 0.1$, $q_{33} = q_{44} = 3283$	99
37	Longitudinal Optimal Feedback Gains for $q_{11} = 0.1$, $q_{22} =$ 0.4 , $q_{33} = 3283$, $q_{44} = 13132$	100
38	ISE and IS θ to 10 ft Command Input for Optimal Longitudinal Equation, with Varying r and q_{ii} ($i = 1,2,3,4$)	
39	Relation of Min. ISE and Max. IS θ vs Weighting Factors Ratio for Longitudinal Equation (lateral eq.) (10 ft. Command Input)	102

LIST OF FIGURES (CON'T.)

<u>Figure No.</u>		<u>Page</u>
40	ISU to 10 ft. Command Input for Optimal Longitudinal Equation, with Varying r and q_{i1} ($i = 1,2,3,4$)	103
41	RMS Longitudinal Position Errors and RMS Controls to Random Gust Input ($\sigma = 20$ ft/s, $d = .314$ rad/s, with Varying r , q_{i1})	104
42	RMS Pitch Attitude Errors Due to Random Gust Input ($\sigma = 20$ ft/sec, $d = .3140$, with Varying r , q_{ii} ($i=1,2,3,4$))	105
43	Root Square Locus with Varying r , $q_{11} = 1.0$ for Lateral Equation	106
44	Root Square Locus with Varying r , $q_{11} = 1.0$, $q_{33} = 820$ for Lateral Equation	107
45	Root Square Locus with Varying r , $q_{11} = 1.0$, $q_{33} = 3280$ for Lateral Equation	108
46	Root Square Locus with Varying r , $q_{11} = 0.1$, $q_{33} = 3283$ for Lateral Equation	109
47	Root Square Locus with Varying r , $q_{11} = 0.01$, $q_{33} = 3283$ for Lateral Equation	110
48	Root Square Locus with Varying r , $q_{11} = q_{22} = 0.1$, $q_{33} = 3283$ for Lateral Equation	111
49	Root Square Locus with Varying r , $q_{11} = q_{22} = 1.0$, $q_{33} = q_{44} = 3283$ for Lateral Equation	112

LIST OF FIGURES (CON'T.)

<u>Figure No.</u>		<u>Page</u>
50	Root Square Locus with Varying r , $q_{11} = q_{22} = 0.1$, $q_{33} = q_{44} = 3283$ for Lateral Equation	113
51	Root Square Locus with Varying r , $q_{11} = 0.1$, $q_{22} = 0.4$, $q_{33} = 3283$, $q_{44} = 13132$	114
52	Lateral Optimal Feedback Gains for the OWEM Method	115
53	Lateral Optimal Feedback Gains for $q_{11} = 1.0$	116
54	Lateral Optimal Feedback Gains for $q_{11} = 1.0$, $q_{33} = 820$	117
55	Lateral Optimal Feedback Gains for $q_{11} = 1.0$, $q_{33} = 3283$	118
56	Lateral Optimal Feedback Gains for $q_{11} = 0.1$, $q_{33} = 3283$	119
57	Lateral Optimal Feedback Gains for $q_{11} = 0.01$, $q_{33} = 3283$	120
58	Lateral Optimal Feedback Gains for $q_{11} = q_{22} = 0.1$, $q_{33} = 3283$	121
59	Lateral Optimal Feedback Gains for $q_{11} = q_{22} = 1.0$, $q_{33} = q_{44} = 3283$	122
60	Lateral Optimal Feedback Gains for $q_{11} = q_{22} = 0.1$, $q_{33} = q_{44} = 3283$	123
61	Lateral Optimal Feedback Gains for $q_{11} = 0.1$, $q_{22} = 0.4$, $q_{33} = 3283$, $q_{44} = 13132$	124
62	ISE and IS θ to 10 ft. Command Input for Optimal Lateral Equation, with Varying r , q_{ii} ($i = 1,2,3,4$)	125
63	ISU to 10 ft. Command Input for Optimal Lateral Equation, with Varying r and q_{ii} ($i = 1,2,3,4$)	126

LIST OF FIGURES (CON'T.)

<u>Figure No.</u>		<u>Page</u>
64	RMS Lateral Position Errors and RMS Controls to Random Gust Input ($\sigma = 20$ ft/s, $d = .314$ rad/s) with Varying r, q_{ii}	127
65	RMS Roll Attitude Errors Due to Random Gust Input ($\sigma = 20$ ft/s, $d = .314$ rad/s), with Varying r, q_{ii} ($i = 1,2,3,4$)	128
66	Effects of Gust with Different Psd Bandwidths to Rms Lateral Attitude Errors	129
67	Root Square Locus OWEM for Longitudinal Equation (Approach Phase)	130
68	Root Square Locus OWEM for Lateral Equation (Approach Phase)	131
69	Root Square Locus OWEM with ESM for Longitudinal Equation	132
70	Root Square Locus OWEM with ESM for Lateral Equation	133
71	Longitudinal Gains OWEM with ESM (1:1:4:4)	134
72	Lateral Gain OWEM with ESM (1:1:4:3)	135

LIST OF SYMBOLS

a	:	velocity damping, sec^{-1}
a_{ij}	:	(i,j) element of A
b	:	control derivative
c	:	noise derivative
c	:	(i,j) element of C
d	:	cutoff frequency of p.s.d. of gust model
e	:	error between command input and output
$g(s)$:	transfer function
k_{ij}	:	(i,j) element of K
K_x	:	feedback gains of x and \dot{x}
p_i	:	i-th row of P
q_{ii}	:	(i-i) element of Q
r	:	command input or a scalar control weighting
s	:	Laplace operator $s = \sigma \pm j\omega$
s_1	:	zeroes of root square locus
s_2	:	
s_i	:	
s_{i+1}	:	eigenvalues of the autopiloted hovering helicopter dynamics
u	:	m control vector
x	:	position state of a second order system
	:	n state vector
y	:	p output vector
$x(0)$:	initial position error

LIST OF SYMBOLS (CON'T.)

A	:	$n \times n$ system matrix
A*	:	$n \times n$ desirable decoupled system matrix
B	:	$n \times m$ control derivative matrix
B*	:	$n \times m$ desirable decoupled control derivative matrix
C	:	$m \times n$ control decoupling matrix, $n \times 1$ noise derivatives
G	:	$m \times n$ feedback gain matrix
F	:	$n \times n$ closed loop system matrix
G(j ω)	:	frequency response of transfer function
I	:	identity matrix
I _i	:	i -th order integral
ISE	:	integral squared error
ISU	:	integral squared control
IS θ	:	integral squared pitch attitude angle, deg ² sec.
IS ϕ	:	integral squared roll attitude angle, deg ² sec.
IS ψ	:	integral squared yawing angle, deg ² sec.
J	:	performance index cost
J _{min}	:	minimum value of J
K	:	$n \times n$ state feedback gain matrix for decoupling
\bar{K}	:	$n \times n$ decoupling matrix with defined eigenvalues
L	:	Lagrangian equation
M	:	P-Pe
M ₁	:	1×1 matrix

LIST OF SYMBOLS (CON'T.)

N	:	lxl noise intensity matrix
P	:	nxn solution matrix of riccati equation
	:	pxn output matrix
Q	:	nxn state weighting matrix
\underline{Q}	:	$Q^T Q$
R	:	mxm control weighting matrix
S_{ij}^k	:	sensitivity of k-th characteristic root to a_{ij} variation
T_e	:	equivalent time constant, sec
T_{ex}	:	equivalent time constant of the longitudinal control
T_{ey}	:	equivalent time constant of the lateral control
T_{ez}	:	equivalent time constant of the vertical control
$T_{e\psi}$:	equivalent time constant of the yaw control
TSD	:	total system damping
U_m	:	equivalent mean control
Y_i	:	i-th output
X_0	:	n initial state vector
$X_a(t)$:	equivalent deterministic gust input
Y^*	:	$\mathcal{E}\{y-y^T\}$
U^*	:	$\mathcal{E}\{u-u^T\}$

LIST OF SYMBOLS (CON'T.)

Helicopter and V/STOL Notations

- x, y, z : longitudinal, lateral and vertical positions
perturbations, ft.
- u, v, w : longitudinal, lateral and vertical velocity
perturbations, ft/sec.
- θ, ϕ, ψ : pitch, roll and yaw attitude angle perturbations
rad.
- p, q, r : rolling, pitching and yawing angular velocity
perturbations, rad/sec.
- U_0, V : airspeed, ft/sec
- γ_0 : flight path angle, rad.
- X_{Bl_s} : longitudinal control input, rad.
- A_{l_s} : lateral cyclic control input, rad.
- δ_c : collective control input, rad.
- δ_r : yaw rudder control input, rad.
- m : mass of helicopter, V/STOL, slugs
- I_x, I_y, I_z : inertia moments about longitudinal, lateral
and vertical axis, slug ft²
- I_{xz} : product of inertia moment, slug ft²
- X : longitudinal force, pound
- X_u, X_v, X_w : longitudinal force derivatives, $\frac{1}{m} \frac{\partial X}{\partial u}$, $\frac{1}{m} \frac{\partial X}{\partial v}$, etc.
- X_p, X_q, X_r
- Y : lateral force, pound

LIST OF SYMBOLS (CON'T.)

Y _u , Y _v , Y _w Y _p , Y _q , Y _r	: lateral translational force derivatives, $\frac{1}{m} \frac{\partial Y}{\partial u}$, $\frac{1}{m} \frac{\partial Y}{\partial v}$, $\frac{1}{m} \frac{\partial Y}{\partial p}$, etc.
Z	: vertical force, pound
Z _u , Z _v , Z _w Z _p , Z _q , Z _r	: vertical translational force derivatives, $\frac{1}{m} \frac{\partial Z}{\partial u}$, $\frac{1}{m} \frac{\partial Z}{\partial v}$, $\frac{1}{m} \frac{\partial Z}{\partial w}$, etc.
L	: rolling moment, ft. pound
L _u , L _v , L _w L _p , L _q , L _r	: rolling moment derivatives, $\frac{1}{I_x} \frac{\partial L}{\partial u}$, $\frac{1}{I_x} \frac{\partial L}{\partial v}$ $\frac{1}{I_x} \frac{\partial L}{\partial w}$, etc.
M	: pitching moment, ft. pound
M _u , M _v , M _w M _p , M _q , M _r	: Pitching moment derivative, $\frac{1}{I_y} \frac{\partial M}{\partial u}$, $\frac{1}{I_y} \frac{\partial M}{\partial v}$, $\frac{1}{I_y} \frac{\partial M}{\partial w}$, etc.
N	: yawing moment, ft. pound
N _u , N _v , N _w N _p , N _q , N _r	: Yawing moment derivatives, $\frac{1}{I_z} \frac{\partial N}{\partial u}$, $\frac{1}{I_z} \frac{\partial N}{\partial v}$, $\frac{1}{I_z} \frac{\partial N}{\partial w}$, etc.
X _{B1s} , X _{A1s}	: longitudinal force control sensitivity derivatives,
X _{δ_c} , X _{δ_r}	: $\frac{1}{m} \frac{\partial Y}{\partial B_{1s}}$, $\frac{1}{m} \frac{\partial X}{\partial A_{1s}}$, $\frac{1}{m} \frac{\partial X}{\partial \delta_c}$, $\frac{1}{m} \frac{\partial X}{\partial \delta_r}$

LIST OF SYMBOLS (CON'T.)

- Y_{B1s}, Y_{A1s} : lateral force control sensitivity derivatives,
 $Y_{\delta_c}, Y_{\delta_r}$: $\frac{1}{m} \frac{\partial Y}{\partial B_{1s}}, \frac{1}{m} \frac{\partial Y}{\partial A_{1s}}, \frac{1}{m} \frac{\partial Y}{\partial \delta_c}, \frac{1}{m} \frac{\partial Y}{\partial \delta_r}$
 Z, Z : vertical force control sensitivity derivatives,
 Z_{B1s}, Z_{A1s} : $\frac{1}{m} \frac{\partial Z}{\partial B_{1s}}, \frac{1}{m} \frac{\partial Z}{\partial A_{1s}}, \frac{1}{m} \frac{\partial Z}{\partial \delta_c}, \frac{1}{m} \frac{\partial Z}{\partial \delta_r}$
 $Z_{\delta_c}, Z_{\delta_r}$: $\frac{1}{m} \frac{\partial Z}{\partial B_{1s}}, \frac{1}{m} \frac{\partial Z}{\partial A_{1s}}, \frac{1}{m} \frac{\partial Z}{\partial \delta_c}, \frac{1}{m} \frac{\partial Z}{\partial \delta_r}$
 L_{B1s}, L_{A1s} : rolling moment control sensitivity derivatives,
 $\frac{1}{m} \frac{\partial L}{\partial B_{1s}}, \frac{1}{m} \frac{\partial L}{\partial A_{1s}}, \frac{1}{m} \frac{\partial L}{\partial \delta_c}, \frac{1}{m} \frac{\partial L}{\partial \delta_r}$
 $L_{\delta_c}, L_{\delta_r}$: $\frac{1}{I_x} \frac{\partial L}{\partial B_{1s}}, \frac{1}{I_x} \frac{\partial L}{\partial A_{1s}}, \frac{1}{I_x} \frac{\partial L}{\partial \delta_c}, \frac{1}{I_x} \frac{\partial L}{\partial \delta_r}$
 M_{B1s}, M_{A1s} : pitching moment control sensitivity
 $M_{\delta_c}, M_{\delta_r}$: derivatives, $\frac{1}{I_y} \frac{\partial M}{\partial B_{1s}}, \frac{1}{I_y} \frac{\partial M}{\partial A_{1s}}, \frac{1}{I_y} \frac{\partial M}{\partial \delta_c},$
 $\frac{1}{I_y} \frac{\partial M}{\partial \delta_r}$
 N_{B1s}, N_{A1s} : yawing moment control sensitivity derivatives,
 $N_{\delta_c}, N_{\delta_r}$: $\frac{1}{I_z} \frac{\partial N}{\partial B_{1s}}, \frac{1}{I_z} \frac{\partial N}{\partial A_{1s}}, \frac{1}{I_z} \frac{\partial N}{\partial \delta_c}, \frac{1}{I_z} \frac{\partial N}{\partial \delta_r}$
 $M_{\theta nf}, M_{cv}$: pitching moment control sensitivity derivatives,
 $\frac{1}{m} \frac{\partial M}{\partial \delta_{nt}}, \frac{1}{m} \frac{\partial M}{\partial \delta_v}$
 X_{cv} : longitudinal force control sensitivity derivatives,
 $\frac{1}{m} \frac{\partial X}{\partial \delta_v}$

LIST OF SYMBOLS (CON'T.)

Z_{cs}, Z_{nf}	:	vertical control force sensitivity derivatives, $\frac{1}{m} \frac{\partial Z}{\partial \delta_s}, \frac{1}{m} \frac{\partial Z}{\partial \delta_{nt}}$
δ_v	:	incremental collective fan input
δ_{nf}	:	incremental nose fan input
δ_s	:	incremental fan stagger input
$[\cdot]$:	new derivatives after cancelling inertia coupling terms
$[\bar{\cdot}]$:	scaled computer variables
$K_x, K_u, K_\theta,$		
K_q	:	(optimal) feedback gains of $x, u, \theta,$ and q
$K_y, K_v, K_\phi,$		
K_p	:	(optimal) feedback gains of $y, v, \phi,$ and p
α	:	any scalar number
δ	:	control input
δ_{op}	:	optimal control input
$\delta(\cdot)$:	Dirac's delta function
Δ	:	small variation, summation
ρ^2	:	trade off parameter
σ	:	rms value of random gust, ft/sec.
$\sigma_x, \sigma_y, \sigma_z$:	rms longitudinal, lateral and vertical position errors, ft.
$\sigma_\theta, \delta_\phi, \delta_\psi$:	rms pitch, roll and yaw attitude errors, degree.
λ	:	Lagrange's multiplier

LIST OF SYMBOLS (CON'T.)

ω	:	undamped natural frequency, rad/sec.
ω_g	:	gust disturbance
$[\cdot]^T$:	transpose of a matrix
$[\cdot]^{-1}$:	inverse of a matrix
$ \cdot $:	determinant of a matrix
cofactor (a_{ij})	:	determinant of a matrix excepting i-th row and j-th column
$[\cdot]_m$:	mean value
$\ \cdot\ $:	euclidean norm
$[\dot{\cdot}]$:	time derivative
$T_r[\cdot]$:	summation of diagonal elements of a square matrix
\approx, \simeq	:	nearly equal to
$\mathcal{E}\{\cdot\}$:	expectation
$\{\cdot\}^*$:	optimal

CHAPTER I
INTRODUCTION

This study will explore the use of linear optimal control methods to design the automatic controller of a hovering helicopter. Generally the pilots workload is rather high for stabilizing a hovering helicopter [Fig. 2] and keeping position in the presence of gust over a designated point. Furthermore, to keep an accurate position may become more difficult if the motions [Fig. 3] among each axis are highly coupled.

In design of the multivariable and multi input systems, the conventional techniques such as root locus, frequency response, and describing function analysis which are based on the single input-single output systems, have been employed in trial and error fashion. Design techniques using the optimal control theory applied to multivariable systems in the state space have become popular and have been applied for the flight controller design or optimal control of aircraft [Ref. 1&2].

The optimal control design technique utilizes the minimization of a performance criteria; one of which is a quadratic cost function, such as Eq. (3-1). Adequate selection of weightings in the quadratic cost function yields a stable closed loop system [Ref. 3]. However, the following questions remain to be answered:

How should the weighting matrices be selected.

Where are the poles of the closed loop system in s plane located when control technique is used.

What are the system responses for a command input.

How is the system influenced by random gust inputs.

This work attempts to provide an answer to these questions and examines two methods for selecting weighting matrices, namely; the method of authorities [Ref. 6] and the optimal weighting selection method (OWEM) [Ref. 7]. The approach used in this investigation is as follows: First, the equation of motion of a helicopter comparable to a CH54B are decoupled, and the results are confirmed by an analogue computer study. Secondly, for each set of decoupled equations are derived the optimal controls with its feedback gains. For a range of selected factor weightings, analysis has been made for the root loci of the closed loop system, optimal feedback gains, the integral squared position error (ISE), attitude errors ($IS\theta$, $IS\phi$) and controls (ISU) to a command input. Also are investigated the root mean squared position errors, attitude errors and control motion for a random gust input. For the chosen pole location in s plane, the closed loop gains are determined, and command inputs response (ISE, $IS\theta$, etc.) and gust responses (rms errors) are calculated.

In Chapter II, is reviewed the application of optimal linear control theory, and an outline of the performed work is given. Also is discussed the areas that need further study and investigation.

In Chapter III, the details of optimal controller design are described for the vertical and yawing motion, followed by the longitudinal and lateral motions of the hover helicopter.

In Chapter IV, conclusions and recommendations on the optimal flight controller design using these methods are discussed.

In the appendices are reviewed some of the theoretical aspects of linear optimal control theory and model following. It appears that the OWEM design method is also applicable to model following, as outlined in Chapter II. Theoretical work has been extracted from Ref. [7], applications and calculations from Ref. [34] and the Appendix [6] from Ref. [35].

CHAPTER 2

REVIEW OF THE APPLICATION OF LINEAR OPTIMAL CONTROL THEORY

The purpose of this study is to apply optimal control methods for a controller design for helicopter at hover and in the approach phase. The design procedures in this report utilize first the decoupling of the helicopter dynamics (Appendix B). The system to be controlled consists of the decoupled helicopter dynamic equations.

In state variable form, the equations of motion are given by:

$$\dot{x}(t) = Ax(t) + Bu(t) \quad (2-1)$$

In most cases, x (n dimensional state vector), represents the state variables of motion of a hovering helicopter, which are, respectively, x , u , θ , q , z , w , y , v , ϕ , p , ψ , and r . The control variable u (m dimensional vector), represents control inputs which are respectively B_{1s} , A_{1s} , δ_r , and δ_c . In a few cases, the state vector x also can include the output of servo controller and so on.

The output vector $y(t)$ of helicopter is assumed to be the state vector $x(t)$ itself,

$$y(t) = Hx(t) = x(t) \quad (2-2)$$

$H = I : n \times n$ identity matrix

The advantages of state variable formulation is significant in the case of multi-variable and multi-input systems.

The design method uses an optimal control method with a quadratic performance index that minimizes the performance index given by the following equation:

$$J = \frac{1}{2} \int_0^{\infty} (x^T(t) Qx(t) + u^T(t) Ru(t)) dt \quad (2-3)$$

The matrices Q and R in Eq. (2-3) are respectively n by n and n by m weighting matrices which place relative weights on quadratic quantities x^2 , u^2 , θ^2 , ..., B_{1s}^2 ..., θ_0^2 . These state variables represent small displacements and their incremental rates from an equilibrium point. Therefore, the minimization of the performance index (2-3) minimizes the energy in the state and control displacements.

The linear optimal quadratic control law yields linear feedback of states and results in a reasonable damped, stable closed loop system. The quadratic cost function may be regarded as a generalized weighted mean square error criterion for the multi-variable system working under the penalties on the control variables.

The quadratic cost function for this problem is written with a weighting matrix Q for the state (or the output), and a scalar weighting $R = \rho^2$ for the control as follows:

$$J^* = \text{Min}_u \int_0^{\infty} [x^T(t) Qx(t) + \rho^2 u^2(t)] dt \quad (2-4)$$

The optimal control law $u(t)$ is obtained as

$$u(t) = -R^{-1}B^TKx(t) \quad (2-5)$$

It has been shown that the gain matrix K must satisfy the algebraic matrix Riccati equation:

$$KA + A^TK - \frac{1}{\rho^2} KBB^TK + Q = 0 ; \text{ where } Q > 0 \quad (2-6)$$

which yields a feedback control system with the stable, closed loop roots:

$$R_e\{\lambda_i[F]\} \equiv R_e\{\lambda_i[A - \frac{1}{\rho^2} BB^TK]\} < 0 \text{ for all } i = 1,2,3,4$$

To solve Eq. (2-6) for K matrix, the weighting matrix Q must be selected. For example, the longitudinal dynamic equations for a hovering helicopter (4th order system), one can write:

$$u(t) = -R^{-1}B^TKx(t) = -G_1x_1(t) - G_2x_2(t) - G_3x_3(t) - G_4x_4(t) \quad (2-7)$$

where

$$\begin{aligned} K &\equiv \{k_{ij}\} ; i, j = 1,2,3,4 \\ G_1 &= (X_{B1}k_{21} + M_{B1}k_{41}) / \rho^2 \\ G_2 &= (X_{B1}k_{22} + M_{B1}k_{42}) / \rho^2 \\ G_3 &= (X_{B1}k_{23} + M_{B1}k_{43}) / \rho^2 \\ G_4 &= (X_{B1}k_{24} + M_{B1}k_{44}) / \rho^2 \end{aligned}$$

After the Laplace transform, the control law Eq. (2-7) can be written as:

$$B_{1s}(s) = - G_x(T_x s + 1) x(s) - G_\theta(T_\theta s + 1) \theta(s) \quad (2-8)$$

where

$$G_x = G_1, G_\theta = G_3, T_x = G_2/G_1, T_\theta = G_4/G_3 \quad (2-9)$$

The optimal control system theory attempts to provide an analytical design procedure that lessens the designer's load in the design task, and locates more of the load on the computational machines. The problem is to find an optimal linear controller for a linear plant by minimizing the above quadratic system performance criterion or a quadratic cost function. The optimal linear-quadratic control theory provides a well organized design procedure for a linear system with a feedback structure. The linear feedback structure would probably be, from the practical point of view, the most beneficial result of optimal linear-quadratic control theory. The application of the theory, even the multiloop system design, which is often difficult in the conventional approach, may be thought to become easily accessible for system designers. All the possible feedback loops are taken into account and all the corresponding feedback gains are determined in the design procedure. The resulting closed loop system appears to be not only a stable system, but also a minimum weighted mean square error system.

The benefits and the mathematical beauty of the optimal linear-quadratic control theory might give a false impression that almost all the difficulties in linear system design have been eliminated. The entire theory has been developed under the presumption that the weighting matrices in the quadratic cost function are somehow given a priori. They are completely left open for the designer's choice.

The weighting matrices are usually selected only for their diagonal elements by the practical system designer on the basis of his engineering experience, coupled with simulation runs for different trial values. One can be obliged to do a tediously long trial-and-error approach, especially in the design of multiloop systems. Many of the attractive features of optimal linear-quadratic control theory seem to disappear. The optimal linear-quadratic control theory may be even worse than the conventional methods for multiloop system designs, because the weighting matrices have no apparent quantitative relationships with the closed loop system dynamical characteristics. None the less, the weighting matrices determine, to a large extent, on the resulting system dynamical characteristics. Hence, the selection of weighting matrices often become a considerably difficult task. One may be able to say that most of the potential difficulties of multiloop system design have been concentrated on the selection of weighting matrices, and the optimal control theory does not ease essential difficulties in the system design.

Accordingly, the selection of weighting matrices really has a crucial significance in the practical system design through the optimal linear-quadratic control theory. Some of the qualitative properties of weighting

matrices are summarized in Ref. [26]. They may help designers to select the trial weighting matrices. In order for the theory to be practically applicable, however, it is necessary to develop a reasonable and unified way for the quantitative selection of weighting matrices. This is one of the topics considered in this work.

Two methods for the quantitative selection of these weighting matrices have been available.

1. Method of Authorities of Variables (Refs. [27] and [28])

This method is based on the normalization of output variables and control variables. Every weighting factor for the output variables and the control variables is inversely proportional to the square of the prescribed maximum for that variable. The quadratic cost function becomes a linear combination of normalized mean square errors and controls. This method only provides an initial estimate for the weighting matrices, which are assumed to be of diagonal forms. However, there are no clear-cut reasons for the weighting matrices to be necessarily of a diagonal form, since the output components are usually coupled with one another. In order to refine the resulting system, a trial-and-error approach would be inevitable. Besides, it is often a difficult task to estimate the maximum values of all the output and the control components. Even if it is possible, there is no guarantee that all the outputs and the controls of the resulting system are suppressed within the prescribed maximum values.

2. Closed Loop Pole Allocation (Refs. [20] and [6])

This method achieves the specified closed loop poles by appropriately

choosing the weighting matrices in the quadratic cost function. The original work for this method has probably been done by E.J. Ellert (Ref. [6]). W.M. Wonham proved in Ref. [35] that it is possible to implement arbitrarily assigned poles on the complex plane with some linear feedback control law, if the open loop system is completely controllable. However, this has been proved independently of quadratic cost functions. More recent studies (Refs. [36] and [37]) on the inverse problem of linear feedback control show that every linear feedback control minimizes a quadratic cost function with certain weighting matrices. Combining Wonham's work and the results out of the inverse problem, it is possible to place the closed loop poles anywhere on the complex plane by choosing appropriate weighting matrices. However, the difficulty is how to allocate all (but not some) of the closed loop poles, especially in high-order systems. The dominant closed loop pole allocation has also been studied (Ref.[20]). This is a method to approximately obtain the desired dominant poles. However, this does not answer the essential difficulties in deciding the number of dominant poles, and in choosing the dominant poles. Besides, this approach usually yields a system with very high feedback gains, and requires complicated computational procedures. If the desired closed loop poles can be assigned, the optimal linear-quadratic control theory may not be necessary, but some other direct approach may be more convenient (example: Ref. [31]).

Thus, there is still a large gap between the optimal linear-quadratic control theory and its application to practical system design. Until such a gap is bridged by developing a reasonable, simple, and well-unified method to select the weighting matrices, the optimal linear-quadratic control theory would remain to be just a "theory" and would not be accessible to the

designers of practical systems.

This work is based upon Ref. [7], which attempts to bridge the gap. Below and in Appendix E is given a summary of the two new methods described in Ref. [7], to select the weighting matrices of general forms (not necessarily diagonal matrices).

3. OWEM Design Method (Ref. [7])

Based on the thought that the quadratic cost function is a legitimate system performance measure in the linear-quadratic control theory, the minimum quadratic cost function with the optimal linear feedback control law is actively used as the criterion to select the weighting matrices. First, the nature of the minimum quadratic cost function has been examined for particular sequences of weighting matrices. It leads to the necessity of some constraints on the weighting matrices, as a minimum equal to zero occurs when the weighting matrices are zero. In Ref. [7], reasonable constraints are explored to make the optimal weighting matrices not equal to zero or finite, and this appears to be a determinant constraint. Under this constraint, the minimum quadratic cost function is further minimized with respect to weighting matrices. The resulting weighting matrices are based upon the system noise characteristics, and hence, the minimum of the quadratic cost function becomes a function of the noise N or $J_{\min}(N, Q, R)$. The resulting closed loop system dynamics is a system that minimizes the effect of the noise or disturbance for which it was designed. It was also shown that the resulting optimal weighting matrices Q and R were inversely proportional to the output covariance matrix, and the induced covariance matrix of optimal controls, respectively. Obviously, they are not necessarily diagonal matrices. Note that these results are quite similar to the weightings proposed by Gauss for the weighted least-square estimation problem.

The optimal weighting matrices appropriately normalize the output and the control variables, and also equalize in groupwise all the additive terms appearing in the quadratic cost function. The two functions, i.e., the normalization and the equalization, are fundamental roles required for the weighting matrices in quadratic cost functions. Because of the normalizing effect of weighting matrices, the resulting closed loop system dynamics became irrelevant to the physical dimensions which were used to express the plant dynamical equations.

It was also shown that the ratio $\rho = |R|/|Q|$ between the prescribed determinants of R and Q represented some kind of measure about the trade-off between the contribution of control variables, and that of system output variables to the quadratic cost function. The tradeoff parameter ρ would play the key role for determining the closed loop system bandwidth.

The method described above provided a well formulated set of necessary and sufficient conditions for reasonable optimal weighting matrices with only one unknown parameter or trade-off parameter equal to ρ . It required the a priori knowledge about the system noise intensity matrix N since the criterion $J_{\min}(N;Q,R)$ was a function of N. The a priori knowledge about the plant noise may not be available in many cases. Then, the second method for the selection of the weighting matrices was developed by introducing a new criterion which is independent of the noise intensity matrix N.

The concept of n-dimensional hyper error ellipsoid (state error set) is used and a measure of the state error set was defined by its n-dimensional volume ($V(t)$). The "Relative Rate of Convergence of Error Sets" was defined as $|\frac{1}{V(t)} \frac{dV(t)}{dt}|$, and this represents a sort of generalized system response speed. This new criterion is independent of the plant noise intensity

matrix N , and was shown to be exactly the same as the so-called "Total System Damping". The well formulated necessary and sufficient conditions for the noise-free optimal weighting matrices are derived as the solution of the Mini-Max problem for the RERACES (or TSD).

It has been shown that, using the second method selection of the Q matrix yields the same result as the first method, if the noise characteristics (see Fig. 1) are assumed to be white noise disturbances with $N_e = kR^{-1}$. In other words, a white noise disturbance in $u(t)$. The effect of noise or disturbance bandwidths in the helicopter application is discussed in Chapter 3, and is often small for the range of operating conditions used in that application.

The initial application of this method for determining the Optimal Weighting Matrices to second through fifth order example in Ref. [38] indicates the advantages of this approach. For these examples, the conventional and optimal methods have been used extensively, and the results are well known. For these examples, the area of the pole location for the precision hover of a helicopter has been well established, and each of the above methods can be applied yielding (often by trial and error), about the same results. However, it has been demonstrated, by these examples, that the application of the OWEM method yields, without a trial and error method, a good and well damped solution to the problem.

This solution is independent of scaling (dimensions) of the problem statement, and assumes in the first instance, that there is no a priori different penalty on error, gain, frequency, etc., among the state variables.

In summary, for the OWEM design method it is required to know:

1. the system matrix
2. the control matrix
3. the noise or disturbance matrix

The OWEM design method then determines the weighting matrices Q and R for minimizing the quadratic performance index under the assumption that all errors are equally important, and hence, these matrices for the calculation of the feedback gains. When the noise N is unknown, Q and R can be computed by the mini-maximization of TSD with respect to Q and R under prescribed determinant constraints. This is equivalent to a white noise disturbance with a magnitude N_e inversely proportional to the control weighting R, and the minimization of TSD is equivalent to the minimization of $J_{\min}(N_e; Q, R)$.

The OWEM design method is based upon minimization of known or estimated disturbances and results in a control system with adequate stability or damping. In the generalized formulation no consideration is given to system limitations, such as acceleration limits, gain limitations, and so on. Hence, in the design of a flight controller, the performance and control boundaries must be considered. These boundaries are essential in the practical application of the design method. For example, take the case of a hovering helicopter (longitudinal).

A design is to be made for an automatic control system. However, the assumption is made that when the system is switched to manual control, it is desirable that the mode frequencies do not change appreciably. Hence,

the boundaries for the automatic system should be similar to those of manual control. The longitudinal control of the precision hover of a helicopter is in principle dominated by 2 modes; a "position" mode corresponding to the "outer loop" and a "attitude mode" corresponding to the "inner loop" of the feed control system.

An estimate of the boundaries of the "position" mode is given in Ref. [22], and summarized below.

A massless point controlled according to a linear error control law, $\dot{e} = -Ke$, would result in a first order system with a closed loop bandwidth $\omega_{CL} = 1/\tau_{CL} = K$. Instantaneous speed changes not being possible, even the simplest model has to incorporate the inertia. This leads to a second order system for control. The most significant assumption in this very simple model is that tilting the thrust vector and changing its magnitude, is possible with negligible delay compared with the position keeping bandwidth. The block diagram of such a simplified model is shown in Illustration (2-1).

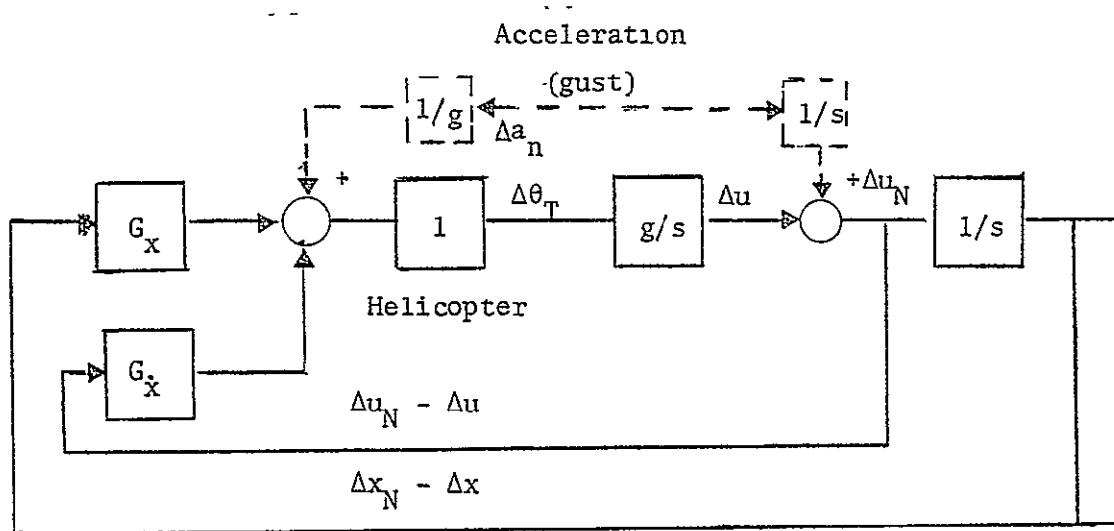


Illustration 2-1. Simplified Block Diagram of a Hovering Helicopter

The input to the longitudinal positioning loop is shown as Δa_N , the acceleration disturbance. The gains $\bar{g}G_x$ and gG_x determine the acceleration per foot error and per ft/sec error rate, respectively. The following fundamental relationships are easily deduced from the block diagram.

The natural frequency and therefore, the bandwidth of the position loop is

$$\omega_p = \sqrt{gG_x} \quad ; \quad (2-10)$$

gG_x is the "spring constant" of the position loop. The relative damping ratio is

$$\zeta_p = (\sqrt{g}/2) (G_x^*/\sqrt{G_x}) = 2.83 (G_x^*/\sqrt{G_x}) \quad (2-11)$$

The relationship between the bandwidth and the damping ratio is determined by

$$G_x^*/G_x = 2(\zeta_p/\omega_p) \quad (2-12)$$

and, for a predetermined bandwidth and damping ratio

$$G_x = (1/g) \omega_p^2 \quad \text{and} \quad G_x^* = (2/g) \zeta_p \omega_p$$

In the case of a constant acceleration disturbance, the steady state error is $ag/\omega_p^2 = a/G_x$. The simple model provides reasonable estimates of the

relationship between bandwidth gains and errors as long as the bandwidth of the attitude control loops is several times faster than that of the station keeping loop. Such a separation is feasible and appears desirable in most applications.

For the choice of bandwidth of the position loop, the following considerations can be made. A large ω_p leads to a high error gain G_x , a small ω_p results in a large steady state error for constant acceleration disturbance.

The table below shows some characteristic values of bandwidth, gain and error.

ω_p (rad/sec)	.1	.2	.5	1.0
G_x (deg/ft)	.018	.07	.45	1.8
steady state error (ft)				
for .1g acceleration	320	80	13	3.2

This table helps to narrow the choice of ω_p to between approximately .3 and .5. With values under .3, the error becomes excessive, above .5 the thrust angle variations with even small errors are rapidly becoming too large.

The desirability to make the bandwidth of the "attitude" mode faster than that of the "position" mode is limited by the manual attitude control loop. This results in an "attitude" mode of frequency in the order of $\omega > 1.0$ to 2 rad/sec.

In the conventional control system design method, the gain limitations are taken into account for choosing the "inner" and "outer" loops. In these

hovering helicopter examples a "tight" inner loop (altitude) is designed with sufficient damping by adjusting G_θ and $G_{\dot{\theta}}$, the outer loop (position) is determined by the position gain limitation G_x ; the velocity gain $G_{\dot{x}}$ is adjusted to provide sufficient damping.

In the OWEM design method as developed does not take into consideration gain limitations. When there are no gain limitations, the operating point in the linear quadratic optimal design is determined by the control weighting. This number is determined by the control limitations, and the maximum expected disturbances, and/or command inputs.

However, the OWEM design method can be easily adapted by additional information, into the design.

When no additional information is used, the computational procedure regards the errors and the associated feedback gains, etc., equally important. Hence, in this design method, the root location tends to be circular with more damping than the Butterworth configuration. After the initial design is made, the resulting mode frequencies, errors, gains, etc., can be analyzed. When the value of these quantities are not in conflict with the practical design requirements, then one can consider the design to be completed.

However, in many cases, practical physical limitations have to be imposed on errors, loop gains, mode frequencies, etc. For example, in the hovering helicopter, the position mode frequency is acceleration limited e.g., .3 to .5 radians/sec.

On the other hand, the attitude loop should be a much higher frequency, e.g., 1-3 rad/sec.

In Appendix E is shown in the calculation of the optimal weighting matrices the groups wise equalization matrix (S) is equal to the unity matrix. This imposes an equal weighting on the elements of the $y^* Q y^{*T}$. In engineering terms, this implies that all the mean square error associated control, gains, etc., are of equal importance.

The initial design is done on the digital computer using $S = I$. The resulting design is then examined with respect to errors, control and gain limitations. For example, one can examine errors and mode frequencies as a function of the control weighting ρ . When this examination shows that the control weighting ρ determined by the control limitation, no other boundaries (imposed or desired) are violated, then the design is finished. If, however, one finds that for the desired control weighting ρ , one of the pre-determined requirements is not met or gain boundaries are violated, then one should determine the violated boundary on the Optimal Root Location (ORL) plot.

In the example shown for the longitudinal hovering helicopter, the position acceleration limitation limits the ρ to approximately equal to 800 (.3 to .5 rad/sec.), while the desired altitude boundary yields a ρ approximately equal to 3200. This implies that in order to reach the control boundary and acceleration boundary at the same time, one should use an equalization matrix which has a value of 1/4 for the state variables associated with this limitation.

In other words, one can assign a different weighting on the system errors if this also is equivalent to assigning a diagonal Error Scaling Matrix (ESM). The designer is free to investigate the effect of the ESM matrix upon the final system design. Note that the ESM matrix is a diagonal matrix, so that the elements of the matrix are easily interpreted.

In this manner, an objective measure of an error criteria is used to determine the weighting matrices. The approach taken in this work imposes the boundaries more or less by engineering judgement in terms of errors. A very important further theoretical investigation with significant practical aspects is the introduction of constraints in the OWEM design.

The OWEM design method is also directly applicable in model following for the determination of the weighting matrix \hat{Q} (Appendix G1, Eq. G1-22). The weighting matrix \hat{Q} in the model reference system is composed of the original weighting factors Q of linear feedback systems. The OWEM method determines the Q matrix for minimization of disturbances. Hence, a weighting matrix determined by this principle should yield a prefilter model reference control system that minimizes the errors due to the disturbances.

Another important investigation will be the practical aspects of the use of OWEM design criteria for incomplete measurement and feedback of all state variables.

CHAPTER 3

CONTROLLER DESIGN FOR A HELICOPTER (OWEM)

1. A Helicopter system and control equations

In this chapter the optimal control design will be illustrated on the controller design of a helicopter. The system to be controlled is a system representative of an uncoupled hovering helicopter CH54B given by Eq. 3-1.

$$\begin{bmatrix} \dot{u} \\ \dot{\theta} \\ \dot{q} \\ \dot{w} \\ \dot{v} \\ \dot{\phi} \\ \dot{p} \\ \dot{r} \end{bmatrix} = \begin{bmatrix} X_u & -g & X_q & 0 & 0 & 0 & 0 & 0 \\ 0 & 0 & 1 & 0 & 0 & 0 & 0 & 0 \\ M_u & 0 & M_q & 0 & 0 & 0 & 0 & 0 \\ \gamma & 0 & 0 & Z_w & 0 & 0 & 0 & 0 \\ 0 & 0 & 0 & 0 & Y_v & g & Y_p & Y_r \\ 0 & 0 & 0 & 0 & 0 & 0 & 1 & 0 \\ 0 & 0 & 0 & 0 & L_v & 0 & L_p & 0 \\ 0 & 0 & 0 & 0 & 0 & 0 & 0 & N_r \end{bmatrix} \begin{bmatrix} u \\ \theta \\ q \\ w \\ v \\ \phi \\ p \\ r \end{bmatrix} +$$

$$\begin{array}{c}
 \begin{array}{cc|cc}
 \bar{X}_{B_{1s}} & 0 & 0 & 0 \\
 0 & 0 & 0 & 0 \\
 M_{B_{1s}} & 0 & 0 & 0 \\
 \hline
 0 & Z_{\delta_c} & 0 & 0 \\
 \hline
 0 & 0 & Y_{A_{1s}} & 0 \\
 0 & 0 & 0 & 0 \\
 0 & 0 & L_{A_{1s}} & 0 \\
 \hline
 0 & 0 & 0 & N_{\delta_r}
 \end{array}
 &
 \begin{array}{c}
 \bar{B}_{1s} \\
 \delta_c \\
 A_{1s} \\
 \delta_r
 \end{array}
 &
 (3.1)
 \end{array}$$

For the optimal design, the following equations are used and solved with the aid of a digital computer.

System dynamics: $\dot{x}(t) = Ax(t) + Bu(t) + Cn(t)$ (3.2)

$$y(t) = Hx(t)$$
 (3.3)

where $x(t)$: n dimensional state vector
 $u(t)$: m dimensional control vector ($m \leq n$)
 $y(t)$: p dimensional output vector ($p \leq n$)
 $n(t)$: l dimensional noise vector ($l \leq n$)

$E\{n(t)\} = 0$
 $Cov\{n(t);n(\tau)\} = N\delta(t-\tau)$ (unknown)
 A, B, C and H : $n \times n$, $n \times m$, $n \times l$ and $p \times n$ constant matrices, respectively.

Cost function: $J_{\min}(N; Q, R) = \text{Min}_{u(t)} \left\{ \text{Lim}_{T \rightarrow \infty} \frac{1}{2T} \int_{-T}^T [y^T(t)Qy(t) + u^T(t)Ru(t)] dt \right\}$

$$= \text{Tr}[CNC^T K]. \quad (N: \text{unknown}) \quad (3.4)$$

If $N_e = kC^+BR^{-1}B^T(C^+)^T$, then

$$J_{\min}(N_e; Q, R) = k\text{Tr}[BR^{-1}B^T K] \quad (3.5)$$

where C^+ : $l \times n$ pseudo-inverse matrix of C , i.e.,
 $(= (C^T C)^{-1} C^T)$

Optimal control law: $u(t) = -R^{-1}B^T Kx(t)$ (3.6)

where K : $n \times n$ unique positive definite solution of (3.7)

$$KA + A^T K - KBR^{-1}B^T K + H^T QH = 0 \quad (3.7)$$

The optimal control law (3.7) can be computed without knowing N if Q and R are given.

If the Q and R matrices are estimated, then for these Q and R values the optimal control law can be calculated.

When the values for the matrices Q and R are not estimated, then one needs an additional criteria. For example, minimizing total system error in total system damping, etc. as discussed in Ref. (7). Assuming that gust or noise information is not available, the selection of optimal weighting matrix is done by minimizing the criterion $L(Q, \rho^2)$, as discussed in Ref. 7 and Appendix E.

Auxiliary performance index

Total System Damping = TSD: the negative sum of the closed loop roots

$$L^* = \text{Min}_Q \text{Max}_R \{ \text{TSD} \} = \text{Min}_Q \text{Max}_R \{ \text{Tr}[-(A - BR^{-1}B^T K)] \} \quad (3.8)$$

or equivalently

$$L^* = \text{Min}_Q \text{Max}_R \{ \text{Tr}[BR^{-1}B^TK] \} \quad (\because A = \text{constant matrix})$$

$$\text{subject to } KA + A^TK - KBR^{-1}B^TK + H^TQH = 0$$

Note: (1) TSD is equivalent to the Relative Rate of Change of Error Sets (RERACES, see Ref. [7], Chapter IV), and is a generalized system response speed.

(2) The extremum (minimax) of TSD does not exist unless Q and R are appropriately constrained.

Constraints on Q and R

$$|Q| = 1, \quad |R| = \rho^2$$

where

$$|(\cdot)| : \text{the determinant of } (\cdot) \quad (3.9)$$

Optimal weighting matrices

$$Q = \sqrt{|HPH^T|} \cdot (HPH^T)^{-1} \quad (3.10)$$

$$R = \rho^{2/m} \frac{B^TKB - B^TKPKB}{\sqrt[m]{|B^TKB - B^TKPKB|}} \quad (3.11)$$

$$\text{where } FP + PF^T + BR^{-1}B^T = 0 \quad (3.12)$$

$$F = A - BR^{-1}B^TK$$

The latter equations are solved on the digital computer for the matrix Q. The optimal weighting matrices are then used in the Riccati Eq. 3-8 which yields the optimal control law (Eq. 3-7).

For a hovering helicopter CH54B, the numerical values for Eq. 3-2 are shown in Eq. 3-13.

$$A = \begin{bmatrix} -.0169 & -32.2 & .661 & 0.0 & 0.0 & 0 & 0.0 & 0.0 \\ & & 1.00 & & & & & \\ .0024 & 0 & -.257 & 0.0 & 0.0 & 0 & 0.0 & 0.0 \\ 0.0 & 0 & 0.0 & -.269 & 0.0 & 0 & 0.0 & 0.0 \\ 0.0 & 0 & 0.0 & 0.0 & -.0405 & 32.2 & -.895 & 0.0 \\ & & & & & & 1.00 & \\ 0.0 & 0 & 0.0 & 0.0 & -.0200 & 0 & -1.14 & 0.0 \\ 0.0 & 0 & 0.0 & 0.0 & 0.0 & 0 & 0.0 & -.591 \end{bmatrix}$$

$$B = \begin{bmatrix} 35.6 & 0.0 & 0.0 & 0.0 \\ 0 & 0 & 0 & 0 \\ -5.66 & 0.0 & 0.0 & 0.0 \\ 0.0 & -292. & 0.0 & 0.0 \\ 0.0 & 0.0 & 36.1 & 0.0 \\ 0 & 0 & 0 & 0 \\ 0.0 & 0.0 & 24.6 & 0 \\ 0.0 & 0.0 & 0.0 & -10.9 \end{bmatrix} \quad (3.13)$$

These equations can be divided into four separate systems of equations, namely:

1. Vertical Control System
2. Yaw Control System
3. Longitudinal Control System
4. Lateral Control System

For a helicopter in the approach phase, the numerical values for Eq. 3-2 are shown below in Eq. 3-14.

$$A^* = \begin{bmatrix} -.0221 & -32.2 & 1.515 & | & 0.0 & | & 0.0 & 0 & 0.0 & | & 0.0 \\ & & 1.0 & | & & | & & & & | & \\ .0020 & 0 & -.4251 & | & 0.0 & | & 0.0 & 0 & 0.0 & | & 0.0 \\ \hline 0.0 & 0 & 0.0 & | & -.5333 & | & 0.0 & 0 & 0.0 & | & 0.0 \\ \hline 0.0 & 0 & 0.0 & | & 0.0 & | & -.0711 & 32.2 & -1.788 & | & 0.0 \\ & & & | & & | & & & 1.0 & | & \\ 0.0 & 0 & 0.0 & | & 0.0 & | & -.0113 & 0 & -1.488 & | & 0.0 \\ \hline 0.0 & 0 & 0.0 & | & 0.0 & | & 0.0 & 0 & 0.0 & | & -.937 \end{bmatrix}$$

$$B^* = \begin{bmatrix} 33.12 & 0.0 & 0.0 & 0.0 \\ 0 & 0 & 0 & 0 \\ -5.35 & 0.0 & 0.0 & 0.0 \\ \hline 0.0 & -304.4 & 0.0 & 0.0 \\ \hline 0.0 & 0.0 & 35.35 & 0.0 \\ 0 & 0 & 0 & 0 \\ 0.0 & 0.0 & 24.06 & 0 \\ \hline 0.0 & 0.0 & 0.0 & -9.53 \end{bmatrix} \quad (3-14)$$

B Controller Design for Vertical and Yaw Control

In hovering, the helicopters have inherent rate damping in vertical and yawing motions with stable vertical speed and yaw rate characteristics. However, with regard to the position stability, both the position control equations are neutrally stable due to pole located at origin. This means that the helicopter, if uncontrolled and if exposed to disturbances, will drift away from desired hover points. Taking these into account, the following design objectives are recommended for precision hovering.

- (1) To obtain the stable well damped position control system
- (2) Good system response to position command input, with a small or no overshoot, and minimizing integral square error (ISE)
- (3) Minimizing root mean square position errors and resulting controls to random gust input.

Some of these requirements oppose each other and a compromise becomes necessary.

The characteristics of the decoupled (uncoupled) motion of vertical and yawing equations are of the second order rate command systems as in Eq. (3-14).

$$\ddot{x}(t) + a\dot{x}(t) = b\delta(t) + (cw_g(t)) \quad (3-15)$$

where

$x(t)$: position Z , ft or ϕ , rad

$\dot{x}(t)$: rate of position Z , ft/sec or r , rad/sec

a : rate damping Z_w or N_r , sec^{-1}

- b : control derivatives Z_{θ} , ft/sec²rad or N_{δ_r} , rad/sec²rad
 $\delta(t)$: control input δ_c or δ_r , rad
 $w_g(t)$: vertical gust or sideway gust, ft/sec
 c : gust derivatives, Z_w , 1/sec or N_v , 1/sec ft

We assume for calculation purposes that disturbances even in decoupled yaw equation has effect on control through N_v term.

Design Method by Conventional Selection of Weighting Factors

The optimal control is derived by minimizing, in a disturbed system the following integral without w_g

$$\frac{1}{2} \int_0^{\infty} (q_{11} x^2(t) + q_{22} \dot{x}^2(t) + r \delta^2(t)) dt \quad (3-16)$$

- Where q_{11} : weighting factor for position
 q_{22} : weighting factor for rate
 r : weighting factor for control

Selection of Weighting Elements q_{11} , q_{22} and r

In both systems the closed loop system characteristics are covered by selection of non-zero diagonal q_{11} , q_{22} and r only, as shown in Appendix D. The weighted quadratic terms in the integral should be non-dimensionalized. The following units are selected for q_{11} , q_{22} and r .

	Vertical	Yaw	
q_{11}	ft ⁻²	rad ⁻²	(3-17)
q_{22}	ft ⁻² .sec ²	rad ⁻² sec ²	
r	rad ⁻²	rad ⁻²	

The values of weighting factors are specified by choosing an equivalence of the values of position errors (Z, ϕ) , rate errors (\dot{Z}, \dot{r}) and resulting control (δ_c, δ_r) . The selection is as follows:

$$\text{Vertical } (10 \text{ ft})^2 = (5 \text{ ft/sec})^2 = (0.1 \text{ rad})^2 \quad (3-18)$$

$$\text{Yawing } (0.2 \text{ rad})^2 = (0.1 \text{ rad/sec})^2 = (0.1 \text{ rad})^2 \quad (3-19)$$

These weighting factors correspond to the case (5) with $r = 100$ in Table 1 below, where a number of computed numerical examples are listed.

Table 3.1. Computed Numerical Examples

Case No.	Weighting factors		
	q_{11}	q_{22}	r
(1)	1.0	0	$0 \rightarrow \infty$
(2)	1.0	0.25	$0 \rightarrow \infty$
(3)	1.0	1.0	$0 \rightarrow \infty$
(4)	1.0	2.0	$0 \rightarrow \infty$
(5)	1.0	4.0	$0 \rightarrow \infty$
(6)	1.0	16.0	$0 \rightarrow \infty$

Note that only the relative magnitudes (values) have effects on the characteristics of the closed loop system (see Appendix D).

Optimal Control. The optimal control to minimize the performance index (Eq. 3-16) is given as function of q_{11} , q_{22} and r (Appendix D).

$$\delta_{op}(t) = -\sqrt{\frac{q_{11}}{r}} x - \left(\frac{a}{b} + \sqrt{\left(\frac{a}{b}\right)^2 + \frac{2}{b} \sqrt{\frac{q_{11}}{r} + \frac{q_{22}}{r}}} \right) \dot{x}(t) \quad (3-20)$$

Substituting this into Eq. (3-15) gives the closed loop system

$$\ddot{x}(t) + \sqrt{a^2 + 2b\sqrt{\frac{q_{11}}{r}} + b^2 \frac{q_{22}}{r}} \dot{x}(t) + b\sqrt{\frac{q_{11}}{r}} x(t) = 0 \quad (3-21)$$

This derivation and its properties are shown in Appendix D.

The optimal control, in general, has been solved for the system without noise as shown in Appendix D. The separation theory in Refs. (26, 27, 39) warrants the optimal control to be optimal for the system with gaussian white noise. However, unfortunately it is not guaranteed to be still optimal for the system with nonwhite or nongaussian gust.

Root Locus for some q_{22} 's and $q_{11} = 1.0$. The root loci with varying r are shown in Figs. (6 and 7) for vertical and yaw equations, respectively. The complex roots are circumferently distributed to the origin. These numerical examples are of the following numbers.

Vertical

$$\begin{aligned} a &= Z_{\dot{w}} = -.269 \text{ 1/sec} \\ b &= Z_{\delta} = -292 \text{ ft/sec}^2/\text{rad} \\ c &= -Z_{\dot{w}} = -.269 \text{ 1/sec} \end{aligned} \quad (3-22)$$

Yawing

$$\begin{aligned} a &= N_r = -.482 \text{ 1/sec} \\ b &= N_{\delta_r} = -8.95 \text{ rad/sec}^2/\text{rad} \\ c &= -N_v = -.0019 \text{ rad/ft/sec} \end{aligned} \quad (3-23)$$

Notice that the closed loop system is sufficiently stabilized by weighting q_{11} and r only, and the damping ratio approaches .707 as r becomes smaller. These poles are called 2nd order Butterworth poles (Ref. 9). Addition of q_{22}

gives rise to a more damped system. The damping ratio and undamped natural frequency are given as:

$$\zeta = \frac{1}{2} \sqrt{2 + \frac{a^2}{b} \sqrt{\frac{r}{q_{11}}} + bq_{22} \sqrt{\frac{1}{rq_{11}}}} \quad (3-24)$$

$$\omega_n = \sqrt{b \sqrt{\frac{q_{11}}{r}}} \quad (3-25)$$

The latter determines the system response speed, or accuracy, which is inversely proportional to quartic root of control weighting r . When the weighting q_{22} satisfies the following inequality

$$\sqrt{\frac{q_{11}}{q_{22}}} \leq |a| \quad (3-26)$$

Then all roots are on negative real axis, since $S_1 = -\sqrt{\frac{q_{11}}{q_{22}}}$ has the role of a zero in the root locus. It is observed that such selection of weightings as in this case 'that is' no cross product terms in Eq. (3-16), place the closed loop system poles in certain limited left half plane. A desirable region of pole location closely relate with the requirements (2) and (3). In spite of increasing accuracy or speed of response, placing poles too far away in the left half plane, by increasing feedback gains or control action, is likely to excite the structural vibration mode of the helicopter. On the other hand, poles near the origin present a slow response and roughness of control.

The feedback gains are shown in Figs. (8) and (9), which also show the corresponding augmented damping and stiffness. The feedback gains increase as r becomes smaller, and increase in q_{22} raises the rate feedback gains.

The optimal feedback controls for both vertical and yawing systems do not yield a system which has an overshoot for a step input. Hence, some of our design objectives (stable, no overshoot) are definitely obtained.

ISE and ISU Evaluation for Command Input. In general, the ISE and ISU for the second order system to a unit command step input are given as

$$\text{ISE} = \frac{1}{\omega_n} \left(\zeta + \frac{1}{4\zeta} \right) \quad (3-27a)$$

$$= \int_0^{\infty} x^2 dt \left| \begin{array}{l} x(0) = 1.0 \\ \dot{x}(0) = 0.0 \end{array} \right. \quad (3-27b)$$

$$\text{ISU} = \frac{\omega_n (a^2 + \omega_n^2)}{4\zeta} \quad (3-28a)$$

$$= \int_0^{\infty} \delta^2 dt \left| \begin{array}{l} x(0) = 1.0 \\ \dot{x}(0) = 0 \end{array} \right. \quad (3-28b)$$

where

ω_n : closed loop undamped natural frequency rad/sec

ζ : closed loop damping ratio

a : open loop damping

which are sketched as a function of ζ in Figure 10 where the minimum ISE is attained when $\zeta = 0.500$, and the ISU is inversely proportional to ζ . In the s-plane the curves for ISE = const. and ISU = const. are shown in Figure (18).

Using Eqs. (3-24), (3-25), (3-27) and (3-28), the integrated square errors and controls to command step input are computed with varying r , some q_{22} 's and $q_{11} = 1.0$ as shown in Figs. (11) and (12). The ISE value approaches the minimum as r goes zero, while the ISU goes to infinity. The minimum ISE value of the optimal control system is given by substituting Eqs. (3-24) and (3-25) into Eq. (3-27),

$$\text{Min. ISE} = \frac{1}{2} \sqrt{\frac{q_{22}}{q_{11}}} \quad (3-29)$$

at $r = 0$ where the ISU becomes infinity. This value would become criterion for selection of q_{11} and q_{22} , known as that of the model equation given by Eq. (D2-21) in Appendix D. For reference of ISE values, it is desirable to compare with the ISE of the first order system of which command response is easily depicted in mind. Therefore, the following time constant may become an index:

$$T_e = \text{time constant of the first order system with same ISE} \quad (3-30)$$

which is labeled in Figs. (10), (11), (12), (38) and (63). Similarly , one may define the following equation as mean control acceleration.

$$U_m = \sqrt{\frac{1}{T_e} ISU} \quad (3-31)$$

which would be a rule of thumb for the upper limit of ISU. It is interesting to see that ISE of the optimal control system is a little bit larger than the true minimum ISE as shown in Figure 10.

Gust Response. The requirement for gust response supercedes that for command input in position keeping such as hovering. In addition, knowledge of the gust response is important since the optimal control is obtained independently of the random gust. The assumed gust model is of the following power spectrum density (p.s.d.).

$$S_{rr}(\omega) = \frac{2\sigma^2 d}{d^2 + \omega^2} \quad (3-32)$$

where

d : bandwidth of p.s.d. of the random gust

σ : rms value of random gust

The numerical examples are given by

$$\begin{aligned} \sigma &= 10 \text{ ft/sec} \\ d &= .314, 1.0, 2.0 \text{ rad/sec} \end{aligned} \quad (3-33)$$

which is a considerable gusty condition.

The rms position error and control are calculated with varying r as shown in Figs. (13) to (16) for both vertical and yawing equations. From these figures, the gust response would be alleviated by increasing q_{22} , or increasing rate feedback (see Figs. 8,9), with less control effort. It is much more reduced by decreasing r 'that is' increasing rms control action. As r goes to zero, the rms control force (acceleration) increases to cancel the random gust force with little excess as shown in Figs. (13) and (14). Note that excess control action is caused by control system time lag.

For different bandwidths of p.s.d. of random gust under its constant intensity, the rms position errors and controls are studied in Figs. (15) and (16). These results show that random gust with higher frequency component bring less effect on both rms position error and resulting control.

These results are explained by the frequency domain analysis as follows:
The rms value of the gust response is described as (Appendix G1-3)

$$\text{RMS value} = \frac{1}{\pi} \int_0^{\infty} |G(j\omega)|^2 S_{rr}(\omega) d\omega \quad (3-34)$$

where $G(j\omega)$ is the frequency response of the transfer function to the gust. For example, the frequency responses of the transfer function of vertical position error and control to the gust input are shown in Figs. (17) and (18). The following three cases are pictured here:

Case No.	Weighting factors			Undamped	
	q_{11}	q_{22}	r	Damping	Natural Frequency
(1)	1.0	0	13130	0.71	0.9
(2)	1.0	0	8190	0.71	1.8 (3-35)
(3)	1.0	4.0	8190	1.9	1.8

The broken lines indicate the p.s.d. of the random gust. The rms position error in case (1) becomes larger than the others because of the higher gain as shown in Fig. (17). On the other hand, the control action becomes smaller since the relative magnitude of control is smaller. In case (3), though the control response can be influenced by a high frequency component of random gust, the gust under consideration does not include such frequency component, and therefore the rms resulting control is smaller compared to case (2). Similarly, it is recognized that the random gust with higher bandwidth of its power spectrum density has less effect on both rms position errors and control.

Now, assume that requirements are chosen as follows:

$$\text{rms vertical position error} \leq 5 \text{ ft} \quad (3-36a)$$

$$\text{Integral squared position error} \leq 5 \text{ ft}^2 \text{ sec} (T_e=1.0) \quad (3-36b)$$

$$\text{Integral squared control} \leq 9.0 \text{ ft}^2 \text{ sec}^{-3} (U_m=3.0 \text{ ft/sec}^2) \quad (3-36c)$$

Eq. (3-36a) would supercede the others in keeping position.

The lower limit of r is prescribed by only ISE requirement. We should choose q_{11} and q_{22} as necessary,

$$q_{22}/q_{11} \leq 1.0 \quad (3-37)$$

and r should satisfy the following inequality

$$1200(8.5) \leq \frac{r}{q_{11}} \leq 2,200(6.2) \quad (3-38)$$

for $q_{11} = 1.0$ and $q_{22} = 0.0$.

The requirements for yawing cases are chosen as follows:

$$\text{rms yawing error} \leq 1.0 \text{ degrees} \quad (3-39a)$$

$$\text{ISE} \leq .50 \text{ deg}^2\text{sec} \quad (T_e = 1.0 \text{ sec}) \quad (3-39b)$$

$$\text{ISU} \leq 9. \text{ deg}^2\text{sec}^{-3} \quad (U_m = 30 \text{ deg/sec}) \quad (3-39c)$$

Then, we should choose as necessary

$$q_{22}/q_{11} \leq 1.0 \quad (3-40)$$

and r should satisfy, for $q_{11} = 1.0$, $q_{22} = 0$

$$1.1 (8.5) \leq r/q_{11} \leq 3(5.2) \quad (3-41)$$

Note that numerical numbers in the parenthesis indicate ratios of expected controls and position errors due to weightings, and the ratios are almost the same in both cases. There is a big difference between selected r due to the differences in control derivatives.

The desirable root location to meet all requirements (Eq. 3-36), which varies as requirements alternate, is sketched in Fig. (18).

Owem Design Method. The optimal control is given by, as shown in Appendix E2.

$$\bar{\delta}_{\text{opt}}(t) = - \frac{b \frac{1}{3} x(t) - (-\frac{a}{b} + \sqrt{(\frac{a}{b})^2 + \frac{3}{\frac{2}{b^3} \frac{2}{r^3}}})}{r \frac{2}{5}} \dot{x}(t) \quad (3-42)$$

Note that the optimal control is determined only by r which is called 'trade off parameter' in the Appendix E. This optimal control is also designed to be optimal for the system with a gaussian white noise as shown in the Appendix E, but not for a nonwhite gust.

The close loop system is given by, (See Eq.E2-)

$$\ddot{x}(t) + \sqrt{a^2 + \frac{3b}{r} \frac{4}{3}} \dot{x}(t) + \frac{b}{r} \frac{4}{3} x(t) = 0 \quad (3-43)$$

of which undamped natural frequency and damping ratio are:

$$\omega_n = \frac{b}{r} \frac{2}{3} \quad (3-44)$$

$$\zeta = \frac{1}{2} \sqrt{3 + \frac{a^2}{b} \frac{2}{3} r \frac{2}{3}} \quad (3-45)$$

Root Locus for Varying r

The root loci are sketched in broken lines for vertical and yawing equation in Figs. (6) and (7), respectively. The closed loop system approaches the system with damping ratio = .866 while the poles are pushed away

in the left half s plane as r goes to zero. The distance of the complex roots from the origin is inversely proportional to cubic root of control weighting r. By this method, no overshoot and sufficiently stable system can be obtained and some of our design objectives are achieved.

ISE and ISU for Command Input

The ISE and ISU values are shown in broken lines in Figs. (11) and (12), respectively. These (ISE and ISU with varying r) are calculated by substituting (3-44) and (3-45) into (3-27) and (3-28) and as r goes zero, obviously

$$ISE_{r=0} = 0 \quad (3-46)$$

$$ISU_{r=0} = \text{infinity} \quad (3-47)$$

The requirements described in Eqs. (3-36b,c) and (3-39 b,c) would be satisfied by choosing r properly.

Gust Response

The rms position errors and controls of the gust responses are also shown with broken lines in Figs. (13) and (14). Decreasing a weight r on control or increase in available control reduces the rms position error.

The requirements described in Eqs. (3-36) and (3-39) are satisfied by choosing

$$2700(5.6) \leq r \leq 7500(3.4) \quad (3-48)$$

$$2.6(5.6) \leq r \leq 5.8(3.5) \quad (3-49)$$

Note that the numbers in parenthesis indicate the ratio of expected controls and state errors due to r called tradeoff parameter in the single input cases [sée Appendix E].

In this way, all the design requirements would be satisfied by this method.

Helicopter in Approach Phase

The numerical values for the helicopter in the approach phase (Eq. 3-14), are not sufficiently different from those in Eq. 3-22 and 3-23 to employ a control system with variable gain, especially as the control system is of the first order.

C Controller Design for Longitudinal Equation

A hovering helicopter can have an unstable, oscillatory mode in the longitudinal equation, as shown in Figure 2. Furthermore, the position control equation has another pole at origin. That places much workload on the pilot for precision hovering, especially in gusty conditions. Therefore, the design objectives become, for the automatic controller:

1. To obtain the stable system
2. Good response, such as little-overshoot, minimizing the ISE, IS θ , ISU to a command input
3. To minimize RMS of the position error, attitude error, and resulting control to gust input

The longitudinal equation is given by

$$\begin{aligned} \dot{u} - X_u u - X_q \dot{\theta} + g\theta &= X_{B1s} B_{1s} - X_u u_g \\ -M_u \ddot{u} + \ddot{\theta} - M_q \dot{\theta} &= M_{B1s} B_{1s} - M_u u_g \end{aligned} \quad (3-50)$$

In the state variable form, including position variables

$$\begin{bmatrix} \dot{x} \\ \dot{u} \\ \dot{\theta} \\ \ddot{q} \end{bmatrix} = \begin{bmatrix} 0 & 1 & 0 & 0 \\ 0 & X_u & -g & X_q \\ 0 & 0 & 0 & 1 \\ 0 & M_u & 0 & M_q \end{bmatrix} \begin{bmatrix} x \\ u \\ \theta \\ q \end{bmatrix} + \begin{bmatrix} 0 \\ X_{B1s} \\ 0 \\ M_{B1s} \end{bmatrix} B_{1s} + \begin{bmatrix} 0 \\ -X_u \\ 0 \\ -M_u \end{bmatrix} u_g \quad (3-51)$$

where

x	:	longitudinal position	, ft
u	:	longitudinal velocity	, ft/sec
θ	:	pitch attitude angle	, rad
q	:	pitch rate	, rad/sec
B_{1s}	:	longitudinal cyclic pitch	, rad
u_g	:	gust input	, ft/sec
X_u	:	rate of change of longitudinal force, 1/sec with velocity	
X_q	:	rate of change of longitudinal force, ft/sec with pitch rate	
M_u	:	rate of change of pitching moment, rad/ft sec with velocity	
M_q	:	pitch rate damping	, 1/sec
$X_{B_{1s}}$:	longitudinal control derivatives	, ft/sec ² /rad
$M_{B_{1s}}$:	longitudinal control derivatives	, rad/sec ² /rad
g	:	gravitational force	, 32.2 ft/sec ²

The performance index to be minimized is given as follows:

$$\frac{1}{2} \int_0^{\infty} (q_{11}x^2 + q_{22}u^2 + q_{33}\theta^2 + q_{44}\dot{\theta}^2 + rB_{1s}^2) dt \quad (3-52)$$

Selection of q_{ii} ($i = 1, 2, 3, 4$) and r .

The selection of diagonal Q or q_{ii} places the poles of the closed loop system in a restricted part of the left half s plane. (Appendix E). The following units are selected for q_{11} , q_{22} , q_{33} , q_{44} and r .

$$\begin{array}{ll}
q_{11} & \text{ft}^{-2} \\
q_{22} & \text{ft}^{-2} \text{sec}^2 \\
q_{33} & \text{rad}^{-2} \\
q_{44} & \text{rad}^{-2} \text{sec}^2 \\
r & \text{rad}^{-2}
\end{array} \tag{3-53}$$

Their values are specified by choosing an equivalence of x , u , θ , q and B_{1s} in the integral of Eq. (3-52). The selection is as follows:

$$1 \text{ ft} = 1 \text{ ft/sec} = 1 \text{ degree} = 1 \text{ degree/sec} = 0.1 \text{ rad} \tag{3-54}$$

Equation (3-54) is expressed as Case No. (7) with $r = 100$ in Table 3.2 where the selected diagonal weighting q_{ii} ($i = 1,2,3,4$) are shown. Note that attitude errors θ , $\dot{\theta}$ are specified in degrees, while in the equation the units are radians.

Table 3-2. Numerical Examples for q_{ii}

Case No.	q_{11}	q_{22}	q_{33}	q_{44}
(1)	1.0	---	---	---
(2)	1.0	---	820	---
(3)	1.0	---	3,280	---
(4)	0.1	---	3,280	---
(5)	0.01	---	3,280	---
(6)	1.0	---	3,280	3,280
(7)	1.0	1.0	3,280	3,280
(8)	0.1	0.1	3,280	---
(9)	0.1	0.1	3,280	3,280
(10)	0.1	0.4	3,280	13,130

Root Square Locus.

The root loci for the longitudinal system is shown in Figs. (19) through (27). A stable system is obtained using only a weighting q_{11} of the Q matrix and r. Two of the poles approach the asymptote $\zeta = 0.707$ while attitude poles approach the zeroes, as shown in Fig. (19). The root loci starts from stable poles which are then shifted to mirror image in the left half plane of the original unstable poles. Increasing the attitude weighting factors q_{33} from a zero value, induces the more damping to the attitude poles, and further increases in q_{33} moves the attitude poles away from the asymptote and shifts the position poles into the left half plane as shown in Figs. (20) to (23). As a result, the attitude control or inner loop control becomes much faster than the outer loop or position control. The boundary condition, whether or not the locus of the attitude poles bends inwards, depends on the weighting ratio of q_{11} and q_{33} . The zero locus is drawn as a function of q_{33}/q_{11} in Fig. (22). This indicates that an increase in the relative weighting q_{33} to q_{11} brings two zeroes to the origin. Addition of either q_{22} or q_{44} yields another zero on real axis and provides more damping to both the attitude and position poles, as shown in Figs. (24) to (27). Especially, imposition of q_{33} on $\dot{\theta}$ locate a zero near $Z_1 = -\sqrt{\frac{q_{33}}{q_{44}}}$. Hence, only one root goes to infinity along the negative real axis, while the others approach the zeroes, and the system is more damped. The closed loop system with damping ratio more than 0.707 would be achieved by the adequate selection of q_{11} , q_{22} , q_{33} , q_{44} and r, where obviously more weighting would be imposed on q_{33} and q_{44} .

By the OWEM method, the root locus is uniquely determined with choice of r only. Four poles move to infinity along $\zeta \approx .65$ and $\zeta \approx .95$, and the closed loop systems are sufficiently damped.

In this way, some of the design requirements are attained without difficulty. The feedback gains are shown in Figs. (28) to (37). Using these diagrams, the optimal control is obtained as:

$$B_{1s} = K_x x + K_u u + K_\theta \theta + K_q q \quad (3-55)$$

At infinite r , both feedback gains K_θ and K_q approaches nonzero gains, so that the unstable poles are shifted to the mirror image in the left half plane. For the conventional selection method of q_{ii} and r , the outer loop, feedback gain is given by:

$$K_x = \sqrt{\frac{q_{11}}{r}} \quad (3-56)$$

which specifies the systems accuracy. From this point of view, Eq. (3-56) helps select q_{11} and r .

ISE, IS θ and ISU for a Command Input.

The integral squared position and attitude error to a 10 ft. command input is shown in Fig. (38). In position control, the hovering helicopter is desirable to follow the command input as fast as possible without excessive attitude change or its rate. As r goes to zero, the ISE value approaches the minimum given by that of model equation corresponding the zeroes, while the IS θ reaches the maximum as shown in Fig. (38). These values at null r are sketched as a function of ratio of weighting factors q_{11} and q_{33} in Fig. (39).

They show that the reduction in ISE increases $IS\theta$ in Fig. (39). Hence, a compromise is necessary. The addition of the weighting factor, q_{44} decreases the $IS\theta$ considerably, with little increase in the ISE. Finally, the amount of control available in Fig. (40) is limited by the power limitation and mechanical strength of the helicopter.

As shown in Fig. (38), the integral squared control increases as r decreases and decreases more when a weighting is placed on the attitude or its rate.

It is observed that the OWEM has features similar to, but better than, Case 1 in Table 2, indicating $ISE = 0$, $IS\theta = ISU = \infty$ at $r = 0$.

Gust Response

The rms position and attitude errors to the random gust are shown in Figs. (41) and (42), for some q_{ii} 's and varying r . The assumed gust model is of the same as Eq. (3-33) and numerical example is made assuming quite strong gusty conditions.

$$\sigma = 20 \text{ ft/sec} \quad (3-58)$$

$$d = .314, 1.0, 2.0 \text{ rad/sec}$$

The rms position error decreases as r/q_{11} becomes smaller and depends slightly on q_{33}/q_{11} . Effects of q_{22} and q_{44} are negligible, and hence, not shown in the figure. On the other hand, the rms attitude error, due to the gust, depends strongly on r/q_{11} and selected q_{ii} ($i = 1,2,3,4$). Adding a weighting factor, q_{22} or q_{44} improves the error considerably. In the range of q_{ii} considered here, the ratio of q_{33}/q_{11} governs entirely the order of magnitude of the rms value.

The rms longitudinal cyclic control and position error is shown in Fig.(41). The root mean squared position, attitude errors, and different bandwidths of the power spectrum density for a gust with constant intensity are computed. It is clear that the rms position errors are less influenced by the gust with higher bandwidth. On the other hand, the rms attitude errors are affected less at a large r, but become more affected at smaller r by the gust components of higher frequency, as shown in Fig.(67).

The gust responses for the OWEM, shown with broken lines in Figs. (41) and (42) are better than Case 1.

A ranking of all requirements for precision hover can be done as shown below. A compromise between them must be found as it is desirable that all requirements are simultaneously satisfied. Take, for example, the following case:

$$\text{root mean squared position error} \leq 1.0 \text{ ft.} \quad (3-57a)$$

$$\text{root mean squared attitude error} \leq 0.3 \text{ deg.} \quad (3-57b)$$

$$\text{integral squared position error} \leq 400 \text{ ft}^2\text{sec} \ (\tau_e \leq 8) \quad (3-57c)$$

$$\text{integral squared attitude} \leq 16 \text{ deg}^2\text{sec} \ (\theta_m \leq 2 \text{ deg.}) \quad (3-57d)$$

$$\text{integral squared control} \leq 0.05 \text{ rad}^2\text{sec} \ (B_{1sm} \leq .05 \text{ rad}) \quad (3-57e)$$

$$\text{acceleration limits} \leq \text{none}$$

The righthandside of Eqs. (3-57a) and (3-57b) vary depending on rms gust velocity or its rate. The upper limits on Eqs. (3-57c) to (3-57e) are altered proportionally to squared magnitudes of command inputs. However,

$T_{e_{max}}$, θ_{max} , and U_{max} may be independently prescribed.

Equation (3-57a) exclusively determines the upper limits of r , though ISE and rms attitude error requirements may influence this considerably. The lower limit of r is described by Eqs. (3-57d) and (3-57e). The way of choosing q_{ii} could be found out by requirements (3-57b), (3-57d), and (3-57e).

If one considers the above requirements, then the following set of q_{ii} and r can be chosen as one of desirable sets of q_{ii} and r .

$$\begin{aligned} r &= 2.0 \cdot 10^4 \\ q_{11} &= .1, \quad q_{33} = 3280 \end{aligned} \tag{3-58}$$

With the feedback gains

$$\begin{aligned} K_x &= -.0071 \\ K_u &= -.026 \\ K_\theta &= 1.58 \\ K_q &= .56 \end{aligned} \tag{3-59}$$

It is easily understood in the process of choosing these sets that Case (5) does not satisfy Eq. (3-57c) and Case (1) is unsatisfactory with Eq. (3-57d), because of excessive attitude error. An OWEM method which does not take into account the difference in position and attitude error weighting should also be unsatisfactory (for example, see Eq. (3-57d)).

Helicopter in Approach Phase

The numerical values for the helicopter in the approach phase are given in Eq. (3-14). The root location for the optimal roots as a function of the control weighting r are shown in Figure 67. It appears that the difference in numerical values compared to the hovering case is not sufficiently large enough to justify a control system with variable gains.

OWEM Design Method

Applying the OWEM design method for the longitudinal motion of the helicopter gives a root location as a function of $r = \rho$ obtained by a computer solution as shown in Figure 19.

In the initial approach of an OWEM design, all the constants k_3 of the group-wise equalization of the terms of $\{y^{*T} Q y^*\}$ are chosen to be equal. This corresponds to an equalization matrix $S = I$. Making the equalization matrix not equal to the identity matrix corresponds to an equalization factor of the diagonal terms of the matrix q_{ij} . This principle is illustrated in this example in Figure 19.

In this figure is shown the root location obtained by the initial application of the OWEM method (equalization matrix = identity matrix). The desired root location with associated optimal Q matrix is determined by the acceleration limitation of the helicopter (corresponding to an ω of .3 to 5 rad/sec). Take, for example, that an equalization was desired of one to two for the ratio of the position error to attitude error. The diagonal terms of the Q matrix are associated with the variables $x, \dot{x}, \theta, \dot{\theta}$ respectively. Hence, the equalization is chosen to be 1:1:4:1.

Figure 69 is shown, the root location obtained by the OWEM method, modified with an error scaling matrix (ESM) of 1:1:4:1. For this ESM Q matrix a root square locus diagram is given as a function of the control weighting ρ . The ESM matrix should also change the weighting of the derivatives of θ , as this increases the damping. By trial and error, one can investigate the error scaling matrix for the $\dot{\theta}$ error weighting. In this particular case, 1:1:4:4 was chosen.

In the same illustration is shown the chosen optimal Q matrix, modified with an equalization matrix of 1:1:4:4.

For this equalized Q matrix a root square locus diagram is given as a function of the control weighting $r = \rho$. (curve no. 2)

For a control weighting of 3200, the (negative) feedback gains are:

$$\begin{aligned}G_x &= -.0015 \text{ rad/ft} = -.084 \text{ deg/ft.} \\G_{\dot{x}} &= -.0074 \text{ rad/ft} = -.420 \text{ deg/ft.} \\G_\theta &= .56 \text{ rad/rad} = .56 \text{ deg/deg.} \\G_{\dot{\theta}} &= .42 \text{ rad/rad} = .42 \text{ deg/deg.}\end{aligned}\tag{3-60}$$

The root locations are shown in Figure 69, with the associated feedback gains in Figure 72. The corresponding error and control measures are shown in Figures 40, 41 and 42.

It should be emphasized that, in this work the acceleration limitations have been introduced as an "afterthought" in the OWEM design. In the OWEM calculations the acceleration limitations were simulated by an "error weighting". In principle, it should be possible to introduce constraints directly into the OWEM design method, thereby eliminating the trial and error aspect.

In the hovering helicopter example, feedback gain limitations on the position state variable (equivalent to an acceleration limit) should more or less "freeze" the position mode when a certain control power is reached. A further increase in control power should only affect the θ mode. This procedure would eliminate the trial and error procedure of the $\dot{\theta}$ error weighting. However, these theoretical aspects need first to be further investigated.

D Controller Design for Lateral Equation

In a hovering helicopter, the lateral equation uncoupled with yaw becomes unstable and poses a comparatively short period mode (see Figs. (2,3)). Therefore, our design objectives are composed of the same ones as the longitudinal case. The lateral equations are given by:

$$\begin{aligned} \dot{v} - Y_v v - Y_p p - g\phi &= Y_{A1s} A_{1s} - Y_v v_g \\ -L_v v + \ddot{\phi} - L_p \dot{\phi} &= L_{A1s} A_{1s} - L_v v_g \end{aligned} \quad (3-61)$$

In the state variable form, including position variable

$$\begin{bmatrix} \dot{y} \\ \dot{v} \\ \dot{\phi} \\ \dot{p} \end{bmatrix} = \begin{bmatrix} 0 & 1 & 0 & 0 \\ 0 & Y_v & g & Y_p \\ 0 & 0 & 0 & 1 \\ 0 & L_v & 0 & L_p \end{bmatrix} \begin{bmatrix} y \\ v \\ \phi \\ p \end{bmatrix} + \begin{bmatrix} 0 \\ Y_{A1s} \\ 0 \\ L_{A1s} \end{bmatrix} A_{1s} + \begin{bmatrix} 0 \\ -Y_v \\ 0 \\ -L_v \end{bmatrix} v_g \quad (3-62)$$

where

- y : lateral position ,ft
- v : lateral velocity ,ft/sec
- φ : roll angle ,rad
- p : roll rate ,radsec⁻¹

A_{1s}	: lateral cyclic pitch	, rad
v_g	: gust input	, ft/sec
Y_v	: rate of change of lateral force with velocity	, sec ⁻¹
Y_p	: rate of change of lateral moment with roll velocity	, sec ⁻¹
L_v	: rate of change of lateral moment with velocity	, rad/sec ft
L_p	: roll rate damping	, sec ⁻¹
Y_{Als}	: lateral control derivatives,	, ft.sec ⁻² rad
L_{Als}	: lateral control derivatives,	, 1/sec ²
g	: gravitational force	, 32.2 ftsec ⁻²

The performance index to be minimized is given by:

$$\int_0^{\infty} (q_{11}y^2 + q_{22}v^2 + q_{33}\phi^2 + q_{44}p^2 + rA_{1s}^2) dt \quad (5-63)$$

Selection of q_{ii} , $i = 1, 2, 3, 4$ and r .

The diagonal weighting matrices Q might place the poles of the closed loop systems in restricted parts of the left half plane. The selection of Q would be done in the same way as in the longitudinal case and the same q_{ii} 's are used as numerical examples [see Table 3.2].

Root Square Locus

The root loci are shown in Figs. (43) to (51). The stable closed loop system is obtained by a weighting factor q_{11} only. Addition of q_{33} gives more damping to the system, especially to attitude control loop. Further increase in q_{33} finally moves the poles of the attitude loop further in the left half plane, while the poles of position move to the right, 'that is' the position loop reduces stability as shown in Figs. (45 to (47). It is seen in Fig. (46) that the attitude poles start going far away for a set of $q_{11}=.1$, $q_{33}=3280$ unlike the longitudinal case. These tendencies seem desirable since the inner loop control is desirable to be much faster than the outer loop position control. The broken line of Fig. (44) indicates the zero locus as a function of the parameter of q_{33}/q_{11} . It starts from the point $\zeta=-2.33\pm j4.06$ and approaches the zero along the asymptote $\zeta=.707$. Addition of q_{22} or q_{44} yields another zero on negative real axis and provides more damping to both the attitude and position poles as shown in Figs. (48, 49, 50 and 51). Selection of q_{22} locates the zero in the far left of the negative real axis. On the other hand, selection of q_{44} locates the zero on $Z_1 = -\sqrt{\frac{q_{33}}{q_{44}}}$. As a result, only one root goes to infinity on the negative real axis while the others approach zeroes and the system is more damped. The closed loop system with damping ratio more than 0.707, if desired, would be achieved by adequate selection of q_{11} , q_{22} , q_{33} , q_{44} and r .

The feedback gains are shown in Figs. (52) to (61), where it is noted that the augmented dampings are equivalent to those of longitudinal ones at the same r/q_{11} , though feedback gains being smaller than longitudinal ones

except K_y given by

$$K_y = \sqrt{\frac{q_{11}}{r}} \quad (3-64)$$

which specify the system control precision. At infinite r , K_ϕ and K_p are nonzero similarly as in longitudinal cases. Using these gain diagrams, the optimal control is obtained as:

$$A_{1s}^* = K_y y + K_v v + K_\phi \phi + K_p p \quad (3-65)$$

ISE, IS ϕ , and ISU for Command Input

The integral squared position error, attitude and control to a 10 ft. command input is shown in Figs. (62) to (63). Effects of r and q_{ij} on these results are almost the same as the longitudinal case. When compared to the longitudinal case, the IS θ came out larger in spite of the use of less control amount (ISU) due to the larger control derivative. Accordingly, the command input response becomes faster, that is, less ISE. The min. ISE and max. IS θ at zero r are nearly equivalent to those of the longitudinal case because both model equations are almost the same. Note that the ISE goes zero while the IS θ increases to infinity as r goes zero for the OWEM.

Gust Responses

Figs. (64) to (67) show that rms lateral position error (ISE), attitude error (IS ϕ) and resulting control (ISU). From these figures, it is confirmed that the lateral motion is much stronger influenced by gust through large gust derivatives, Y_v and L_v , compared to longitudinal motion. The control

necessary to trim the translational force and upset moment due to gust amounts is twice as large as that of a longitudinal case. Keeping lateral position as precise as longitudinal control requires more feedback gains corresponding to smaller r .

Figure (66) indicates the effect of gust with different frequency components under its constant intensity to attitude errors. It turns out that the gust with cut-off frequency $d = 1.0$ rad/s influences the lateral attitude most, while the pitch attitude is most influenced with cut-off frequency $d = .314$ rad/s at large r . These characteristics are explained by the fact that the basic helicopter dynamics have modes excited around frequency of $.36$ rad. in longitudinal motion and frequency of $.85$ rad. in lateral axis.

Take, for example, the following case similarly to the Eqs. (3-57a) to (3-57e):

$$\text{rms position error} \leq 1.0 \text{ ft.} \quad (3-66a)$$

$$\text{rms roll attitude error} \leq 0.3 \text{ deg.} \quad (3-66b)$$

$$\text{ISE} \leq 400 \text{ ft}^2 \text{sec} \quad (T_{em} \leq 8 \text{ sec}) \quad (3-66c)$$

$$\text{IS}\theta \leq 16 \text{ deg}^2 \text{sec} \quad (\theta_m \leq 2 \text{ deg}) \quad (3-66d)$$

$$\text{ISU} \leq 0.05 \text{ rad}^2 \text{sec} \quad (A_{1sm} \leq .05 \text{ rad}) \quad (3-66e)$$

$$\text{Acceleration limits} \leq \text{none}$$

The design approach is similar to that of the longitudinal case.

For the closed loop system, to satisfy all requirements, the following set of q_{ii} and r is chosen as one of the desirable sets of q_{i1} and r

$$r = 1.5 \cdot 10^3 \quad (3-67)$$

$$q_{11} = .1, q_{33} = 3280$$

Then, the feedback gains are:

$$\begin{aligned} K_y &= -.026 \text{ rad/ft} \\ K_v &= -.087 \text{ rad/ft/s} \\ K_\phi &= -4.8 \text{ rad/rad} \\ K_\dot{\phi} &= -.46 \text{ rad/rad/s} \end{aligned} \quad (3-68)$$

In a practical application, the acceleration limits will show that these gains are too high.

Helicopter in Approach Phase

The numerical values for the helicopter in the approach phase are given in Eq. (3-14). The root location for the optimal roots as a function of the control weighting ρ is shown in Figure 68. It appears that the difference in numerical values, compared to the hovering case, is not sufficiently large enough to justify a control system with variable gains.

OWEM Design Method

Using the approach similar to that of the longitudinal case, the root locations using the OWEM design is shown in Figure 43. For an error scaling matrix, chosen was 1:1:4:3, and, the feedback gains for $\rho = 1300$ are:

$$\begin{aligned} K_y &= -.00075 \\ K_v &= -.0025 \\ K_\phi &= -.18 \\ K_\dot{\phi} &= -.09 \end{aligned} \quad (3-69)$$

The root locations as a function of $r = \rho$ are shown in Figure 70 with the associated feedback gains in Figure 72. The corresponding errors and con-

trol measures are shown in Figures 62, 63 and 64.

CHAPTER 4

CONCLUSIONS AND RECOMMENDATIONS

The optimal linear-quadratic control theory provides a well organized design procedure for the automatic controller design of a multivariable system. In this design process an optimal linear feedback control law is found, which minimizes a quadratic cost function.

It is usually assumed that the weighting matrices in quadratic cost functions are given a priori. However, the resulting optimal feedback control system is a function of the selected weighting matrices. The functional relationships between the weighting matrices and dynamical characteristics of the resulting system are rather obscure. Therefore, the selection of weighting matrices is often a major problem in the practical applications of the optimal linear-quadratic control theory.

In this report the weighting matrices are selected by the OWEM design method as described in Ref. [7] and Appendix E. Also in this work the weighting matrices using the OWEM design method are obtained by direct calculation and not mainly by a creative trial and error approach. The OWEM design method is compared with other methods for finding the weighting matrices. The results indicate that the use of this approach gives at least as good results as obtained by other classical design methods.

Much work still has to be done, especially in the case of multivariable input-output systems, and a priori imposed limitations of the practical system. However, from the examples in this work, it can be recommended that the OWEM

design method is a good candidate to use for the selection of weighting matrices. Moreover, the OWEM design method does not require any lengthy and laborous estimations of weighting matrices in quadratic cost function. A completely computerized system design becomes possible, which can provide quick results even for complicated systems. The decision which has to be made by the designer after the computerized system design is to choose an appropriate trade-off parameter by considering the corresponding feedback gains, system dynamical characteristics and other practical situations. Practically, of course, further refinements for such a computerized system design would have to be done for a few choices of trade-off parameters. In the long run, when the given system is highly complicated, for example, a system with many feedback loops and/or multiple controls, the computerized system design procedure associated with the OWEM method can save large amounts of time usually required in the early stage of system designs.

In conclusion, the OWEM method provides an objective measure to determine the weighting factors in the performance index based upon an error criteria. Initially, the system errors are assumed to be equally important, however, directly from missions requirements one can determine which are the important errors, and use this additional information together with the other system requirements to obtain an improved design. The resulting OWEM design is a control system that minimizes the errors due to disturbances and has good transient responses.

This work explores the application of the OWEM design method to an automatic controller design for a helicopter at hover and approach. The examples demonstrate that this approach is feasible and is a good candidate for the control system design.

Areas of further studies are:

1. Further investigation of the practical aspects of system disturbances in the selection of the weighting matrices, i.e., how are the weighting matrices and the resulting optimal feedback gains changed if the noise characteristics are varied.
2. Investigation of the effect of a priori imposed limitations (control and/or system boundaries) on the OWEM design method, i.e., in this work imposed limitations were combined with an assigned error scaling matrix ESM derived from physical limitations. Further investigation of the practical aspects of a priori imposing design limitations would be highly desirable.
3. An investigation of the practical aspects of the effects of an incomplete measurement system and feedback of the state variables in the OWEM design method.
4. Further investigation of the application of the OWEM design method in model following control systems. In theory, the OWEM method can yield the weighting or Q matrix for the prefilter model reference control system. However, the practical aspects should be investigated.

REFERENCES

1. Robinson, A.C., "Survey of Dynamics Analysis Methods for Flight Control Design", *Journal of Aircraft*, Vol. 6, No. 2, March-April 1969.
2. Paiewonsky, B., "Optimal Control: A Review of Theory and Practice", *AIAA Journal*, Vol. 3, No. 11, November 1965.
3. Athans, M. and Falb, P.L., "Optimal Control", McGraw Hill Inc., New York, 1966.
4. Chang, S.S.L., "Synthesis of Optimal Control Systems", McGraw Hill Book Company, Inc., New York, 1961.
5. Kalman, R.E., "When is a Linear Control System Optimal", *Journal of Basic Engineering*, March 1964.
6. Ellert, F.J., "Indices for Control System Design Using Optimization Theory", Ph.D. Thesis, Dept. of Electrical Engineering, Rensselaer Polytechnic Institute, New York, 1963.
7. Kawahata, N., "Linear Control System Optimization by Optimal Selection of the Weighting Matrices in Quadratic Cost Functions", Ph.D. Thesis, Dept. of Aerospace and Mechanical Sciences, Princeton University, Princeton, N.J., September 1972.
8. Skelton, G.B., "Investigation of the Effects of Gust on V/STOL Craft in Transition and Hover", AFFDL TR-68-65, Wright Patterson AFB, Ohio, October 1968.
9. Seckel, E., "Stability and Control of Airplanes and Helicopters", Academic Press Inc., New York, 1964.
10. Nikolsky, A.A., "Helicopter Analysis", John Wiley and Sons, Inc., New York, 1951.
11. Curtiss, H.C., Jr., "Some Notes on VTOL Stability and Control", Princeton University Course Notes, August 1971.
12. McRuer, D.I., Ashkenas, I., and Graham, D., "Aircraft Dynamics and Automatic Control", System Technology Inc., Hawthorn, California, Princeton University, 1974.
13. Morgan, B.S., Jr., "The Synthesis of Linear Multivariable Systems by State Variable Feedback", *IEEE Transactions on Automatic Control*, Vol. AC-9, October 1964.

REFERENCES

(2)

14. Falb, P.L. and Valvoich, W.A., "Decoupling in the Design and Synthesis of Multivariable Control Systems", IEEE Transaction of Automatic Control, Vol. AC-12, No. 6, December 1967.
15. Gilbert, E.G., "The Decoupling of Multivariable Systems by State Feedback", SIAM J. Control, Vol. 7, No. 1, February 1969.
16. Panda, S.P., "Compensator Design for Decoupling of Multivariable Systems by State Feedback", Int. J. Control, Vol. 13, No. 1971.
17. Mufti, T.H., "Some Results on the Decoupling of Multivariable Systems", Int. J. Control, Vol. 14, No. 3, 1971.
18. McRuer, D.T., et al, "Human Pilot Dynamics in Compensatory Systems", System Technology, Inc., AFFDL-TR-65-15, July 1965.
19. Kwakernaak, H. and Sivan, R., "Linear Optimal Control Systems", John Wiley & Sons, Inc., New York 1972.
20. Anderson, B.D.O and Moore, J.B., "Linear Optimal Control", Prentice Hall Inc., Englewood Cliffs, New Jersey, 1971.
21. Rynaski, E.G. and Whitbeck, R.F., "The Theory and Application of Linear Optimal Control", Cornell Aeronautical Laboratory, Cal. No. 1H-1943-F-1, Buffalo, New York, October 1965.
22. Dukes, T.A., "Helicopter Station Keeping", Princeton University, USA ECOM-TR-02412-9, September 1972.
23. Kalman, R.E. and Bucy, R.S., "New Results in Linear Filtering and Prediction Theory", Trans. ASME J. Basic Engineering, Ser. D, Vol. 83, March 1961.
24. Luenberger, D.G., "Observers for Multivariable Systems", IEEE Tr. on AC, Vol. AC-11, No. 2, April 1966.
25. Bryson, A.E. and Hall, W.E., "Synthesis of Hover Autopilots for Rotary-Wing VTOL Aircraft", Stanford University, SUDAAR Rpt. No. 446, November 1971.
26. Athans, M., "The Role and Use of the Stochastic Linear-Quadratic-Gaussian Problem in Control System Design", IEEE Trans. Auto. Control, Vol. AC-16, No. 6, December 1971.

REFERENCES

(3)

27. Bryson, A.E. and Ho, Y.C., "Applied Optimal Control", Blaisdell Publishing Company, Waltham, Massachusetts, 1969.
28. Ellert, F.J. and Merriam, C.W., III, "Synthesis of Feedback Controls Using Optimization Theory - An Example", IEEE Trans. Auto. Control, Vol. AC-8, No. 2, April 1963.
29. DeRusso, P.M., Roy, R.J. and Close, C.M., "State Variables for Engineers", John Wiley and Sons, Inc., New York, 1965.
30. Aström, K.J., "Introduction to Stochastic Control Theory", Academic Press, New York, 1970.
31. Muller, J.F., "Stability-Augmentation System Gain Determination by Digital Computer", J. Aircraft, Vol. 4, No. 5, September-October 1967.
32. Kai, Tadao, "Optimal Control Theory Applied to Helicopter in Hover", Princeton University Thesis (M.S.E.) No. 1242-T, AMS Department, July 1975.
33. Born, Gerard and Kai, Tadao, "Linear Optimal Control Applied to a Helicopter in the Hover and Approach Phase", Princeton University Report No. 1205, Princeton, N.J., January 1975.
34. Berman, N. and Born, Gerard, "A Review of Model Following", Princeton University, Instrumentation and Control Laboratory (to be published).
35. Wonham, W.M., "On Pole Assignment in Multi-Input Controllable Linear Systems", IEEE Trans. Auto. Control, Vol. AC-12, No. 6, December 1967.
36. Kreindler, E. and Jameson, A., "Optimality of Linear Control Systems", IEEE Trans. Auto. Control, Vol. AC-17, No. 3, June 1972.
37. Yokoyama, R. and Kinnen, E., "The Inverse Problem of the Optimal Regulator", IEEE Trans. Auto. Control, Vol. AC-17, No. 4, August 1972.
38. Born, G.J. and Kawahata, N., "Control System Design with Optimal Weighting Matrices (OWEM)", Princeton University Report No. 1145, January, 1974.
39. Wonham, W.M., "On the Separation Theorem of Stochastic Control", SIAM J. Control, Vol. 6, No. 2, 1968.

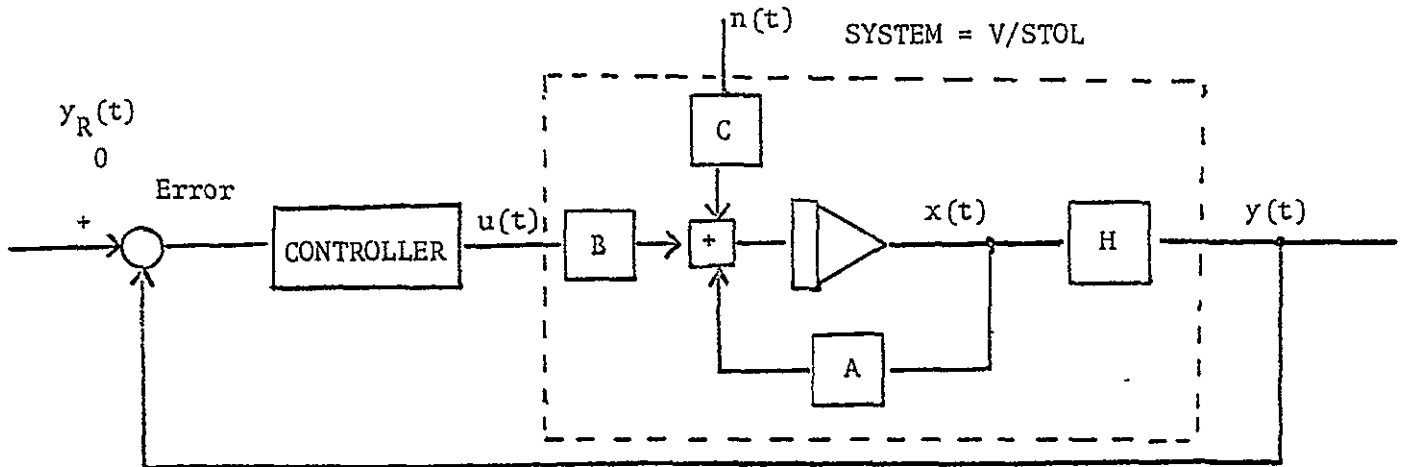


Figure 1. Block Diagram for Decoupling

System dynamics: $\dot{x}(t) = Ax(t) + Bu(t) + Cn(t)$

$y(t) = Hx(t)$

where $x(t)$: n dimensional state vector

$u(t)$: m dimensional control vector ($m \leq n$)

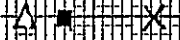
$y(t)$: p dimensional output vector ($p \leq n$)

$n(t)$: l dimensional noise vector ($l \leq n$)

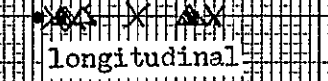
Basic	Decoupled	Uncoupled	$j\omega$
$.136+j.323$	$.130+j.356$	$.131+j.356$	1.0
$-.377$	$-.544$	$-.537$	lateral
$-.219$	$-.269$	$-.269$	
$-.084+j.676$	$.150+j.681$	$.141+j.648$	longitudinal
-1.26	-1.54	-1.46	
$-.557$	$-.496$	$-.591$	

X basic
 Δ decoupled
 ■ uncoupled

lateral

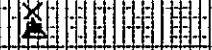


yawing vertical




longitudinal

longitudinal



lateral



-.8

Fig. 2 Roots configuration for basic, decoupled and uncoupled Helicopter dynamics

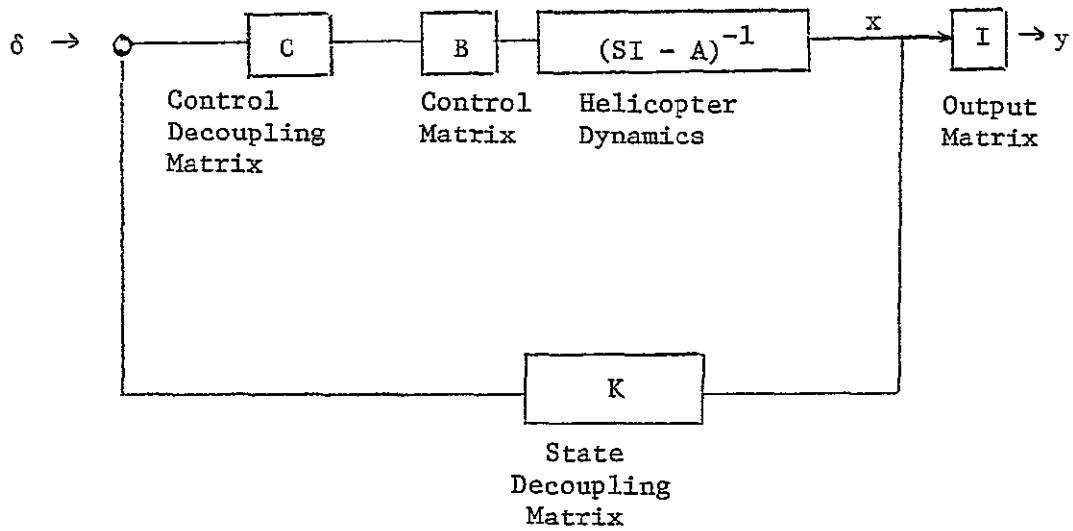


Figure 3. General Construction
for Decoupling Helicopter Dynamics

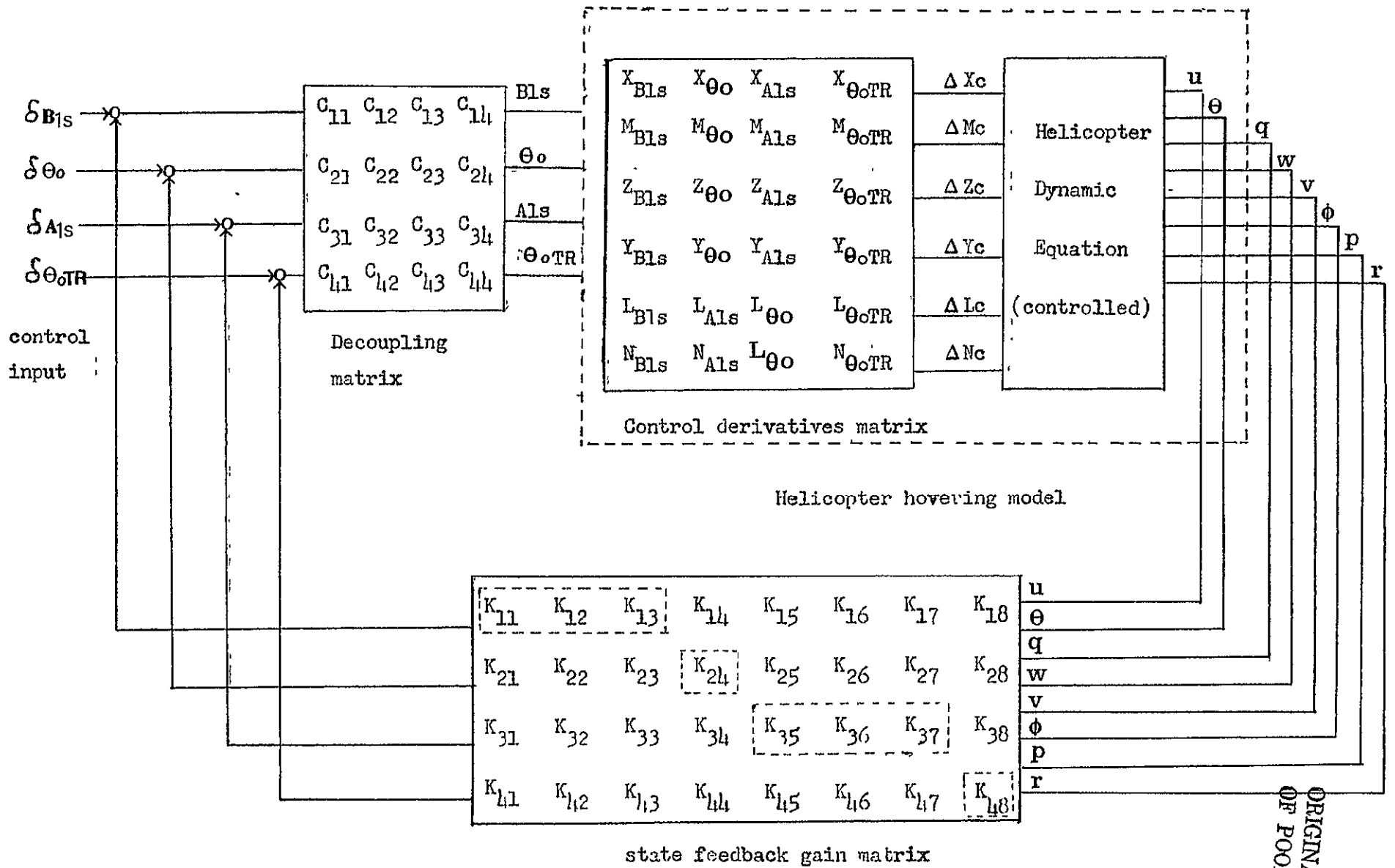


Fig. 4 Construction for decoupling helicopter dynamics

ORIGINAL PAGE IS OF POOR QUALITY

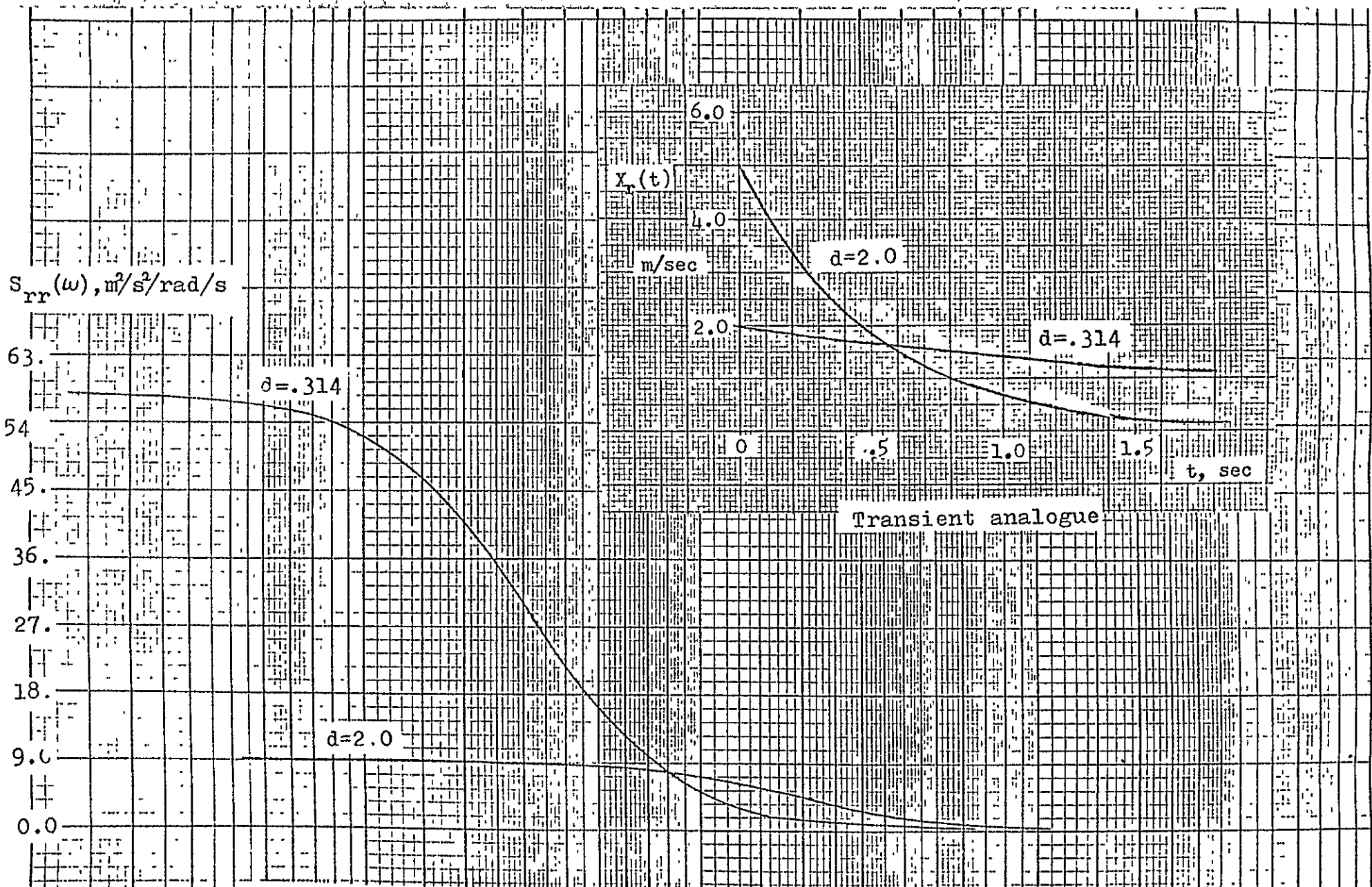


Fig. 5 Power spectrum density and transient analogue of assumed gust model with different bandwidths under constant intensity

69

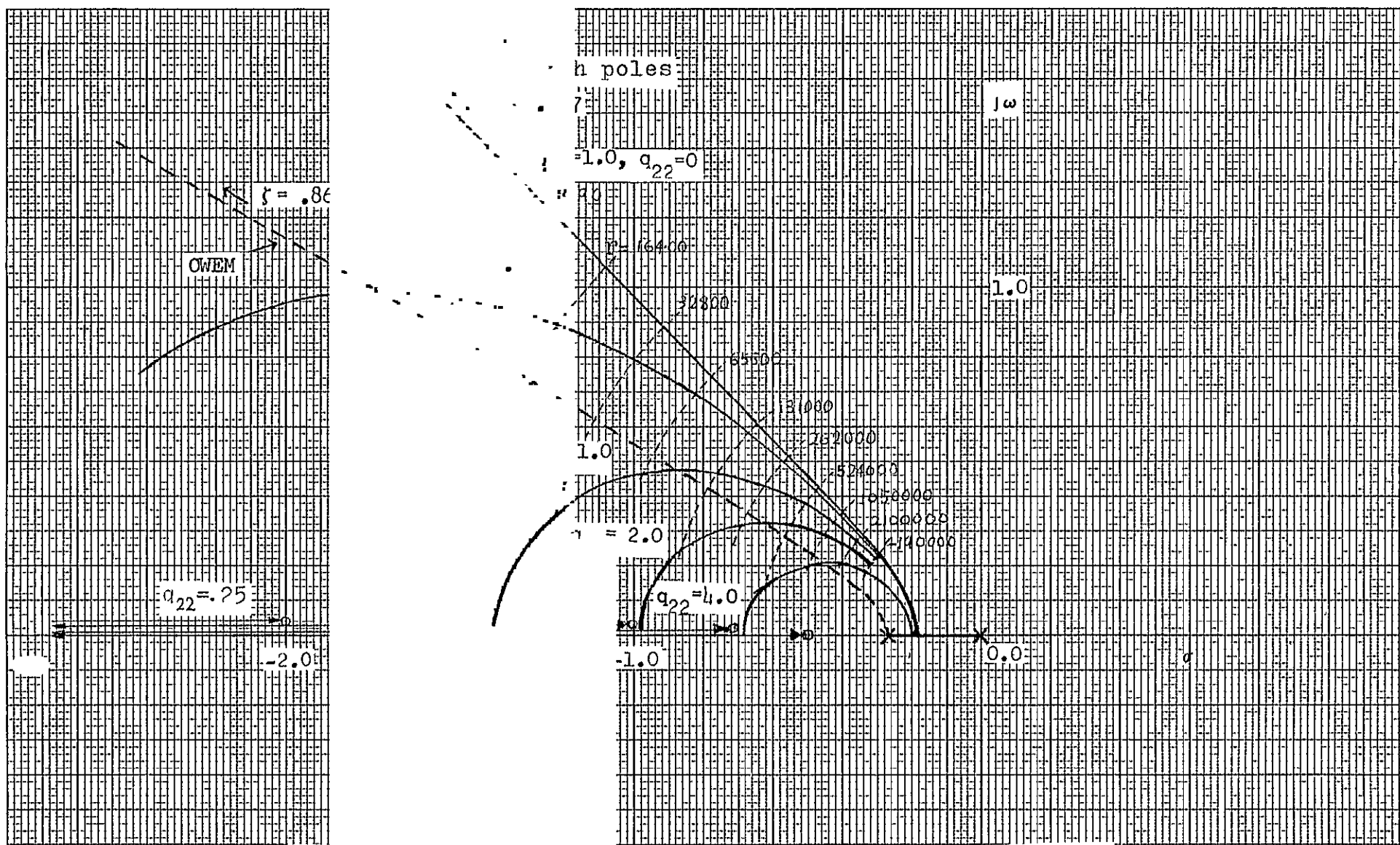


Fig. 6 Root square locus with varying r , some q_{22} 's, and $q_{11} = 1.0$ and by the OWEM method for vertical equation

70

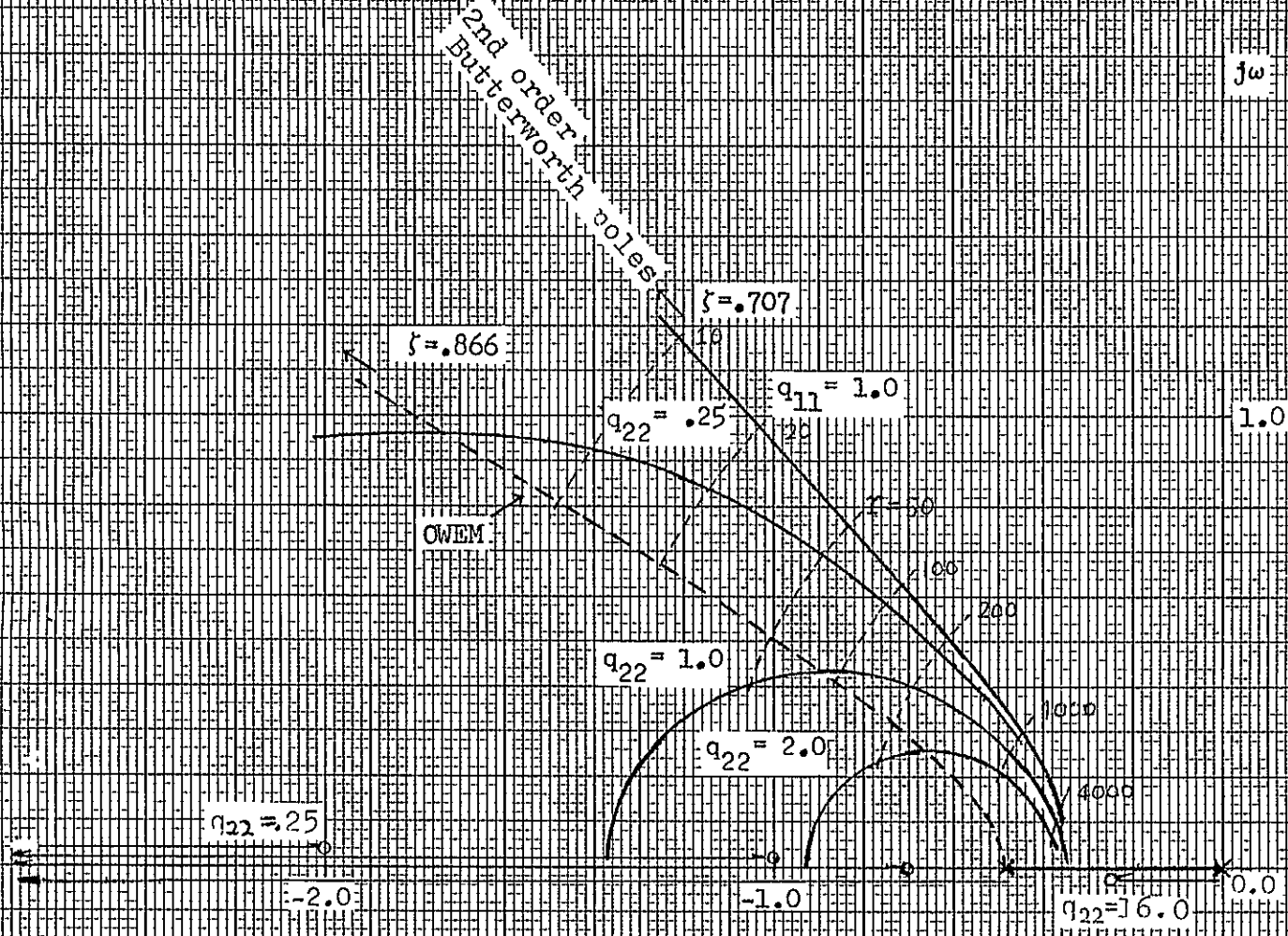


Fig. 7 Root square locus with varying r , some q_{22} 's, and $q_{11} = 1.0$ and by the OWEM method for yawing equation

ORIGINAL PAGE IS
 OF POOR QUALITY

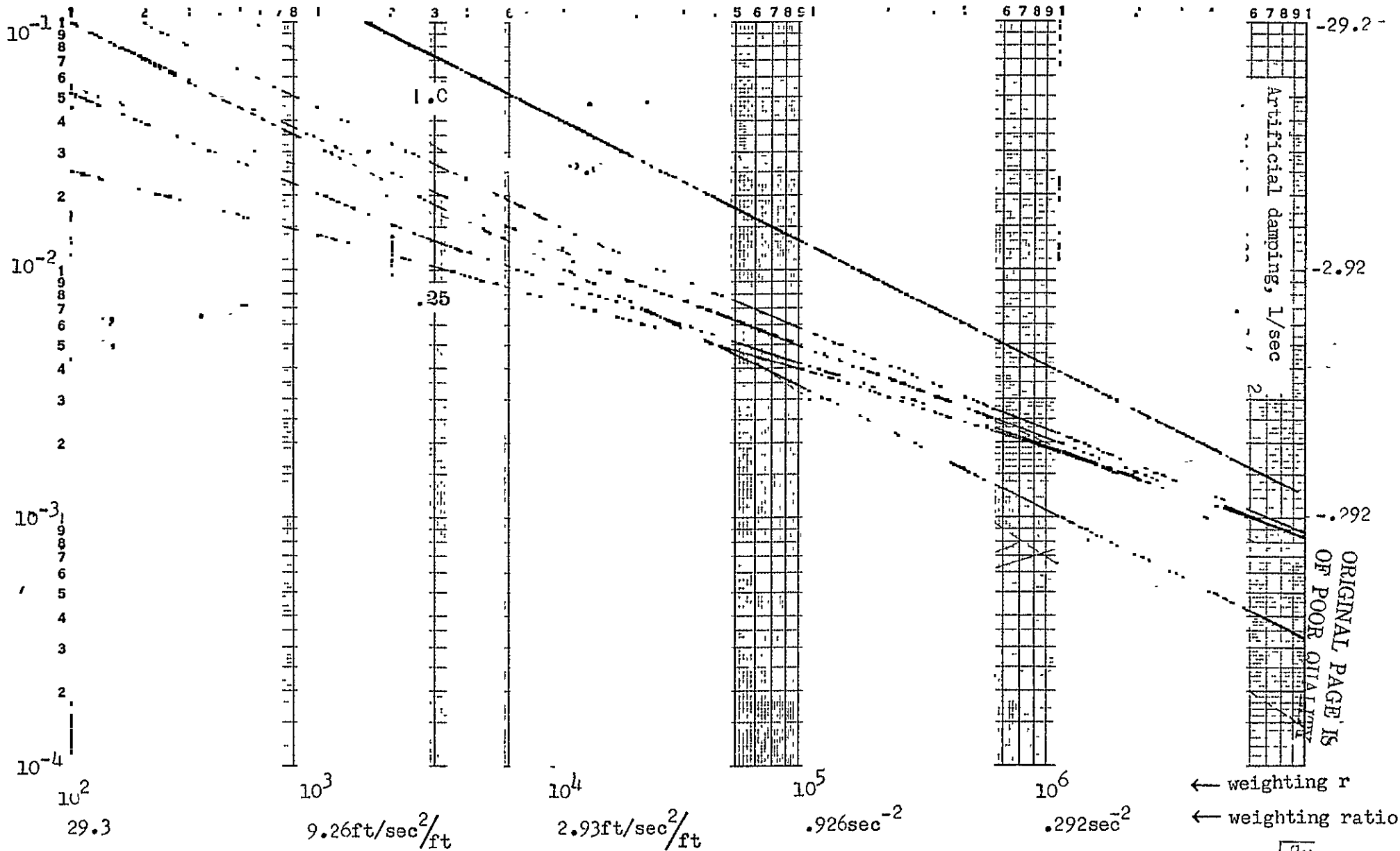


Fig. 8 Vertical optimal feedback gains

$$\sqrt{\frac{q_{11}}{r}}$$

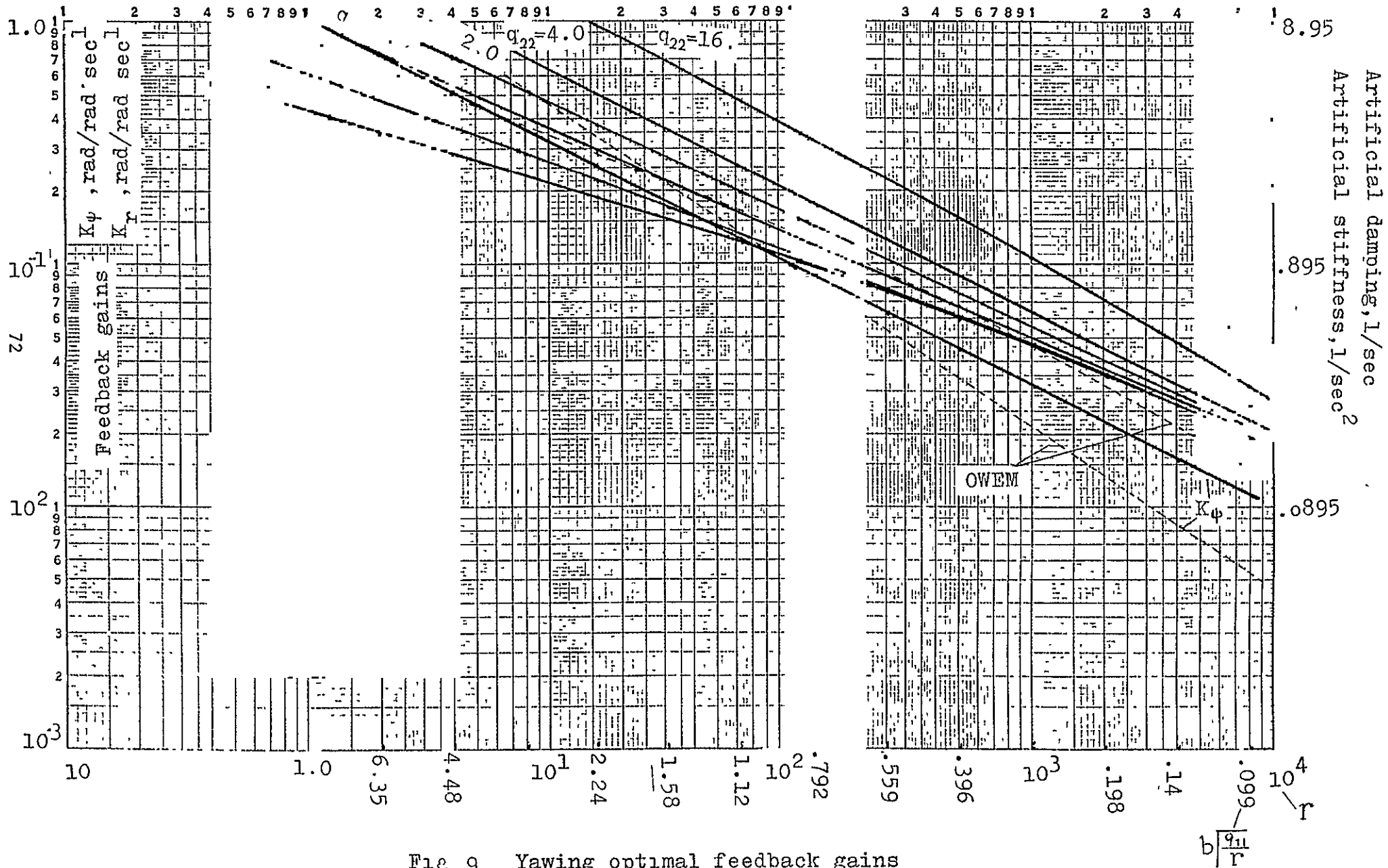


Fig 9 Yawing optimal feedback gains

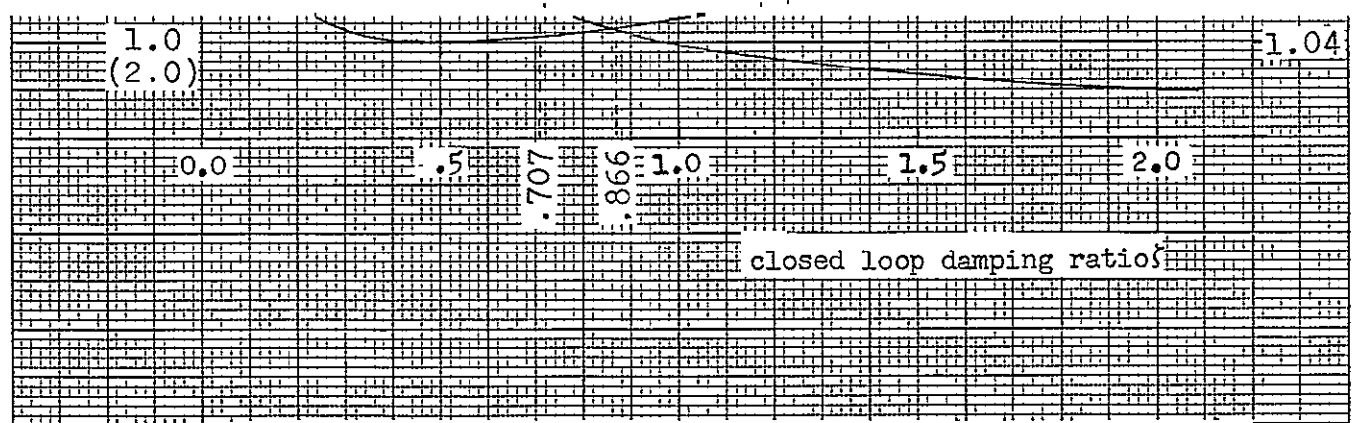
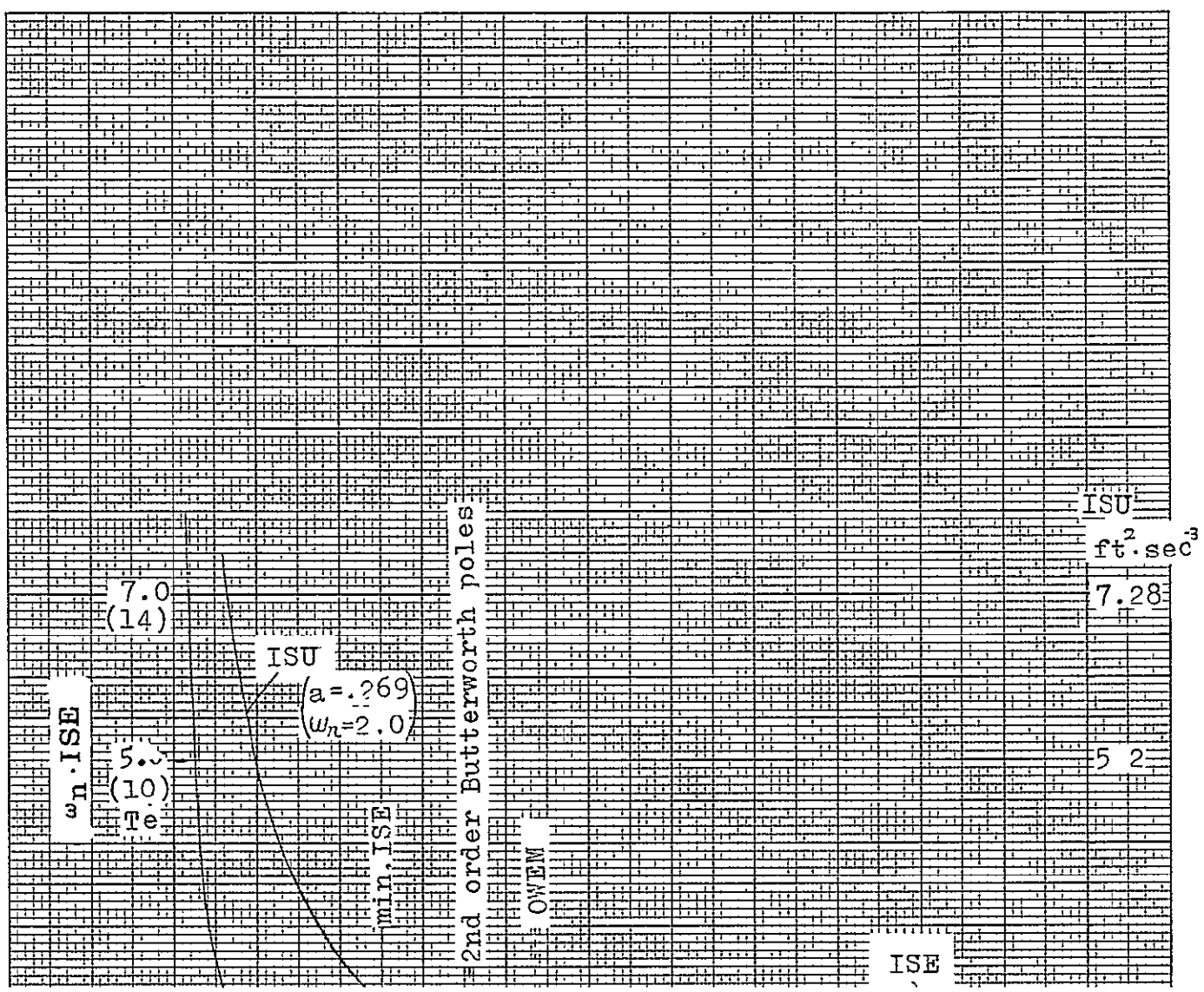
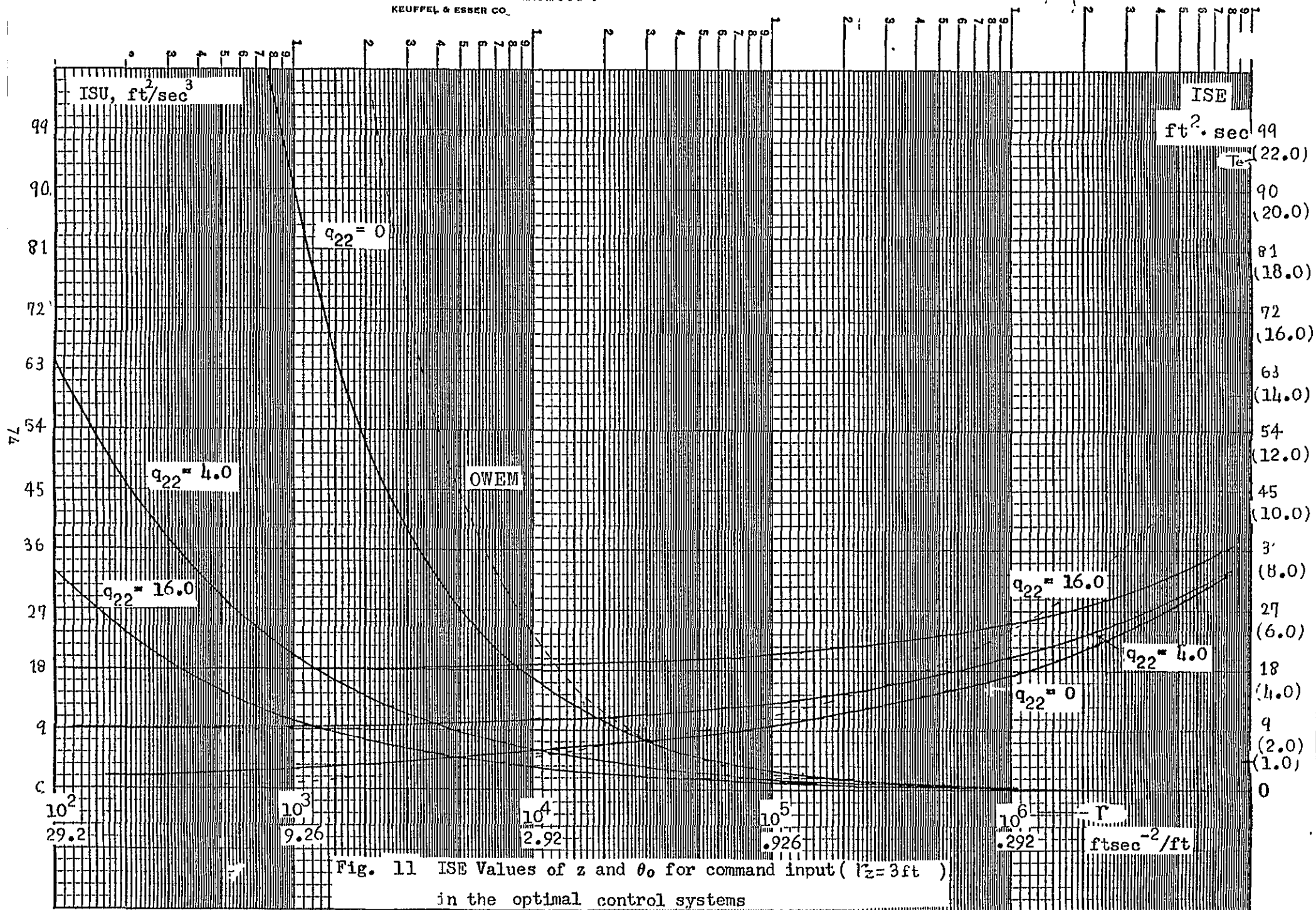


Fig. 10 ISE of Second order rate constant system vs the closed loop system damping ratio ζ , undamped natural frequency ω_n



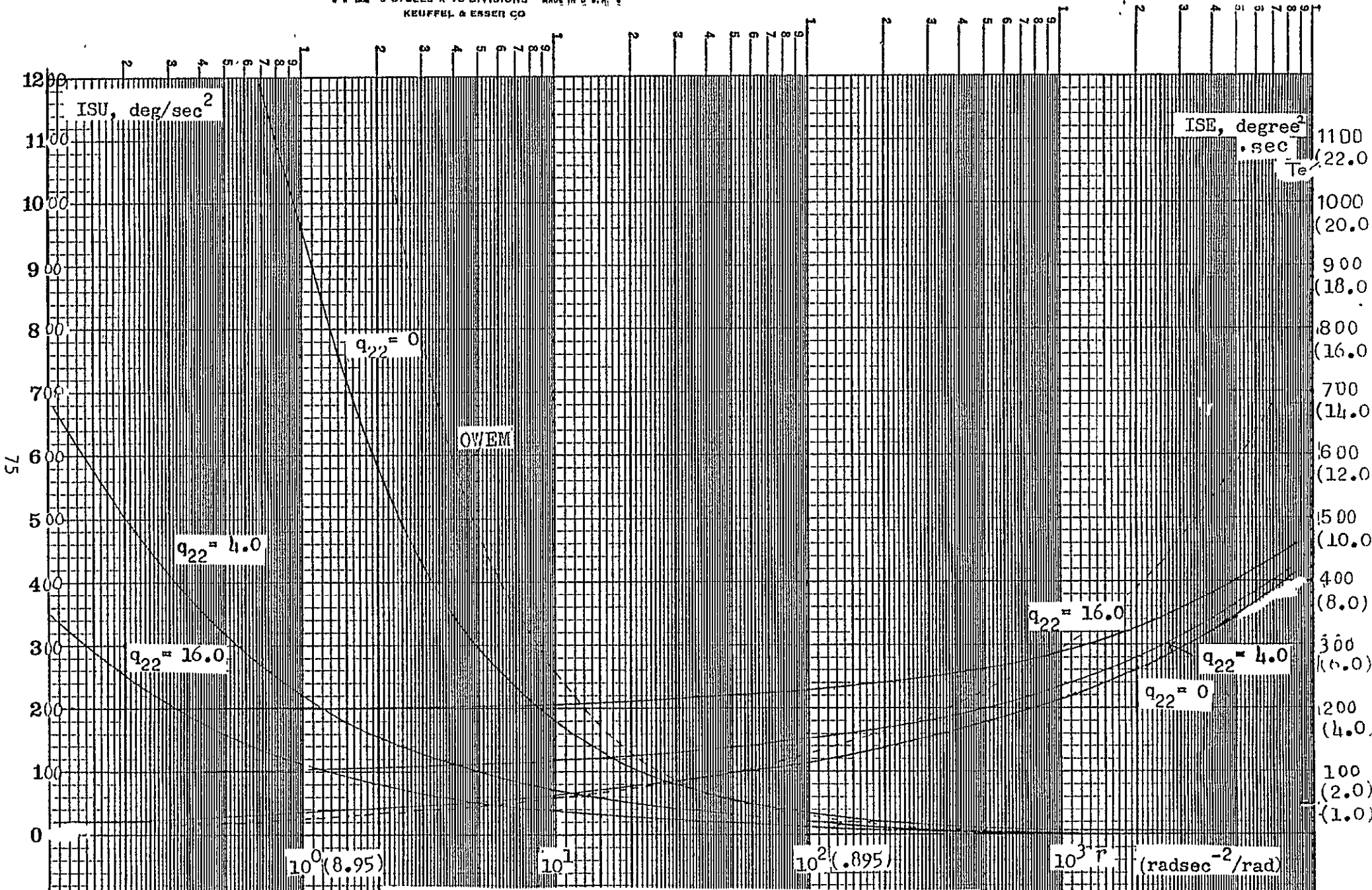


Fig. 12 ISE Values of ψ and θ_{OTR} for command input ($\Gamma_{\psi}=10$ deg.)
 in the optimal yawing control system

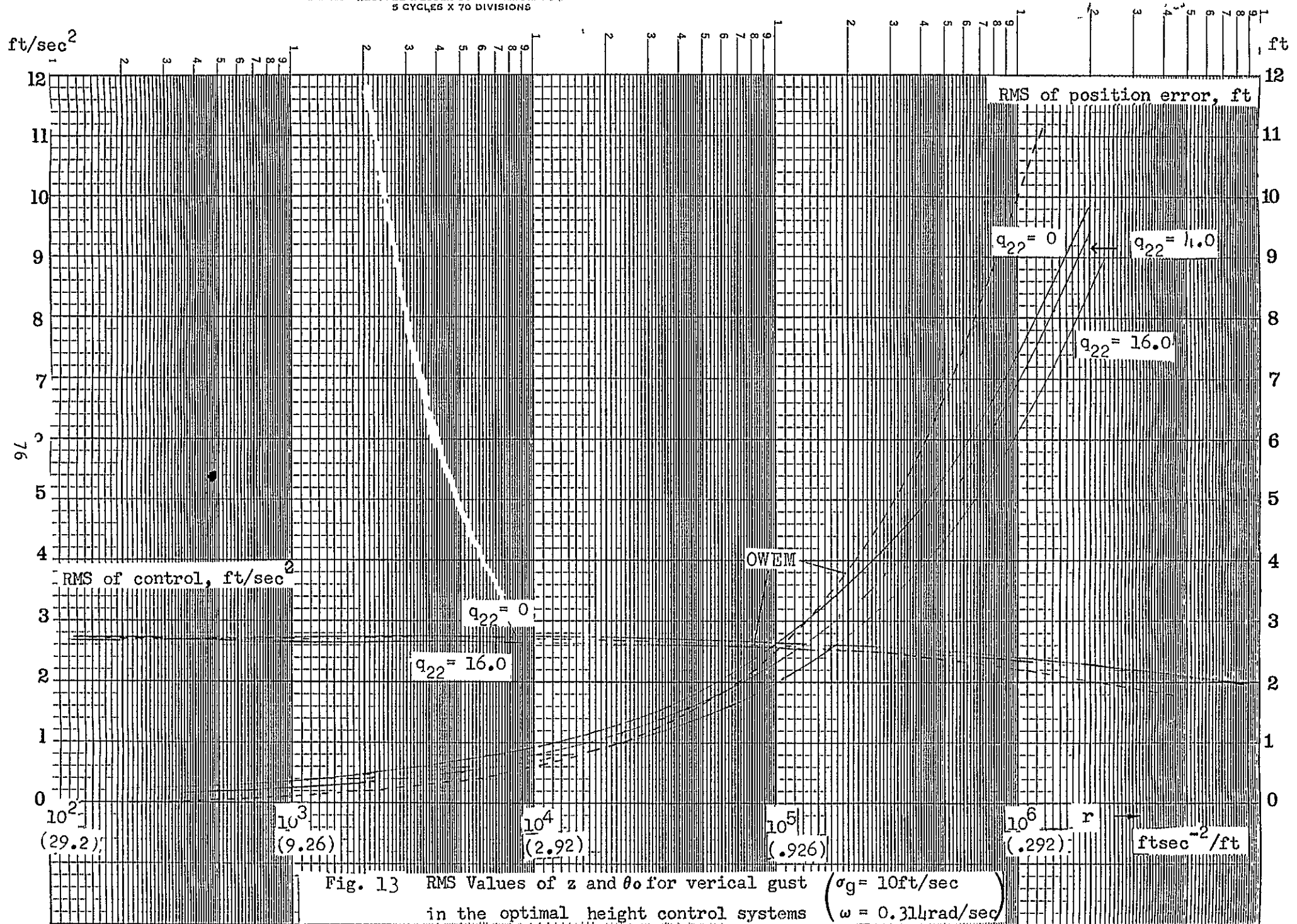


Fig. 13 RMS Values of z and θ for vertical gust ($\sigma_g = 10\text{ft/sec}$)
 in the optimal height control systems ($\omega = 0.314\text{rad/sec}$)

0-2

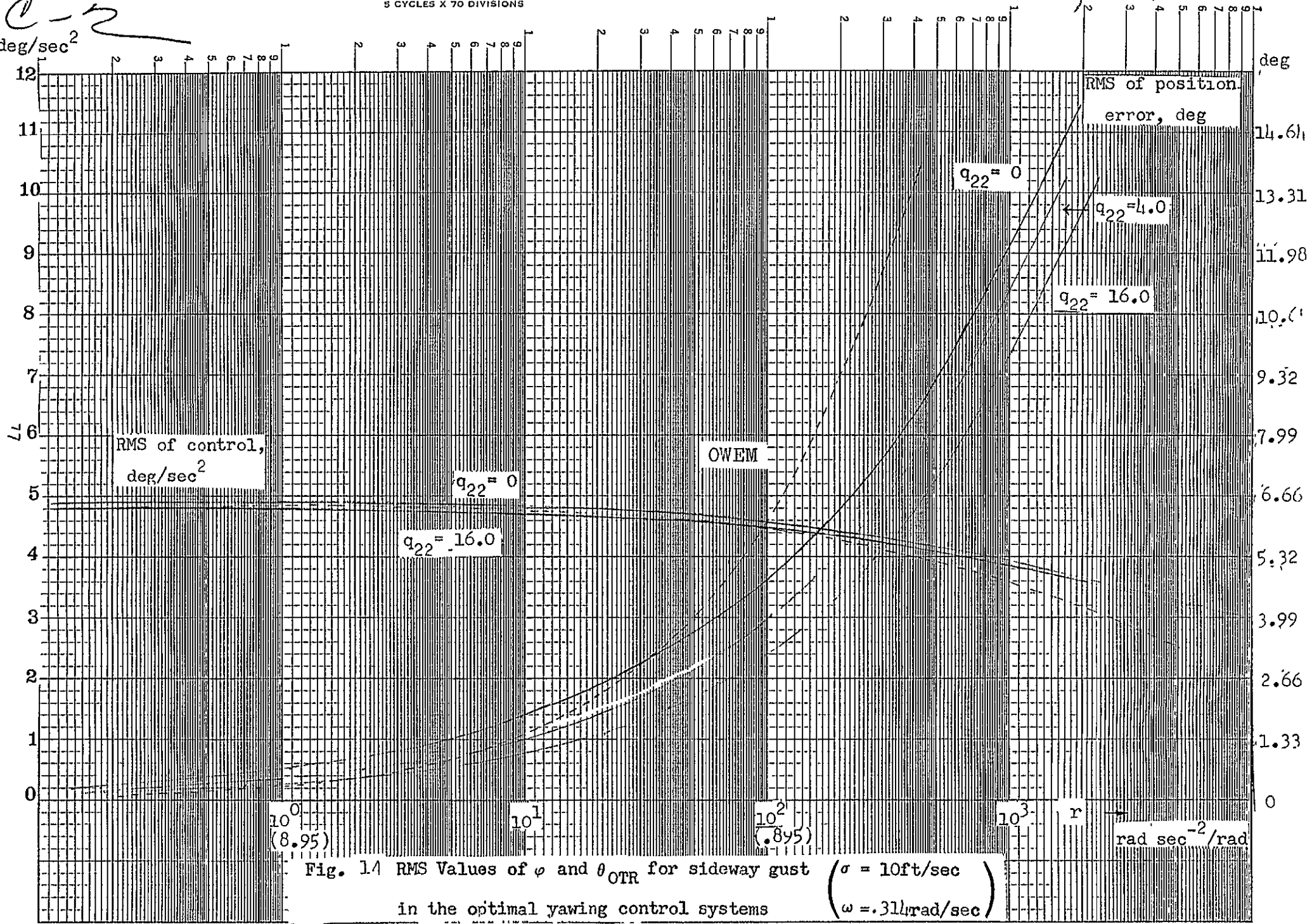


Fig. 1.4 RMS Values of φ and θ_{OTR} for sideway gust ($\sigma = 10\text{ft/sec}$)
 in the optimal yawing control systems ($\omega = .311\text{rad/sec}$)

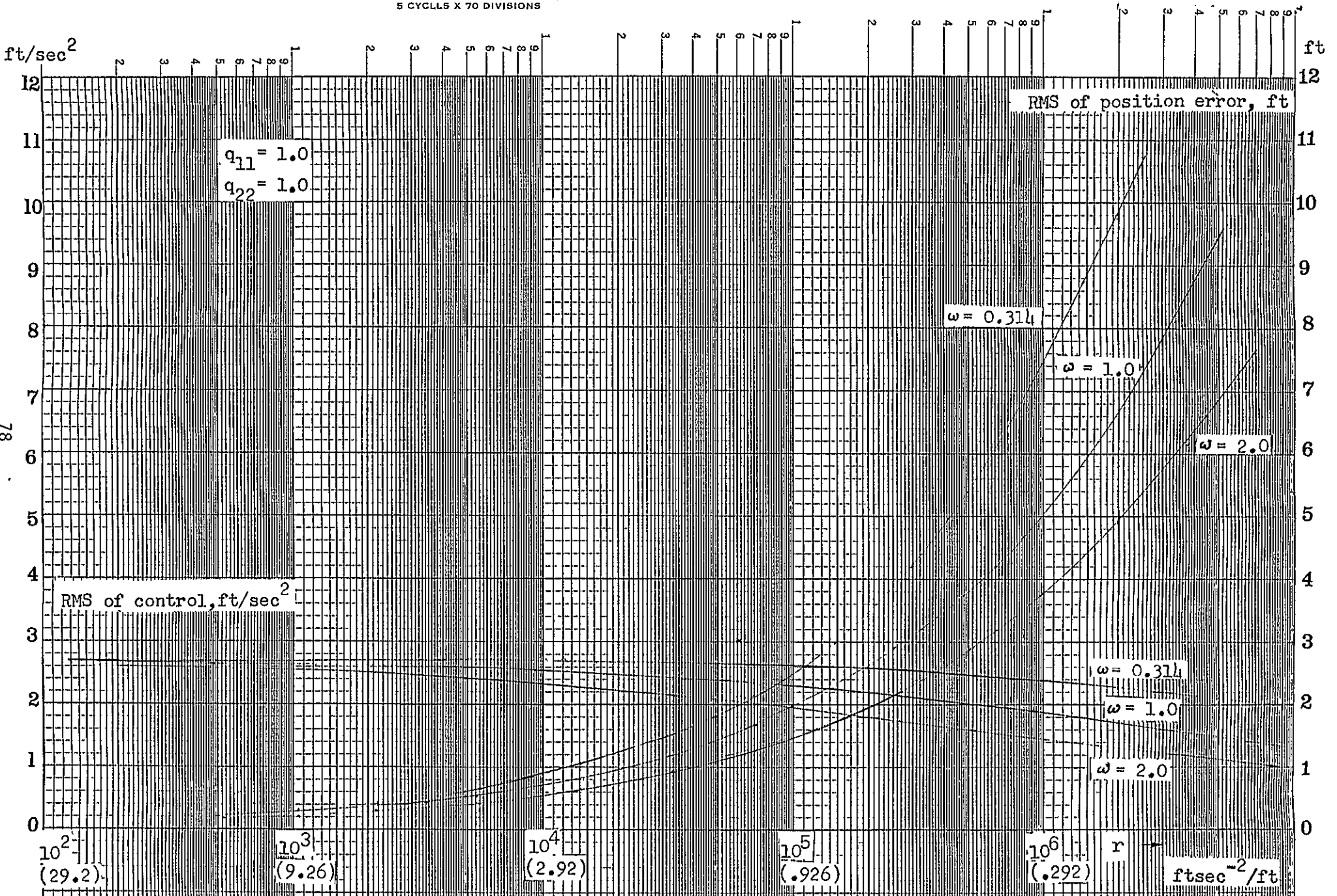


Fig. 15 RMS Values of Z and θ_0 for different vertical gust break frequencies in the optimal height control systems. ($\sigma = 10\text{ft}/\text{sec}$)

78

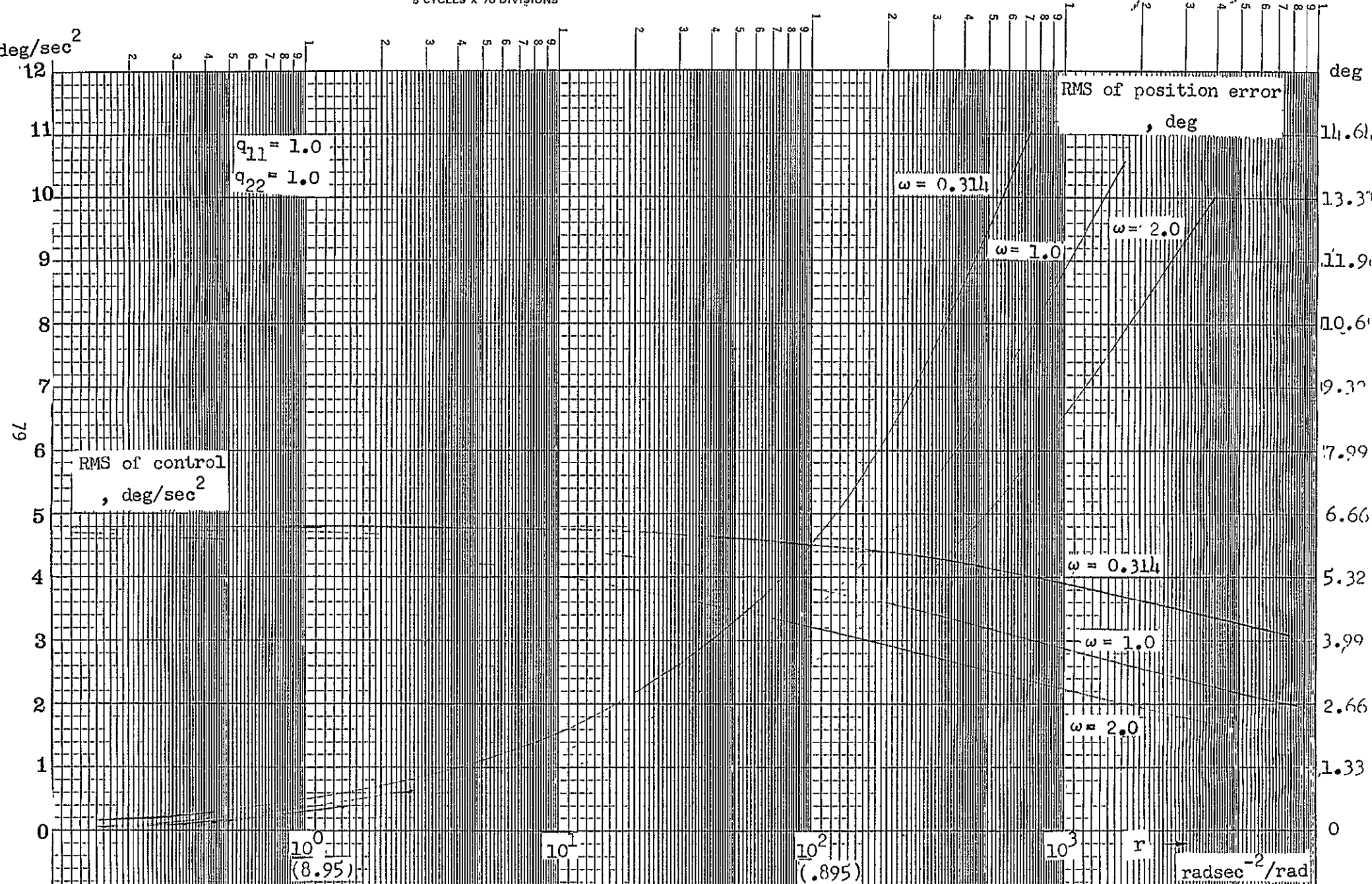


Fig. 16 RMS Values of ϕ and θ_{OTR} for different sideways gust break frequencies
 in the optimal yawing control systems ($\sigma = 10\text{ft/sec}$)

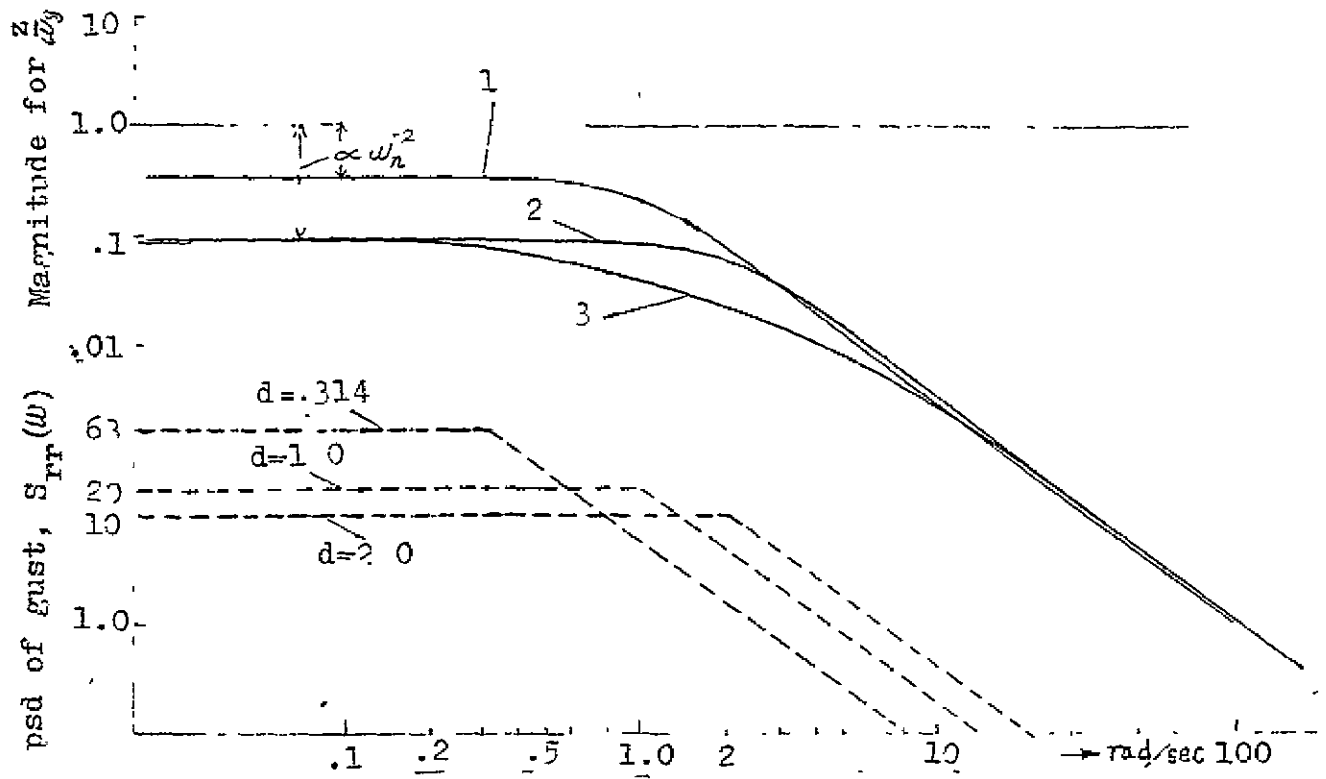


Fig. 17a Frequency response of $w_g \rightarrow z$ transfer function

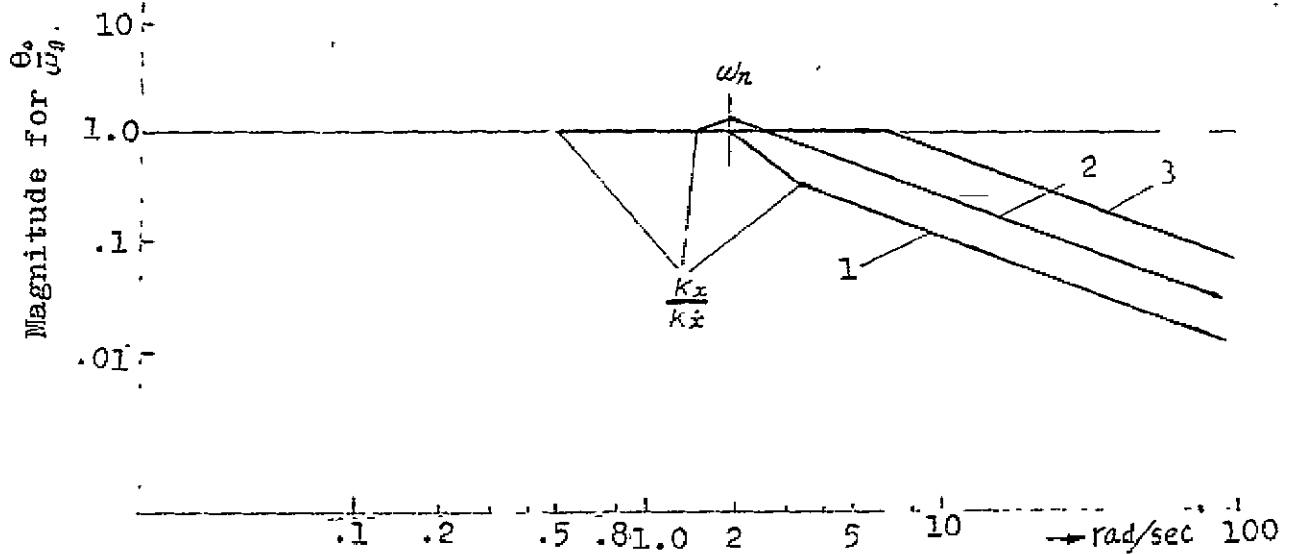


Fig. 17b Frequency response of $w_g \rightarrow \theta_0$ transfer function (straight line approximation)

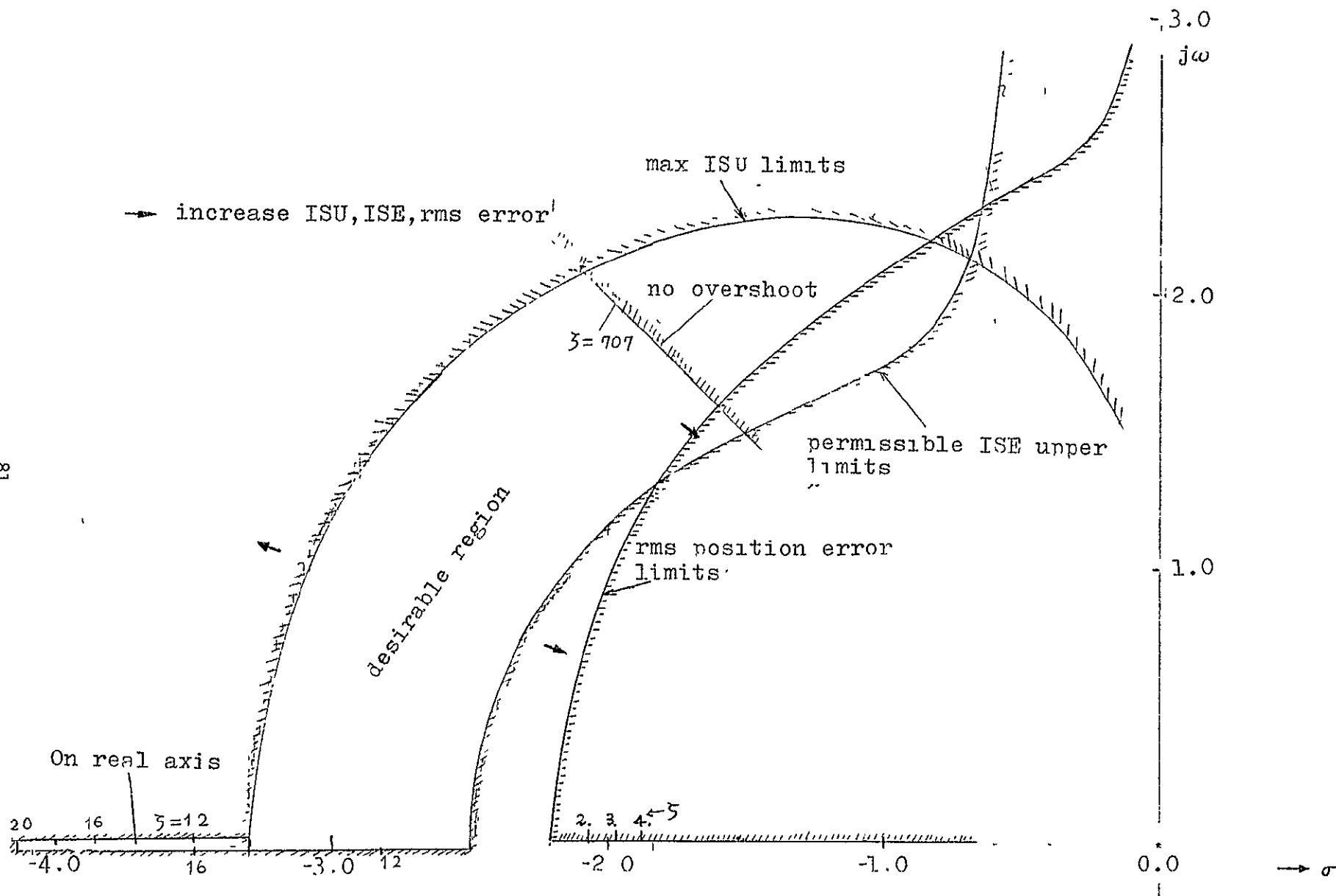


Fig. 18 Desirable roots location for the second order system to satisfy no overshoot, ISE, ISU and rms gust response requirements

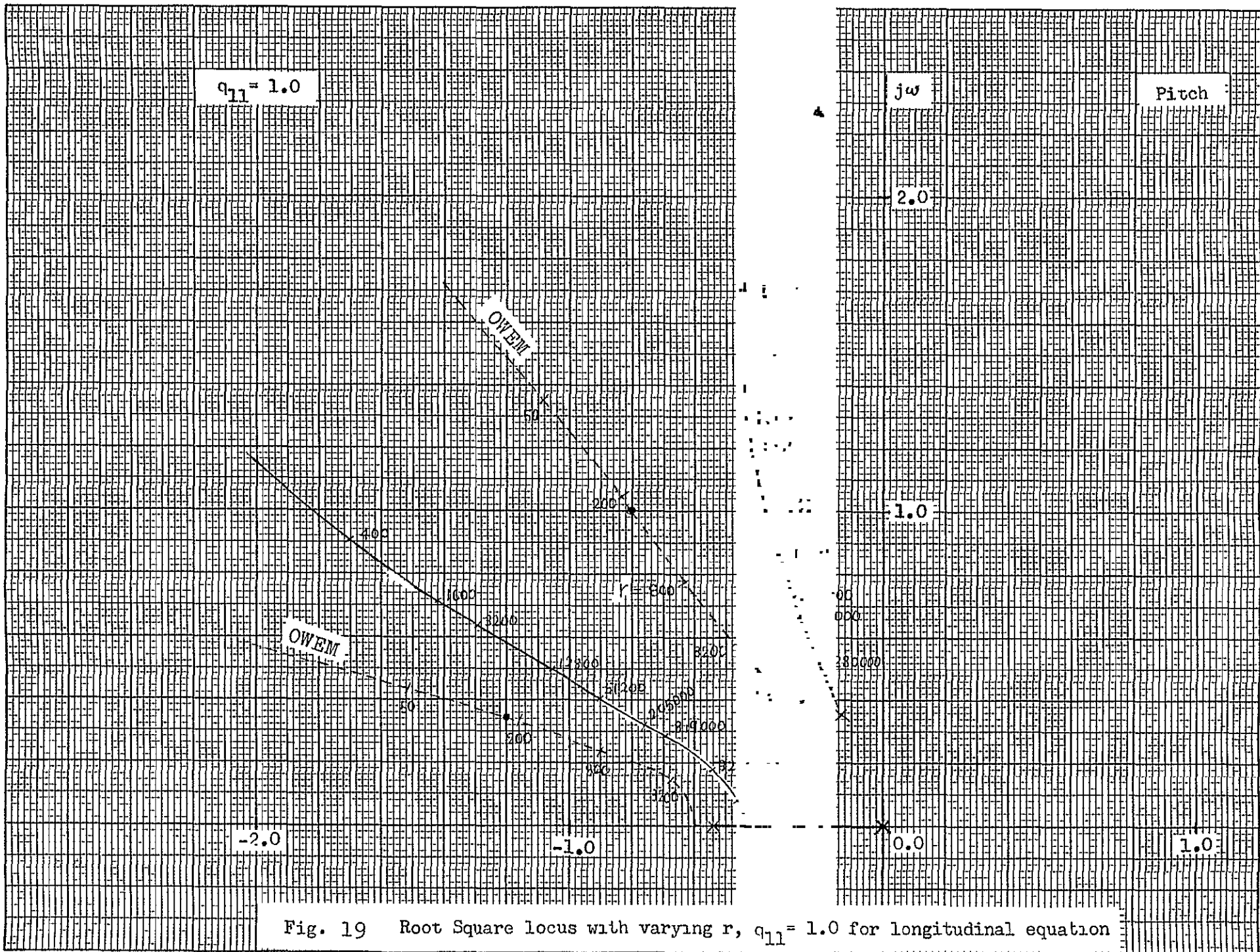


Fig. 19 Root Square locus with varying r , $q_{11} = 1.0$ for longitudinal equation

(2) $q_{11} = 1.0$
 $q_{33} = 820$

(3) Find the case No. of Table 3-2

$j\omega$

Pitch

2.0

1.0

0.0

1.0

200

(5)

(3)

(4)

-2.0

-1.0

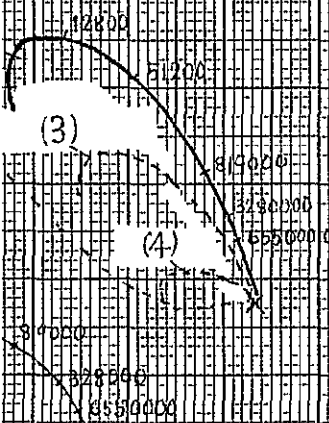


Fig. 20 Root Square locus with varying r , $q_{11} = 1.0$, $q_{33} = 820$ for longitudinal equation

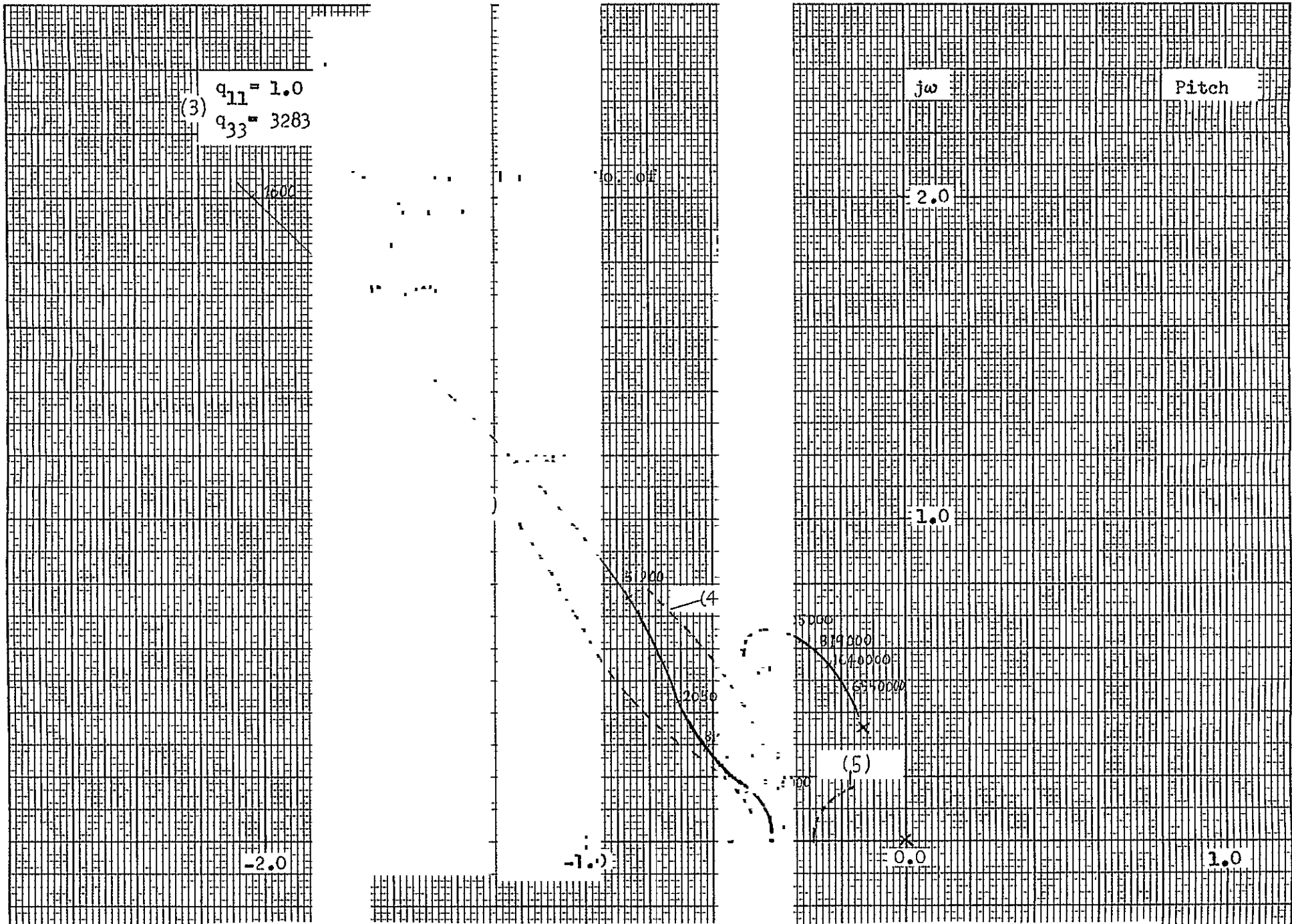


Fig. 21 Root square locus with varying r , $q_{11}=1.0$, $q_{33}=3283$ for longitudinal equation

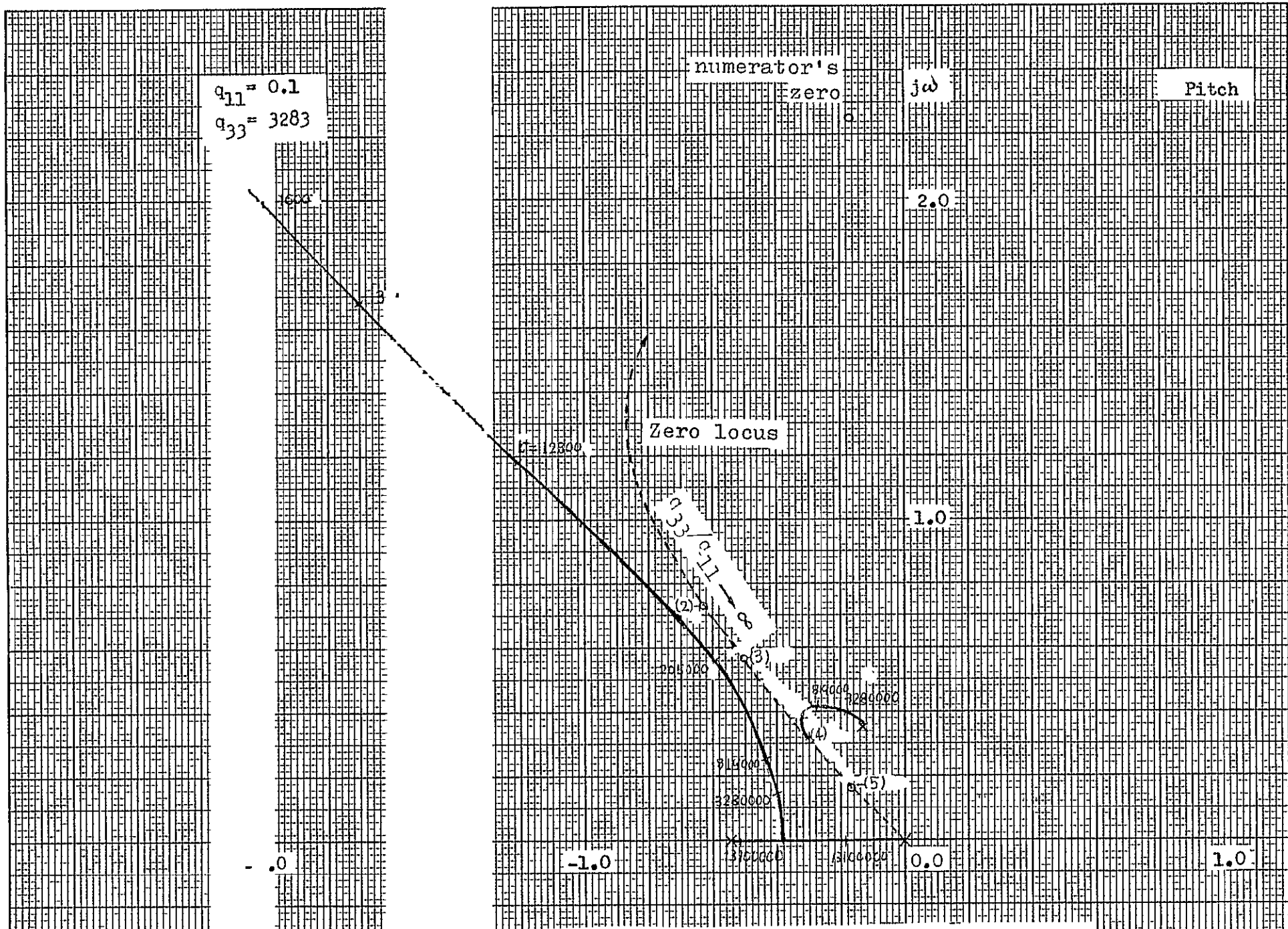
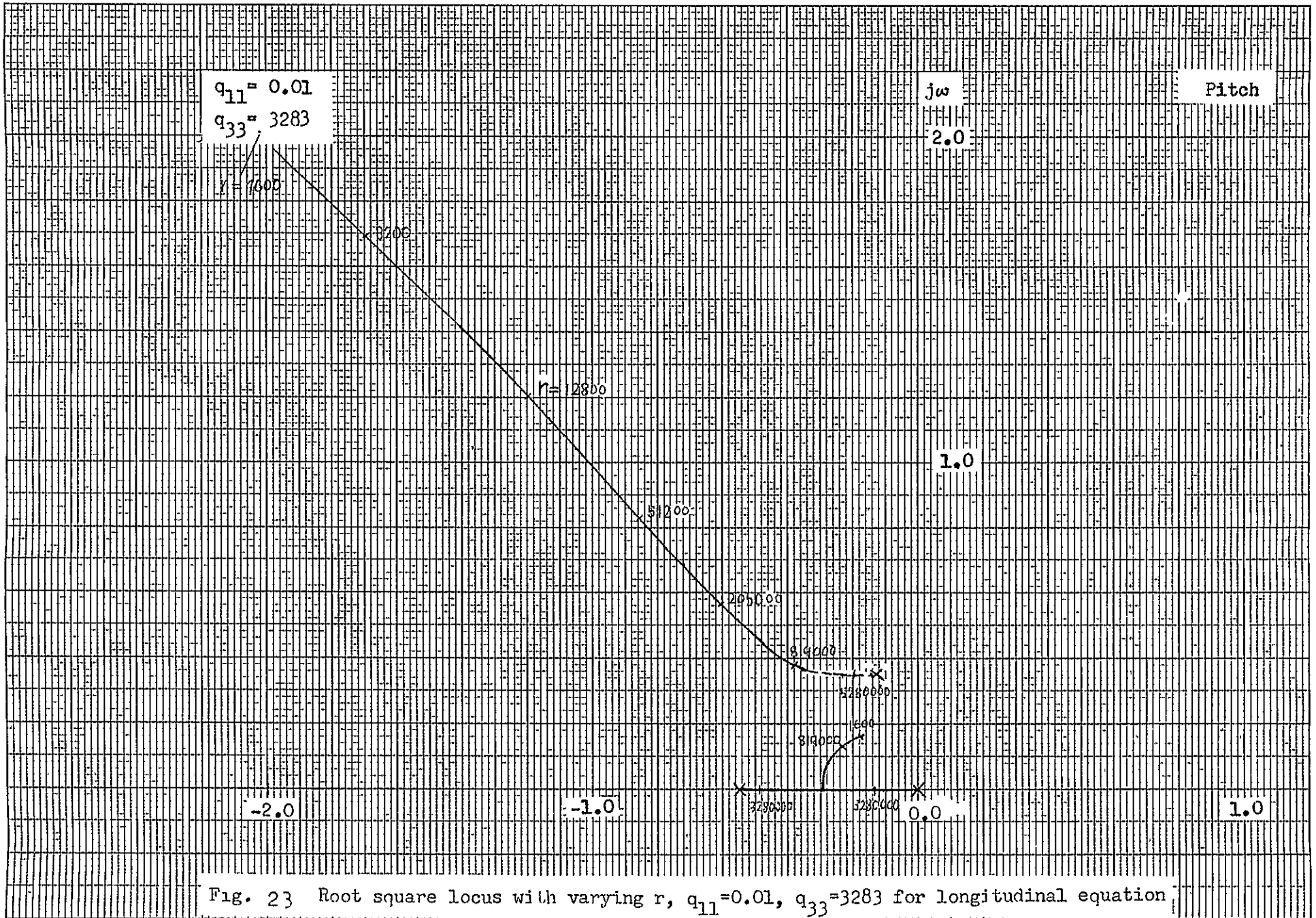


Fig. 22 Root square locus with varying r , $q_{11}=0.1$, $q_{33}=3283$ for longitudinal equation



$q_{11} = 1.0$
 $q_{33} = 3280$
 $q_{44} = 3280$

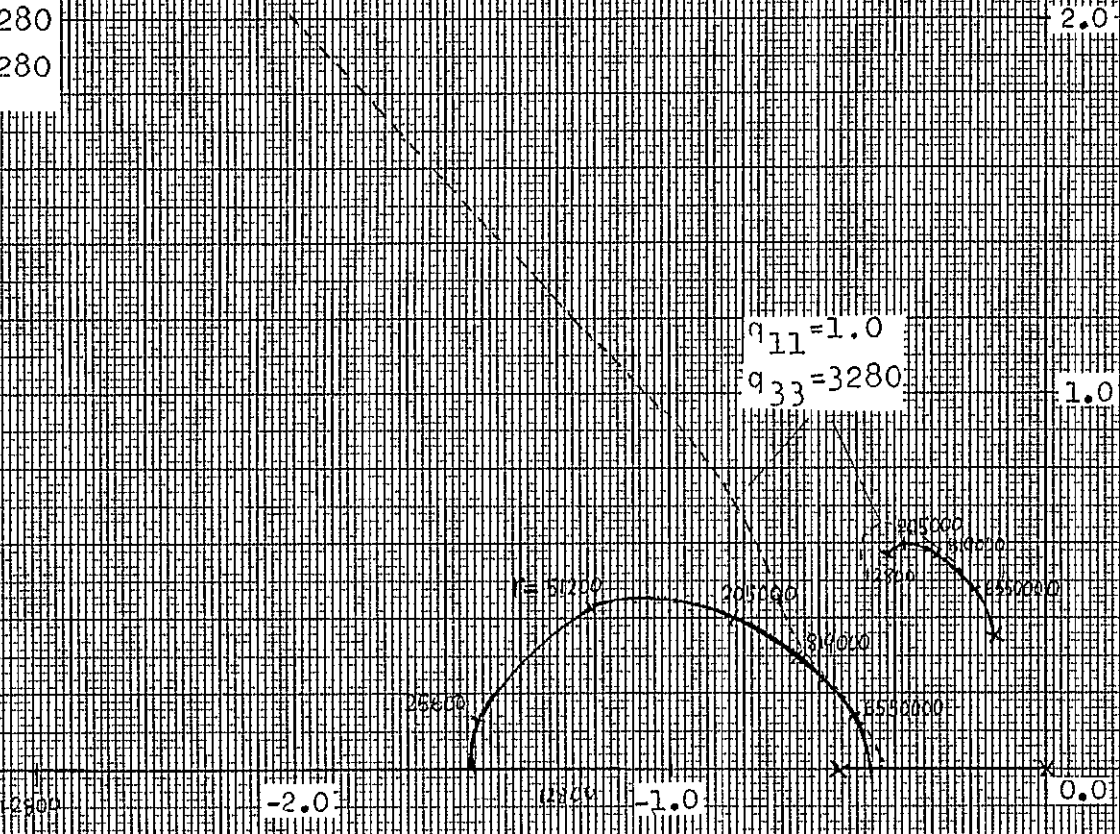


Fig. 24 Root square locus with varying r , $q_{11} = 1.0$, $q_{33} = q_{44} = 3280$ for longitudinal equation

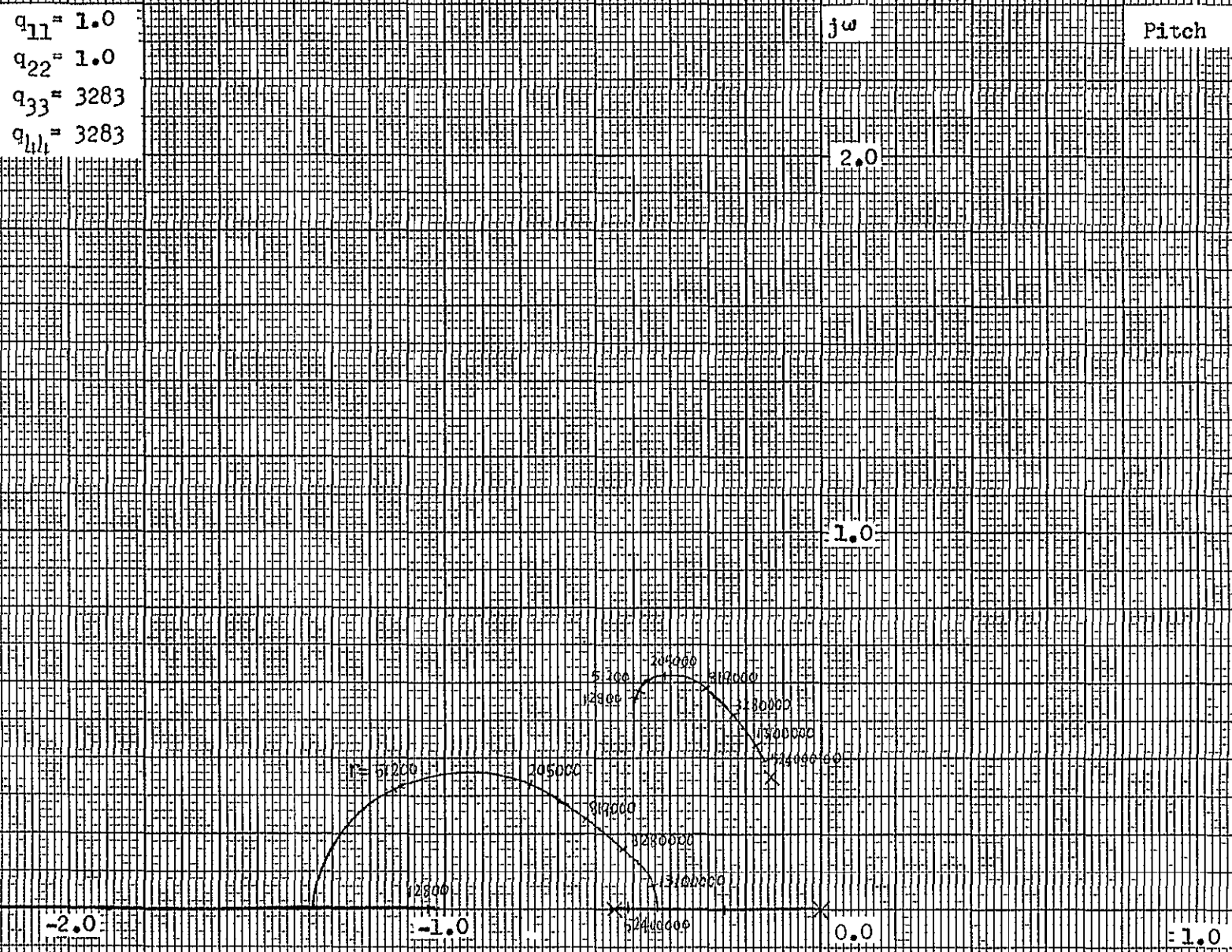


Fig. 25 Root square locus with varying r , $q_{11}=1.0$, $q_{22}=1.0$, $q_{33}=3283$, $q_{111}=3283$
 for longitudinal equation

ORIGINAL PAGE IS
 OF POOR QUALITY

89

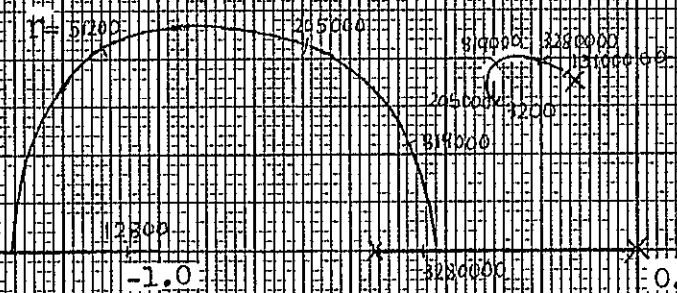
$q_{11} = 0.1$
 $q_{22} = 0.1$
 $q_{33} = 3283$
 $q_{44} = 3283$

$j\omega$

Pitch

2.0

1.0



ORIGINAL PAGE IS
 OF POOR QUALITY

Fig. 26 Root square locus with varying r , $q_{11} = q_{22} = 0.1$, $q_{33} = q_{44} = 3283$ for longitudinal equation

$q_{11} = 0.1$
 $q_{22} = 0.4$
 $q_{33} = 3283$
 $q_{44} = 13132$

$j\omega$ Pitch

2.0

1.0

-2.0

205000

-1.0

205000

0.0

1.0

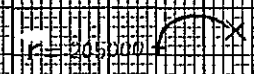


Fig. 27 Root square locus with varying r , $q_{11} = 0.1$, $q_{22} = 0.4$, $q_{33} = 3283$, $q_{44} = 13132$
 for longitudinal equation

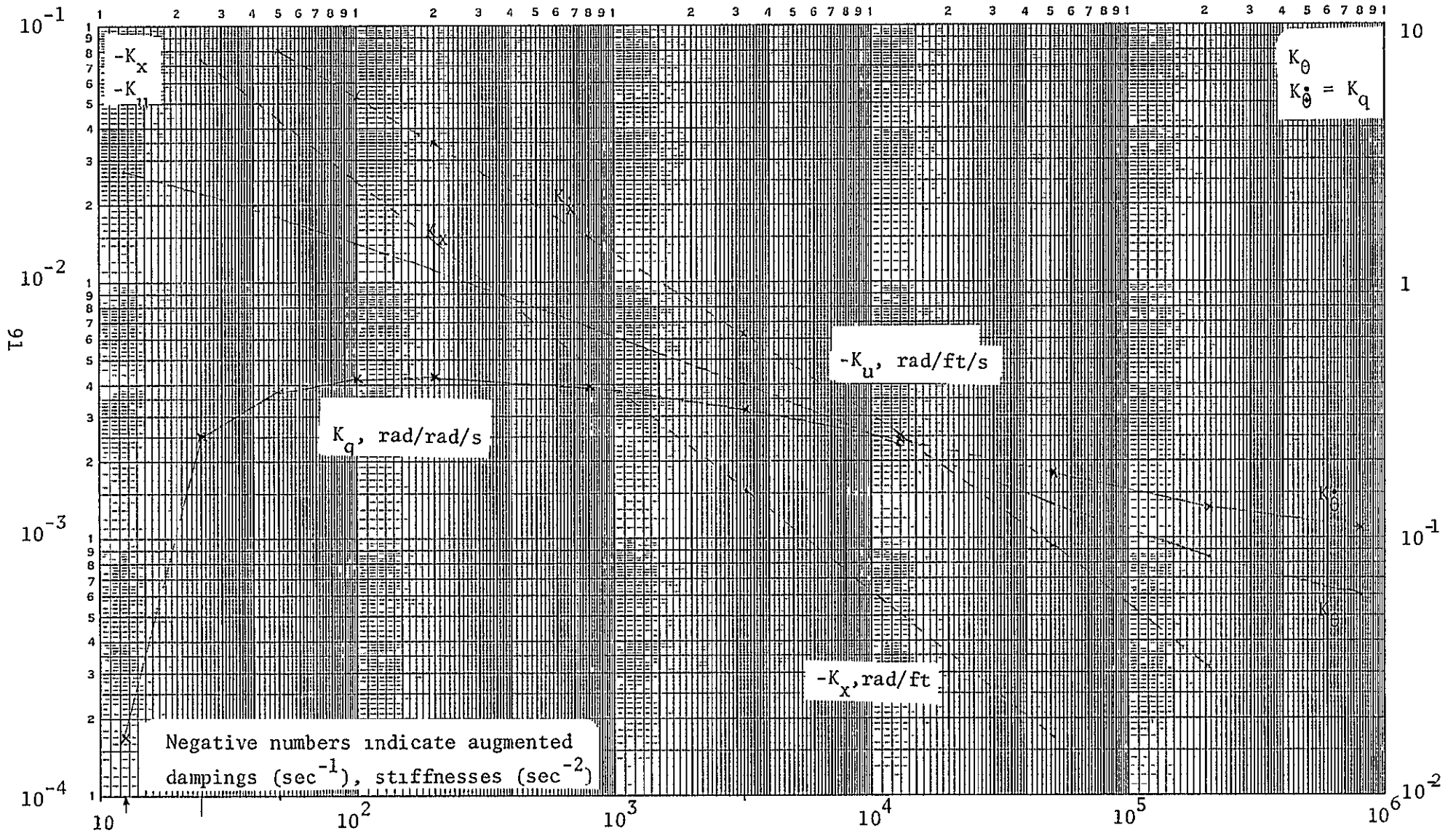


Fig. 28. Longitudinal optimal feedback gains for the OWEM method

→ R

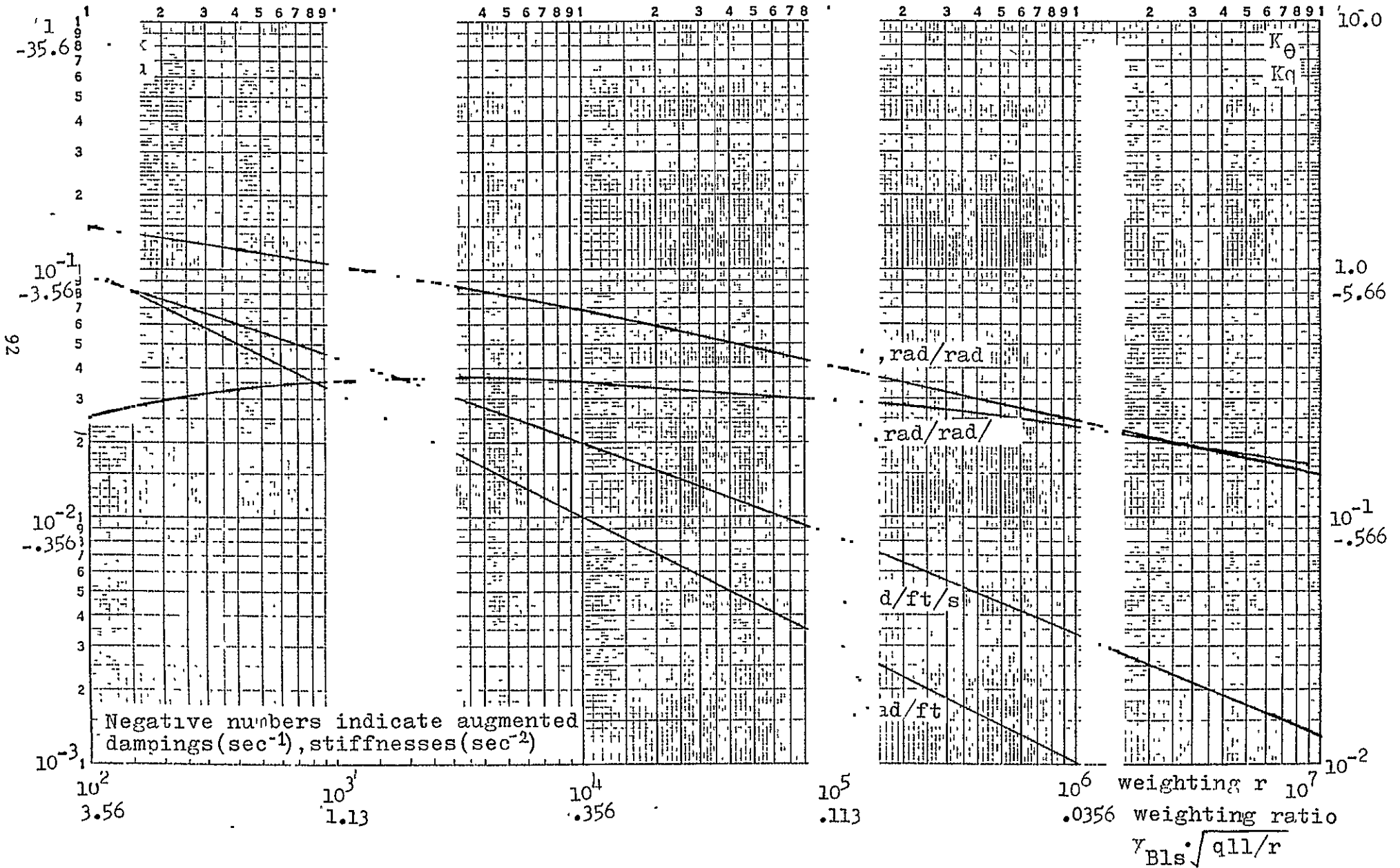


Fig. 29 Longitudinal optimal feedback gains for $q_{11} = 1.0$

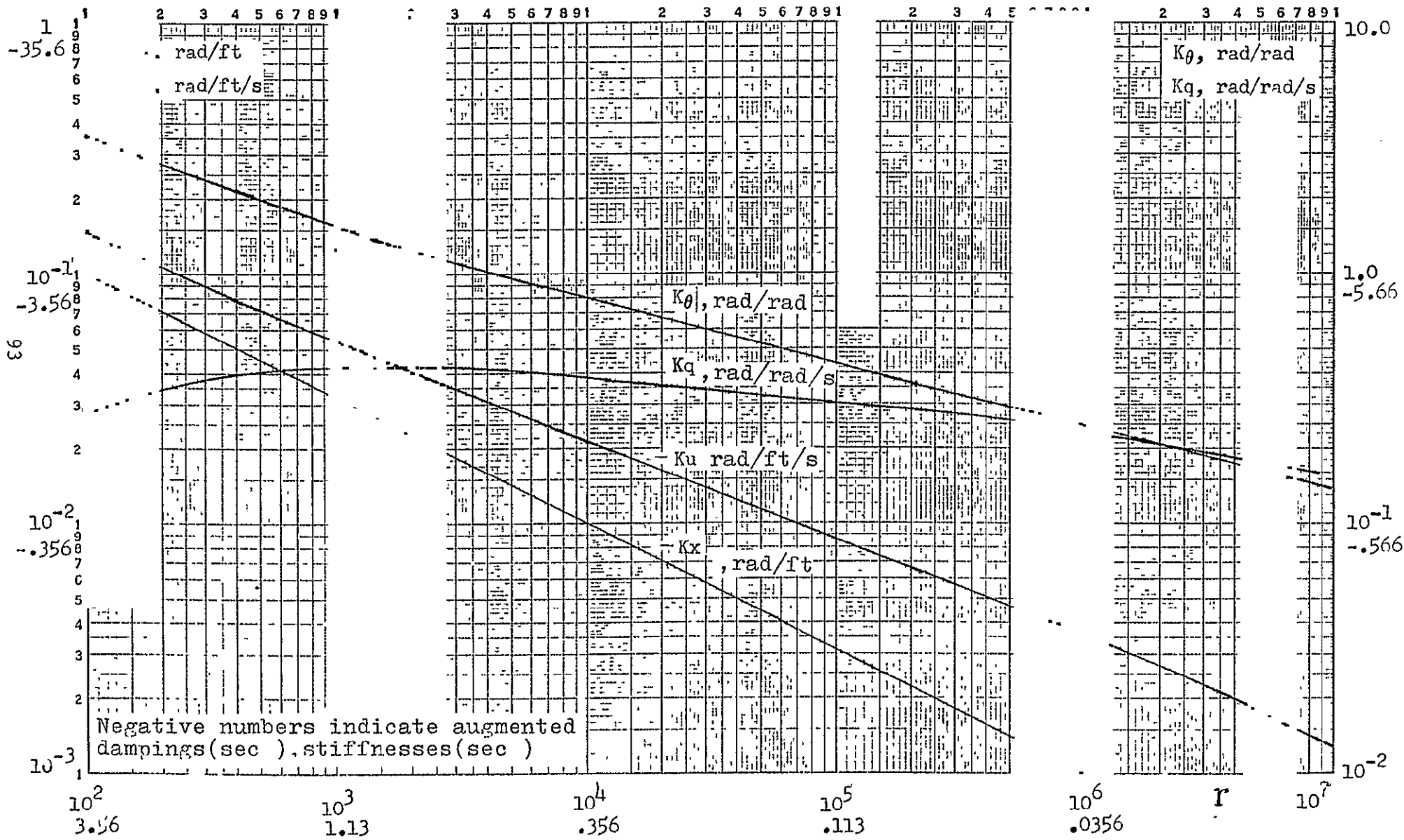


Fig. 30 Longitudinal optimal feedback gains for $q_{11} = 1.0$, $q_{33} = 820$

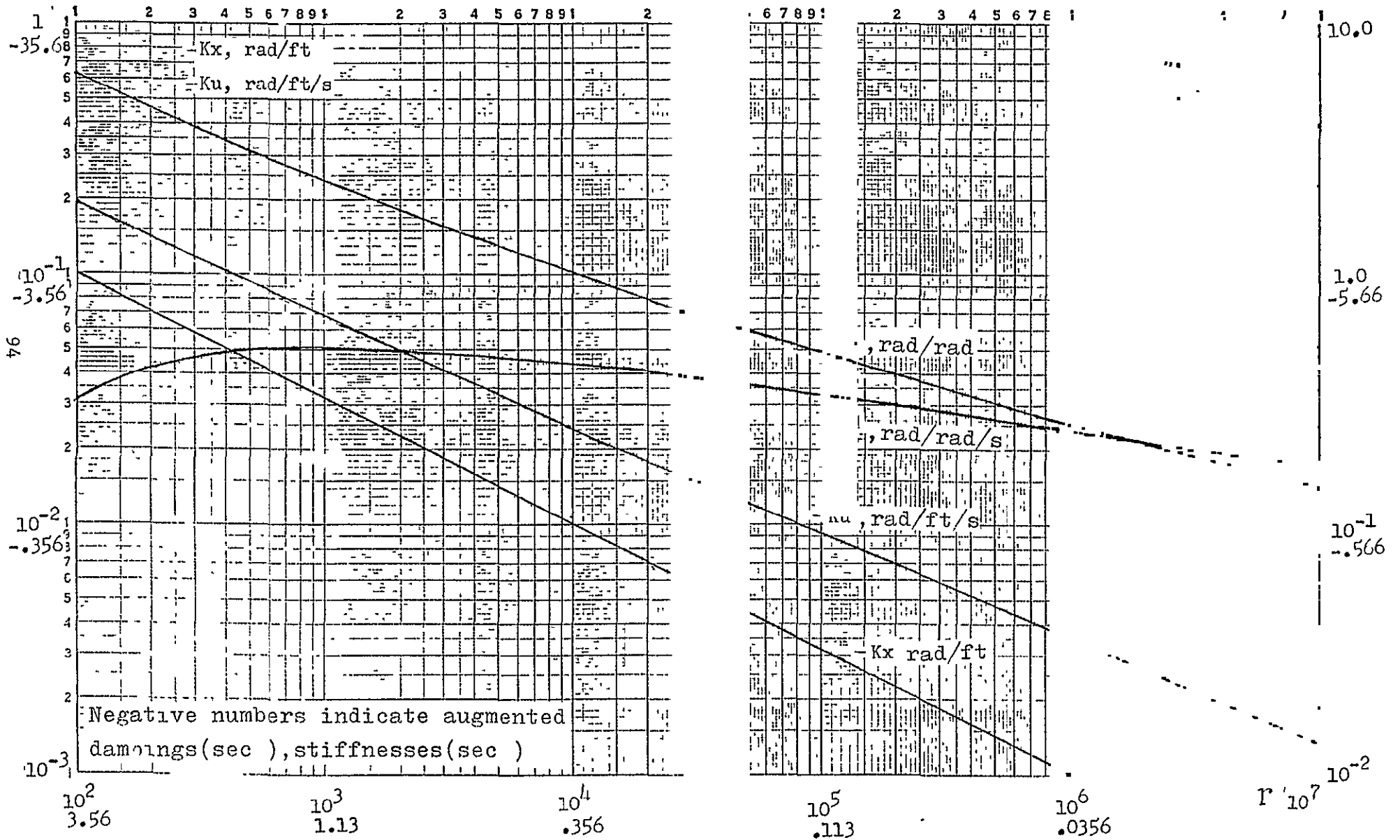


Fig. 31 Longitudinal optimal feedback gains for $q_{11} = 1.0, q_{33} = 3283$

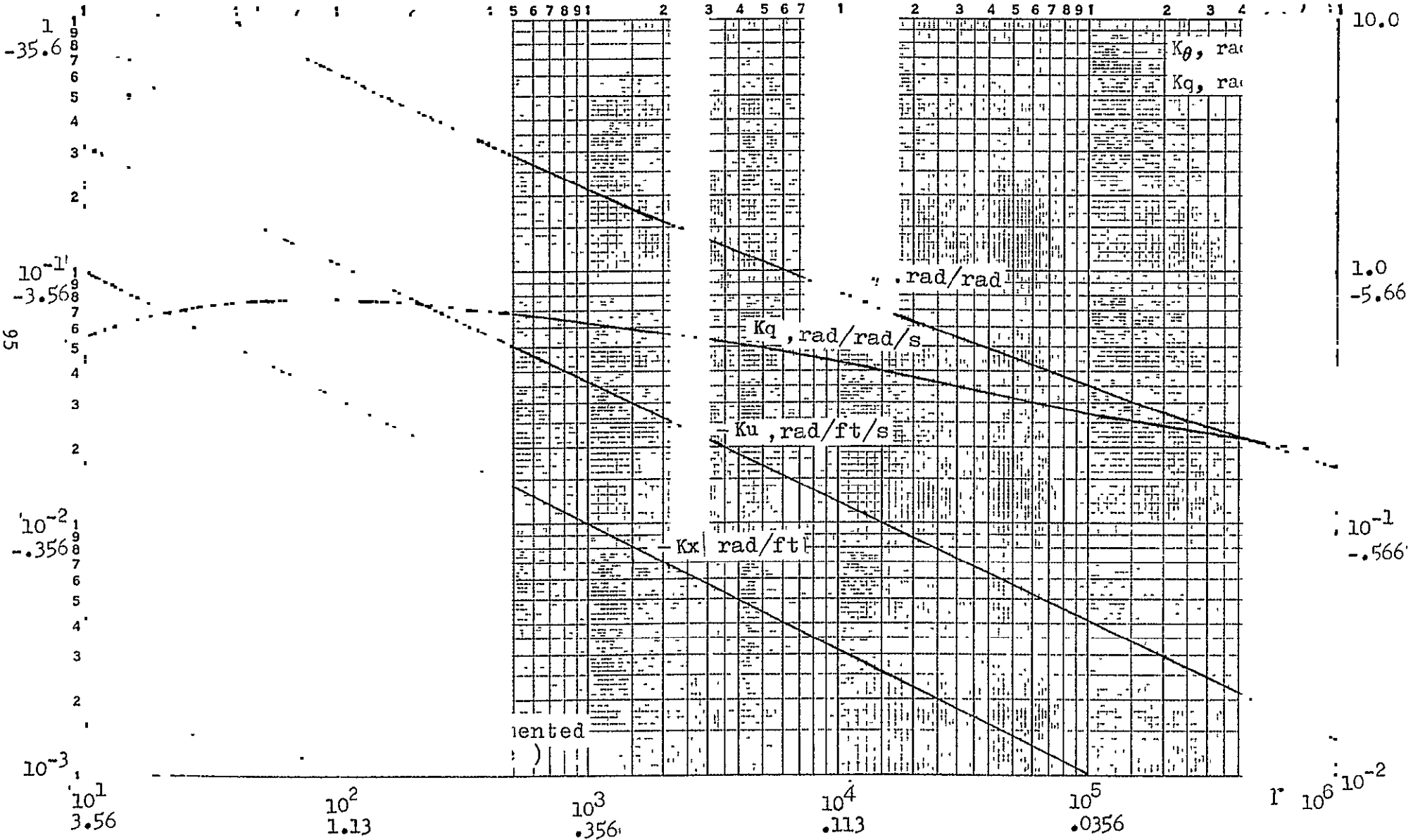


Fig. 32 Longitudinal optimal feedback gains for $q_{11} = 0.1$, $q_{33} = 3283$

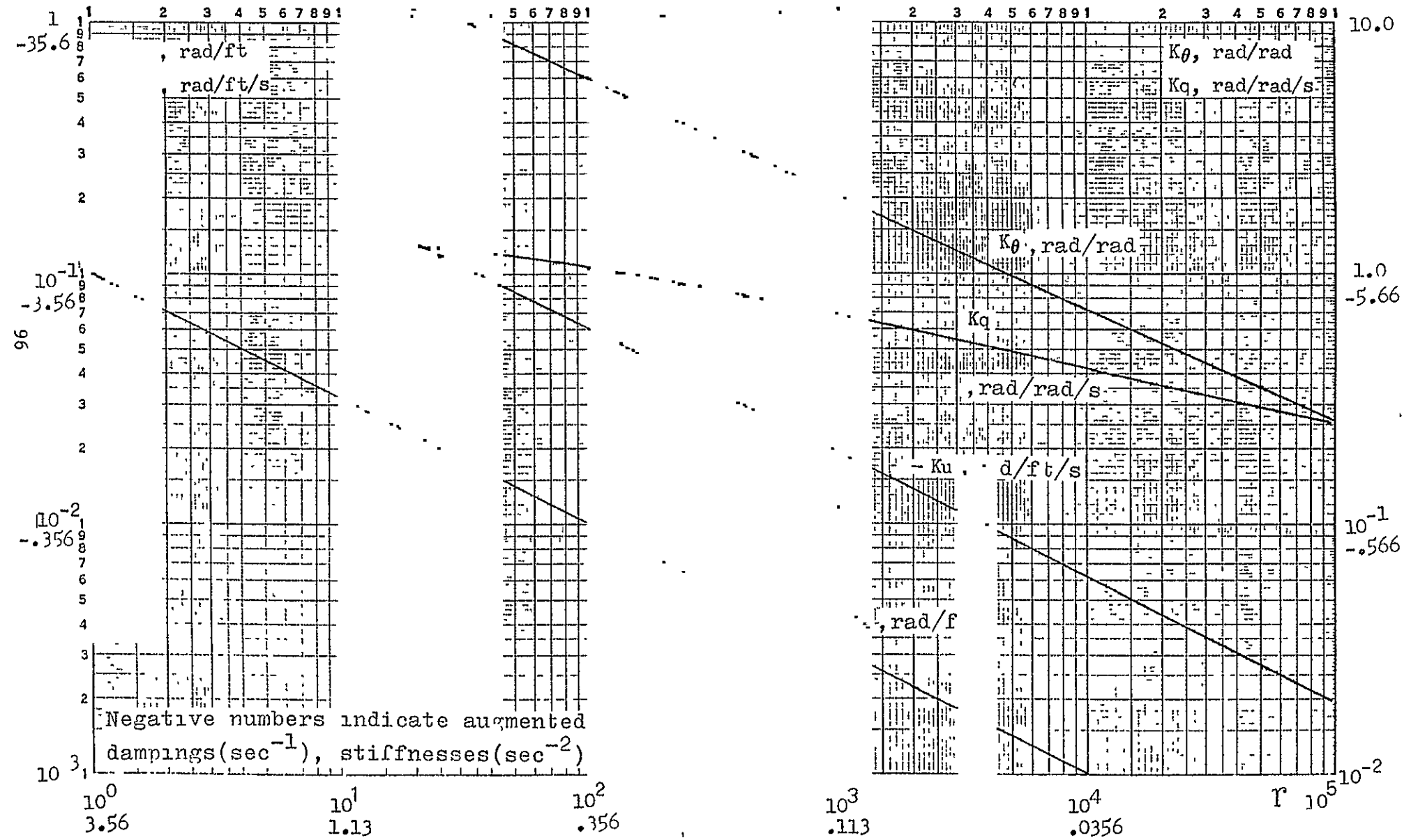


Fig. 33: Longitudinal optimal feedback gains for $q_{11} = 0.01$, $q_{33} = 3283$

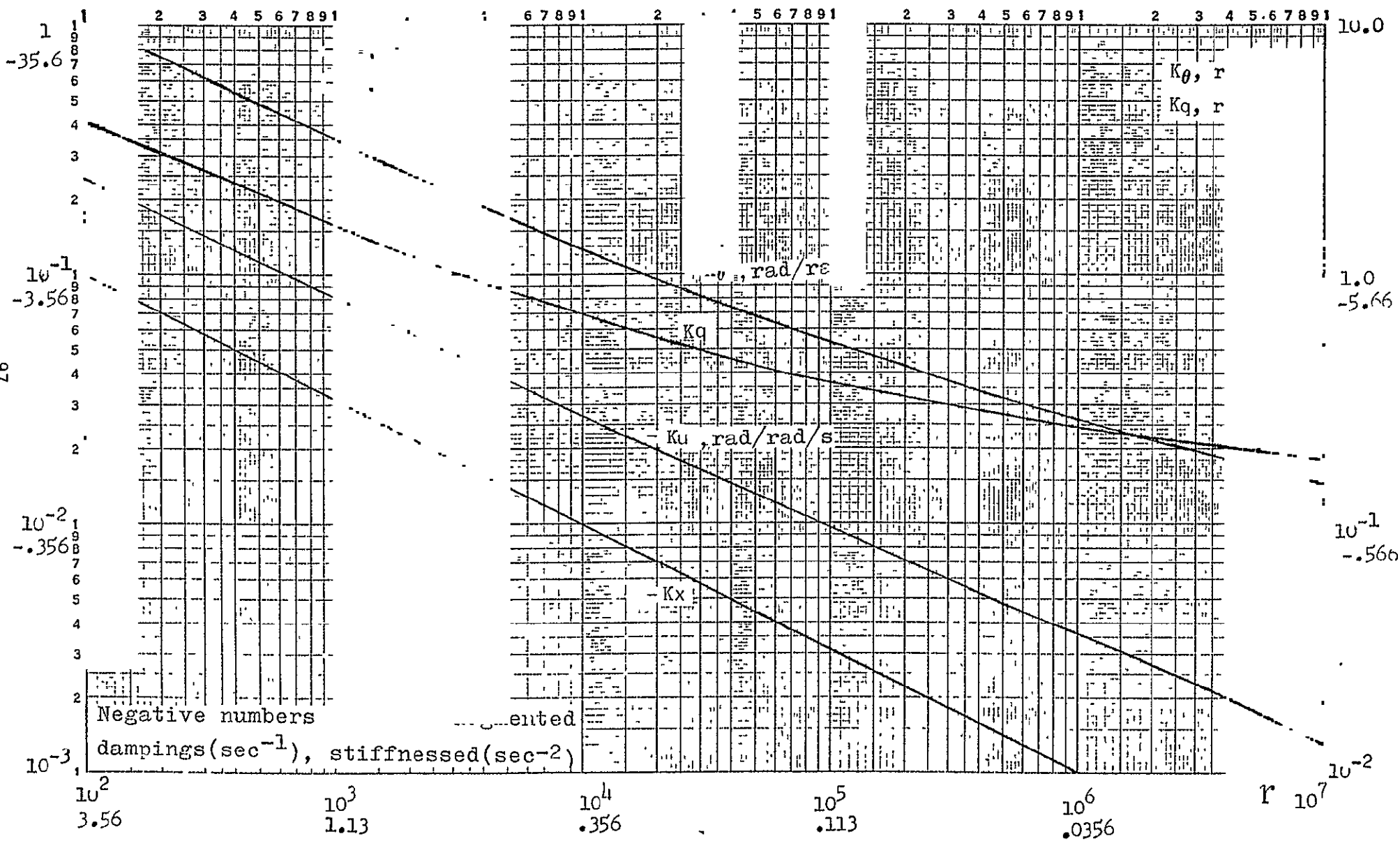
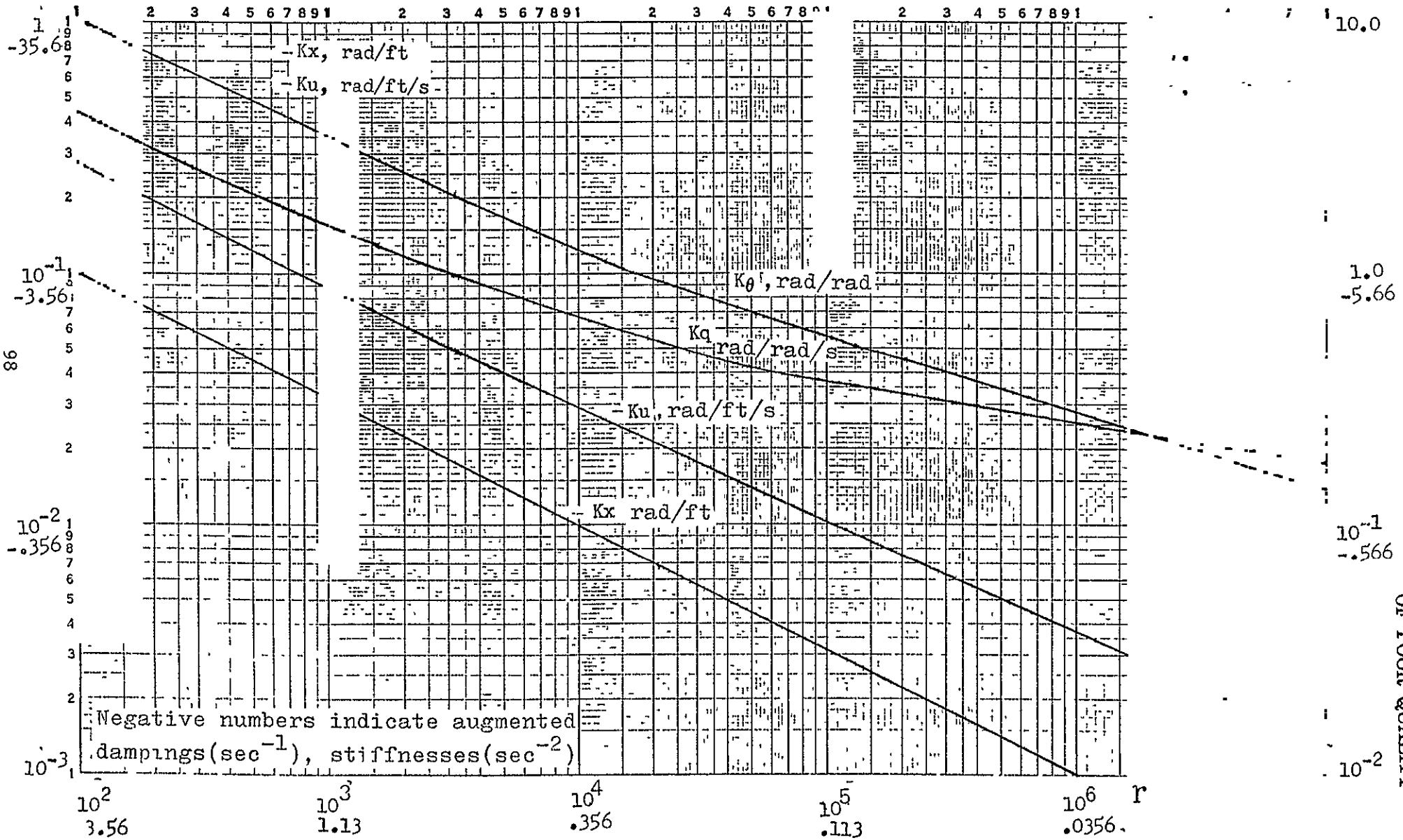
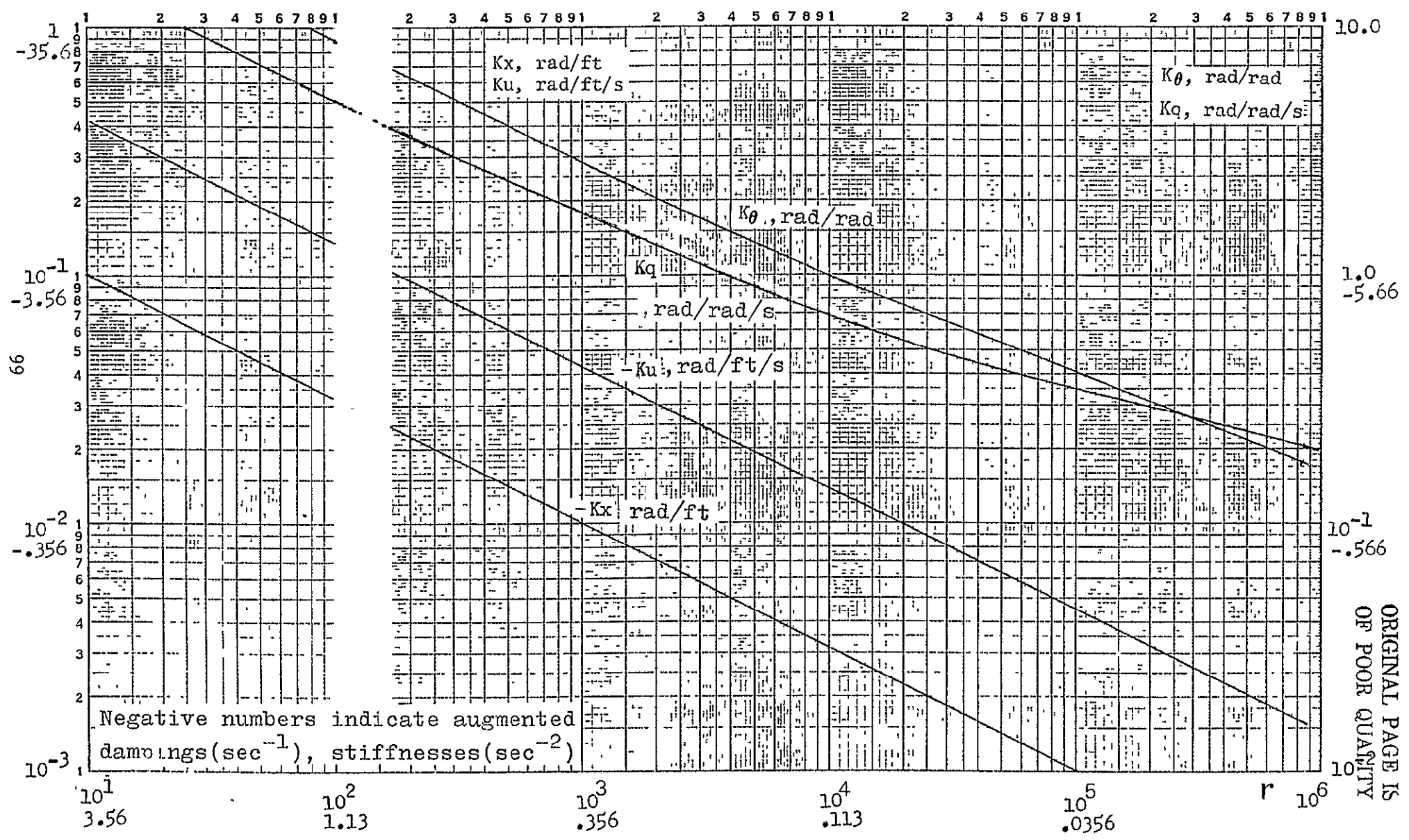


Fig. 34 Longitudinal optimal feedback gains for $q_{11} = 1.0$, $q_{33} = q_{44} = 3283$



ORIGINAL PAGE IS
 OF POOR QUALITY

Fig. 35 Longitudinal optimal feedback gains for $q_{11} = q_{22} = 1.0$, $q_{33} = q_{44} = 3283$



ORIGINAL PAGE IS
 OF POOR QUALITY

Fig. 36 Longitudinal optimal feedback gains for $q_{11} = q_{22} = 0.1$, $q_{33} = q_{44} = 3283$

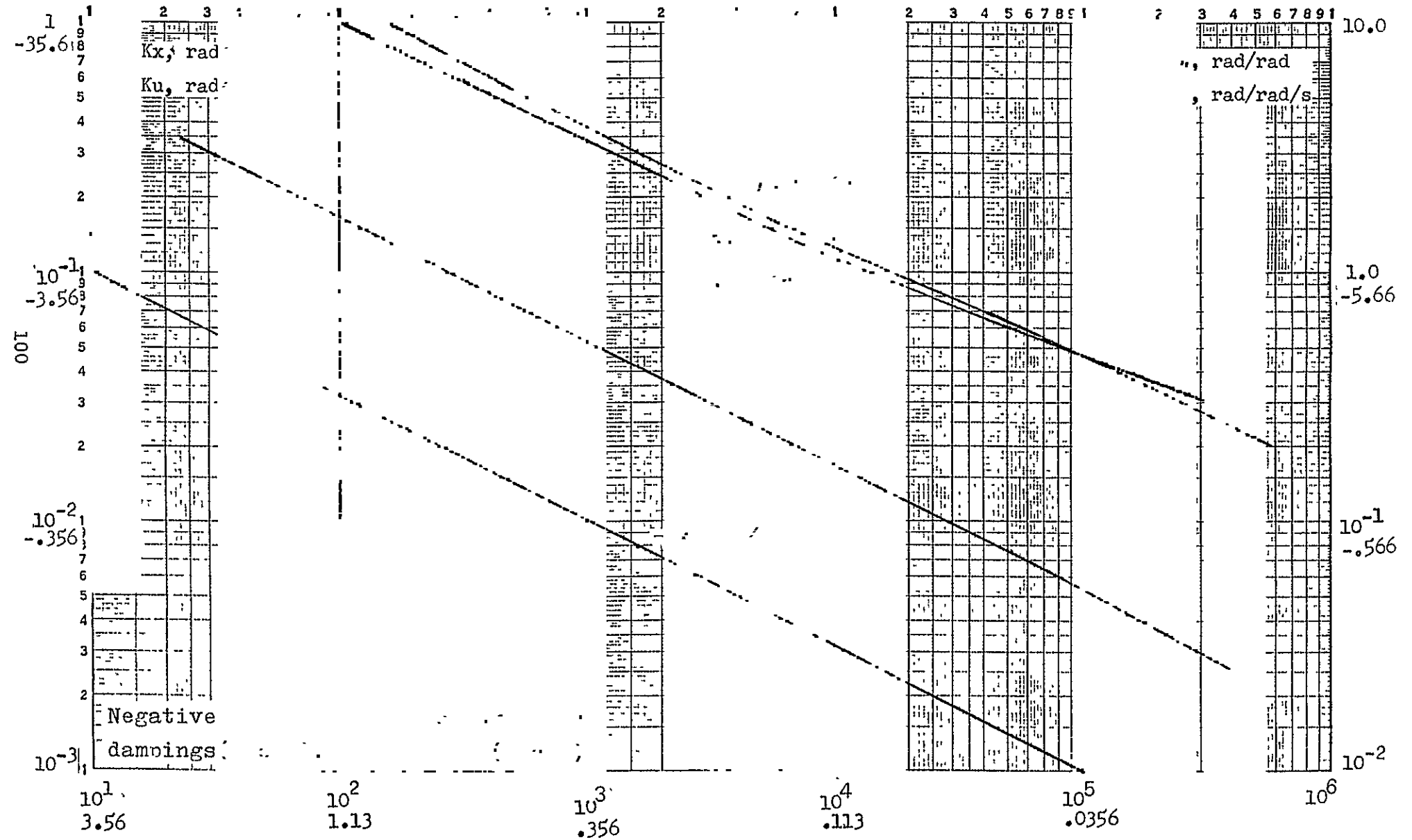


Fig. 37 Longitudinal optimal feedback gains for $q_{11} = 0.1$, $q_{22} = 0.4$, $q_{33} = 3283$, $q_{44} = 3132$

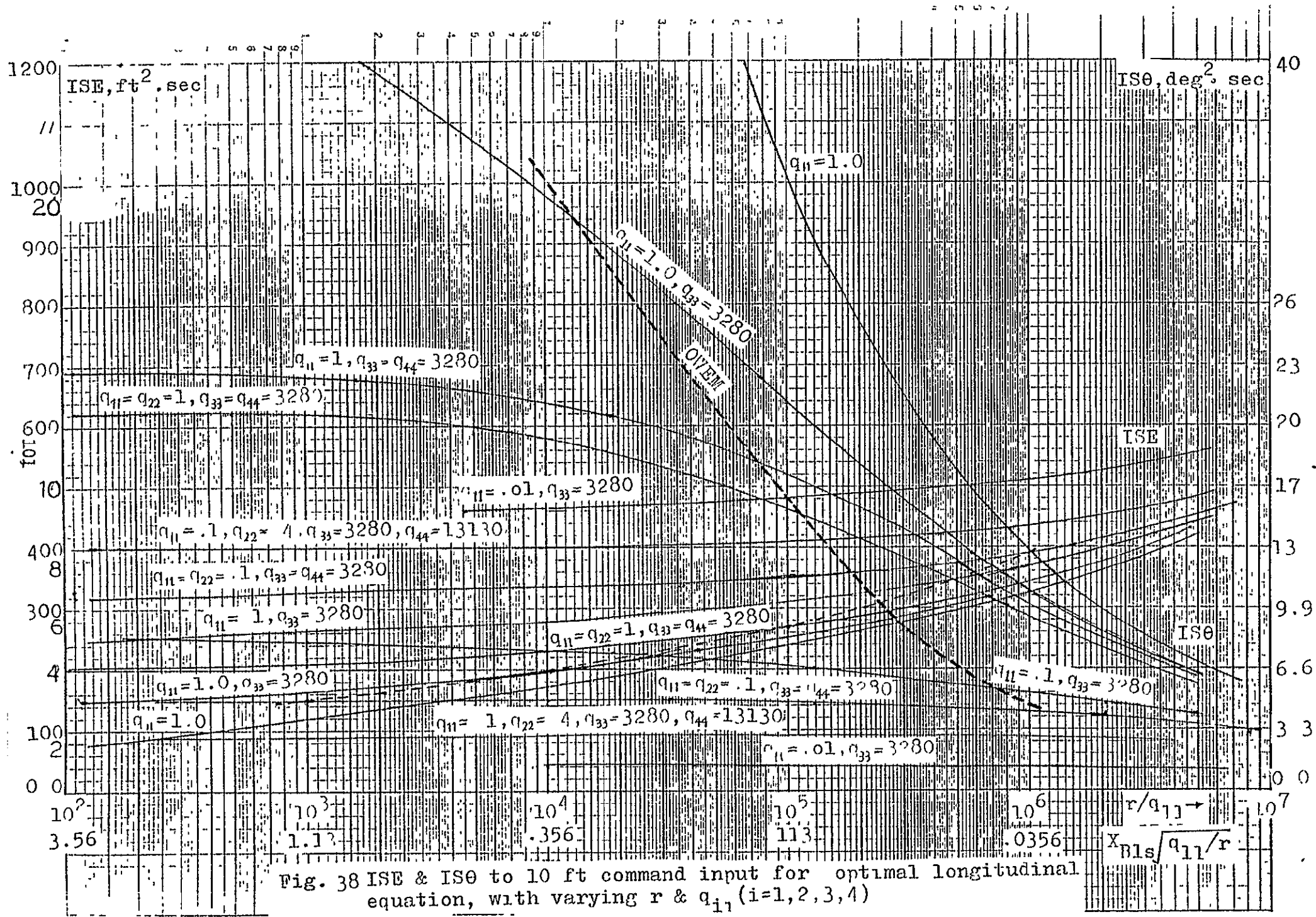


Fig. 38 ISE & ISθ to 10 ft command input for optimal longitudinal equation, with varying r & q_{ii} ($i=1,2,3,4$)

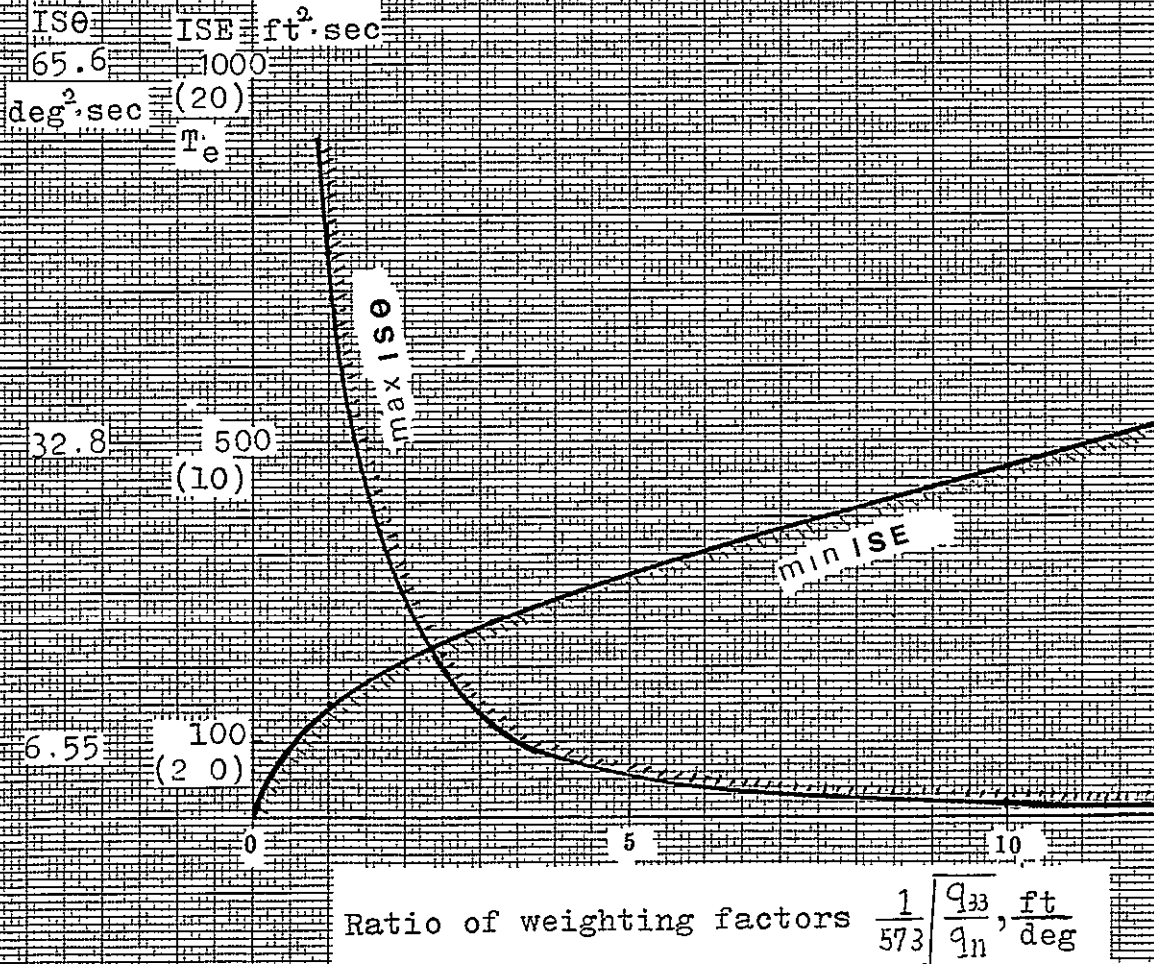


Fig. 39 Relation of min. ISE & max. ISE vs weighting factors ratio for longitudinal equation (lateral eq.)
 (10ft command input)

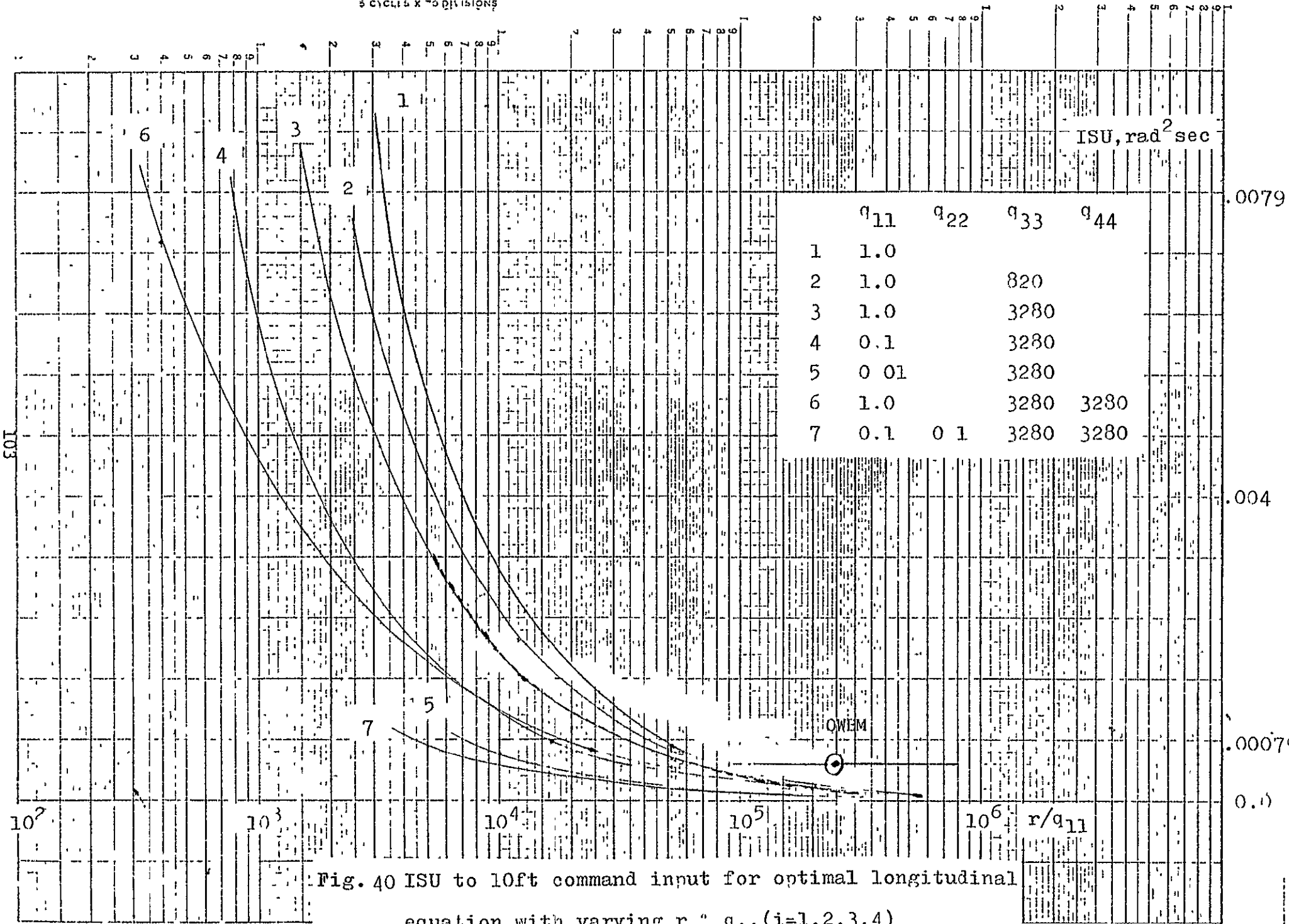


Fig. 40 ISU to 10ft command input for optimal longitudinal equation, with varying r/q_{11} ($i=1,2,3,4$)

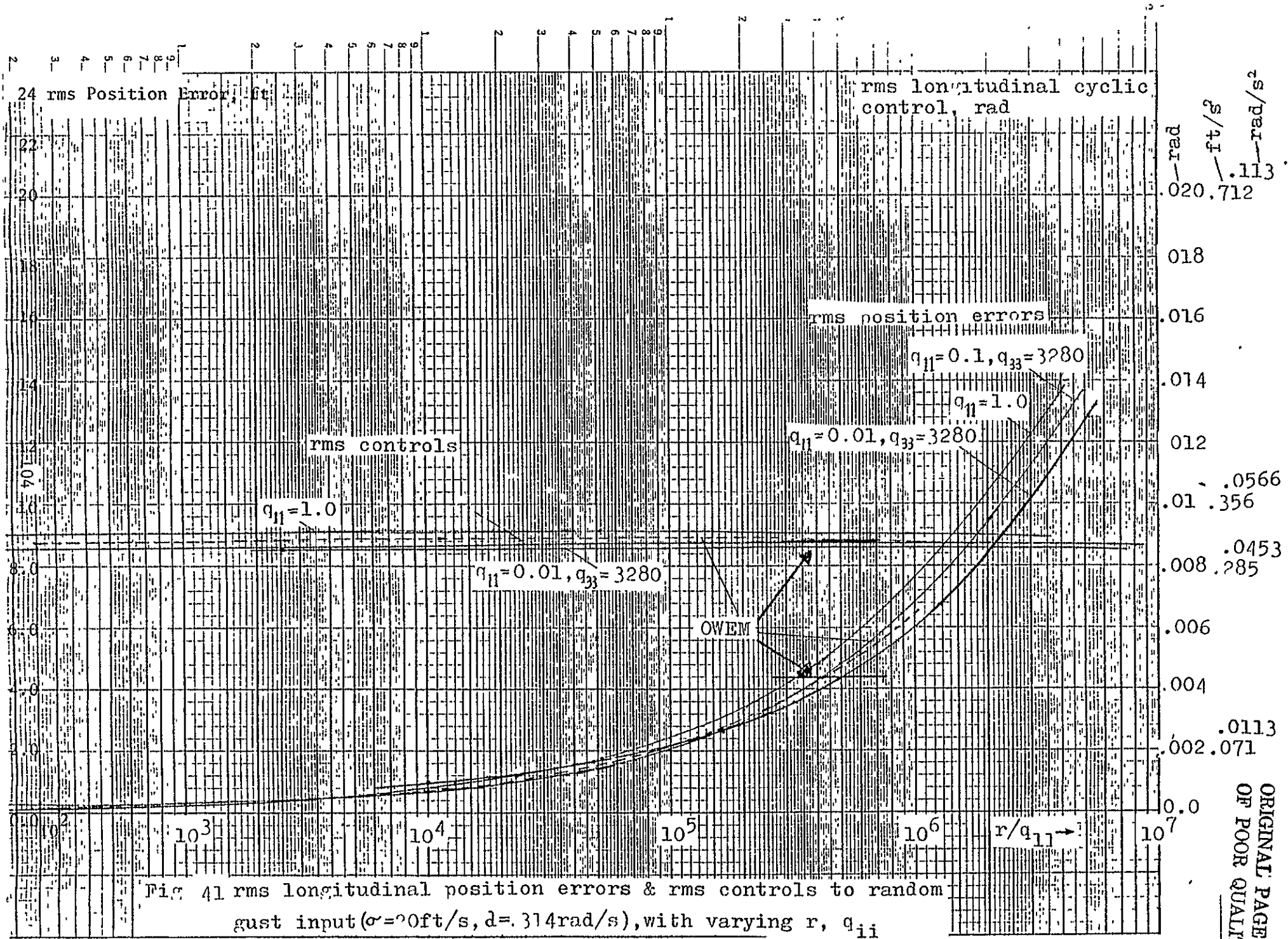


Fig 41 rms longitudinal position errors & rms controls to random gust input ($\sigma=20\text{ft/s}, d=.314\text{rad/s}$), with varying r, q_{ii}

ORIGINAL PAGE IS OF POOR QUALITY

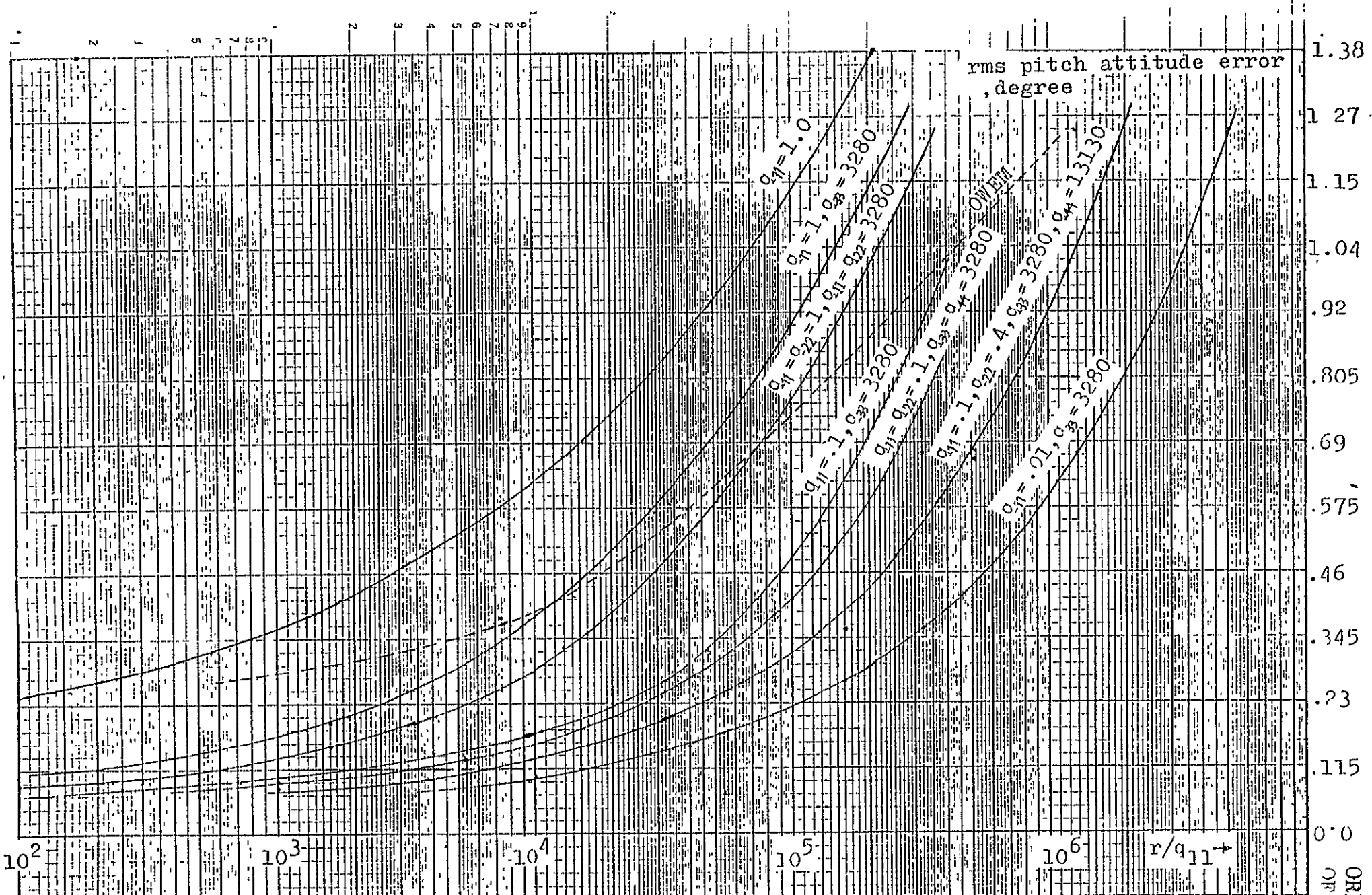


Fig. 42 rms pitch attitude errors due to random gust input ($\sigma=20$ ft/sec, $d=.3140$, with varying $r, q_{ii} (i=1, 2, 3, 4)$)

906

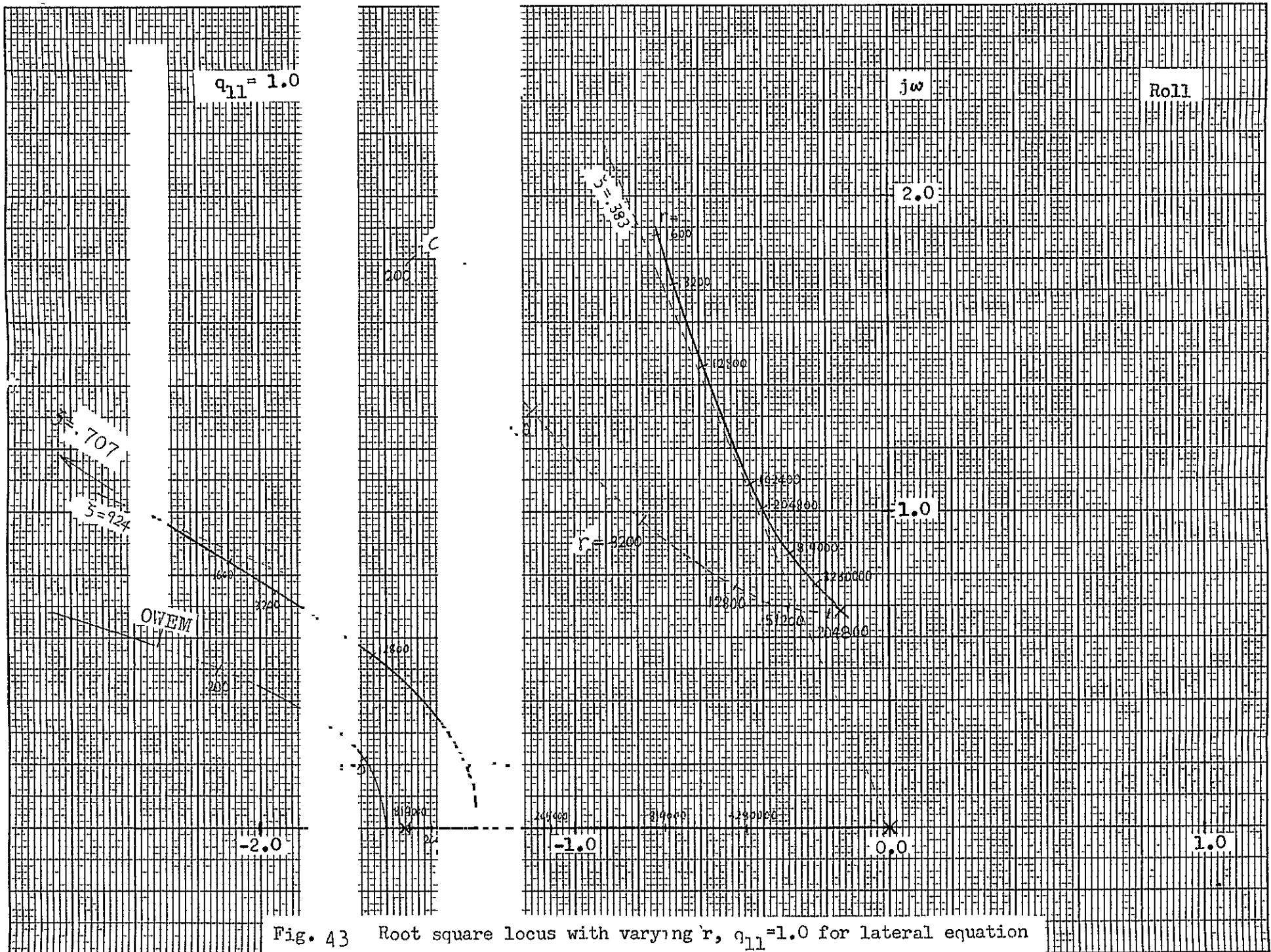


Fig. 43 Root square locus with varying 'r', $q_{11}=1.0$ for lateral equation

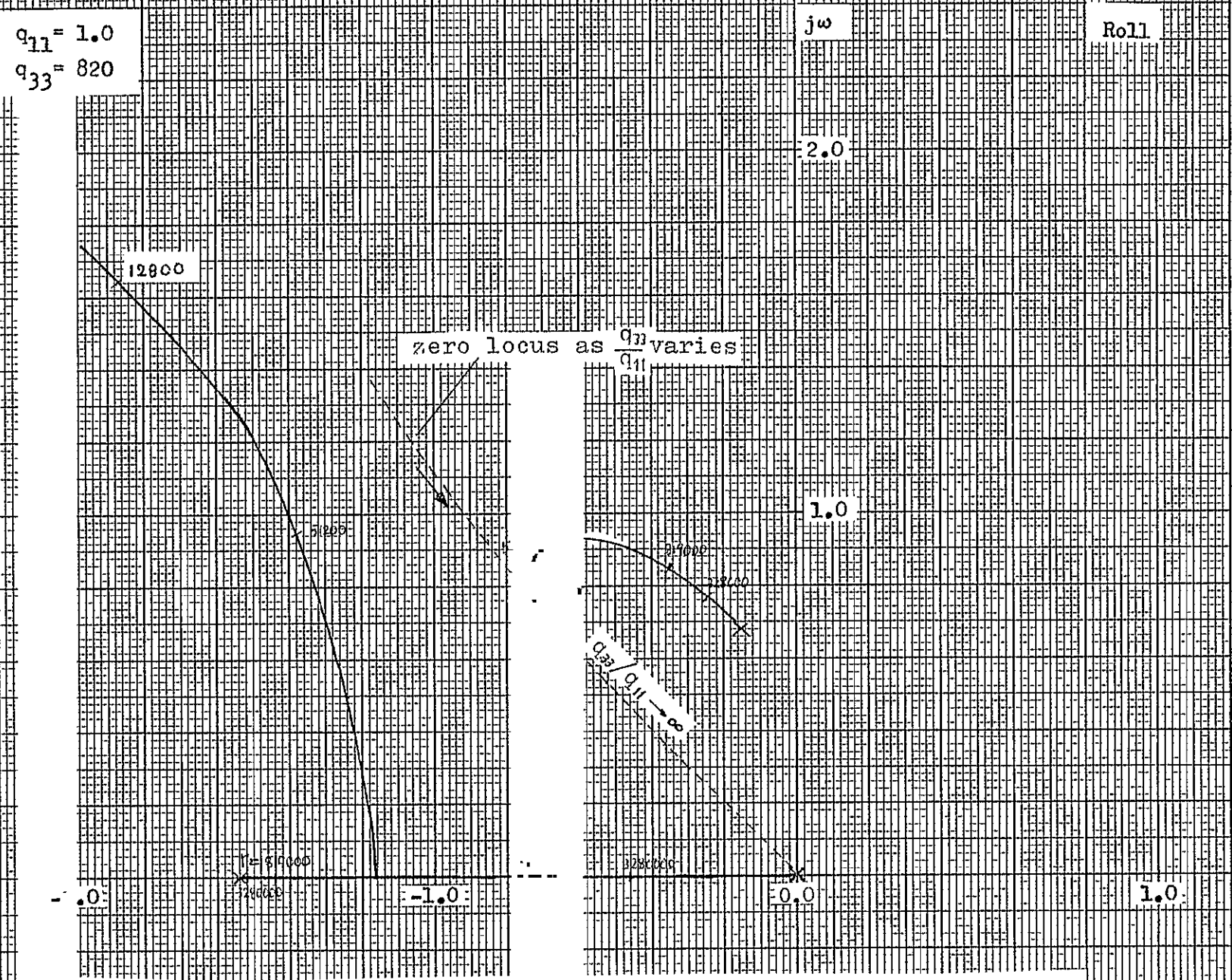


Fig. 44 Root square locus with varying r , $q_{11}=1.0$, $q_{33}=820$ for lateral equation

(4) $q_{11} = 0.1$
 $q_{33} = 3283$

$j\omega$
 2.0
 1.0
 1.0

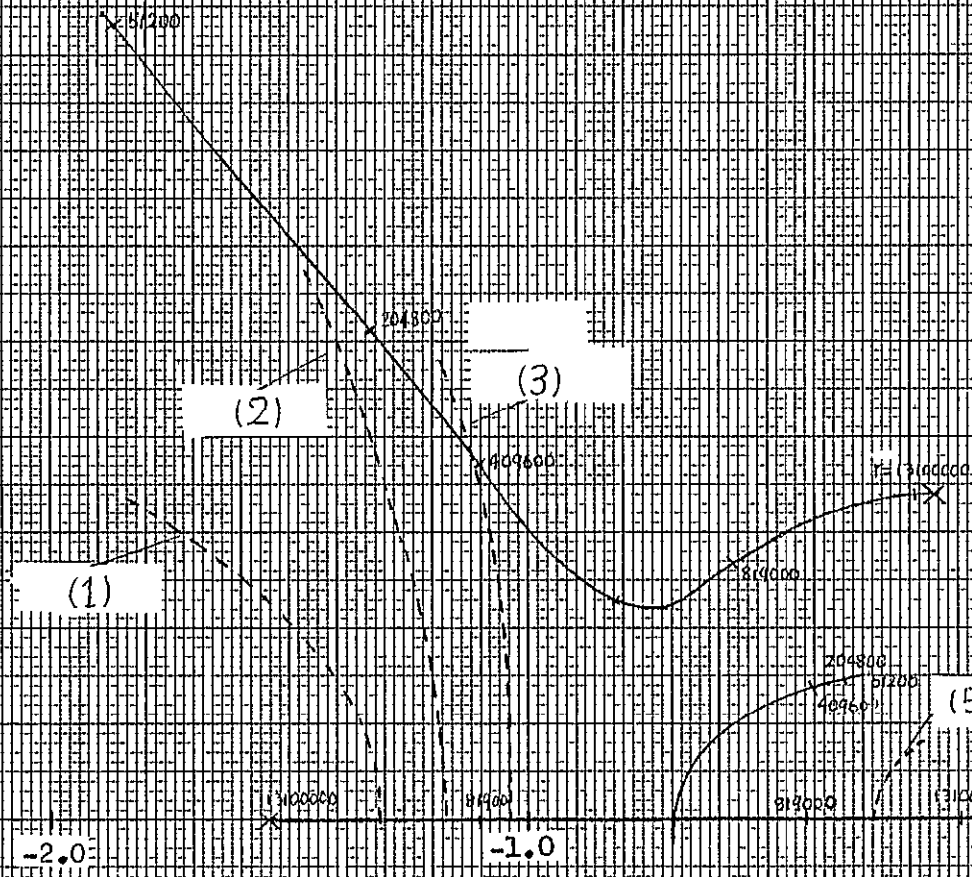


Fig. 46 Root square locus with varying r , $q_{11} = 0.1$, $q_{33} = 3283$ for lateral equation

$q_{11} = 0.01$
 $q_{33} = 3283$

$j\omega$
 2.0
 1.0
 0.0

Roll

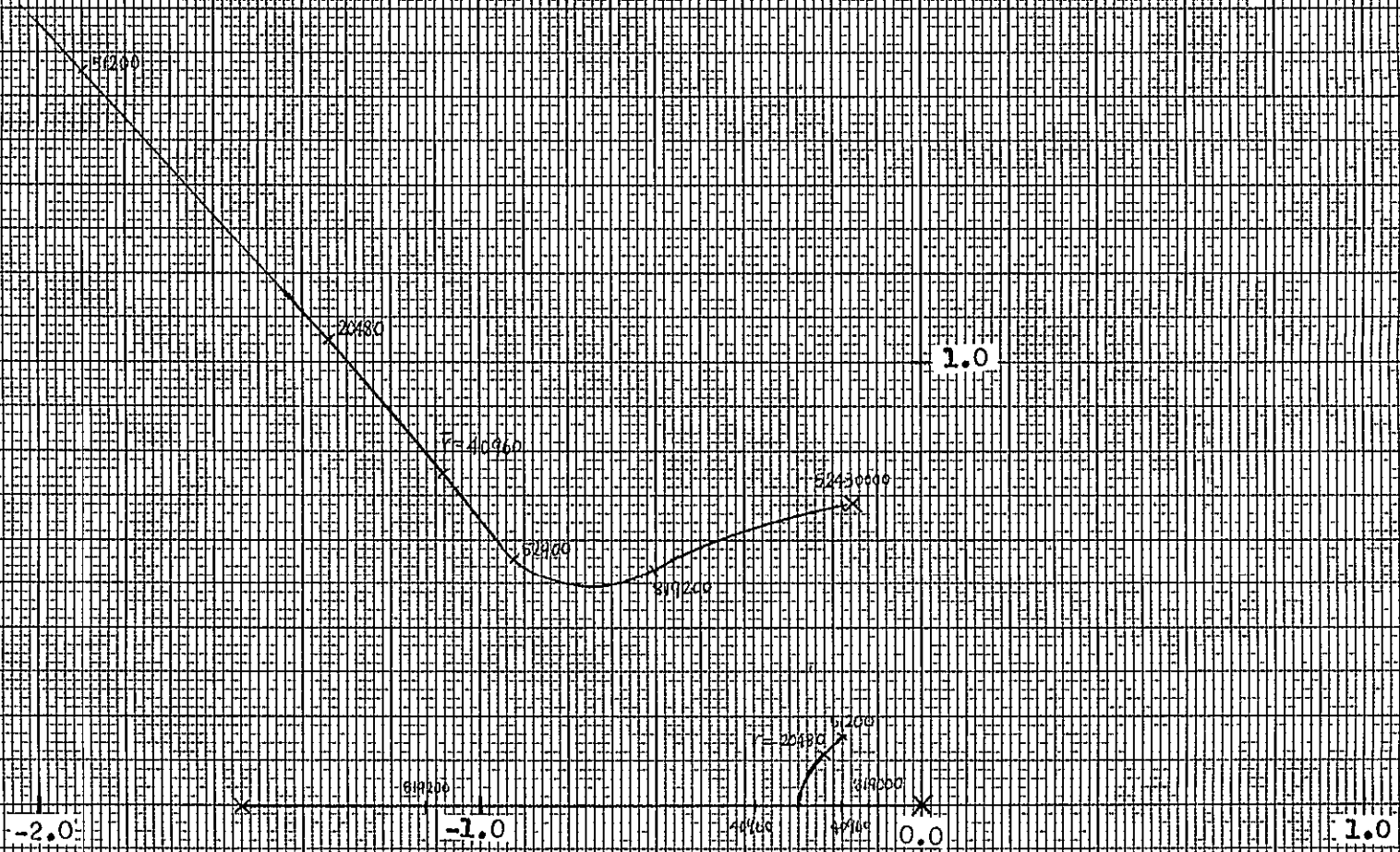


Fig. 47 Root square locus with varying r , $q_{11}=0.01$, $q_{33}=3283$ for lateral equation

110

111

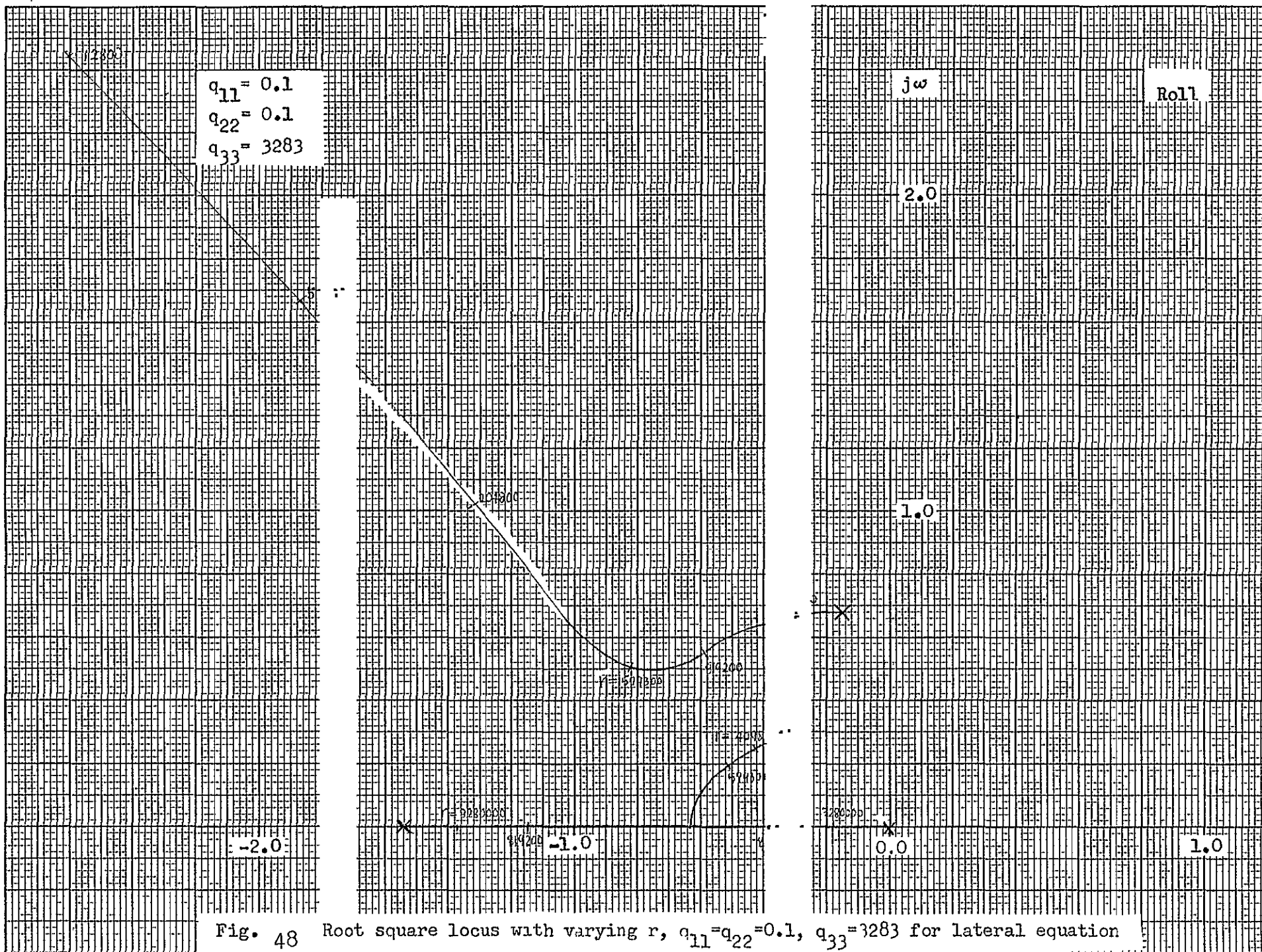


Fig. 48 Root square locus with varying r , $q_{11} = q_{22} = 0.1$, $q_{33} = 3283$ for lateral equation

$q_{11} = 1.0$
 $q_{22} = 1.0$
 $q_{33} = 3283$
 $q_{44} = 3283$

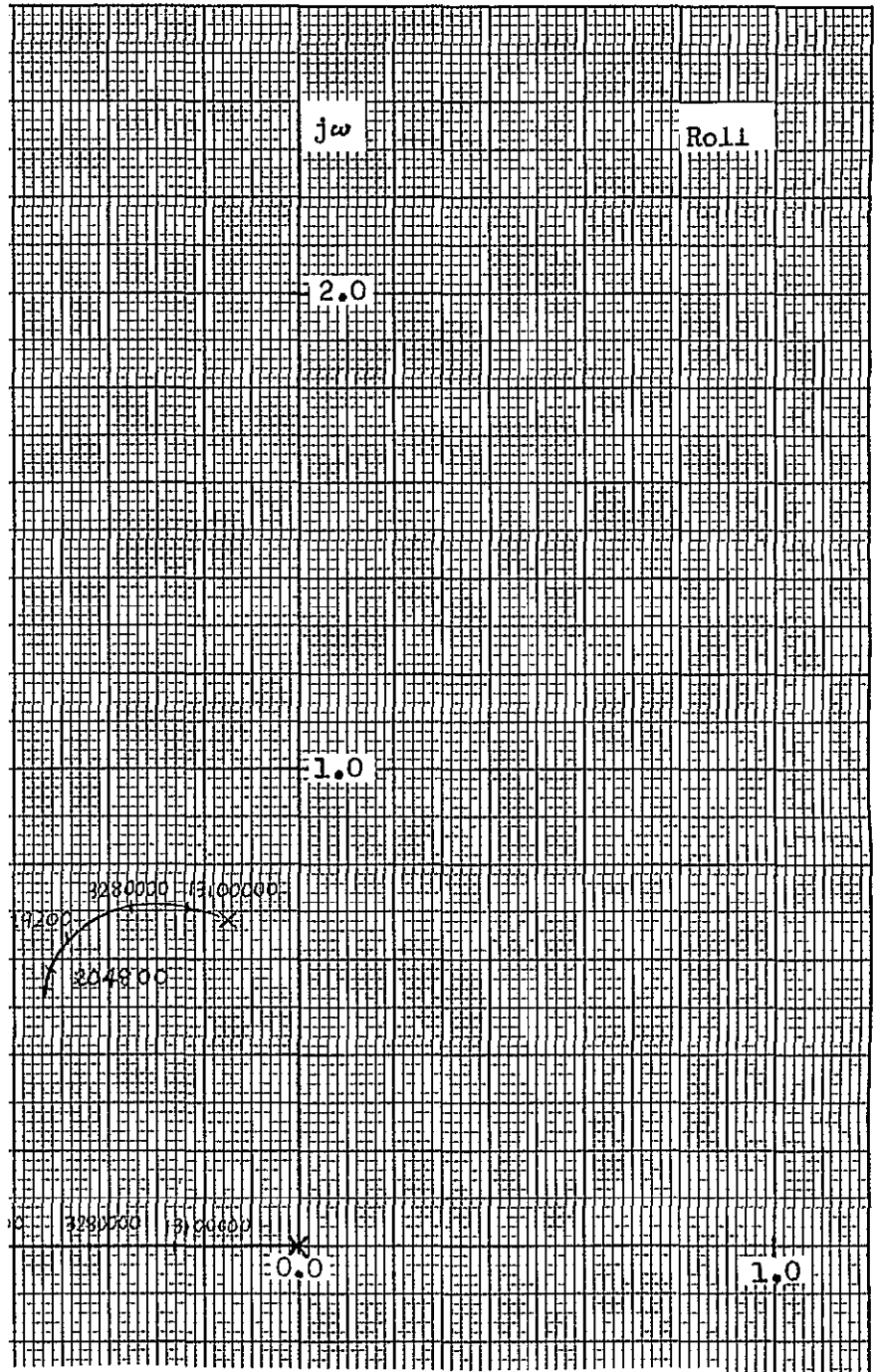


Fig. 49 Root square locus with varying r , $q_{11} = q_{22} = 1.0$, $q_{33} = q_{44} = 3283$ for lateral equation

113

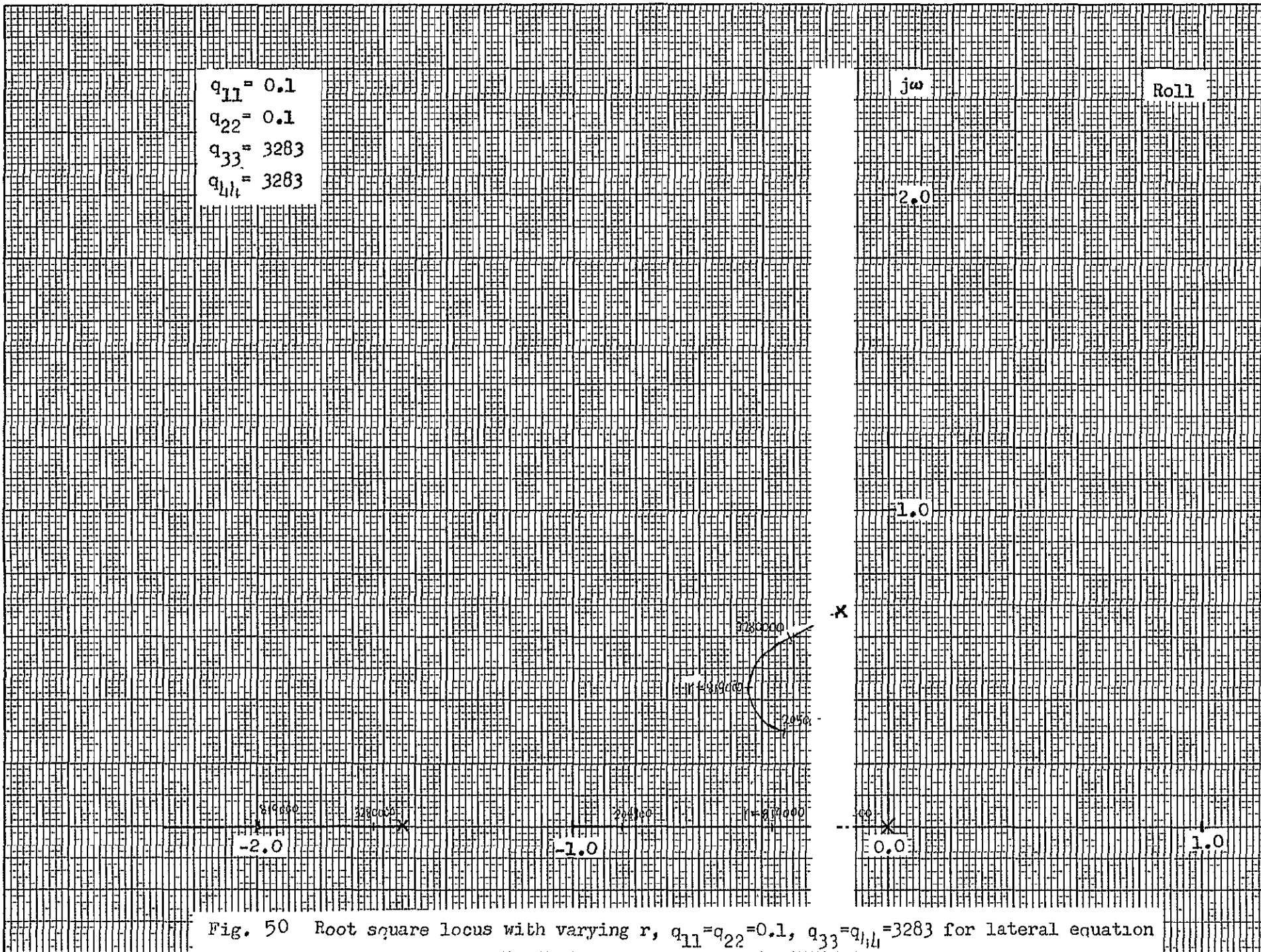


Fig. 50 Root square locus with varying r , $q_{11}=q_{22}=0.1$, $q_{33}=q_{44}=3283$ for lateral equation

114

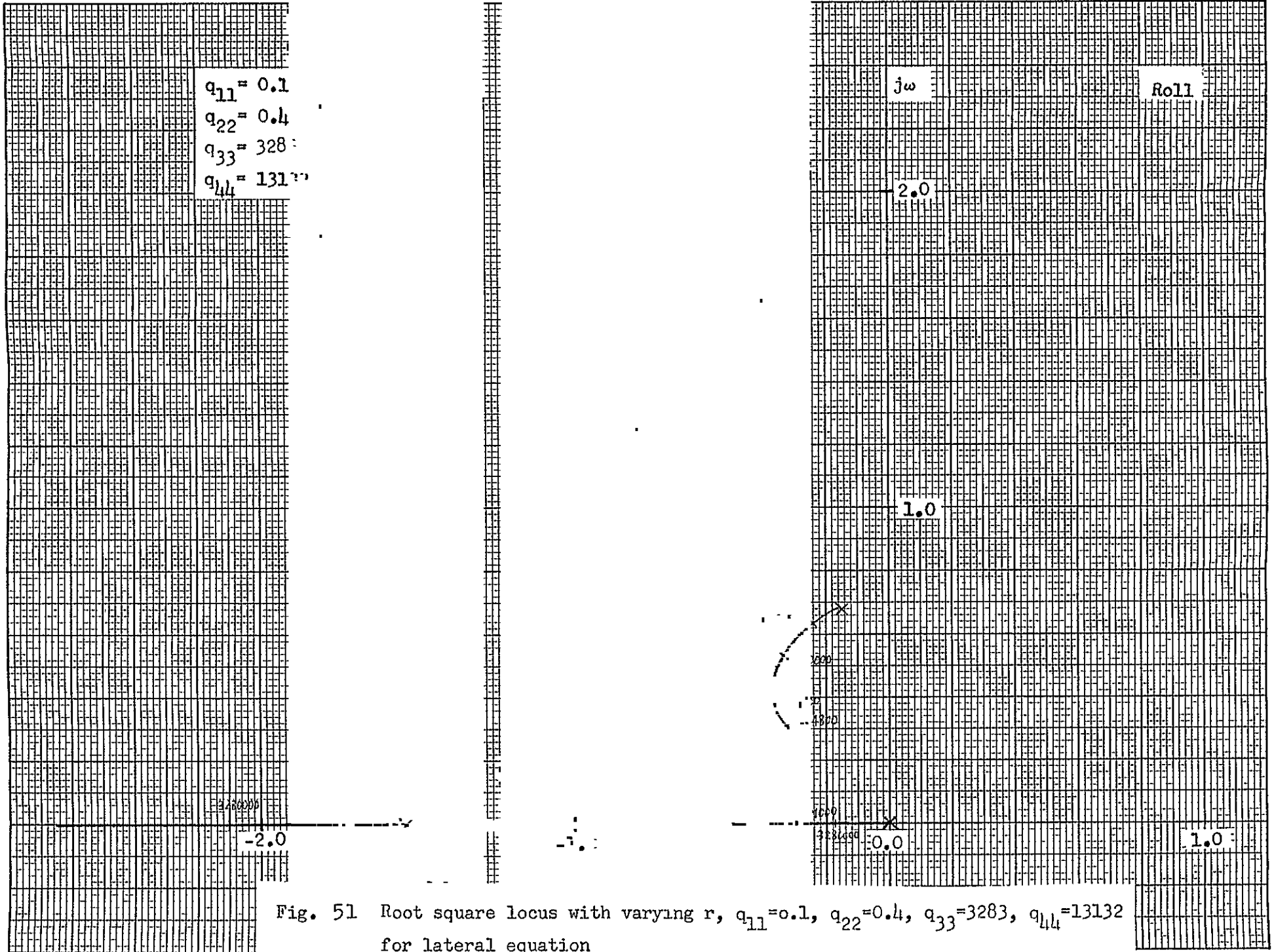


Fig. 51 Root square locus with varying r , $q_{11}=0.1$, $q_{22}=0.4$, $q_{33}=3283$, $q_{44}=13132$ for lateral equation

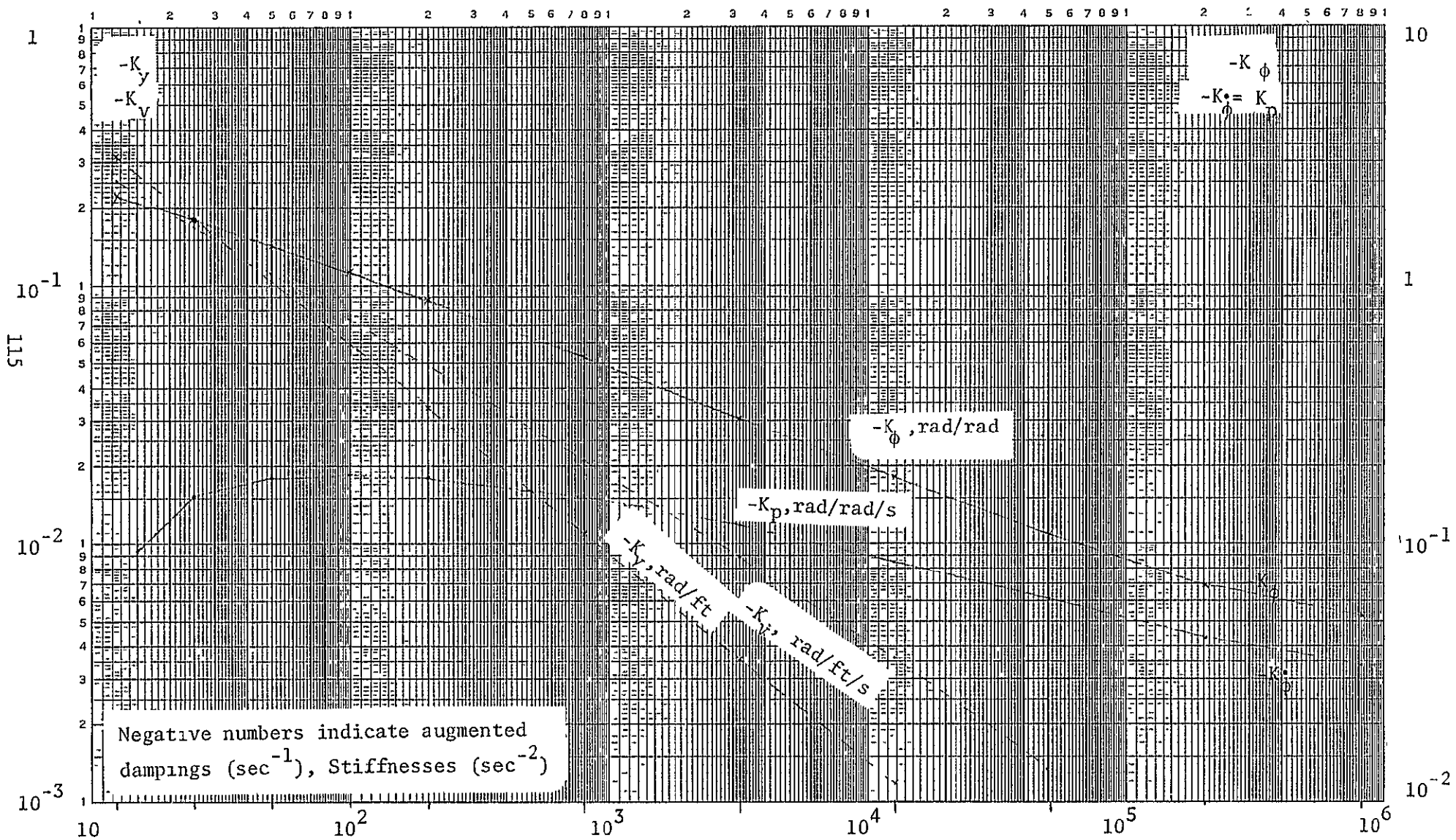


Fig. 52. Lateral optimal feedback gains for the OWEM method

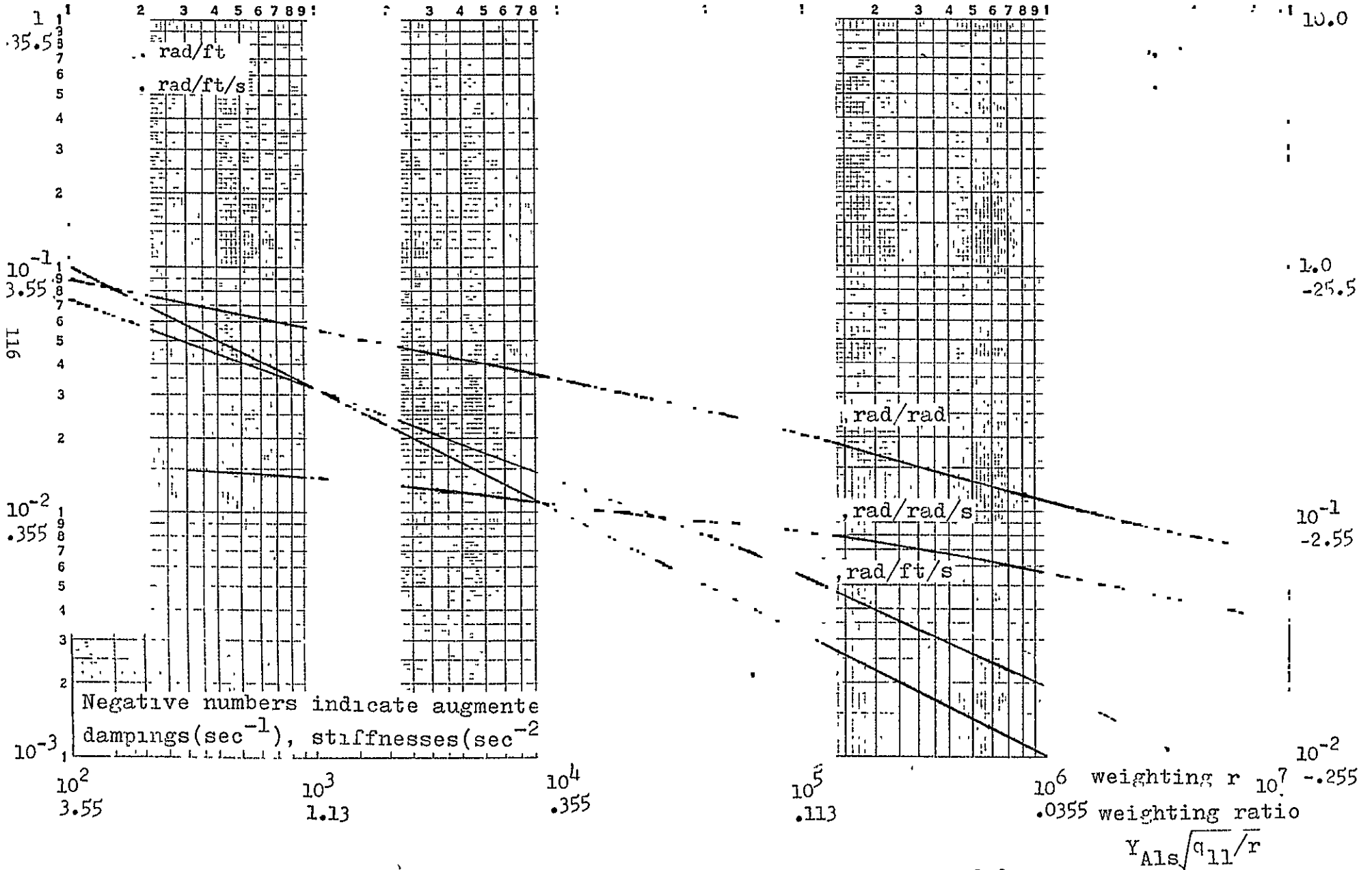


Fig. 53 Lateral optimal feedback gains for $q_{11} = 1.0$

$$Y_{Als} \sqrt{q_{11}/r}$$

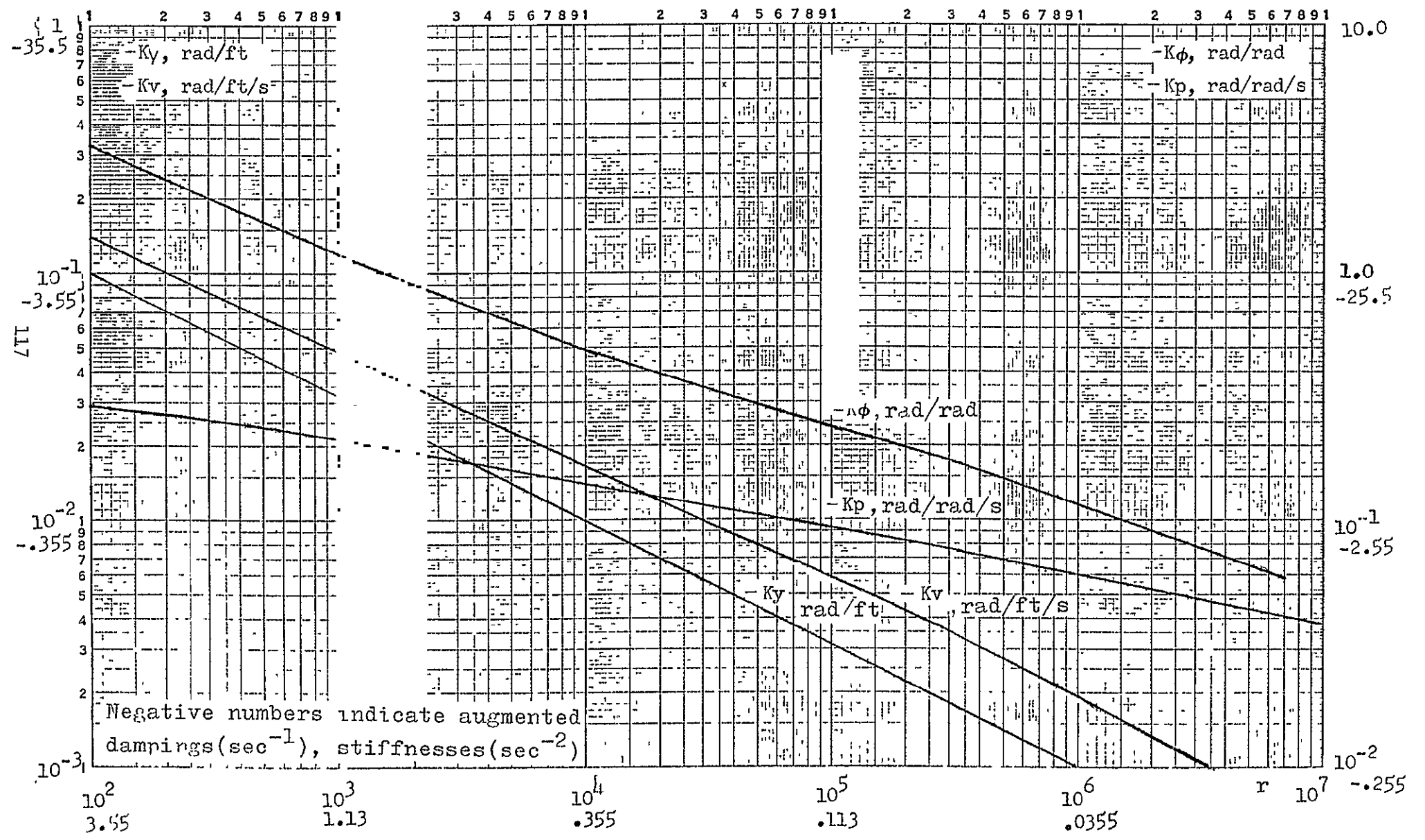


Fig. 54 Lateral optimal feedback gains for $q_{11} = 1.0$, $q_{33} = 820$

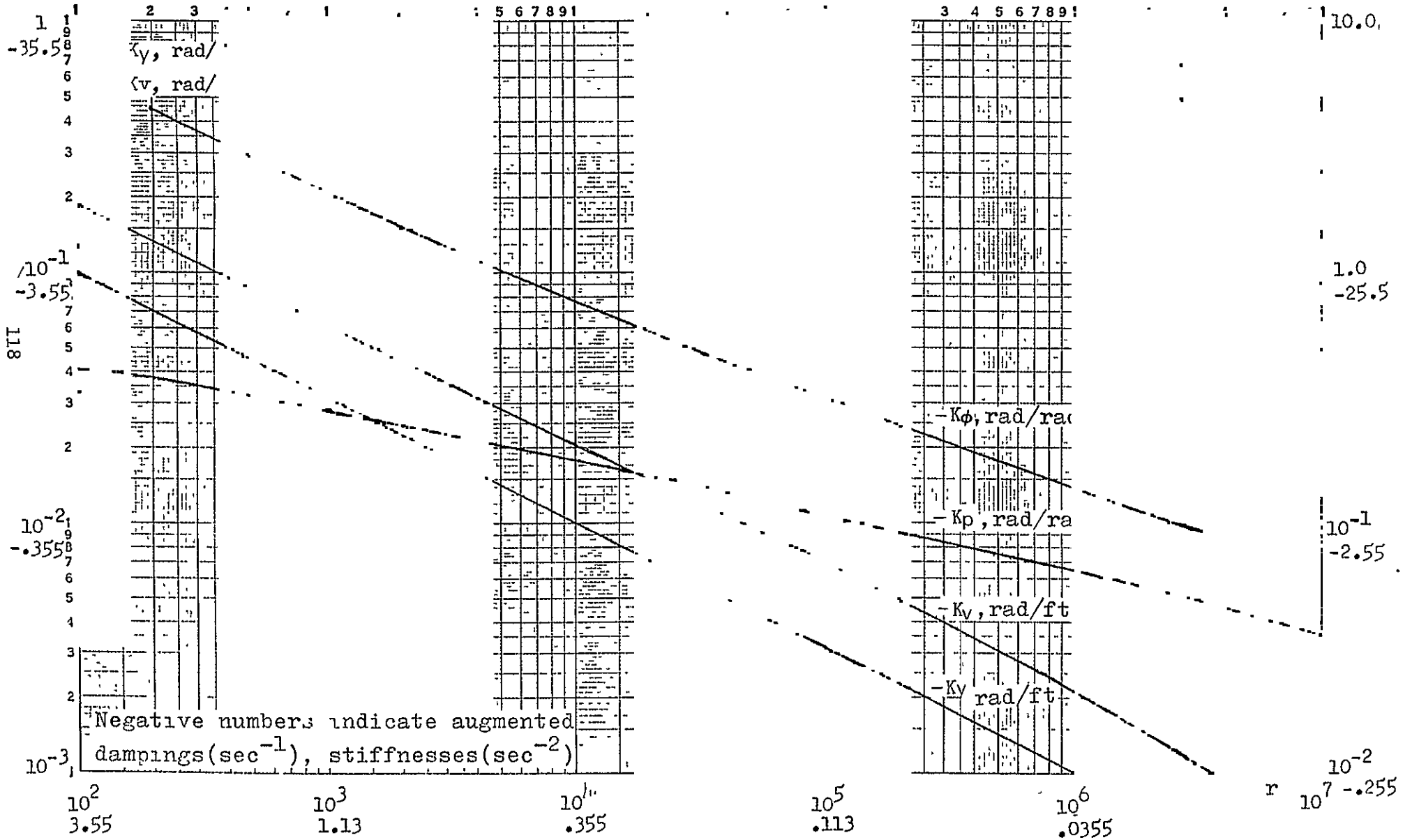


Fig. 55 Lateral optimal feedback gains for $q_{11} = 1.0$, $q_{33} = 3283$

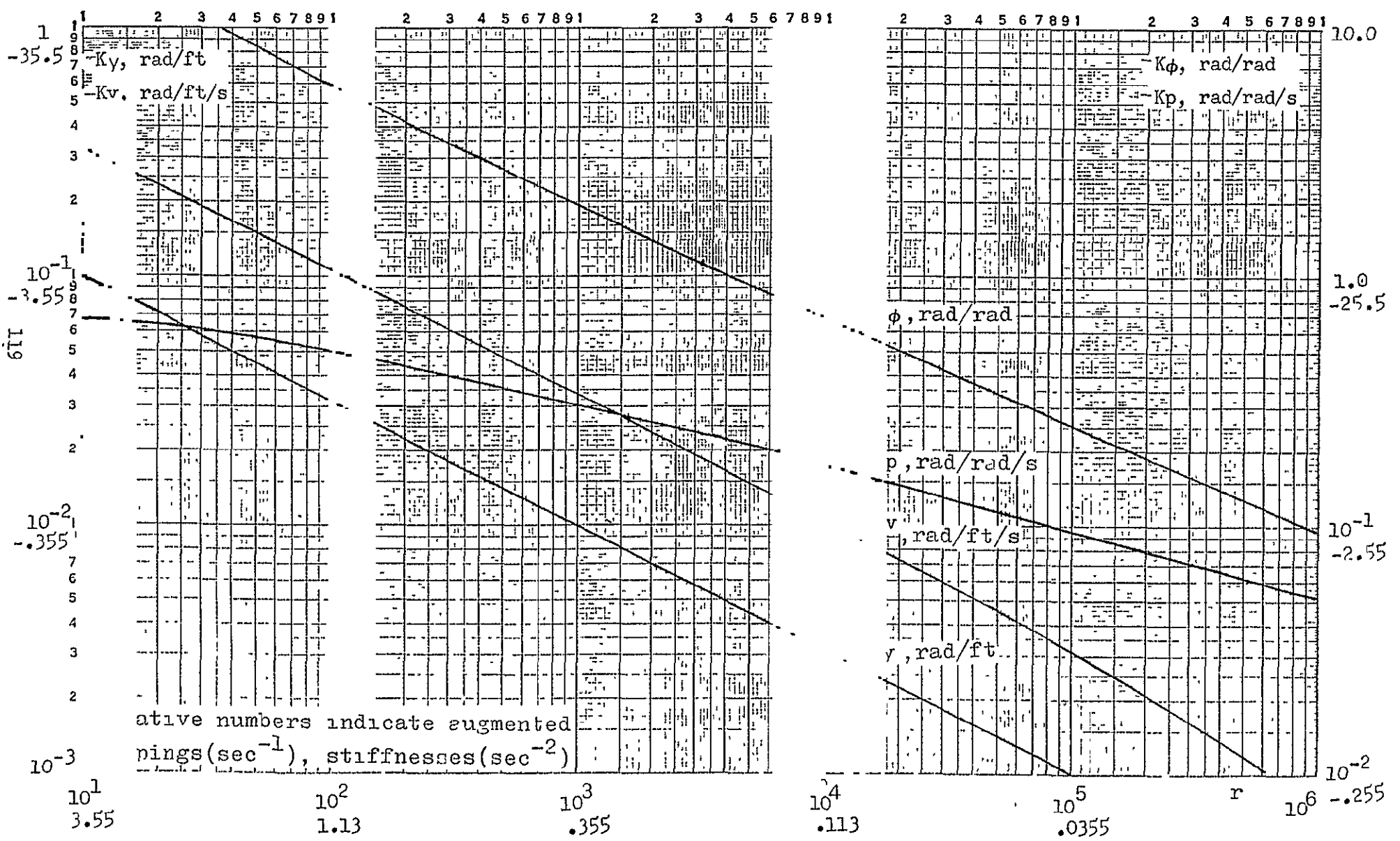


Fig. 56 Lateral optimal feedback gains for $q_{11} = 0.1$, $q_{33} = 3283$

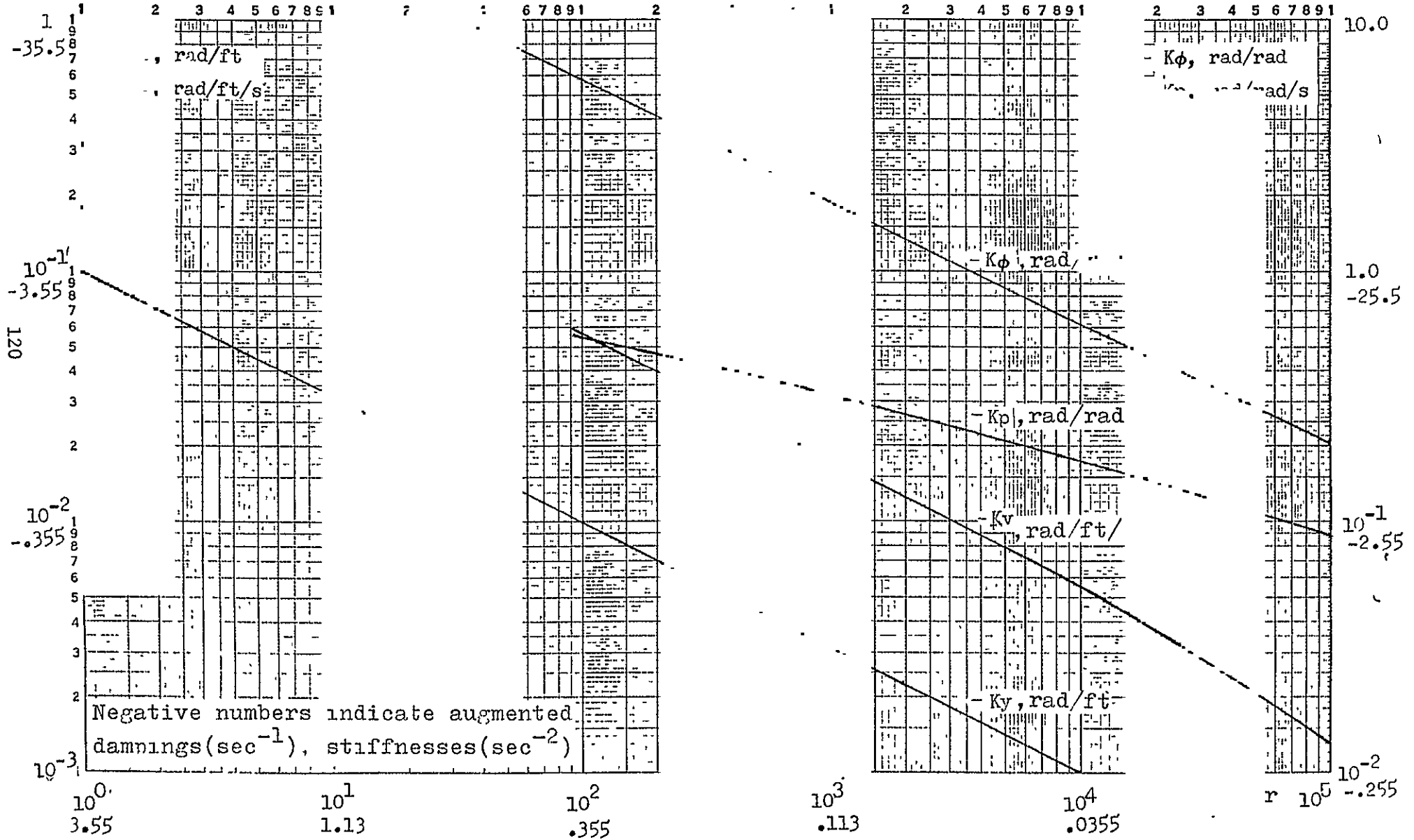


Fig. 57 Lateral optimal feedback gains for $q_{11} = 0.01$, $q_{33} = 3283$

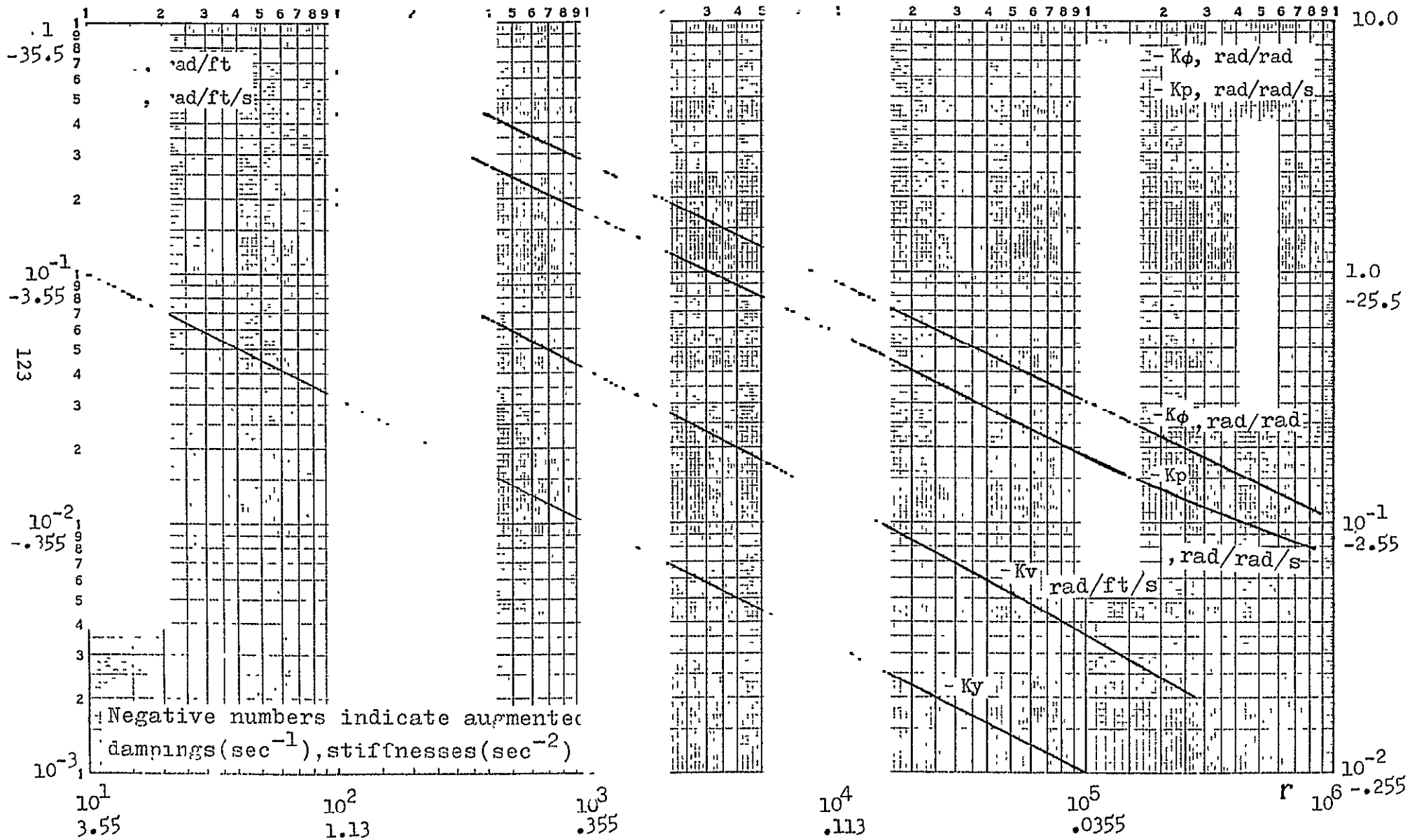


Fig. 60 Lateral optimal feedback gains for $q_{11}=q_{22}=0.1$, $q_{33}=q_{44}=3283$

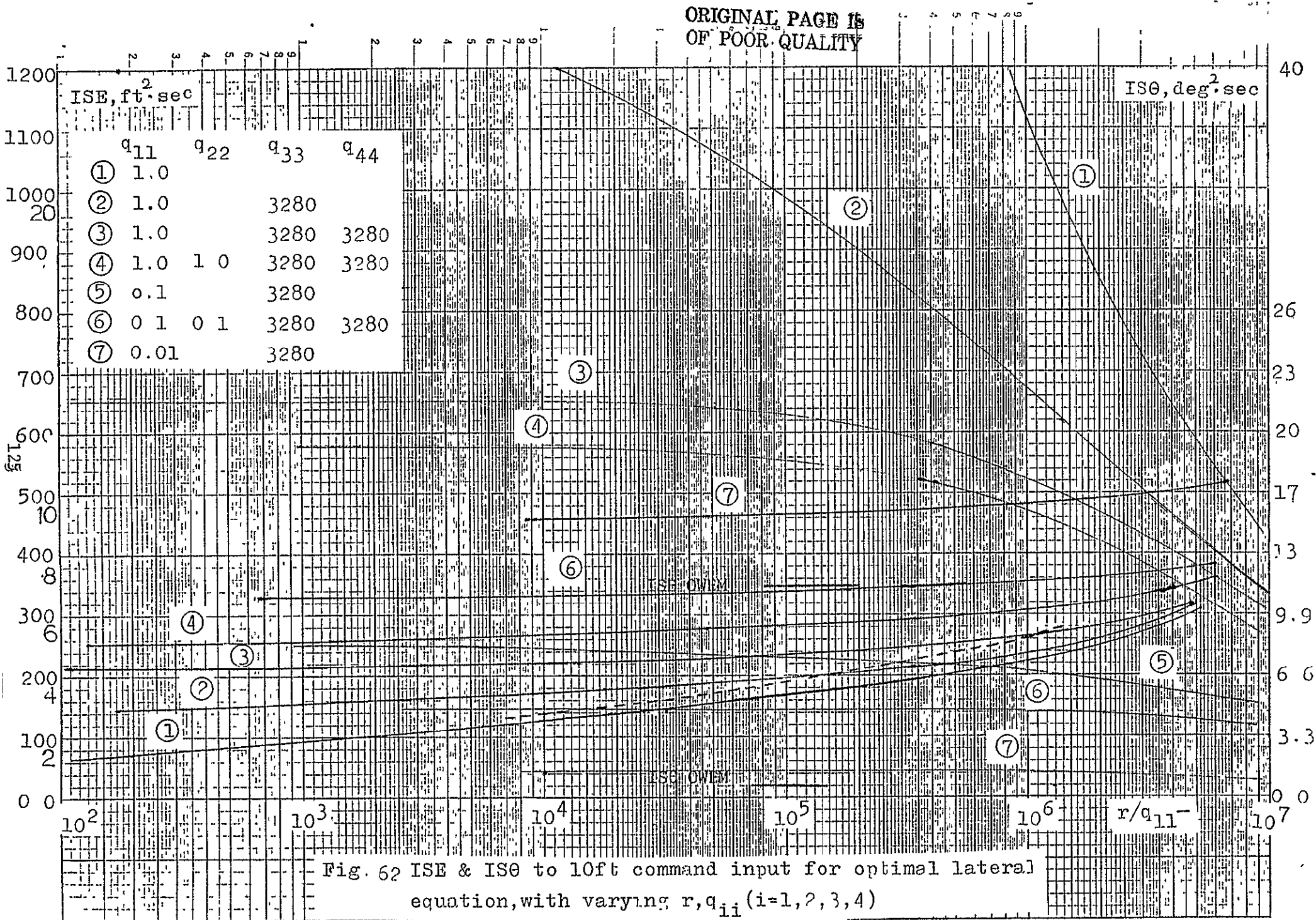


Fig. 62 ISE & ISE0 to 10ft command input for optimal lateral equation, with varying r, q_{ii} ($i=1,2,3,4$)

126

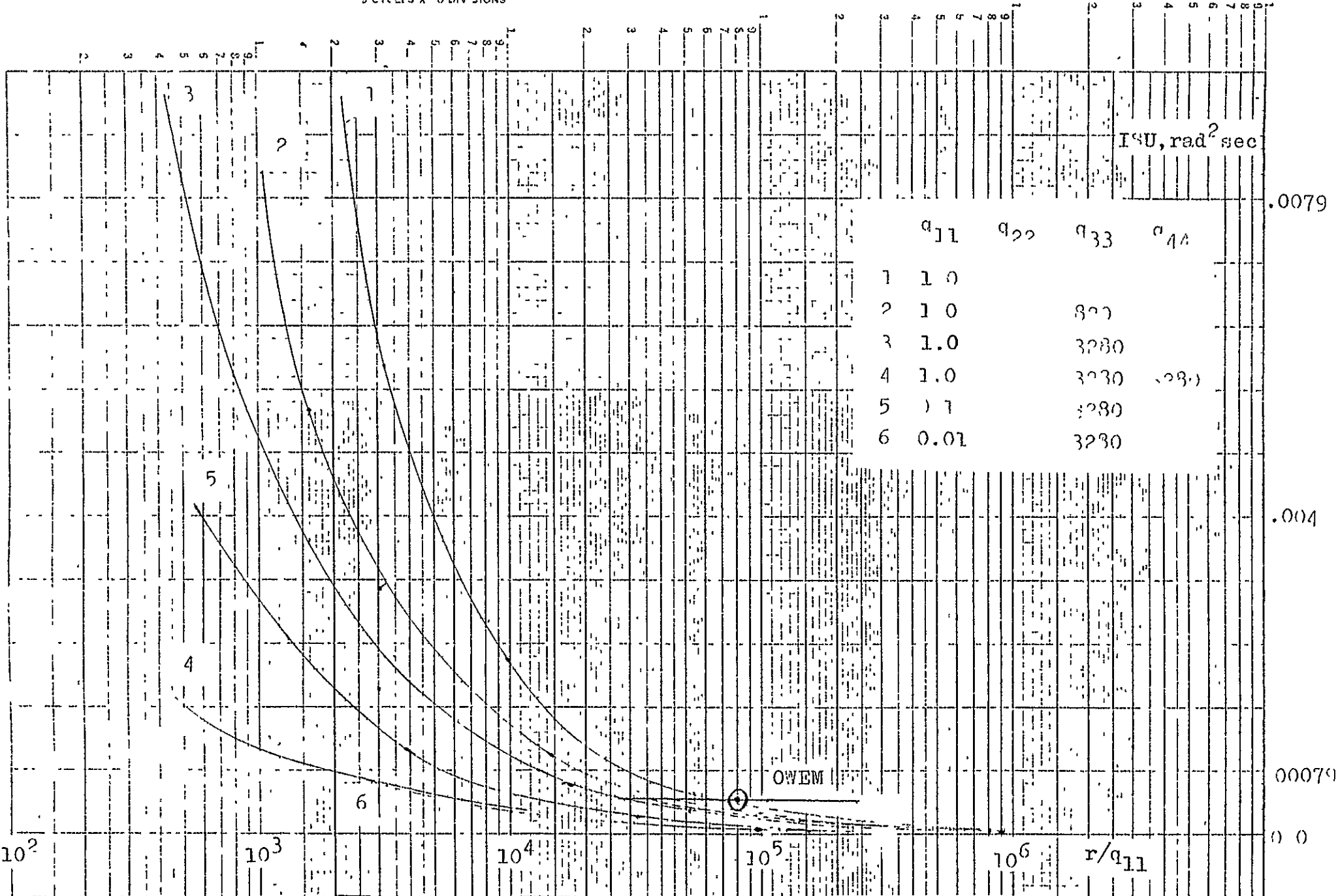


Fig. 63 ISU to 10ft command in ut for optimal lateral equation, with varying r & q_{ii} (i=1 2 3,4)

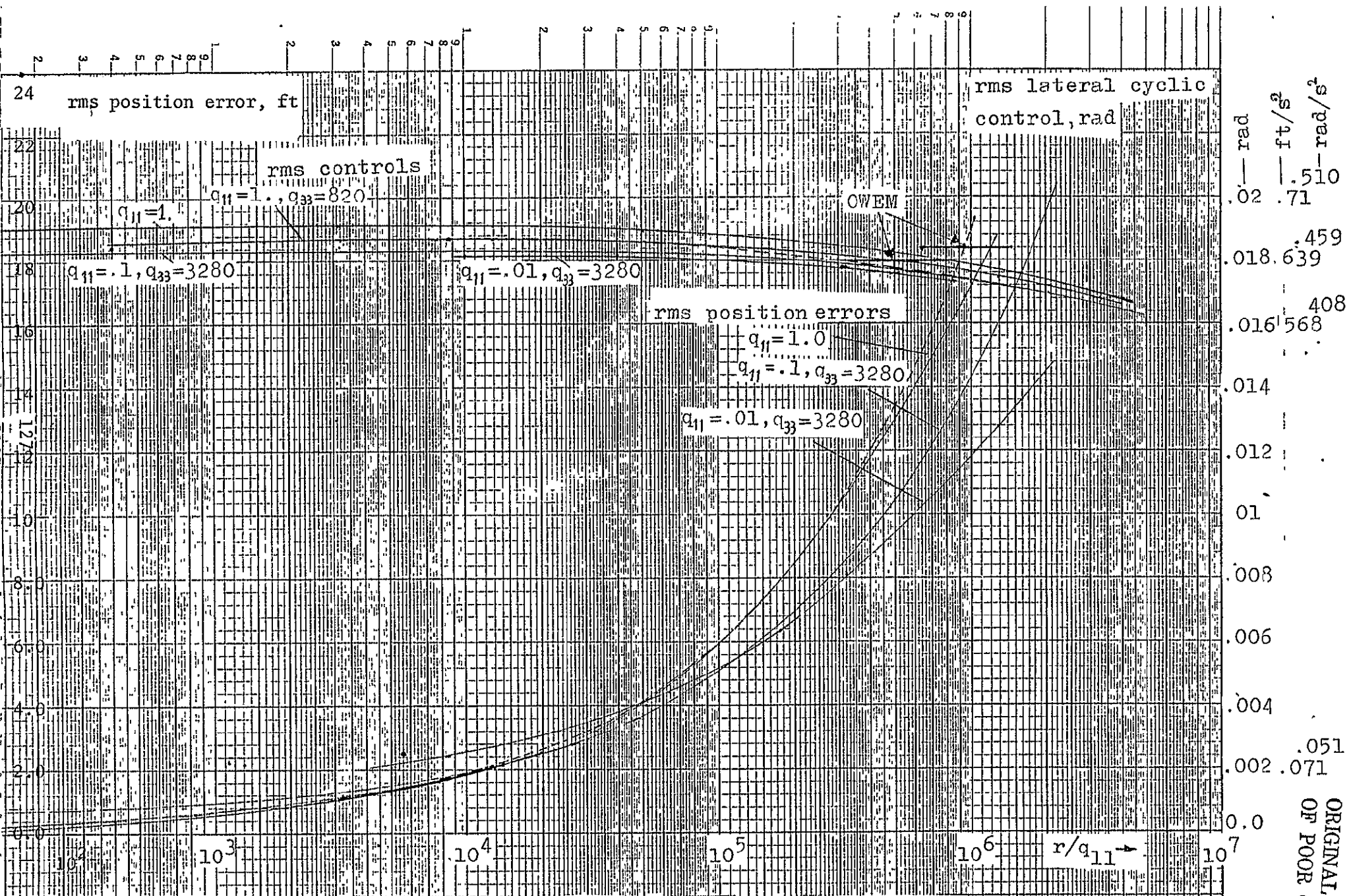


Fig. 64 rms lateral position errors & rms controls to random gust input ($\sigma = 20 \text{ ft/s}, d = .314 \text{ rad/s}$), with varying r, q_{ii}

ORIGINAL PAGE IS OF POOR QUALITY

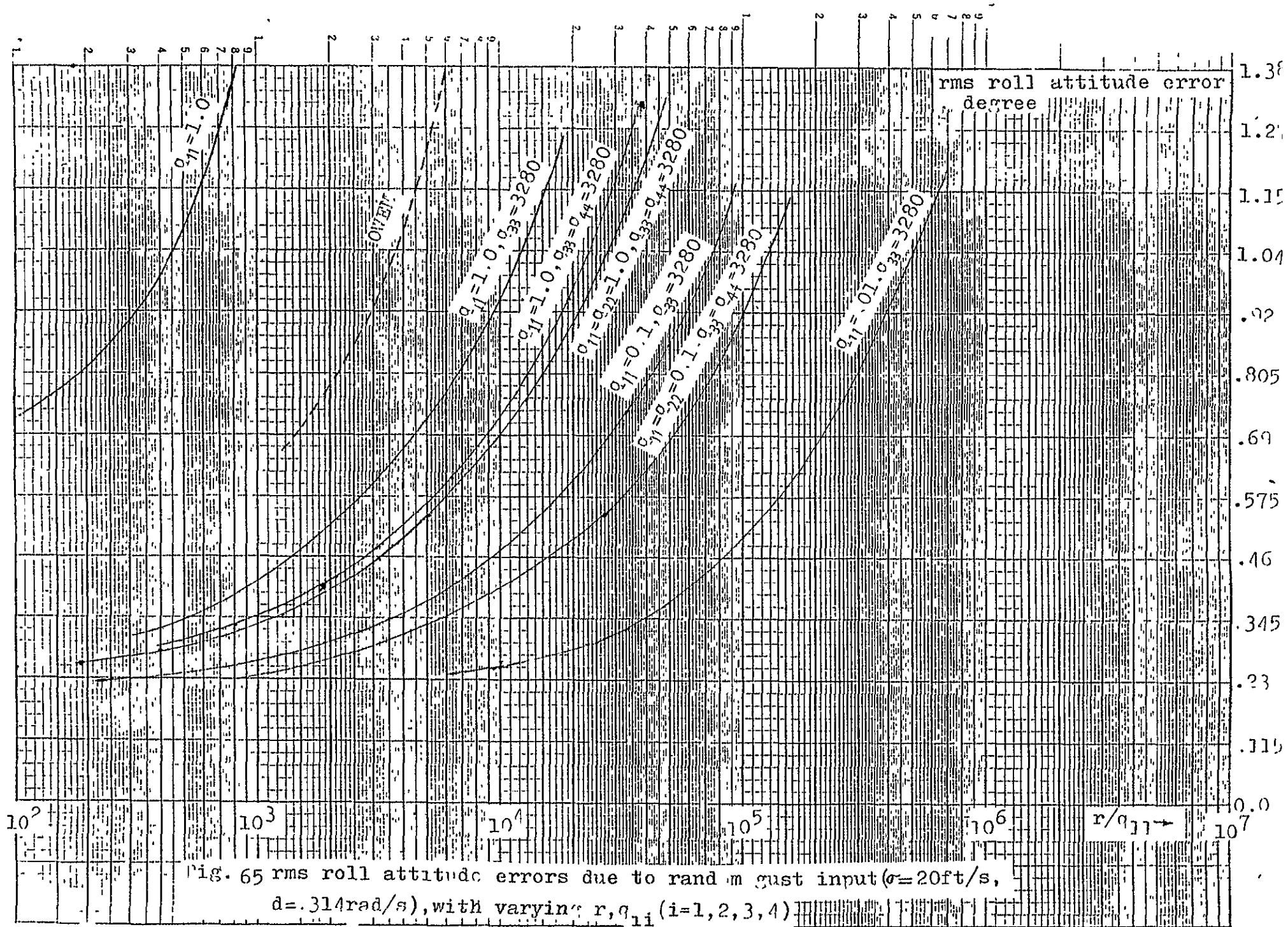
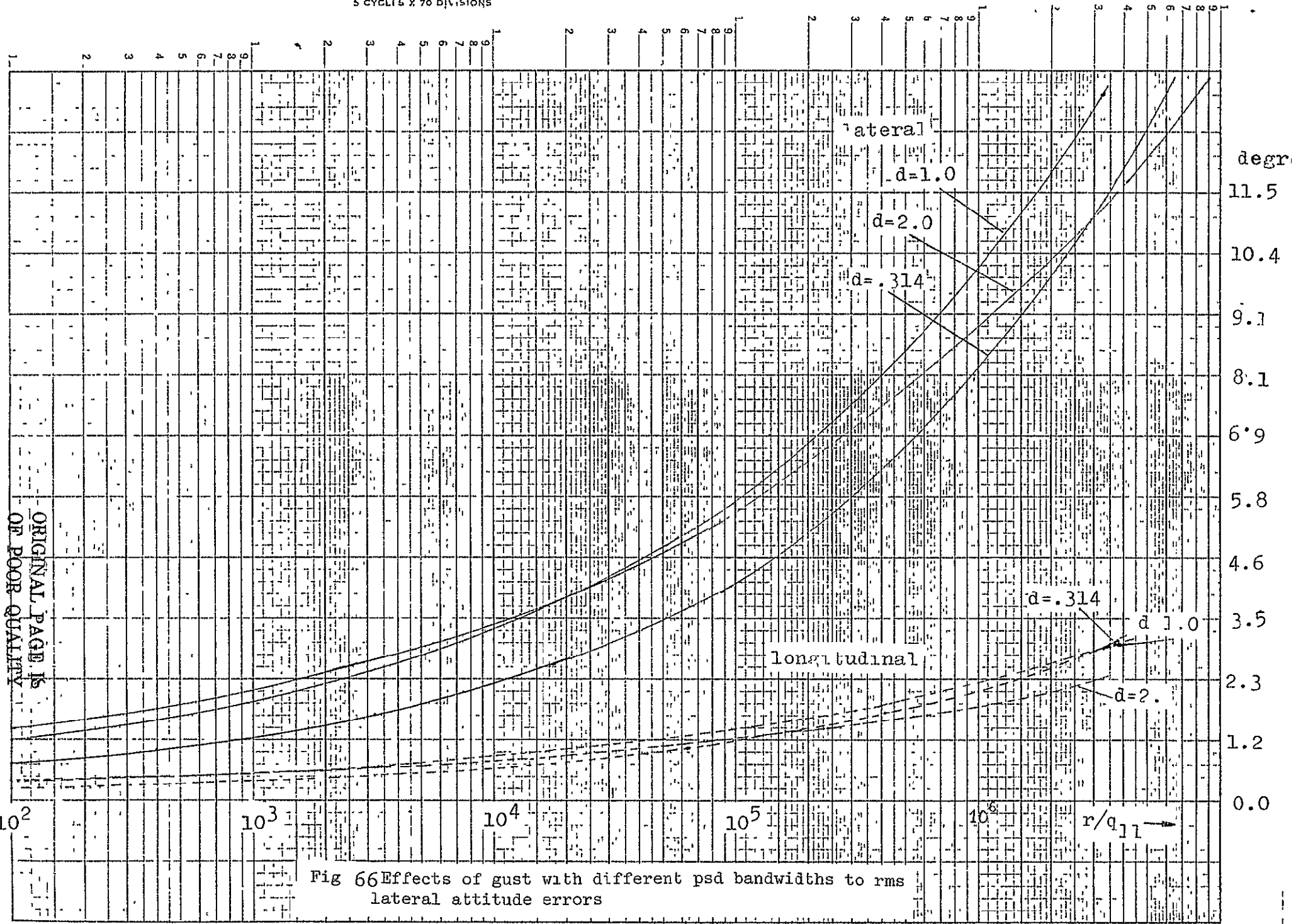


Fig. 65 rms roll attitude errors due to random gust input ($\sigma = 20 \text{ft/s}$, $d = .314 \text{rad/s}$), with varying r, q_{11} ($i = 1, 2, 3, 4$)

129



ORIGINAL PAGE IS
 OF POOR QUALITY

Fig 66 Effects of gust with different psd bandwidths to rms lateral attitude errors

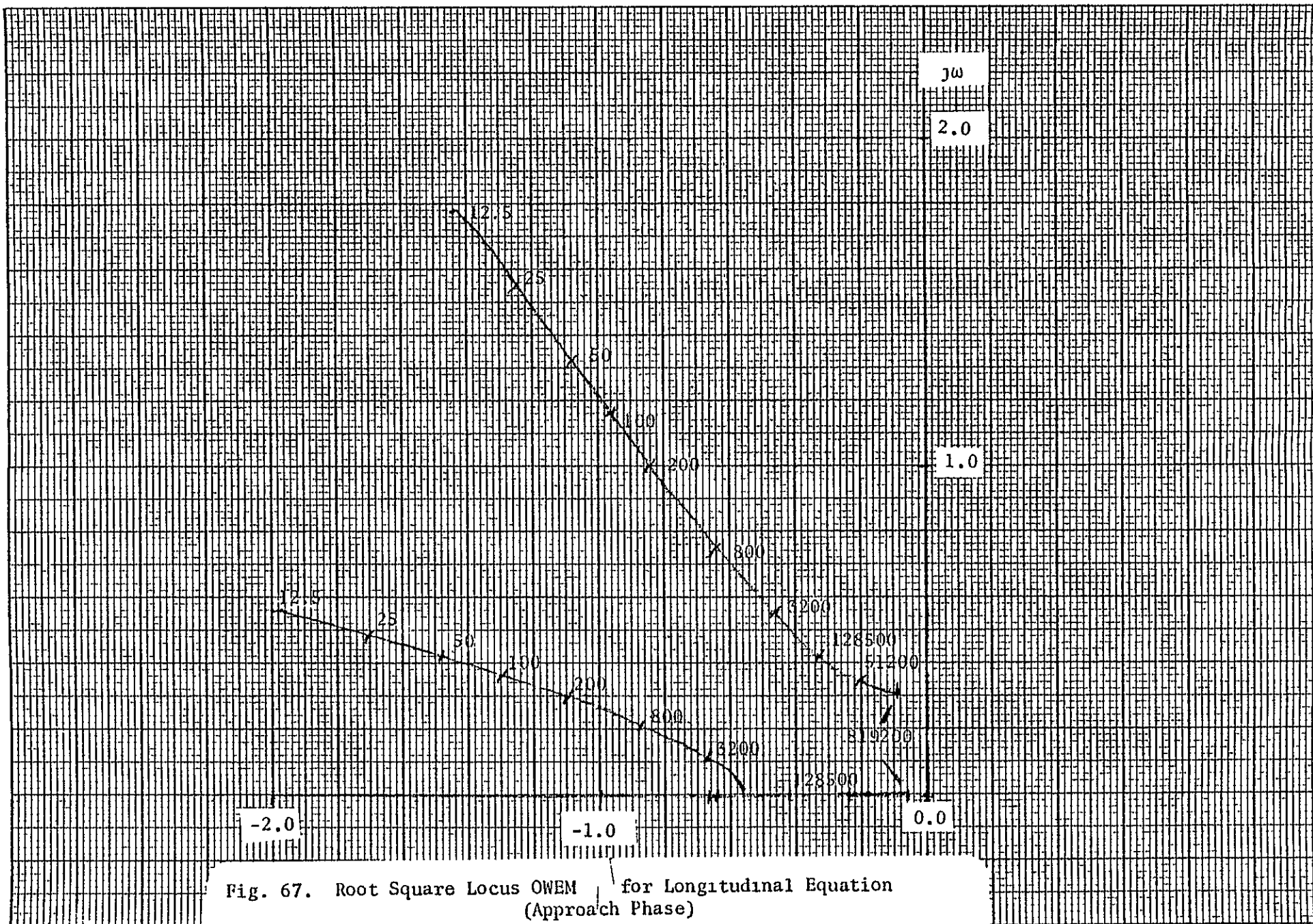


Fig. 67. Root Square Locus OWEM for Longitudinal Equation (Approach Phase)

131
 ORIGINAL PAGE IS
 OF POOR QUALITY

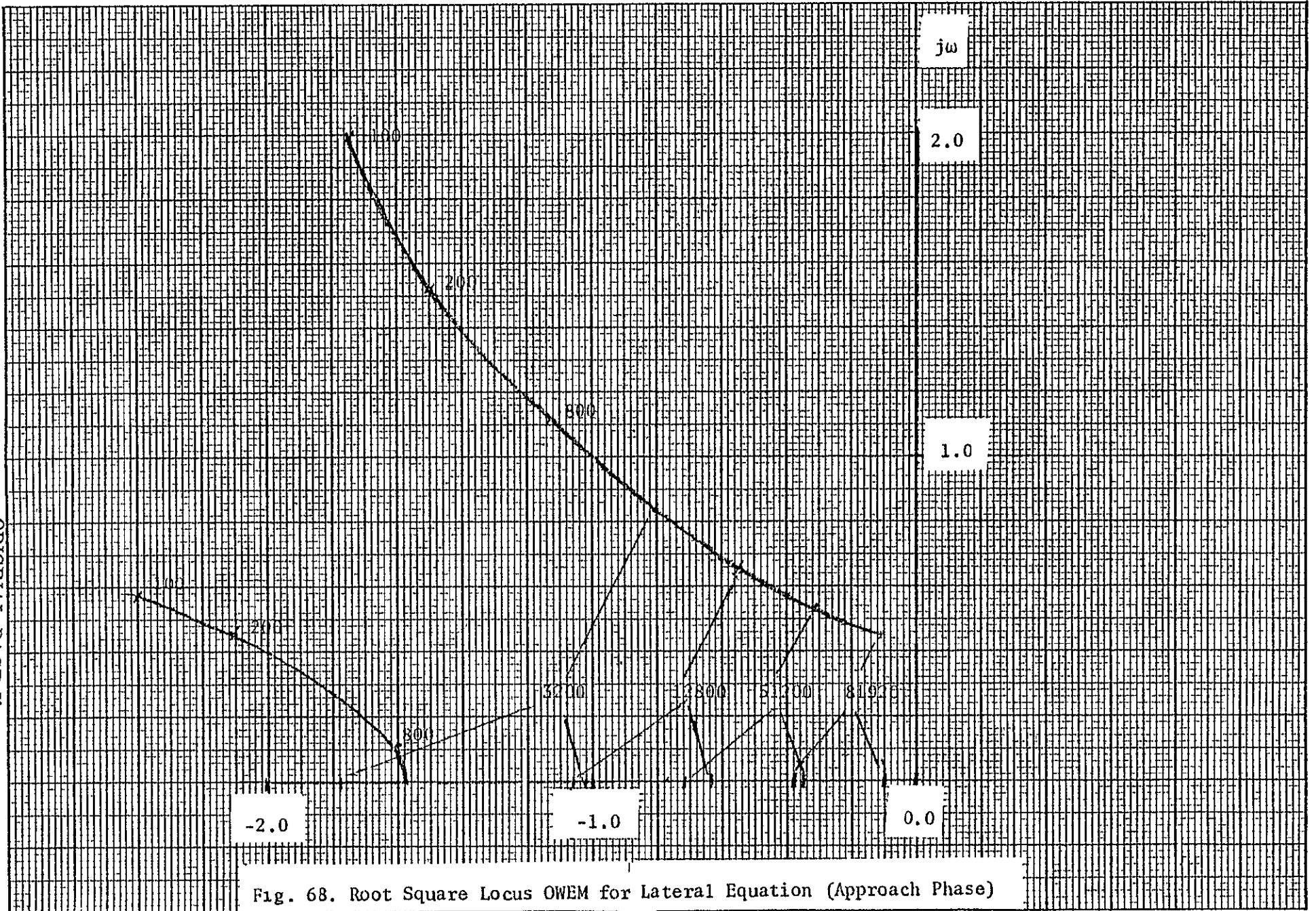
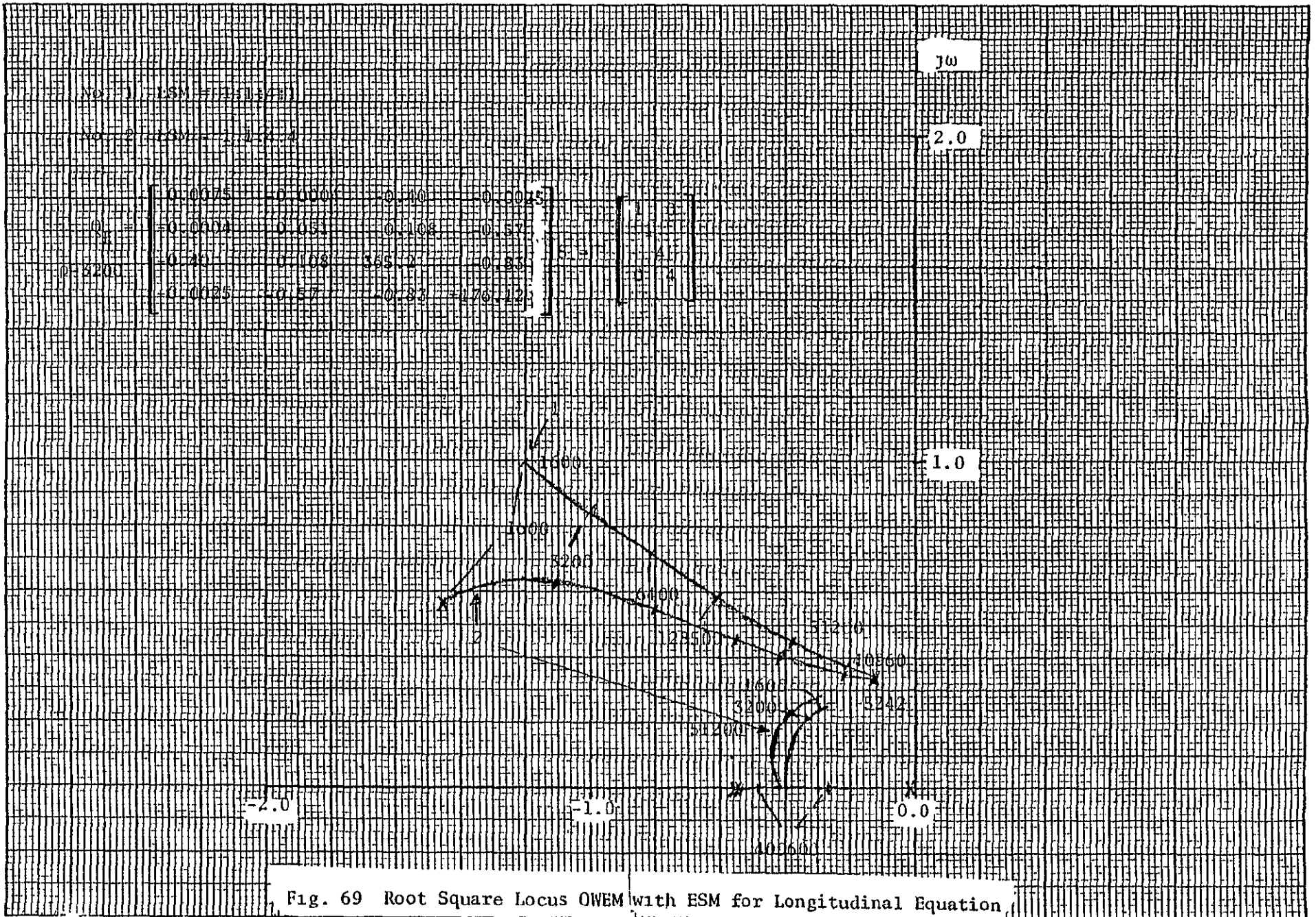


Fig. 68. Root Square Locus OWEM for Lateral Equation (Approach Phase)



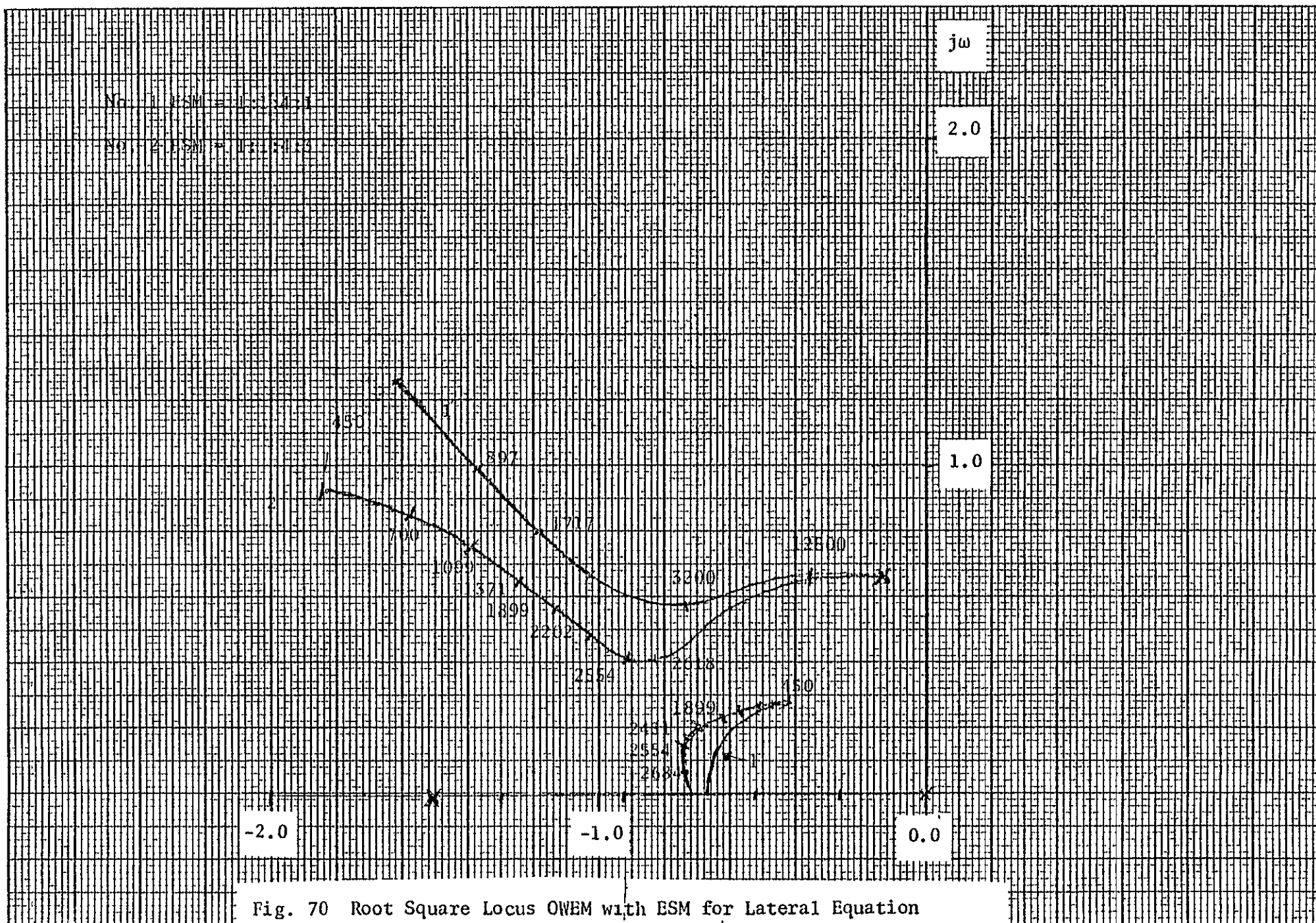


Fig. 70 Root Square Locus OWEM with ESM for Lateral Equation

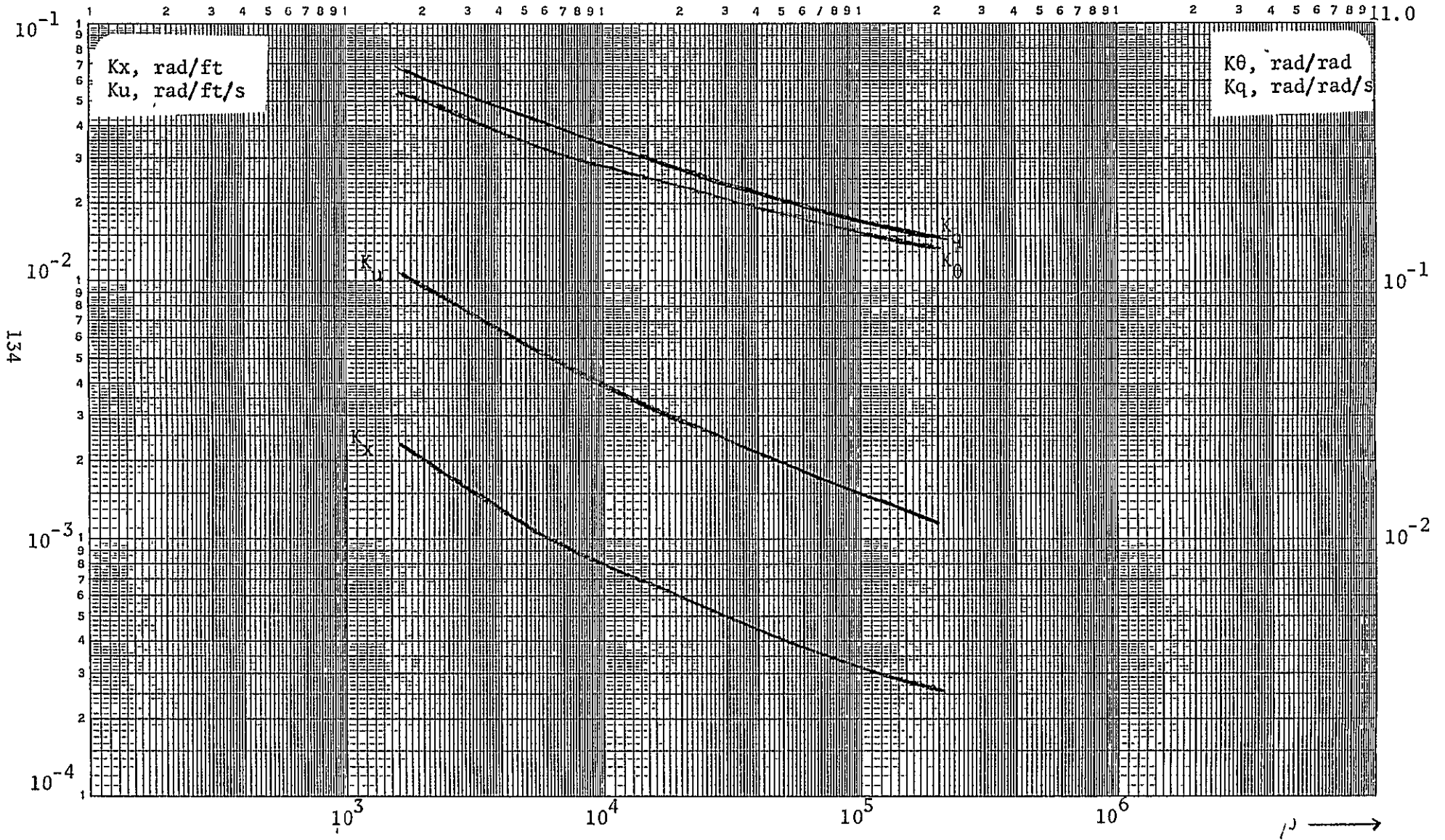


Figure 71. Longitudinal Gains OMEM with ESM (1:1:4:4)

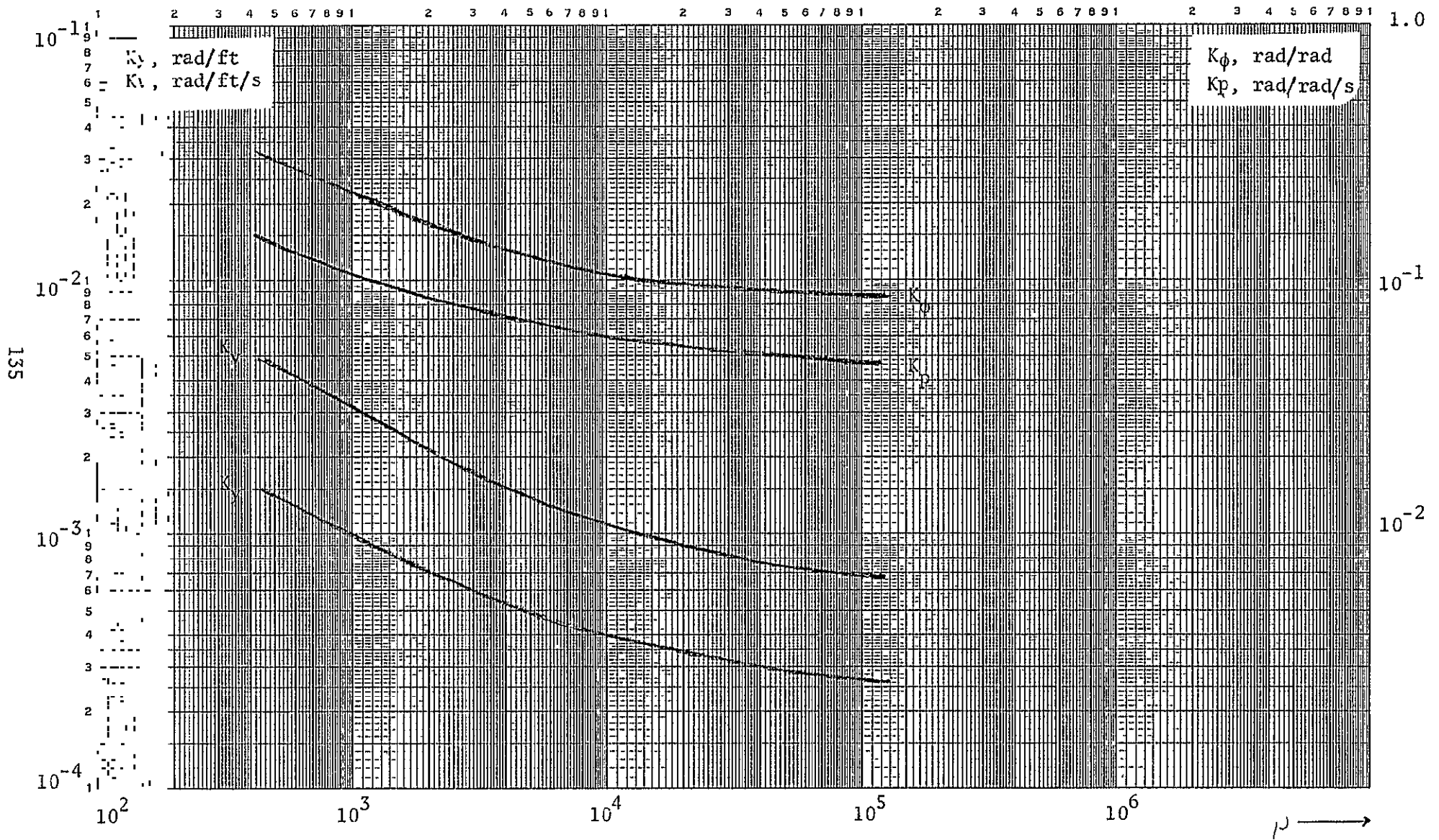


Figure 72. Lateral Gain OMEM with ESM (1:1:4:3)

APPENDIX A1

REVIEW OF HELICOPTER DYNAMICS

Introduction

In a synthesis or analysis of a control system of helicopters, we are confronted with the complexity of the overall helicopter dynamics. Therefore, simplifications often are made and are considered the simplified equations. However, this can be an oversimplification and when the system is constructed, the resulting system may have undesirable properties.

Although the higher order equation can be manipulated by the computer, the analysis and synthesis cannot be easily done. Also the physical insight into the dynamics is often lost during a process of computation. Finally, we would be obliged to use brute forces of computing all parameter variations in order to know their effects. The synthesized controller may become complex, and often becomes more expensive and less reliable. In practice, the precision of hovering can be diminished because of coupling effects.

In general, the complicated dynamics are due to many coupling terms which come from asymmetrical body and power sources. With the exception of a few terms such as (L_r and N_v) which contribute to dynamic stability, they usually bring undesirable effects into the dynamics. These effects can be shown from a sensitivity analysis on coupling terms.

In order to circumvent these things, the dynamics are required to be decoupled. The control of the helicopter then becomes simpler and easier. The analysis and synthesis can be applied to such conventional techniques such as root locus and frequency methods which basically deal with the single

input-single output system. The dynamics can be evaluated by hand calculation. Even in such modern control techniques as optimal control using state space concepts, the analysis and synthesis technique becomes more tractable. This method will be dealt with in the other appendices.

Helicopter Dynamics

In general, the helicopter dynamics are written with respect to the stability axis [Ref. A1]. The following small angle conditions are assumed and higher order terms are neglected.

$$\sin \theta = \theta, \cos \theta = 1, \sin \phi = \phi, \cos \phi = 1 \quad , \quad (A1-1)$$

$$\dot{\theta} = q, \dot{\phi} = p, \dot{\psi} = r$$

$$\dot{u} + g \cos \gamma_o \theta = X_u u + X_v v + X_w w + X_p p + X_q q + X_r r + \Delta X_c$$

$$\dot{v} - g \cos \gamma_o \phi = Y_u u + Y_v v + Y_w w + Y_p p + Y_q q + (Y_r - U_o) r + \Delta Y_c$$

$$\dot{w} + g \sin \gamma_o \theta = Z_u u + Z_v v + Z_w w + Z_p p + (Z_q + U_o) q + Z_r r + \Delta Z_c$$

$$\dot{p} - \dot{r} \frac{I_{xz}}{I_x} = L_u u + L_v v + L_w w + L_p p + L_q q + L_r r + \Delta L_c$$

$$\dot{q} = M_u u + M_v v + M_w w + M_p p + M_q q + M_r r + \Delta M_c$$

$$\dot{r} - \dot{p} \frac{I_{xz}}{I_z} = N_u u + N_v v + N_w w + N_p p + N_q q + N_r r + \Delta N_c$$

(A1-2)

where

$$\begin{aligned}
 \Delta X_c &= X_{B_{1s}} B_{1s} + X_{A_{1s}} A_{1s} + X_{\delta_c} \delta_c + X_{\delta_r} \delta_r \\
 \Delta Y_c &= Y_{B_{1s}} B_{1s} + Y_{A_{1s}} A_{1s} + Y_{\delta_c} \delta_c + Y_{\delta_r} \delta_r \\
 \Delta Z_c &= Z_{B_{1s}} B_{1s} + Z_{A_{1s}} A_{1s} + Z_{\delta_c} \delta_c + Z_{\delta_r} \delta_r \\
 \Delta L_c &= L_{B_{1s}} B_{1s} + L_{A_{1s}} A_{1s} + L_{\delta_c} \delta_c + L_{\delta_r} \delta_r \\
 \Delta M_c &= M_{B_{1s}} B_{1s} + M_{A_{1s}} A_{1s} + M_{\delta_c} \delta_c + M_{\delta_r} \delta_r \\
 \Delta N_c &= N_{B_{1s}} B_{1s} + N_{A_{1s}} A_{1s} + N_{\delta_c} \delta_c + N_{\delta_r} \delta_r
 \end{aligned}
 \tag{A1-3}$$

The new derivatives for cancelling the inertia coupling terms are introduced into the last two equations of (A1-2) [Ref. A2].

$$\begin{aligned}
 -\dot{p} + L'_u \dot{u} + L'_v \dot{v} + L'_w \dot{w} + L'_p \dot{p} + L'_q \dot{q} + L'_r \dot{r} + \Delta L'_c &= 0 \\
 -\dot{r} + N'_u \dot{u} + N'_v \dot{v} + N'_w \dot{w} + N'_p \dot{p} + N'_q \dot{q} + N'_r \dot{r} + \Delta N'_c &= 0
 \end{aligned}
 \tag{A1-4}$$

where

$$L'_u = \frac{L_u + \frac{I_{xz}}{I_x} N_u}{1 - \frac{(L_{xz})^2}{I_x I_z}}, \quad L'_v = \frac{L_v + \frac{I_{xz}}{I_x} N_v}{1 - \frac{(I_{xz})^2}{I_x I_z}}, \quad \dots \text{ etc.}
 \tag{A1-5}$$

$$N'_u = \frac{N_u + \frac{I_{xz}}{I_z} L_u}{1 - \frac{I_{xz}^2}{I_x I_z}}, \quad N'_v = \frac{N_v + \frac{I_{xz}}{I_z} L_v}{1 - \frac{I_{xz}^2}{I_x I_z}}, \quad \dots \text{ etc.}$$

In the same way,

$$\Delta L'_c = L'_{B_{1s}} B_{1s} + L'_{A_{1s}} A_{1s} + I'_{\delta_c} \delta_c + L'_{\delta_r} \delta_r \quad (\text{A1-6})$$

$$\Delta N'_c = N'_{B_{1s}} B_{1s} + N'_{A_{1s}} A_{1s} + N'_{\delta_c} \delta_c + N'_{\delta_r} \delta_r$$

where

$$L'_{B_{1s}} = \frac{L_{B_{1s}} + \frac{I_{xz}}{I_x} N_{B_{1s}}}{1 - \frac{I_{xz}^2}{I_x I_z}}, \quad L'_{\delta_c} = \frac{L_{\theta_0} + \frac{I_{xz}}{I_x} N_{\delta_c}}{1 - \frac{I_{xz}^2}{I_x I_z}}, \quad \dots \text{ etc.} \quad (\text{A1-7})$$

$$N'_{B_{1s}} = \frac{N_{B_{1s}} + \frac{I_{xz}}{I_z} L_{B_{1s}}}{1 - \frac{I_{xz}^2}{I_x I_z}}, \quad N'_{\delta_c} = \frac{N_{\delta_c} + \frac{I_{xz}}{I_z} L_{\delta_c}}{1 - \frac{I_{xz}^2}{I_x I_z}}, \quad \dots \text{ etc.}$$

In hovering, the helicopter dynamics are desirable to be decoupled into the longitudinal, vertical, lateral and yawing motions, though these conditions change in transition and forward flight. The dynamic equations to be decoupled are rewritten in state variable form in Eq. A1-8. The broken lines make 4 x 4 submatrices which clarify main diagonal and off diagonal terms. The uncoupled equations with the noise terms added become as given in Eq. A1-9.

$$\begin{bmatrix} \dot{u} \\ \dot{\theta} \\ \dot{q} \\ \dot{w} \\ \dot{v} \\ \dot{\phi} \\ \dot{p} \\ \dot{r} \end{bmatrix} = \begin{bmatrix} X_u & -g\cos\gamma_0 & X_q & X_w & X_v & 0 & X_p & X_r \\ 0 & 0 & 1 & 0 & 0 & 0 & 0 & 0 \\ M_u & 0 & M_q & M_w & M_v & 0 & M_p & M_r \\ Z_u & -g\sin\gamma_0 & Z_{q+u_0} & Z_w & Z_v & 0 & Z_p & Z_r \\ Y_u & 0 & Y_q & Y_w & Y_v & g\cos\gamma_0 & Y_p & Y_{r-u_0} \\ 0 & 0 & 0 & 0 & 0 & 0 & 1 & 0 \\ L'_u & 0 & L'_q & L'_w & L'_v & 0 & L'_p & L'_{r-u_0} \\ N'_u & 0 & N'_q & N'_w & N'_v & 0 & N'_p & N'_r \end{bmatrix} \begin{bmatrix} u \\ \theta \\ q \\ w \\ v \\ \phi \\ p \\ r \end{bmatrix}$$

$$\begin{bmatrix} X_{B_{1s}} & X_{\delta_c} & X_{A_{1s}} & X_{\delta_r} \\ 0 & 0 & 0 & 0 \\ M_{B_{1s}} & M_{\delta_c} & M_{A_{1s}} & M_{\delta_r} \\ Z_{B_{1s}} & Z_{\delta_c} & Z_{A_{1s}} & Z_{\delta_r} \\ Y_{B_{1s}} & Y_{\delta_c} & Y_{A_{1s}} & Y_{\delta_r} \\ 0 & 0 & 0 & 0 \\ L'_{B_{1s}} & L'_{\delta_c} & L'_{A_{1s}} & L'_{\delta_r} \\ N'_{B_{1s}} & N'_{\delta_c} & N'_{A_{1s}} & N'_{\delta_r} \end{bmatrix} \begin{bmatrix} B_{1s} \\ \delta_c \\ A_{1s} \\ \delta_r \end{bmatrix}$$

(A1-8)

ORIGINAL PAGE IS
OF POOR QUALITY

$$\begin{bmatrix} \dot{u} \\ \dot{\theta} \\ \dot{q} \\ \dot{w} \\ \dot{v} \\ \dot{\phi} \\ \dot{p} \\ \dot{r} \end{bmatrix} = \begin{bmatrix} X_u & -g \cos \gamma_0 & X_q & X_w & 0 & 0 & 0 & 0 \\ 0 & 0 & 1 & 0 & 0 & 0 & 0 & 0 \\ M_u & 0 & M_q & M_w & 0 & 0 & 0 & 0 \\ \hline Z_u & -g \sin \gamma_0 & +u_0 & Z_w & 0 & 0 & 0 & 0 \\ 0 & 0 & 0 & 0 & Y_v & g \cos \gamma_0 & Y_p & -u_0 \\ 0 & 0 & 0 & 0 & 0 & 0 & 1 & 0 \\ q & 0 & 0 & 0 & L'_v & 0 & L'_p & L'_r - u_0 \\ 0 & 0 & 0 & 0 & N'_v & 0 & N'_p & N'_r \end{bmatrix} \begin{bmatrix} u \\ \theta \\ q \\ w \\ v \\ \phi \\ p \\ r \end{bmatrix} +$$

$$\begin{bmatrix} X_{B_{1s}} & X_{\delta_c} & 0 & 0 \\ 0 & 0 & 0 & 0 \\ M_{B_{1s}} & M_{\delta_c} & 0 & 0 \\ \hline Z_{B_{1s}} & Z_{\delta_c} & 0 & 0 \\ 0 & 0 & Y_{A_{1s}} & Y_{\delta_r} \\ 0 & 0 & 0 & 0 \\ 0 & 0 & L'_{A_{1s}} & L'_{\delta_r} \\ \hline 0 & 0 & N'_{A_{1s}} & N'_{\delta_r} \end{bmatrix} \begin{bmatrix} B_{1s} \\ \delta_c \\ A_{1s} \\ \delta_r \end{bmatrix} + \begin{bmatrix} -X_u & -X_w & 0 \\ 0 & 0 & 0 \\ -M_u & -M_w & 0 \\ -Z_u & -Z_w & 0 \\ 0 & 0 & -Y_v \\ 0 & 0 & 0 \\ 0 & 0 & -L'_v \\ 0 & 0 & -N'_v \end{bmatrix} \begin{bmatrix} u_g \\ w_g \\ v_g \end{bmatrix} \quad (A1-9)$$

ORIGINAL PAGE IS
OF POOR QUALITY

In near hover flight one often assumes $u_0 = 0, \gamma_0 = 0$, and the following stability derivatives are often negligibly small and often assumed to be zero or:

$$X'_w = M'_w = Z'_u = 0; X'_{\delta_c} = M'_{\delta_c} = Z'_{B_{1s}} = 0$$

$$N'_p = N'_v = L'_r = 0; Y'_{\delta_r} = L'_{\delta_r} = N'_{A_{1s}} = 0$$

With these assumption Equation A1-9 then becomes:

$$\begin{bmatrix} \dot{u} \\ \dot{\theta} \\ \dot{q} \\ \dot{w} \\ \dot{v} \\ \dot{\phi} \\ \dot{p} \\ \dot{r} \end{bmatrix} = \begin{bmatrix} X_u & -g & X_q & 0 & 0 & 0 & 0 & 0 \\ 0 & 0 & 1 & 0 & 0 & 0 & 0 & 0 \\ M_u & 0 & M_q & 0 & 0 & 0 & 0 & 0 \\ \hline 0 & 0 & 0 & Z_w & 0 & 0 & 0 & 0 \\ \hline 0 & 0 & 0 & 0 & Y_v & g & Y_p & Y_r \\ 0 & 0 & 0 & 0 & 0 & 0 & 1 & 0 \\ 0 & 0 & 0 & 0 & L_v & 0 & L_p & 0 \\ \hline 0 & 0 & 0 & 0 & 0 & 0 & 0 & N_r \end{bmatrix} \begin{bmatrix} u \\ \theta \\ q \\ w \\ v \\ \phi \\ p \\ r \end{bmatrix}$$

(continued next page)

$$\begin{bmatrix}
 X_{B_{1s}} & 0 & 0 & 0 \\
 0 & 0 & 0 & 0 \\
 M_{B_{1s}} & 0 & 0 & 0 \\
 \hline
 0 & Z_{\delta_c} & 0 & 0 \\
 \hline
 0 & 0 & Y_{A_{1s}} & 0 \\
 0 & 0 & 0 & 0 \\
 0 & 0 & L_{A_{1s}} & 0 \\
 \hline
 0 & 0 & 0 & N_{\delta_r}
 \end{bmatrix}
 \begin{bmatrix}
 B_{1s} \\
 \delta_c \\
 A_{1s} \\
 \delta_r
 \end{bmatrix}$$

$$\begin{bmatrix}
 -X_u & 0 & 0 \\
 0 & 0 & 0 \\
 -M_u & 0 & 0 \\
 \hline
 0 & -Z_w & 0 \\
 0 & 0 & -Y_v \\
 0 & 0 & 0 \\
 0 & 0 & -L'_v \\
 0 & 0 & -N'_v
 \end{bmatrix}
 \begin{bmatrix}
 u_{\sigma} \\
 w_{\sigma} \\
 v_{\sigma}
 \end{bmatrix}$$

(A1-10)

Helicopter Transfer Functions

For conventional analysis, the equations of motions are often written in the Laplace domain. The longitudinal and lateral uncoupled equations of motion for the control rate derivatives and gust inputs are:

Longitudinal-Vertical Equations of Motion

Assumptions

$$X_{\dot{w}} = Z_{\dot{w}} = 0, \quad \theta_o = 0,$$

$$X_{\alpha} = Z_{\alpha} = M_{\alpha} = M_{\dot{\alpha}} = 0$$

$$\begin{bmatrix} s-X_u & -X_w & -X_q s + g \cos \gamma_o \\ -Z_u & s-Z_w & -(Z_q + U_o) s + g \sin \gamma_o \\ -M_u & -M_w s - M_w & s^2 - M_q \end{bmatrix} \begin{bmatrix} u \\ w \\ \theta \end{bmatrix} = \begin{bmatrix} X_{B_1 s} + X_{B_1} & X_{\delta_c} \\ Z_{B_1 s} + Z_{B_1} & Z_{\delta_c} \\ M_{B_1 s} + M_{B_1} & M_{\delta_c} \end{bmatrix} \begin{bmatrix} B_{1s} \\ \delta_c \end{bmatrix} +$$

$$\begin{bmatrix} -X_u & -X_w \\ -Z_u & -Z_w \\ -M_u & -M_w \end{bmatrix} \begin{bmatrix} u_g \\ w_g \end{bmatrix}$$

(A1-11a)

Lateral-Directional Equations of Motion

Assumptions

$$Y_{\dot{v}} = L_{\dot{v}} = N_{\dot{v}} = 0$$

$$\begin{bmatrix} s - Y_v & -Y_p s - g \cos \gamma_0 & -Y_r s + U_0 Y_v \\ -L'_v & s^2 - L'_p s & -L'_r s + U_0 L'_v \\ -N'_v & -N'_p s & s^2 - N'_r s + U_0 N'_v \end{bmatrix} \begin{bmatrix} v \\ \phi \\ \psi \end{bmatrix} = \begin{bmatrix} Y_{A_{1s}} & Y_{\delta_r} \\ L'_{A_{1s}} & L'_{\delta_r} \\ N'_{A_{1s}} & N'_{\delta_r} \end{bmatrix} \begin{bmatrix} A_{1s} \\ \delta_r \end{bmatrix} + \\
+ \begin{bmatrix} -Y_v \\ -L'_v \\ -N'_v \end{bmatrix} \begin{bmatrix} v_g \\ \phi_g \\ \psi_g \end{bmatrix} \quad (A1-11b)$$

The basic equations of motion for a helicopter near hover with $\gamma = 0$;

$$U_0 = 0$$

Longitudinal:

$$\begin{bmatrix} s - X_u & -X_w & X_q s + g \\ -Z_u & s - Z_w & -Z_q s \\ -M_u & -M_w & s^2 - M_q s \end{bmatrix} \begin{bmatrix} u \\ w \\ \theta \end{bmatrix} = \begin{bmatrix} X_{B_{1s}} & +X_{B_{1s}} & X_{\delta_c} \\ Z_{B_{1s}} & +Z_{B_{1s}} & Z_{\delta_c} \\ M_{B_{1s}} & +M_{B_{1s}} & M_{\delta_c} \end{bmatrix} \begin{bmatrix} B_{1s} \\ \delta_c \end{bmatrix} + \\
+ \begin{bmatrix} -X_u & -X_w \\ -Z_u & -Z_w \\ -M_u & -M_w \end{bmatrix} \begin{bmatrix} u_g \\ w_g \\ \theta_g \end{bmatrix} \quad (A1-12a)$$

Lateral:

$$\begin{bmatrix} s-Y_v & -Y_p s-g & -Y_r s \\ -L_v & s^2-L_p s & -L_r s \\ -N_v & -N_p s & s^2-N_r s \end{bmatrix} \begin{bmatrix} v \\ \phi \\ \psi \end{bmatrix} = \begin{bmatrix} Y_{A_{1s}} & Y_{\delta_r} \\ L_{A_{1s}} & L_{\delta_r} \\ N_{A_{1s}} & N_{\delta_r} \end{bmatrix} \begin{bmatrix} A_1 \\ \delta_r \end{bmatrix} + \begin{bmatrix} -Y_v \\ -L_v \\ -N_v \end{bmatrix} \begin{bmatrix} v \\ g \end{bmatrix}$$

(A1-12b)

Often are negligible, small and neglected:

$$\begin{aligned} X_w = M_w = Z_u = 0 & & X_{\delta_c} = M_{\delta_c} = Z_{B_{1s}} = 0 \\ N_p = N_v = L_r = 0 & & Y_{\delta_c} = L_{\delta_r} = N_{A_{1s}} = 0 \end{aligned}$$

Also are often neglected the control rate terms

$$X_{B_1} = Z_{B_1} = M_{B_1} = 0 \quad \text{and} \quad X_q = Z_q = 0.$$

The analog computer diagram of the longitudinal and lateral equations of motions are shown in Illustration A1-1 and A1-2.

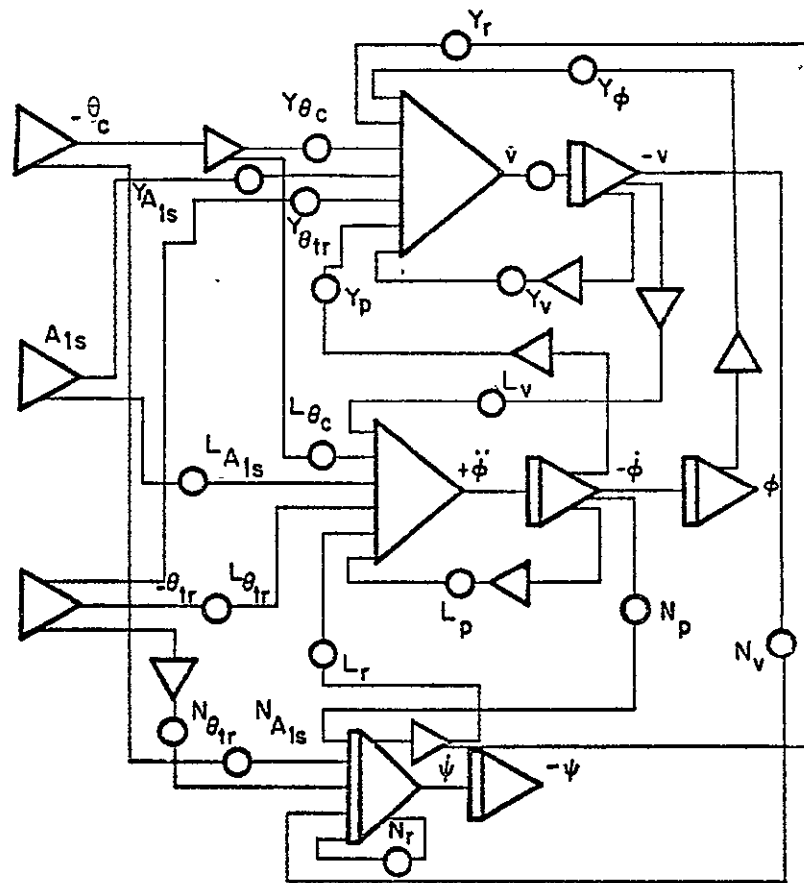


Illustration A-1a. Lateral Equations

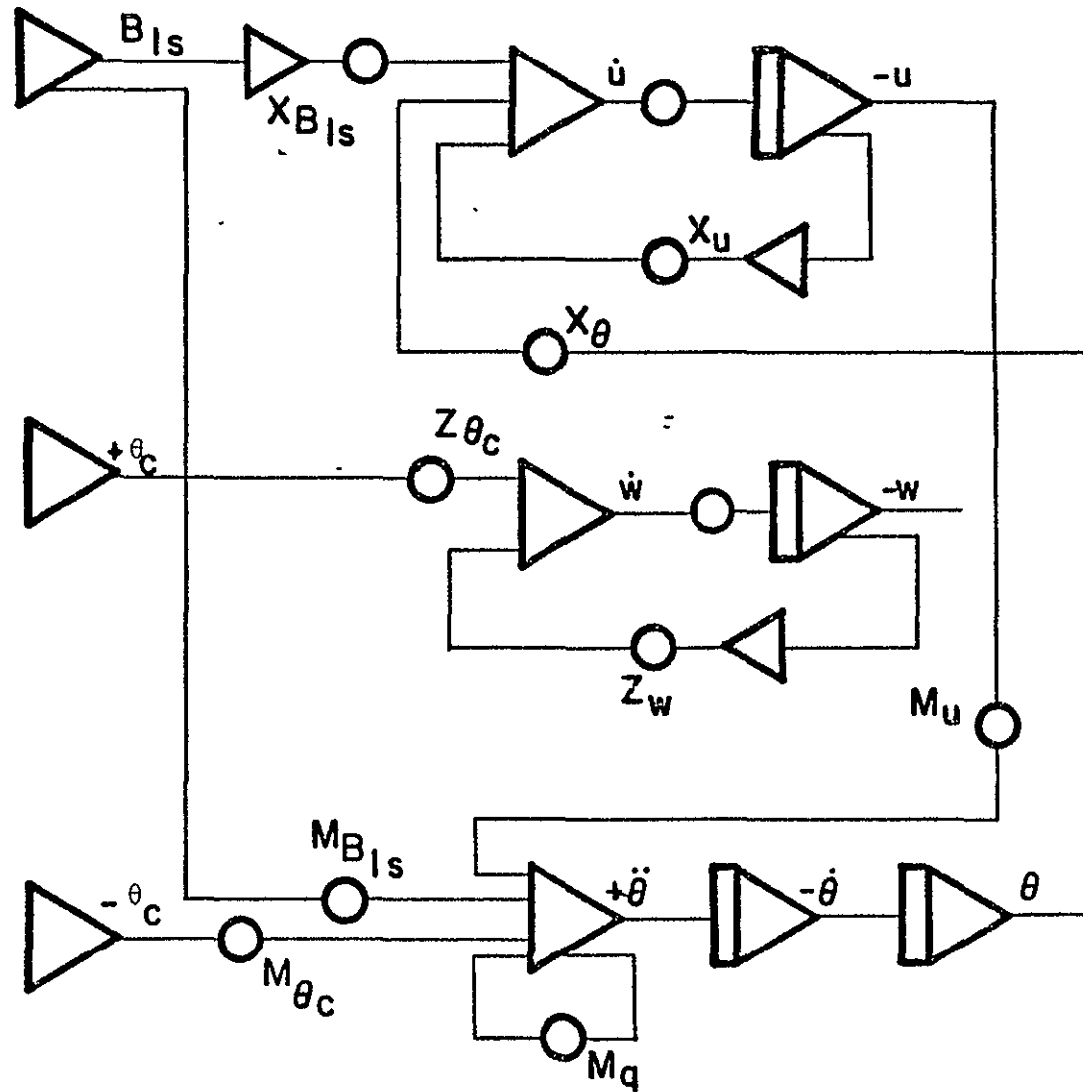


Illustration A-1b. Longitudinal Equation

Input-output Relationships (Hover)

The uncoupled sets of equations can be used to determine the input-output relationships and the effects of gust inputs.

The longitudinal equations are:

$$\begin{bmatrix} \dot{u} \\ \dot{\theta} \\ \dot{q} \end{bmatrix} = \begin{bmatrix} +X_u & -g & X_q \\ 0 & 0 & 1 \\ M_u & 0 & M_q \end{bmatrix} \begin{bmatrix} u \\ \theta \\ q \end{bmatrix} + \begin{bmatrix} X_{B_{1s}} \\ 0 \\ M_{B_{1s}} \end{bmatrix} B_{1s} + \begin{bmatrix} -X_u \\ 0 \\ -M_u \end{bmatrix} u_g \quad (\text{A1-13})$$

The basic equations are:

$$\begin{aligned} \ddot{x} + X_u \dot{x} - g\theta + M_q \dot{\theta} &= X_{B_{1s}} B_{1s} - X_u u_g \\ M_u \dot{x} + \ddot{\theta} + M_q \dot{\theta} &= M_{B_{1s}} B_{1s} - M_u u_g \end{aligned} \quad (\text{A1-14})$$

or

$$\begin{bmatrix} s-X_u & X_q s+g \\ -M_u & s^2-M_q s \end{bmatrix} \begin{bmatrix} u \\ \theta \end{bmatrix} = \begin{bmatrix} X_{B_{1s}} \\ M_{B_{1s}} \end{bmatrix} B_{1s} + \begin{bmatrix} -X_u \\ -M_u \end{bmatrix} u_g \quad (\text{A1-15})$$

The characteristic equation is:

$$\begin{aligned} \Delta &= s(s-M_q)(s-X_u) + M_u X_q s + gM_u \\ &= s^3 - (M_q + X_u)s^2 + (X_u M_q + M_u X_q)s + gM_u \end{aligned} \quad (\text{A1-16})$$

$$N_{B_{1s}}^u = \begin{vmatrix} X_{B_{1s}} & X_q s+g \\ M_{B_{1s}} & s(s-M_q) \end{vmatrix} \quad (\text{A1-17})$$

$$\begin{aligned}
N_{B_1s}^\theta &= \begin{vmatrix} s-X_u & X_{B_1} \\ -M_u & M_{B_1s} \end{vmatrix} \\
&= M_{B_1s} (s-X_u + \frac{X_{B_1s} M_u}{M_{B_1s}})
\end{aligned} \tag{A1-18}$$

The Input-Output Relationships are:

$$\frac{U}{B_{1s}} = \frac{X_{B_1s} (s^2 - (M_q - \frac{M_{B_1s} X_q}{X_{B_1s}}) s - \frac{M_{B_1s}}{X_{B_1s}} g)}{s^3 - (X_u + M_q) s^2 + (X_u M_q - M_u X_q) s + M_u g} \tag{A1-19}$$

$$\frac{X}{B_{1s}} = \frac{1}{s} \cdot \frac{u}{B_{1s}} \tag{A1-20}$$

$$\frac{\theta}{B_{1s}} = \frac{M_{B_1s} (s-X_u + \frac{X_{B_1s}}{M_{B_1s}} M_u)}{s^3 - s^2 (X_u + M_q) + (X_u M_q - M_u X_q) s + M_u g} \tag{A1-21}$$

$$\frac{Q}{B_{1s}} = \frac{M_{B_1s} s (s-X_u + \frac{X_{B_1s}}{M_{B_1s}} M_u)}{s^3 - s^2 (X_u + M_q) + (X_u M_q - M_u X_q) s + M_u g} \tag{A1-22}$$

$$= \frac{s\theta}{B_{1s}}$$

$$\frac{u}{u_g} = \frac{-X_u(s^2 - (M_q - \frac{M_u X_q}{X_u})s - \frac{M_u}{X_u}g)}{s^3 - s^2(X_u + M_q) + (X_u M_q - M_u X_q)s + M_u g} \quad (A1-23)$$

$$\frac{x}{u_g} = \frac{-X_u(s^2 - (M_q - \frac{M_u X_q}{X_u})s - \frac{M_u}{X_u}g)}{s[s^3 - s^2(X_u + M_q) + (X_u M_q - M_u X_q)s + M_u g]} \quad (A1-24)$$

The lateral equations are:

$$\begin{bmatrix} \dot{v} \\ \dot{\phi} \\ \dot{p} \end{bmatrix} = \begin{bmatrix} Y_v & g & Y_p \\ 0 & 0 & 1 \\ L'_v & 0 & L'_p \end{bmatrix} \begin{bmatrix} v \\ \phi \\ p \end{bmatrix} + \begin{bmatrix} Y_{A_{1s}} \\ 0 \\ L_{A_{1s}} \end{bmatrix} A_{1s} + \begin{bmatrix} -Y_v \\ 0 \\ -L'_v \end{bmatrix} v_g \quad (A1-25)$$

The basic equations are:

$$\begin{aligned} \dot{v} &= Y_v v + g\phi + Y_p p + Y_{A_{1s}} A_{1s} \\ \dot{\phi} &= L'_v v + L'_p p + L_{A_{1s}} A_{1s} \end{aligned} \quad (A1-26)$$

or

$$\begin{bmatrix} s - Y_v & -(g + Y_p s) \\ -L'_v & s - L'_p \end{bmatrix} \begin{bmatrix} v \\ \phi \end{bmatrix} = \begin{bmatrix} Y_{A_{1s}} \\ L_{A_{1s}} \end{bmatrix} A_{1s} + \begin{bmatrix} -Y_v \\ -L'_v \end{bmatrix} v_g \quad (A1-27)$$

The characteristic equation is:

$$\Delta = \begin{vmatrix} s - Y_v & -(g + Y_p s) \\ -L_v & s(s - L_p) \end{vmatrix} \quad (\text{A1-28})$$

$$= s^3 - (L_p + Y_v)s^2 + (L_p Y_v - L_v Y_p)s - L_v g$$

$$N_{A_1 s}^v = \begin{vmatrix} Y_{A_1 s} & -(g + Y_p s) \\ L_{A_1 s} & s(s - L_p) \end{vmatrix} \quad (\text{A1-29})$$

$$= Y_{A_1 s} \left[s^2 - \left(L_p - \frac{L_{A_1 s}}{Y_{A_1 s}} Y_p \right) s + \frac{L_{A_1 s}}{Y_{A_1 s}} g \right]$$

$$N_{A_1 s}^\phi = \begin{vmatrix} s - Y_v & Y_{A_1 s} \\ -L_v & L_{A_1 s} \end{vmatrix} \quad (\text{A1-30})$$

$$= L_{A_1 s} \left[s - Y_v + \frac{Y_{A_1 s}}{L_{A_1 s}} L_v \right]$$

$$N_{V_g}^v = \begin{vmatrix} -Y_v & -(g + Y_p s) \\ -L_v & s(s - L_p) \end{vmatrix} \quad (\text{A1-31})$$

$$= -Y_v \left(s^2 - \left(L_p - \frac{L_v}{Y_v} Y_p \right) s + \frac{L_v}{Y_v} g \right)$$

$$N_{Vg}^{\phi} = \begin{vmatrix} s - Y_V & -Y_V \\ -L_V & -L_V \end{vmatrix} \quad (A1-32)$$

$$= -L_V(s - Y_V + Y_V) = -L_V s$$

The input-output relationships are:

$$\frac{Y}{A_{1s}} = \frac{Y_{A_{1s}} [s^2 - (L_p - \frac{L_{A_{1s}}}{Y_{A_{1s}}} Y_p) s + \frac{L_{A_{1s}}}{Y_{A_{1s}}} g]}{s[s^3 - (L_p + Y_V) s^2 + (L_p Y_V - L_V Y_p) s - L_V g]} \quad (A1-33)$$

$$\frac{V}{A_{1s}} = \frac{Y_{A_{1s}} [s^2 - (L_p - \frac{L_{A_{1s}}}{Y_{A_{1s}}} Y_p) s + \frac{L_{A_{1s}}}{Y_{A_{1s}}} g]}{[s^3 - (L_p + Y_V) s^2 + (L_p Y_V - L_V Y_p) s - L_V g]} \quad (A1-34)$$

$$\frac{\phi}{A_{1s}} = \frac{L_{A_{1s}} (s - Y_V + \frac{Y_{A_{1s}}}{L_{A_{1s}}} L_V)}{s^3 - (L_p + Y_V) s^2 + (L_p Y_V - L_V Y_p) s - L_V g} \quad (A1-35)$$

$$\frac{\dot{\phi}}{A_{1s}} = \frac{L_{A_{1s}} s(s - Y_u + \frac{Y_{A_{1s}}}{L_{A_{1s}}} L_u)}{s^3 - (L_p + Y_V) s^2 + (L_p Y_V - L_V Y_p) s - L_V g} \quad (A1-36)$$

$$\frac{Y}{V_g} = \frac{-Y_V [s^2 - (L_p - \frac{L_V}{Y_V} Y_p) s + \frac{L_V}{Y_V} g]}{s[s^3 - (L_p + Y_u) s^2 + (L_p Y_V - L_V Y_p) s - L_V g]} \quad (A1-37)$$

$$\frac{v}{Vg} = \frac{-Y_V (s^2 - (L_p - \frac{L_V}{Y_u} Y_p) s + \frac{L_V}{Y_u} g)}{s^3 - (L_p + Y_V) s^2 + (L_p Y_V - L_V Y_p) s - L_V g} \quad (A1-38)$$

$$\frac{\phi}{Vg} = \frac{-L_V s}{s^3 - (L_p + Y_V) s^2 + (L_p Y_V - L_V Y_p) s - L_V g} \quad (A1-39)$$

$$\frac{\phi}{Vg} = \frac{-L_V s^2}{s^3 - (L_p + Y_V) s^2 + (L_p Y_V - L_V Y_p) s - L_V g} \quad (A1-40)$$

The vertical equation of motion is:

$$\dot{W} = Z_{wW} + Z_{\delta_e} \delta_e - Z_{wW} g \quad (A1-41)$$

The input-output relationships are:

$$\frac{W}{\delta_e} = \frac{Z_{\delta_e}}{s - Z_{wW}} \delta_e \quad (A1-42)$$

$$\frac{Z}{\delta_e} = \frac{Z_{\delta_e}}{s(s - Z_{wW})} \delta_e \quad (A1-43)$$

$$\frac{W}{Wg} = \frac{-Z_{wW}}{s - Z_{wW}} Wg \quad (A1-44)$$

$$\frac{Z}{W_g} = \frac{-X_w}{s(s-X_w)} w_g$$

ORIGINAL PAGE IS
OF POOR QUALITY (A1-45)

The yawing equation of motion is:

$$\dot{r} = N_r r + N_{\delta_r} \delta_r \quad (A1-46)$$

The input-output relationships are:

$$\frac{R}{\delta_r} = \frac{N_{\delta_r}}{s - N_r} \quad (A1-47)$$

$$\frac{\Psi}{\delta_r} = \frac{N_{\delta_r}}{s(s - N_r)} \quad (A1-48)$$

REFERENCES

- A1 Curtiss, H.C., Jr., "Some Notes on VTOL Stability and Control", Princeton University Course Notes, August 1971.
- A2 McRuer, D., Ashkenas, I., & Graham, D., "Aircraft Dynamics and Automatic Control", System Technology Inc., Hawthorne, California (to be published).

Table A1. Numerical Data

In this table the numerical data used in the example is listed. The data is comparable to a heavy lift helicopter CH54B gross weight 47000 lbs.

The inertia are:

$$M = 1460 \text{ slugs}$$

$$I_{xx} = 47,020 \text{ slug ft}^2$$

$$I_{yy} = 192,700 \text{ slug ft}^2$$

$$I_{zz} = 164,100 \text{ slug ft}^2$$

$$I_{xz} = -19,570 \text{ slug ft}^2$$

The full control range is:

$$\delta_c (41.0) \quad .3 \text{ rad}$$

$$A_{1s} (40) \quad .28 \text{ rad}$$

$$B_{1s} (28.5) \quad .455 \text{ rad}$$

$$\delta_t (13.6) \quad .54 \text{ rad w/o.t. with over travel T.R.}$$

The limitations on the controls are (in degrees):

$$\text{Cyclic } 26^\circ \begin{cases} -6^\circ \\ +19^\circ \end{cases}$$

$$\text{Lateral } 16^\circ \begin{cases} -2.5^\circ \\ +13.5^\circ \end{cases}$$

$$\text{Collective } 6.6^\circ - 23.8^\circ$$

$$\text{Directional } 31^\circ \text{ (} 20^\circ \text{ without over travel)}$$

Table A2. Numerical Values CH54B Hover O.G.E.

The dimensional numerical values are normalized by the inertia
 G.W. = 47,000 lbs.

	U	V	W	$P=\dot{\phi}$	$q=\dot{\theta}$	$r=\dot{\psi}$
X	-.0169	-.0008	.0057	-2.3082	.6612	-.2853
Y	.0016	-.0405	-.0160	-.8945	-2.1780	1.2315
Z	.0044	-.0150	-.2689	-.0244	.2014	2.6315
L	.0012	-.0153	-.0032	-1.0937	-1.2943	.3496
M	.0024	.0003	-.0008	.3513	-.3569	-.0072
N	-.0002	.0088	.0028	-.0147	.0750	-.5199

	δ_c	A_{1s}	B_{1s}	δ_t
X	6.1041	-1.2890	+35.6438	-.0159
Y	-18.0959	+36.1232	+1.1884	23.952
Z	-292.260	-2.2376	1.0596	-.0339
L	-5.387	23.4155	-.1215	6.5737
M	-.1719	.0648	-5.6617	-.1756
N	11.627	.0521	.2236	9.5612

Table A3. Numerical Values CH54B Airspeed 60 Knots

The dimensional numerical values are normalized by the inertia
G.W. - 47,000 lbs.

	U	V	W	$p=\dot{\phi}$	$q=\dot{\theta}$	$r=\dot{\psi}$
X	-.0221	-.0028	.0049	-2.073	1.515	-.2431
Y	.0027	-.0717	-.0286	-1.7885	-2.024	1.990
Z	-.100	-.030	-.5533	-1.3915	1.0951	2.1848
L	.0016	-.0168	-.0046	-1.402	-1.2729	.5149
M	.0020	-.0003	-.0016	.2814	-.4254	.0228
N	-.003	.0144	-.0002	.0297	.2506	-.8294

	δ_c	A_{1s}	B_{1s}	δ_t
X	-5.4716	-2.4373	33.1214	-.3398
Y	-15.229	35.353	4.720	20.842
Z	-304.04	-1.440	57.749	.3203
L	-2.2480	22.82	.9092	5.7422
M	1.2833	.2814	-5.355	.0710
N	7.6112	-.1179	.224	-8.3729

APPENDIX B 1

DECOUPLING METHOD (LEAST SQUARES)

Decoupling Using the Least Squares Method

When the number of outputs of interest exceed that of control inputs, the least squares method is employed by minimizing values of coupling terms. Consider the following algebraic matrix equation.

$$\bar{A}X = B \quad (B1-1)$$

where

A : n x m matrix

B : n x 1 matrix

X : m x 1 unknown matrix (m < n)

An approximate solution is obtained by minimizing the following:

$$\text{Minimize } \|\bar{A}X - B\| \quad (B1-2)$$

where $\|\cdot\|$ stands for an enclidean norm given by

$$\|\bar{A}X - B\| = \{\text{Trace}[(\bar{A}X - B)(\bar{A}X - B)^T]\}^{\frac{1}{2}} \quad (B1-3)$$

Then, the solution becomes:

$$X = (A^T A)^{-1} B^T \quad (B1-4)$$

And

$$\bar{A}X = A(A^T A)^{-1} B^T \cong B \quad (B1-5)$$

The proof is as follows:

The solution matrix X is given by:

$$\frac{\partial}{\partial X} \|\bar{A}X - B\| = 0 \quad (B1-6)$$

$$\therefore \frac{\partial}{\partial X} \{ \text{Trace}[(AX-B)(AX-B)^T] \}^{\frac{1}{2}} = 0 \quad (\text{B1-7})$$

$$\therefore A^T(AX-B) = 0 \quad (\text{B1-8})$$

$$\therefore X = (A^T A)^{-1} A^T B, \text{ if } A \text{ has no same column.} \quad (\text{B1-9})$$

This proof uses the following properties of the Trace:

$$\frac{\partial}{\partial X} \text{Trace}[AX] = A^T \quad (\text{B1-10})$$

$$\frac{\partial}{\partial X} \text{Trace}[XX^T] = 2X \quad (\text{B1-11})$$

A weighting for rows of the matrix equation (B3-1) can be used to increase the relative accuracy of approximation. The norm becomes:

$$\| \| Q(AX-B) \| \| = \{ \text{Trace}[(AX-B)^T Q^T Q (AX-B)] \}^{\frac{1}{2}} \quad (\text{B1-12})$$

where the weighting matrix Q is given by:

$$Q = : \begin{bmatrix} q_{11} & 0 \text{-----} 0 \\ & \text{---} q_{22} \text{---} \\ & \vdots \\ 0 \text{-----} & q_{nn} \end{bmatrix} \quad (\text{B1-13})$$

The solution is:

$$X = (A^T Q A)^{-1} A^T Q B \quad (B1-14)$$

where

$$Q = Q^T Q \quad (B1-15)$$

The limitations of this method can be illustrated as follows:

The dynamic equation of the system is:

$$\dot{x} = Ax + Bu \quad (B1-16)$$

$$y = px \quad (B1-17)$$

(A) If B_i (i-th row) = 0, the corresponding i-th state equation should not include coupling terms.

(B) If $y = px$, the output matrix P has only one non-zero element in the same column so that desirable state matrix A^* and control matrix B^* can be defined.

APPENDIX B2

DECOUPLING OF HELICOPTER DYNAMICS

Decoupling in the multivariable systems has been studied by many authors. Morgan (Ref. B1) first posed the decoupling problem. Falb and Volvoich (Ref. B2) gave necessary and sufficient condition for decoupling. Gilbert and some authors (Ref. B3, B4, and B5) extended this method. However, these methods are still cumbersome in algebraic manipulation and are often not applicable to control problems where the number of controls is less than the number of control system outputs.

In this work is used a decoupling method of least squares.

The dynamical equations are given by:

$$\dot{x} = Ax + Bu \quad (B2-1)$$

$$y = x \quad (B2-2)$$

$$u = Ckx + C\delta \quad (B2-3)$$

where

x : n - state vector

y : n - output vector

u : m - control vector

δ : m - control input vector

A : $n \times n$ system matrix

B : $n \times m$ control matrix

C : $m \times m$ control decoupling matrix

K : $m \times n$ decoupling state feedback matrix

Substituting Eq. B2-3 into B2-1 and obtain the following equation:

$$\dot{x} = (A + BCK)x + BC\delta \quad (B2-4)$$

$$y = x \quad (B2-5)$$

Then, the block diagram for decoupling is shown in Illustration B2-1.

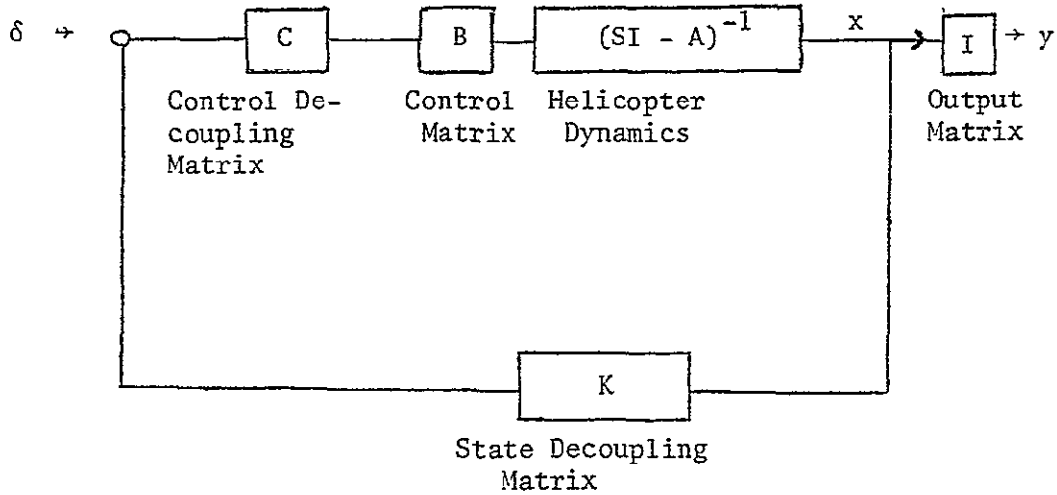


Illustration B2-1. Block Diagram for Decoupling

When the desirable decoupled control matrices are respectively B^* and A^* , then the following relations are satisfied:

$$BC = B^* \quad (B2-6)$$

$$A + BCK = A^* \quad (B2-7)$$

From these equations, using a pseudo-inverse matrix which is a solution of least squares method, as shown in Appendix B1, one obtains the decoupling matrices C and K.

$$C = (B^T B)^{-1} B^T B^* \quad (B2-8)$$

$$K = (C^T B^T B C)^{-1} C^T B^T (A - A^*) \quad (B2-9)$$

$$\dot{z} = (B^{*T} B)^{-1} B^{*T} (A - A^*) z$$

Now, the decoupling matrices (C,K) decouple the system completely or approximately. The practical example of the almost decoupled system is shown in Illustration B2-1. This method is used for decoupling of the helicopter dynamics at hover and approach phase.

Decoupling the helicopter (at hover)

The dynamic equation is rewritten, using a numerical hover example, as follows: (eg. 2.8) with cancelled inertia coupling term)

$$\begin{bmatrix} \dot{u} \\ \dot{\theta} \\ \dot{q} \\ \dot{w} \\ \dot{v} \\ \dot{\phi} \\ \dot{p} \\ \dot{r} \end{bmatrix} = \begin{bmatrix} -.0169 & -32.2 & .661 & .0057 & -.0008 & 0 & -2.31 & -.285 \\ & & 1.0 & & & & & \\ .0024 & 0 & -.257 & -.0008 & .0003 & 0 & .352 & -.0072 \\ -.0044 & 0 & .201 & -.269 & -.015 & 0 & -.0244 & 2.63 \\ .0016 & 0 & -2.18 & -.016 & -.0405 & 32.2 & -.895 & 1.231 \\ & 0 & & & & & 1.0 & \\ .0014 & 0 & -1.39 & -.0046 & -.0200 & 0 & -1.14 & .595 \\ -.0004 & 0 & .241 & .0034 & .0112 & 0 & .120 & -.591 \end{bmatrix} \begin{bmatrix} u \\ \theta \\ q \\ w \\ v \\ \phi \\ p \\ r \end{bmatrix}$$

$$\begin{array}{c}
 + \\
 \left[\begin{array}{cccc}
 35.6 & 6.10 & -1.29 & -.016 \\
 0 & 0 & 0 & 0 \\
 -5.66 & -.172 & .065 & -.176 \\
 \hline
 1.06 & -.292 & -2.24 & .034 \\
 \hline
 1.19 & -18.1 & 36.1 & 23.9 \\
 0 & 0 & 0 & 0 \\
 -.223 & -10.8 & 24.6 & 11.1 \\
 \hline
 .246 & 12.9 & -2.87 & -10.9
 \end{array} \right]
 \begin{array}{c}
 \left[\begin{array}{c}
 B_{1s} \\
 \delta_c \\
 A_{1s} \\
 \delta_r
 \end{array} \right]
 \end{array}
 \end{array}
 \tag{B2-10}$$

And the desirable control matrix B^* and the desirable system matrix A^* are assumed to be given by Eq. (B2-11) and Eq. (B2-12).

$$B^* = \left[\begin{array}{cccc}
 35.6 & 0.0 & 0.0 & 0.0 \\
 0 & 0 & 0 & 0 \\
 -5.66 & 0.0 & 0.0 & 0.0 \\
 \hline
 0.0 & -292. & 0.0 & 0.0 \\
 \hline
 0.0 & 0.0 & 36.1 & 0.0 \\
 0 & 0 & 0 & 0 \\
 0.0 & 0.0 & 24.6 & 0 \\
 \hline
 0.0 & 0.0 & 0.0 & -10.9
 \end{array} \right]
 \tag{B2-11}$$

$$A^* = \begin{bmatrix} -.0169 & -32.2 & .661 & | & 0.0 & | & 0.0 & 0 & | & 0.0 & | & 0.0 \\ & & 1.00 & | & & | & & & | & & | & \\ .0024 & 0 & -.257 & | & 0.0 & | & 0.0 & 0 & | & 0.0 & | & 0.0 \\ \hline 0.0 & 0 & 0.0 & | & -.269 & | & 0.0 & 0 & | & 0.0 & | & 0.0 \\ \hline 0.0 & 0 & 0.0 & | & 0.0 & | & -.0405 & 32.2 & | & -.895 & | & 0.0 \\ & & & | & & | & & & | & 1.00 & | & \\ 0.0 & 0 & 0.0 & | & 0.0 & | & -.0200 & 0 & | & -1.14 & | & 0.0 \\ \hline 0.0 & 0 & 0.0 & | & 0.0 & | & 0.0 & 0 & | & 0.0 & | & -.591 \end{bmatrix} \quad (B2-12)$$

These matrices B* and A* are chosen in such a way that characteristics of the decoupled helicopter are similar to those of the basic helicopter. After being decoupled, the characteristics would be improved by the conventional technique or the optimal control technique.

After simple calculations following Eq. (B2-8) and (Eq. B2-9), one obtains the decoupling matrices C and K given by Eq. (B2-13) and Eq. (B2-14).

$$C = \begin{bmatrix} .998 & -.176 & .042 & -.025 \\ .004 & 1.000 & -.009 & .004 \\ -.014 & -.159 & 1.152 & -.576 \\ -.005 & 1.085 & -.266 & .977 \end{bmatrix} \quad (B2-13)$$

$$K = \begin{bmatrix} -.168 \cdot 10^{-6} & 0.0 & -.611 \cdot 10^{-4} & .155 \cdot 10^{-3} & .232 \cdot 10^{-4} & 0.0 & -.648 \cdot 10^{-1} & -.761 \cdot 10^{-2} \\ -.151 \cdot 10^{-4} & 0.0 & .692 \cdot 10^{-3} & -.237 \cdot 10^{-6} & .514 \cdot 10^{-4} & 0.0 & .834 \cdot 10^{-4} & -.900 \cdot 10^{-2} \\ .478 \cdot 10^{-4} & 0.0 & -.590 \cdot 10^{-1} & -.358 \cdot 10^{-3} & .166 \cdot 10^{-7} & 0.0 & .170 \cdot 10^{-5} & .308 \cdot 10^{-1} \\ .240 \cdot 10^{-4} & 0.0 & -.255 \cdot 10^{-1} & -.531 \cdot 10^{-3} & -.103 \cdot 10^{-2} & 0.0 & .110 \cdot 10^{-1} & .865 \cdot 10^{-2} \end{bmatrix}$$

(B2-14)

The member of the diagonal submatrices of the matrix K are about a factor 10^{-1} less than those of the same column and rows. This means that the feedback gains of the main diagonal submatrices, which artificially govern characteristics of the helicopter dynamics, have no effect on decoupling with exception of the yawing motion. However, the latter is sufficiently stable as is apparent from Eq. (B2-14). This indicates that there exist free choice of main diagonal feedback gains without deficiency in decoupling.

Substituting Eq. (B2-14), (B2-13) into Eq. (B2-4), gives the almost decoupled helicopter dynamics as follows:

$$\begin{bmatrix} \dot{u} \\ \dot{\theta} \\ \dot{q} \\ \dot{w} \\ \dot{v} \\ \dot{\phi} \\ \dot{p} \\ \dot{r} \end{bmatrix} = \begin{bmatrix} -.0169 & -32.2 & .661 & .0001 & -.0001 & 0 & -.0056 & -.0131 \\ & & 1.0 & & & 0 & 0 & \\ .0024 & & -.266 & .0000 & .0001 & 0 & -.0174 & -.0403 \\ .0000 & & -.0005 & -.269 & .0006 & 0 & .0013 & .0030 \\ -.0001 & & -.0203 & -.0021 & -.0381 & 32.2 & -.836 & .137 \\ 0 & & 0 & & & & 1.0 & \\ .0002 & & .0279 & .0029 & -.0233 & 0 & -1.22 & -.189 \\ -.0001 & & -.0159 & -.0016 & .0019 & 0 & .0466 & -.482 \end{bmatrix} \begin{bmatrix} u \\ \theta \\ q \\ w \\ v \\ \phi \\ p \\ r \end{bmatrix}$$

(B2-15)

In order to study the degree of decoupling for a control input, an analogue simulation was done as shown in Figures (B2-1) to (B2-8). The decoupling reduces the longitudinal/lateral coupling terms by a factor of 10 or more. The coupling between the vertical mode and other modes also decreases, showing significant reduction between the vertical and yawing mode. The yawing response is improved for the control input, while its coupling with the other axes decreases significantly. A change in some control derivatives signs accompany turning direction of initial motion opposite to that of basic derivatives. An evaluation of this sign change may require a simulator test by a pilot in the case of an unstable helicopter.

Decoupling the Helicopter (at approach phase)

The dynamic equation, using the numerical example for the approach plane, becomes as follows: (with cancelled inertia coupling term)

$$\begin{bmatrix} \dot{u} \\ \dot{\theta} \\ \dot{q} \\ \dot{w} \\ \dot{v} \\ \dot{\phi} \\ \dot{p} \\ \dot{r} \end{bmatrix} = \begin{bmatrix} -.0221 & -32.2 & 1.515 & .0049 & -.002 & 0 & -2.73 & -.2481 \\ 0 & 0 & 1.0 & 0 & 0 & 0 & 0 & 0 \\ .0020 & 0 & -.4251 & .0016 & .0003 & 0 & .281 & -.228 \\ -.100 & 0 & 7.845 & -.5333 & -.030 & 0 & -1.3915 & 2.1898 \\ .0027 & 0 & -2.024 & -.0286 & -.0711 & 32.2 & -1.788 & 1.990 \\ 0 & 0 & 0 & 0 & 0 & 0 & 1.0 & 0 \\ .0629 & 0 & -1.449 & -.0047 & -.0113 & 0 & -1.488 & 2.169 \\ -.0003 & 0 & .423 & .0057 & .0172 & 0 & .207 & -.937 \end{bmatrix} \begin{bmatrix} u \\ \theta \\ q \\ w \\ v \\ \phi \\ p \\ r \end{bmatrix}$$

(B2-16)

$$+ \begin{bmatrix}
 33.12 & -5.470 & -2.44 & -.361 \\
 0 & 0 & 0 & 0 \\
 -5.35 & 1.28 & .28 & .076 \\
 \hline
 57.75 & -304.04 & -1.44 & .32 \\
 \hline
 4.72 & -15.221 & 35.35 & 20.84 \\
 0 & 0 & 0 & 0 \\
 .86 & -5.69 & 24.06 & 9.70 \\
 \hline
 .122 & 8.29 & -2.98 & -9.53
 \end{bmatrix}
 \begin{bmatrix}
 B_{1s} \\
 \delta_c \\
 \hline
 A_{1s} \\
 \hline
 \delta_r
 \end{bmatrix}
 \tag{B2-17}$$

and the desirable control matrix B^* and the desirable system matrix A^* are assumed to be given by Eq. (B2-18) and Eq. (B2-19).

$$B^* = \begin{bmatrix}
 33.12 & 0.0 & 0.0 & 0.0 \\
 0 & 0 & 0 & 0 \\
 -5.35 & 0.0 & 0.0 & 0.0 \\
 \hline
 0.0 & -304.4 & 0.0 & 0.0 \\
 \hline
 0.0 & 0.0 & 35.35 & 0.0 \\
 0 & 0 & 0 & 0 \\
 0.0 & 0.0 & 24.06 & 0 \\
 \hline
 0.0 & 0.0 & 0.0 & -9.53
 \end{bmatrix}
 \tag{B2-18}$$

$$A^* = \begin{bmatrix} -.0221 & -32.2 & 1.515 & | & 0.0 & | & 0.0 & 0 & 0.0 & | & 0.0 \\ & & 1.0 & | & & | & & & & | & \\ .0020 & 0 & -.4251 & | & 0.0 & | & 0.0 & 0 & 0.0 & | & 0.0 \\ \hline 0.0 & 0 & 0.0 & | & -.5333 & | & 0.0 & 0 & 0.0 & | & 0.0 \\ \hline 0.0 & 0 & 0.0 & | & 0.0 & | & -.0711 & 32.2 & -1.788 & | & 0.0 \\ & & & | & & | & & & 1.0 & | & \\ 0.0 & 0 & 0.0 & | & 0.0 & | & -.0113 & 0 & -1.488 & | & 0.0 \\ \hline 0.0 & 0 & 0.0 & | & 0.0 & | & 0.0 & 0 & 0.0 & | & -.937 \end{bmatrix}$$

(B2-18)

These matrices B^* and A^* are chosen in such a way that characteristics of the decoupled helicopter are similar to those of the basic helicopter. After being decoupled, the characteristics would be improved by the conventional technique or the optimal control technique.

After simple calculations following Eq. (B2-16) and Eq. (B2-17), one obtains the decoupling matrices C and K given by Eq. (B2-21) and Eq. (B2-22).

$$C = \begin{bmatrix} 1.02 & .17 & .08 & -.034 \\ .19 & 1.03 & .010 & .003 \\ -.1 & -.14 & 1.15 & -.5 \\ .13 & .95 & -.30 & .986 \end{bmatrix} \quad (B2-19)$$

$$K = \begin{bmatrix} 0.0 & 0.0 & 0.0 & .151 \cdot 10^{-3} & .102 \cdot 10^{-4} & 0.0 & -.816 \cdot 10^{-1} & -.621 \cdot 10^{-2} \\ -.328 \cdot 10^{-3} & 0.0 & -.360 \cdot 10^{-2} & 0 & .986 \cdot 10^{-4} & 0.0 & .457 \cdot 10^{-1} & -.717 \cdot 10^{-2} \\ .903 \cdot 10^{-4} & 0.0 & -.581 \cdot 10^{-1} & -.603 \cdot 10^{-3} & 0.0 & 0.0 & 0.0 & .670 \cdot 10^{-1} \\ .314 \cdot 10^{-4} & 0.0 & -.443 \cdot 10^{-1} & -.388 \cdot 10^{-3} & -.181 \cdot 10^{-2} & 0.0 & .220 \cdot 10^{-1} & 0.0 \end{bmatrix}$$

(B2-20)

Substituting Equation B2-9 and B2-20 into Equation B2-5, gives the almost decoupled helicopter dynamics as follows.

$$\begin{bmatrix} \ddot{u} \\ \ddot{\theta} \\ \ddot{q} \\ \ddot{w} \\ \ddot{v} \\ \ddot{\phi} \\ \ddot{p} \\ \ddot{r} \end{bmatrix} = \begin{bmatrix} -.0219 & -32.2 & 1.575 & .0001 & 0 & 0 & .025 & -.042 \\ & & 1.0 & & & & 0 & 0 \\ .0020 & & -.425 & .0007 & .0002 & 0 & -.155 & -.26 \\ .0000 & & -.0005 & -.533 & 0 & 0 & 0 & 0 \\ -.0004 & & -.035 & .0066 & -.0716 & 32.2 & -1.788 & .379 \\ 0 & & 0 & & & & 1.0 & \\ .0007 & & -.0514 & .0038 & -.0109 & 0 & 1.48 & -.557 \\ 0 & & 0 & 0 & 0 & 0 & 0 & .936 \end{bmatrix} \begin{bmatrix} u \\ \theta \\ q \\ w \\ v \\ \phi \\ p \\ r \end{bmatrix}$$

(B2-21)

ORIGINAL PAGE IS
OF POOR QUALITY

$$\begin{bmatrix}
 33.02 & .077 & .041 & -.210 \\
 0 & 0 & 0 & 0 \\
 -5.24 & .43 & -.137 & .106 \\
 -.0008 & -304.04 & .0003 & -.0018 \\
 .01 & .077 & 34.76 & 2.10 \\
 0 & 0 & 0 & 0 \\
 1.39 & .11 & 24.8 & -.029 \\
 .79 & -.057 & -.459 & -7.88
 \end{bmatrix}
 \begin{bmatrix}
 B_{1s} \\
 \delta_c \\
 A_{1s} \\
 \delta_r
 \end{bmatrix}
 \tag{B2-22}$$

Note that in the "decoupled" equations, the coupling terms are an order of ten smaller, compared to those of basic equations.

In the numerical values of the above equations is used $(Z_q - U_o)$ with $U_o = 0$. If $Z_q - U_o$ is used with $U_o = 60$ knots/hr, the feedback gains k_{11} remain the same with the exception of k_{34} , which becomes equal to -100 i.e., directly proportional to speed.

Evaluation of Decoupling

The root configuration for basic, decoupled and uncoupled simplified dynamics are shown in Figure 2. The roots of the decoupled longitudinal equations are very close to those of the uncoupled equations. However, decoupling of the lateral equations shifts one of the modes to the right hand side in the s plane, resulting in an unstable mode.

In order to study the degree of decoupling for a control input, an analog simulation was done in Reference (32). The decoupling reduces considerably the longitudinal/lateral coupling terms. The coupling between the vertical mode and other modes also decreases, showing significant reduction between the vertical and yawing mode. The yawing response is improved for the control input, while its coupling with the other axes decreases significantly. A change in some control derivatives signs accompany turning direction of initial motion opposite to that of basic derivatives. An evaluation of this sign change may require a simulator test by a pilot in the case of an unstable helicopter.

Consideration for Practical Design

In general, the stability derivatives and control derivatives are a function of air velocity, altitude and time. Therefore, each element of the decoupling matrices [C,K] must be given by:

$$\begin{aligned} C_{ij} &= C_{ij}(V,h,t) \\ K_{ij} &= K_{ij}(V,h,t) \end{aligned} \tag{B2-23}$$

However, the derivatives are determined at a given air velocity and altitude. In practice, the altitude and time dependence can often be neglected and the derivatives are only a function of air velocity or:

$$C_{ij} = C_{ij}(V)$$

$$K_{ij} = K_{ij}(V)$$

(B2-24)

When the derivatives between different velocities can be approximated by straight lines or simple curves variations in C_{ij} and K_{ij} would be easily programmed.

The decoupling matrices C and K are constructed as shown in Illustration B2-3. The assumptions for the design of the helicopter controller are as follows:

(I) The state variables $u, v, w, \theta, q, \phi, p$ and r can be measured by sensors or approximated.

(II) The fly-by wire system would be desirable.

(III) The measurement of air velocity V is possible.

*

REFERENCES

- B1 Morgan, Bernard S., Jr., "The Synthesis of Linear Multivariable Systems by State Variable Feedback", IEEE Transaction on Automatic Control, Vol. AC-9, pp. 405-411, October 1964.
- B2 Falb, Peter L. and Volvoich, William A., "Decoupling in the Design and Synthesis of Multivariable Control Systems", IEEE Transaction on Automatic Control, Vol. AC-12, No. 6, December 1967.
- B3 Gilbert, Elmer G., "The Decoupling of Multivariable Systems by State Feedback", SIAM J. Control, Vol. 7, No. 1, February 1969.
- B4 Mufiti, I.H., "Some Results on the Decoupling of Multivariable Systems", Int. J. Control, Vol. 14, No. 3, pp. 477-485, 1971.
- B5 Panda, S.P., "Compensator Design for Decoupling of Multivariable Systems by State Feedback", Int. J. Control, Vol. 13, No. 4, pp. 721-735, 1971.

APPENDIX C1

SENSITIVITY ANALYSIS

Sensitivity of Characteristic Roots to Variation in the System

Coefficients (a_{ij})

The system equation with control free is given by (C1-1).

$$\dot{x}(t) = Ax(t) \quad (C1-1)$$

where

$x(t)$: n-state vector

A : n x n system matrix

the n-th order characteristic equation is given by (C1-2).

$$|sI - A| = 0 \quad (C1-2)$$

The sensitivity is defined as

$$S_{ij}^k = a_{ij} \frac{\Delta r_k}{\Delta a_{ij}} \quad (C1-3)$$

where,

S_{ij}^k : sensitivity of k-th characteristic root
to a_{ij} variation

a_{ij} : non-zero (i,j) element of A

Δa_{ij} : variation in a_{ij}

Δr_k : k-th root of the characteristic equation

And, S_{ij}^k is a vector since Δr_k is represented by:

$$\Delta r_k = ||\Delta r_k|| \tan^{-1} \frac{\text{Im}[\Delta r_k]}{\text{Re}[\Delta r_k]} \quad (C1-4)$$

Also, the following equations are easily proved with respect to S_{ij}^k ,

since Trace [A] is the sum of all roots.

$$\sum_{k=1}^n S_{ij}^k = a_{ij} \quad i = j, i, j = 1, 2, \dots, n \quad (C1-5)$$

$$\sum_{k=1}^n S_{ij}^k = 0 \quad i \neq j, i, j = 1, 2, \dots, n \quad (C1-6)$$

Furthermore, the poles and zeros of the root locus of a_{ij} variation are given by roots of (C1-7) and (C1-8) respectively.

$$|sI - A| = 0 \quad (C1-7)$$

$$\text{cofactor } (-a_{ij}) = 0 \quad (C1-8)$$

These are derived as follows:

Letting the variation of the system matrix, ΔA , the characteristic equation is rewritten by:

$$|sI - A - \Delta A| = 0 \quad (C1-9)$$

This equation can be equivalent to (C1-10)

$$|I - (sI - A)^{-1} \Delta A| = 0 \quad (C1-10)$$

$$\therefore \left| I - \frac{\text{adj}(sI-A)\Delta A}{\det(sI-A)} \right| = 0 \quad (C1-11)$$

$$\text{adj}(sI-A) = \begin{bmatrix} \text{cof}(s-a_{11}), \text{cof}(-a_{21}), \dots, \text{cof}(-a_{i1}), \dots, \text{cof}(-a_{n1}) \\ \text{cof}(-a_{12}), \text{cof}(s-a_{22}), \dots, \text{cof}(-a_{i2}), \dots, \text{cof}(-a_{n2}) \\ \vdots \\ \text{cof}(-a_{1j}), \dots, \text{cof}(-a_{ij}), \dots, \text{cof}(-a_{nj}) \\ \vdots \\ \text{cof}(-a_{1n}), \dots, \text{cof}(-a_{in}), \dots, \text{cof}(s-a_{nn}) \end{bmatrix} \quad (C1-12)$$

If one assumes that

$$\Delta A = \begin{bmatrix} 0 & 0 & \dots & 0 & \dots & 0 \\ \vdots & \vdots & & \vdots & & \vdots \\ 0 & \dots & \Delta a_{ij} & \dots & 0 & \dots \\ \vdots & & \vdots & & \vdots & \\ 0 & \dots & 0 & \dots & 0 & \dots \end{bmatrix} \quad (C1-13)$$

then:

$$\text{adj}(sI-A)\Delta A = \begin{bmatrix} 0 & 0 & \dots & \Delta a_{ij} \cdot \text{cof}(-a_{i1}) & \dots & 0 \\ 0 & \dots & \Delta a_{ij} \cdot \text{cof}(-a_{i2}) & \dots & \dots & \dots \\ \vdots & & \vdots & & \vdots & \\ 0 & \dots & \Delta a_{ij} \cdot \text{cof}(-a_{ij}) & \dots & 0 & \dots \\ \vdots & & \vdots & & \vdots & \\ 0 & \dots & \Delta a_{ij} \cdot \text{cof}(-a_{in}) & \dots & 0 & \dots \end{bmatrix} \quad (C1-14)$$

$$\therefore \left| I - \frac{\text{adj}(sI-A)\Delta A}{\det[sI-A]} \right| = 1 - \frac{\Delta a_{ij} \text{cof}(-a_{ij})}{\det[sI-A]} \quad (C1-15)$$

That is, the characteristic equation is:

$$1 - \frac{\Delta a_{ij} \text{cof}(-a_{ij})}{\det[sI-A]} = 0 \quad (C1-16)$$

The poles and zeros are given from (C1-16)

Sensitivites of the Characteristic Roots to the Stability Derivatives

The contributions of stability derivatives to control and dynamic stability are shown in Figures (C-1) to (C-36), with mostly expanded sensitivities. By these figures we can appreciate the following:

- (1) Which roots (or modes) are most sensitive to the specific stability derivative?
- (2) Which roots (or modes) are more sensitive to which stability derivatives?
- (3) Existence of zeroes on real axis can be known.
- (4) From (1) and (2) we can infer degree of coupling.

With respect to L_r and N_u , root locus are shown with reducing L_r and N_u in Figure (C-37) and Figure (C-38), in order to study reduction in stability due to decoupling.

13 1/2 x 10 inch
KEUFFEL & ESSER CO.

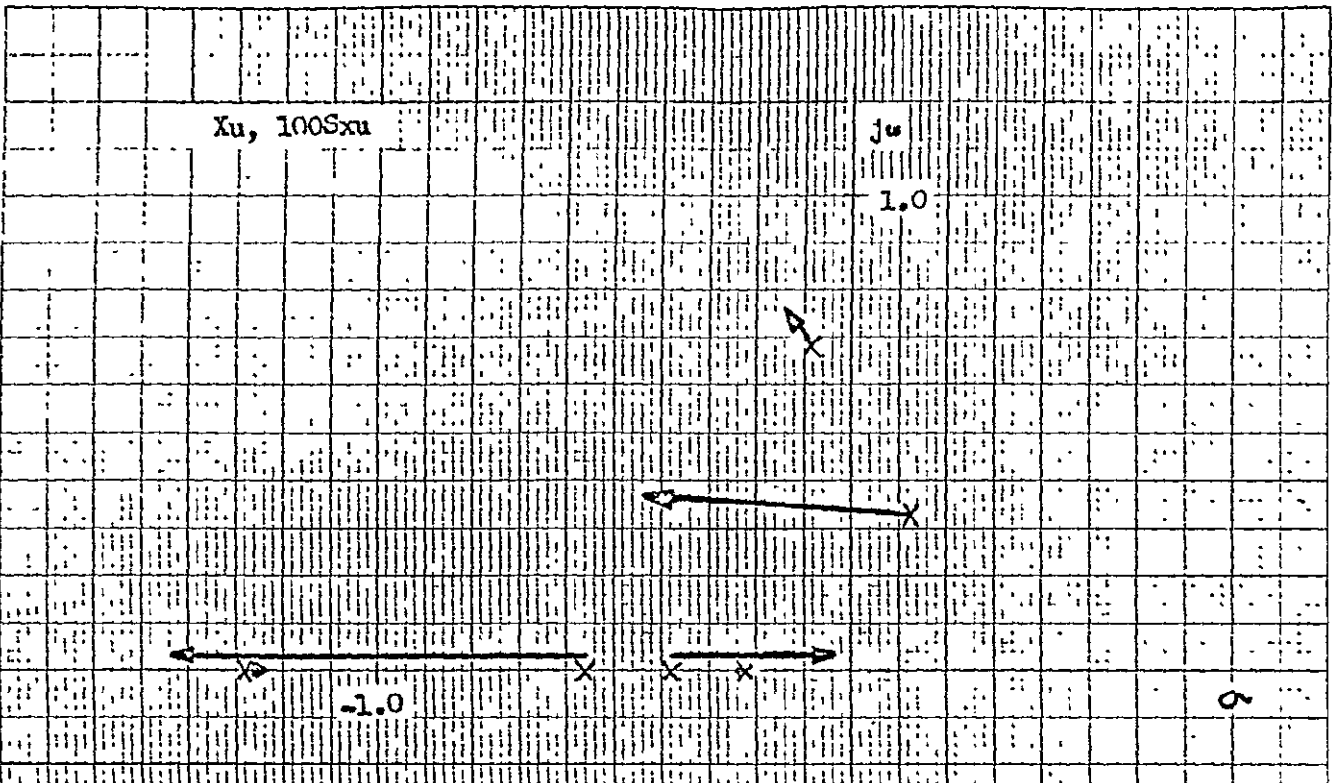


Fig. C-1 Sensitivity to Xu

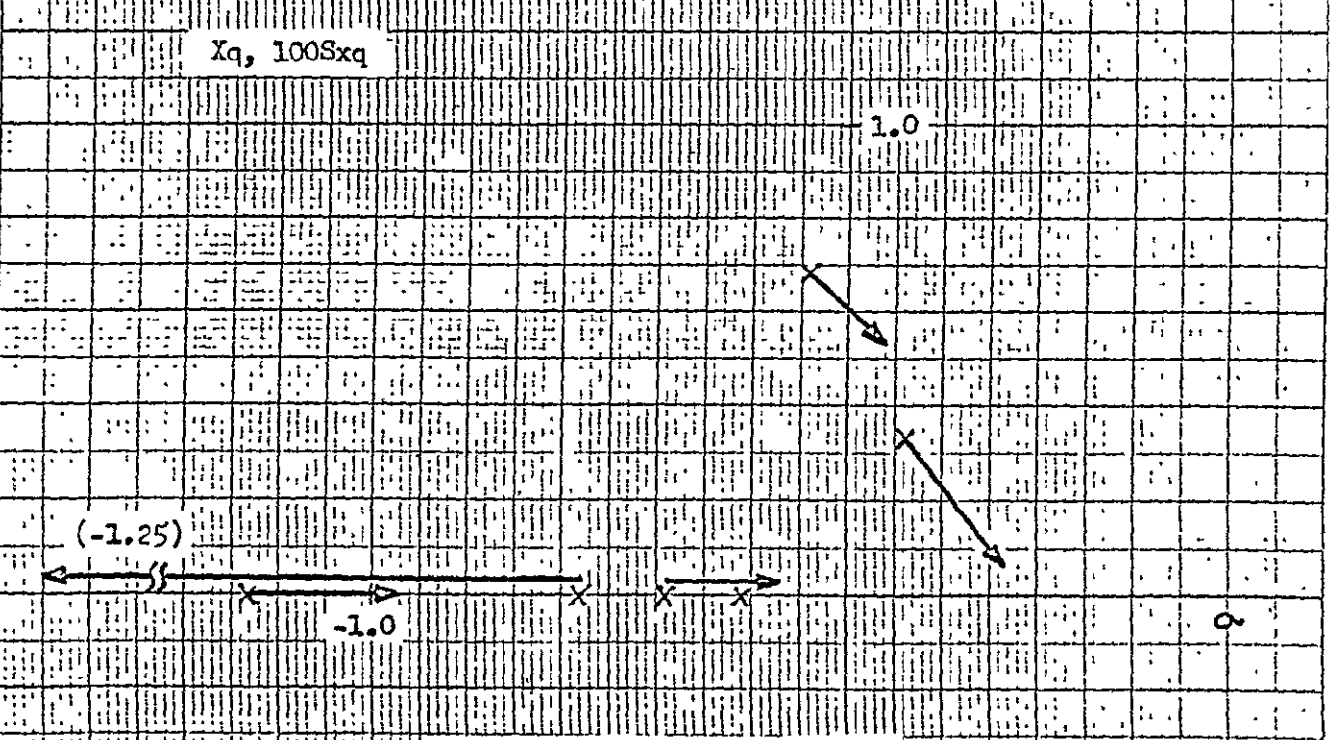


Fig. C-2 Sensitivity to Xq

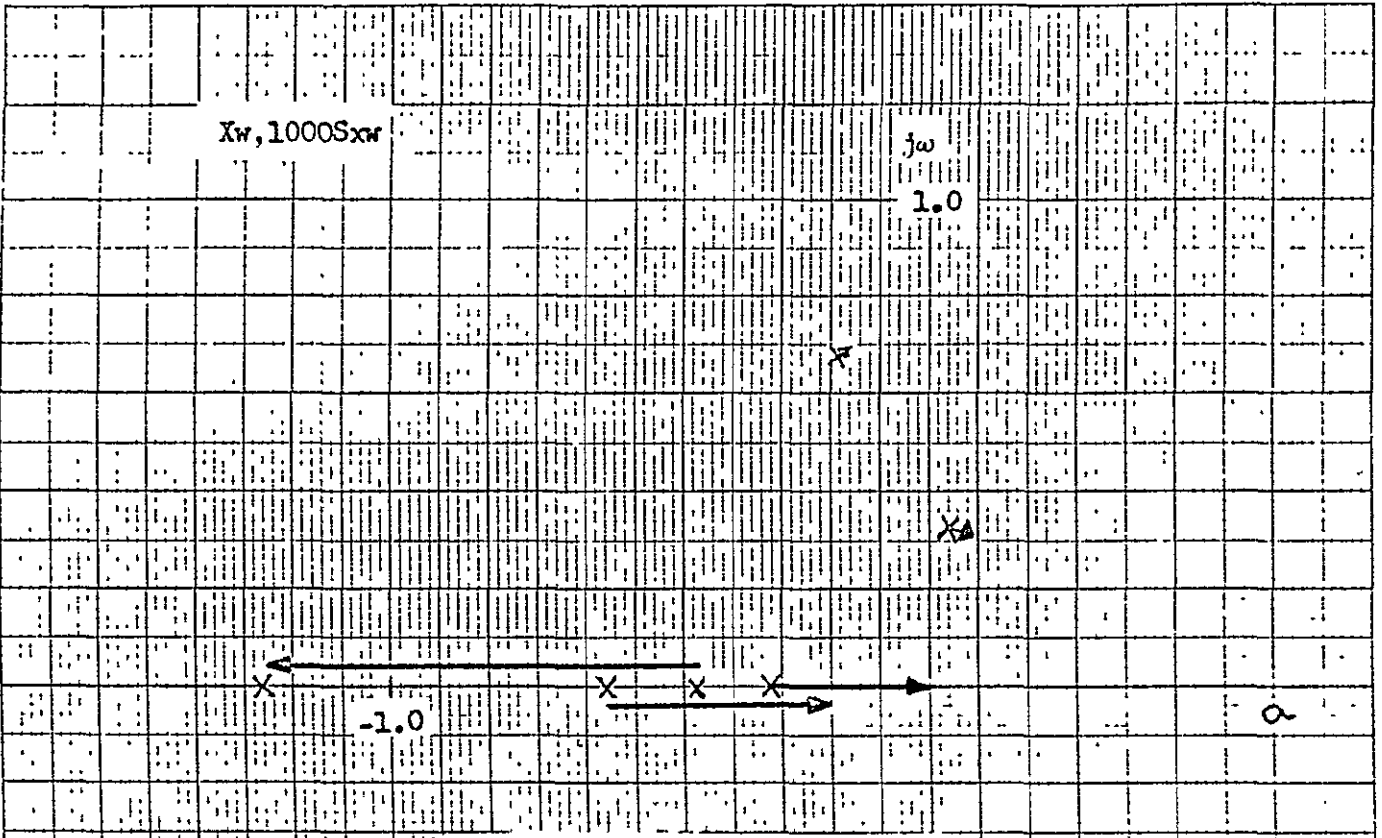


Fig. C-3 Sensitivity to Xw

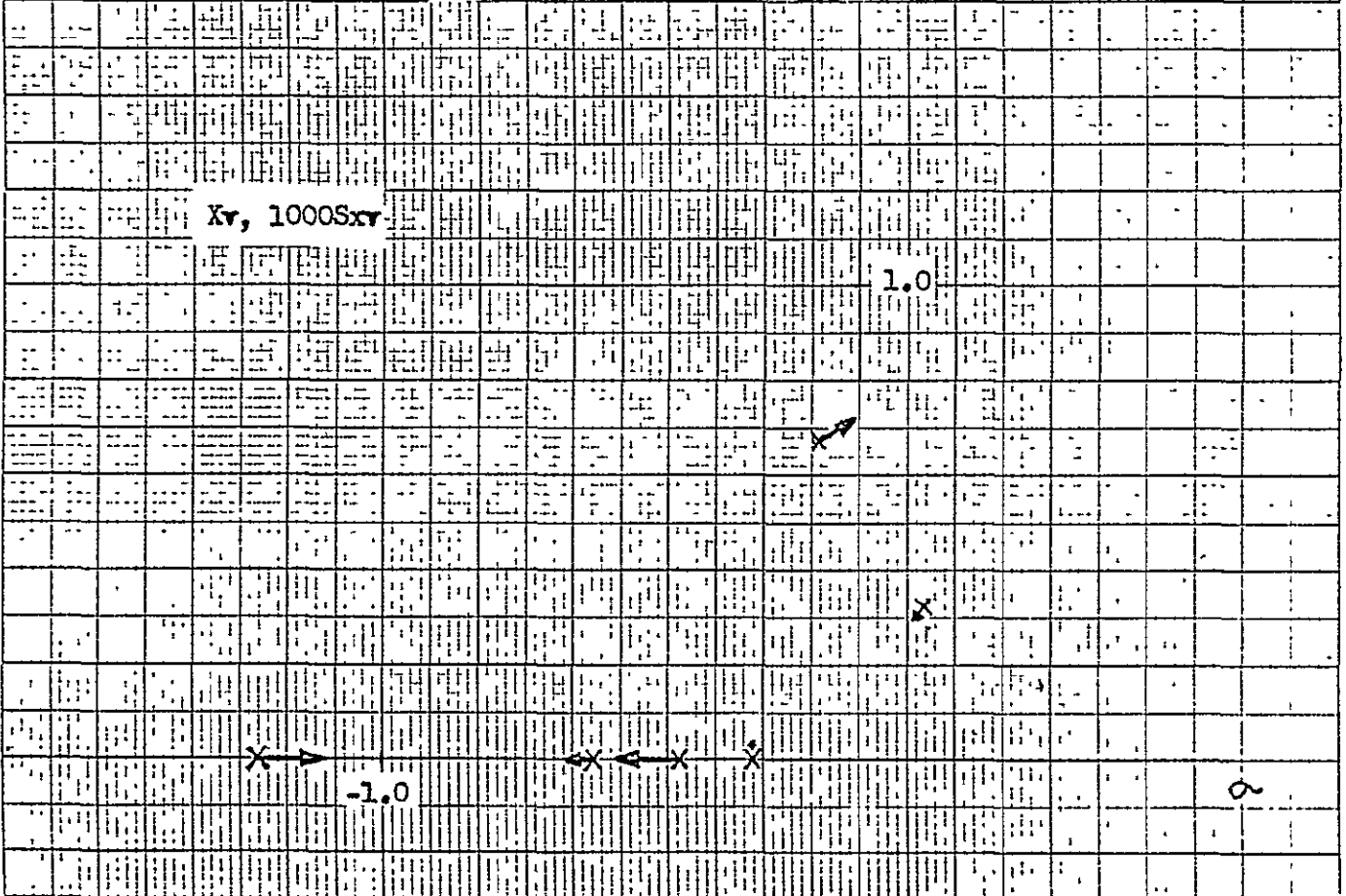


Fig. C-4 Sensitivity to Xv

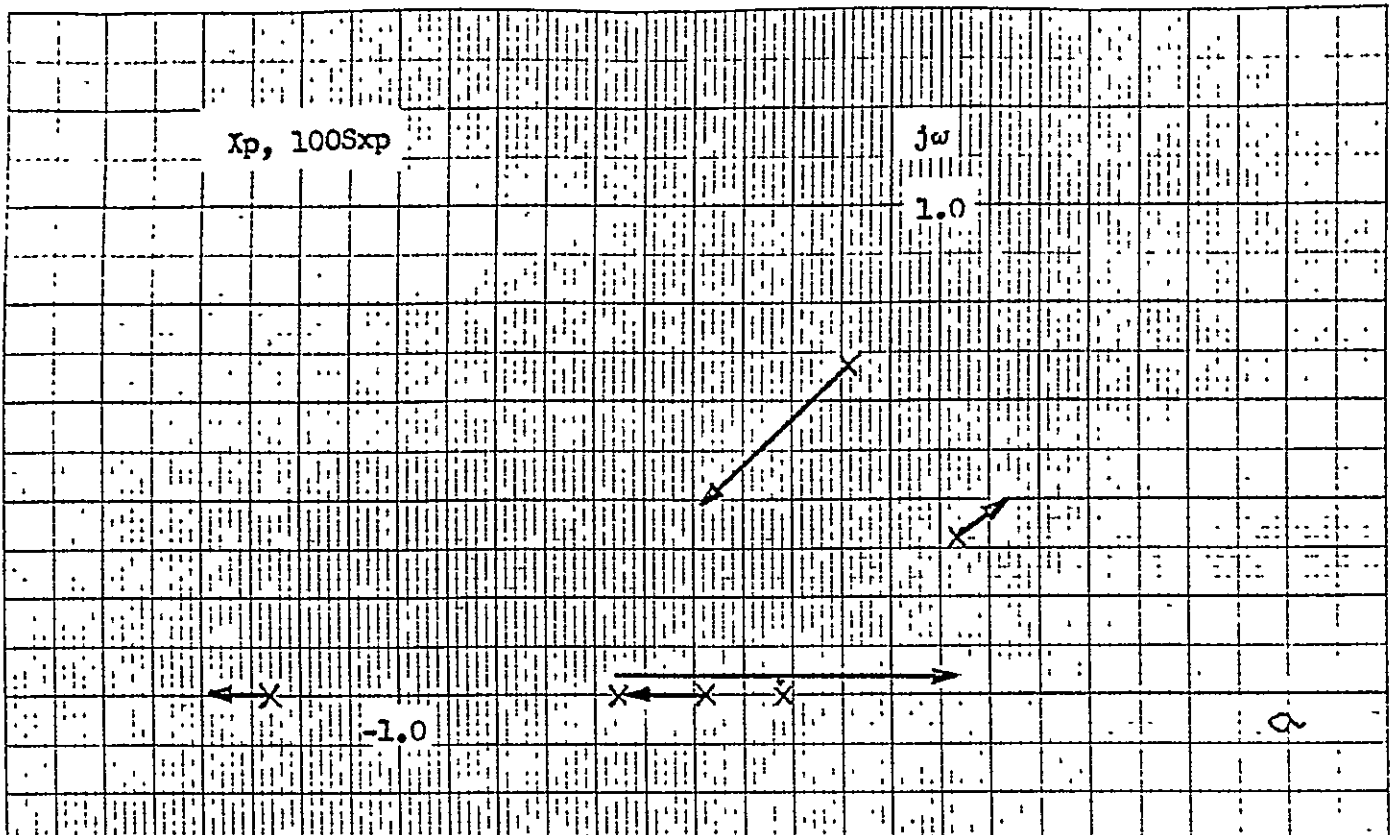


Fig.C-5 Sensitivity to Xp

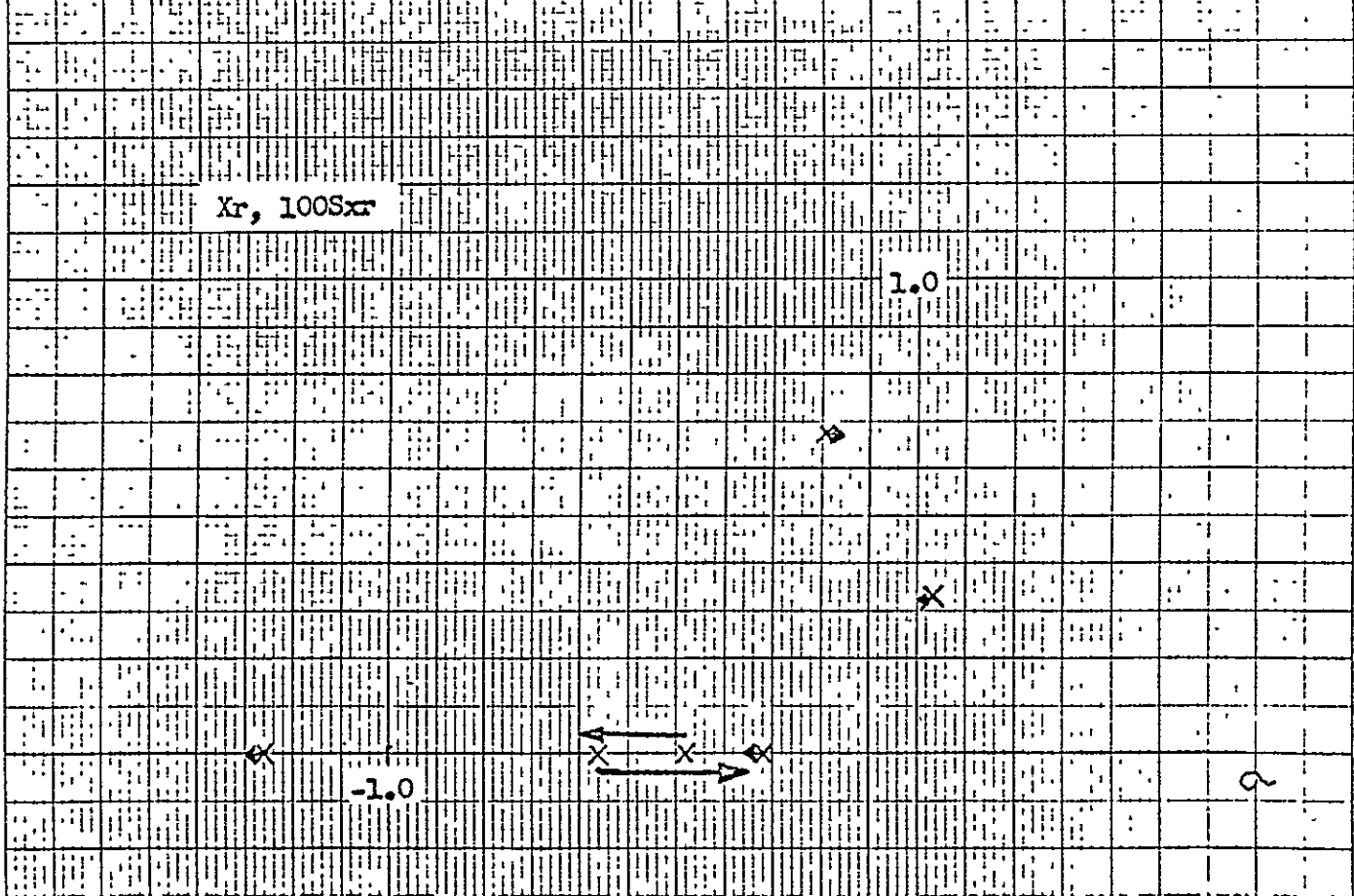
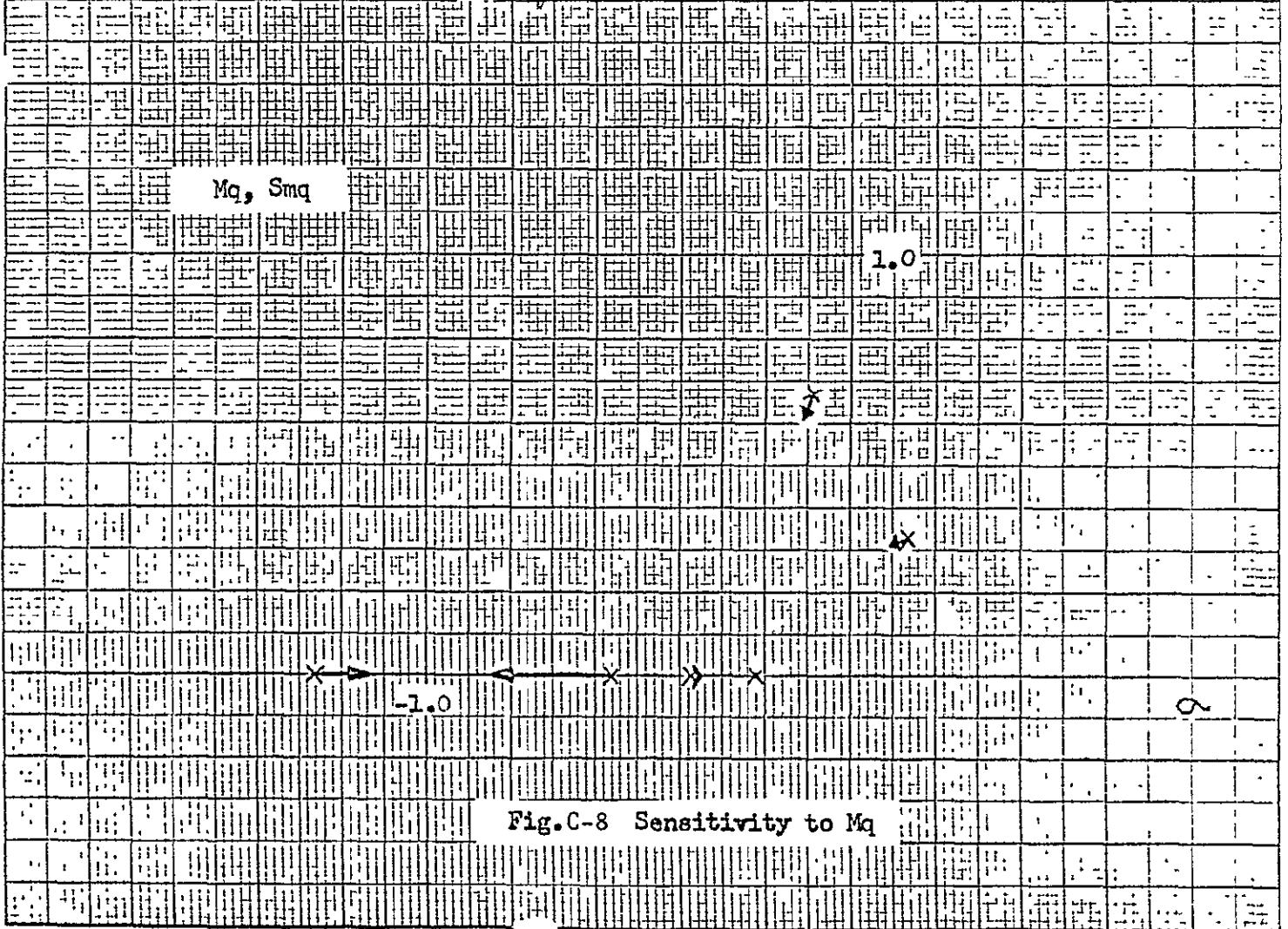
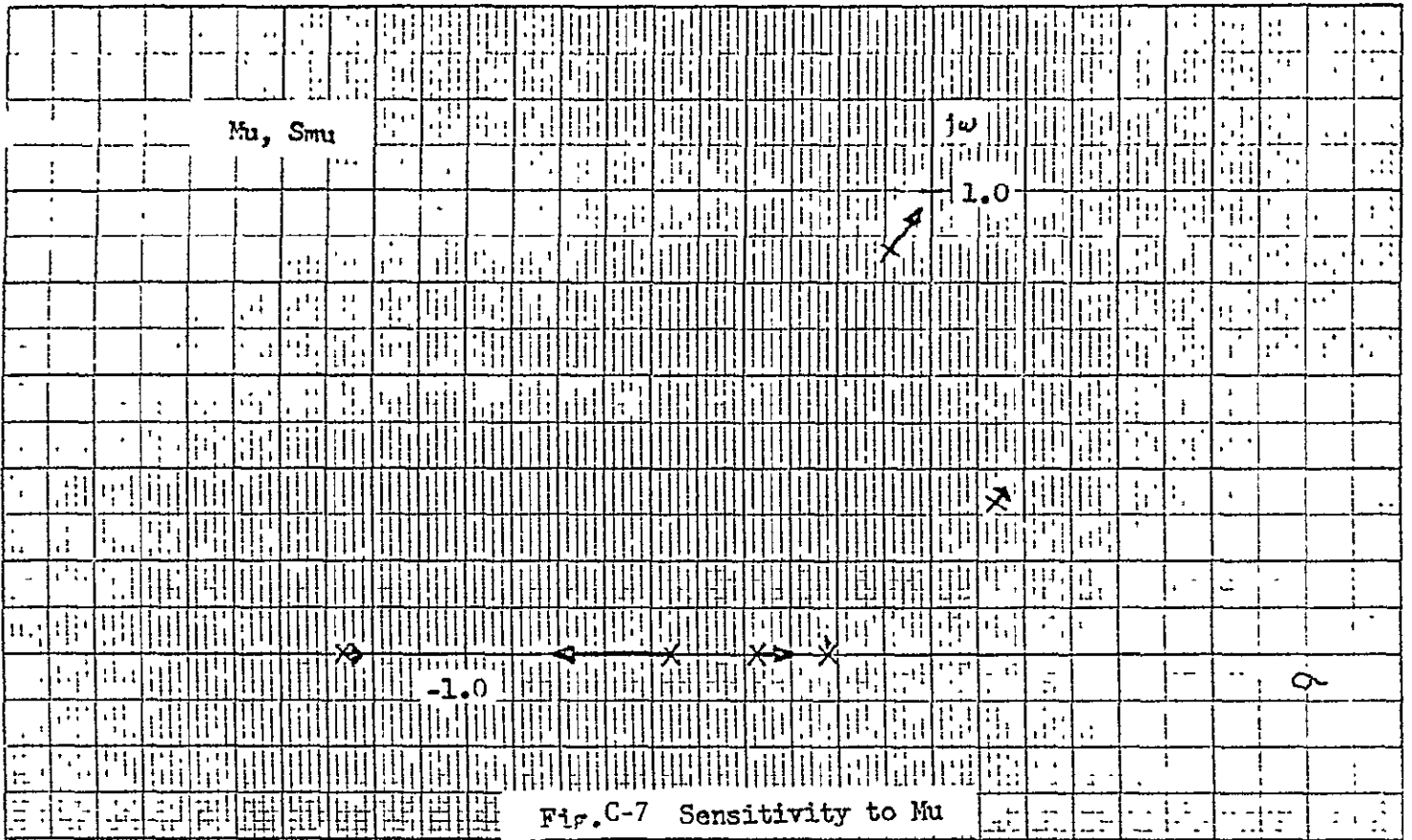


Fig.C-6 Sensitivity to Xr



10 X 10 TO 1/2 INCH 46 1400
 7/8 X 10 INCH 5
 NEUFFEL & ESSER CO.



Fig. C-9 Sensitivity to M_v

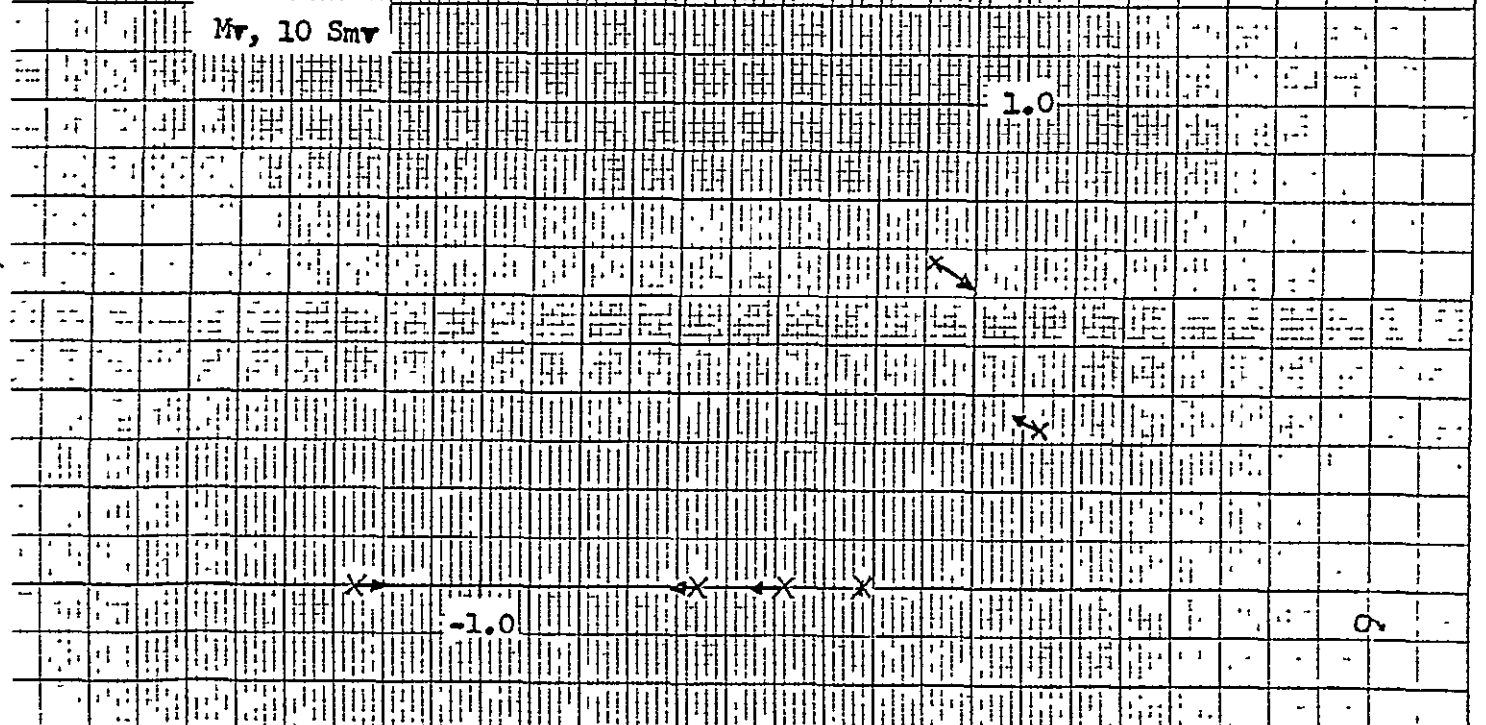


Fig. C-10 Sensitivity to M_v

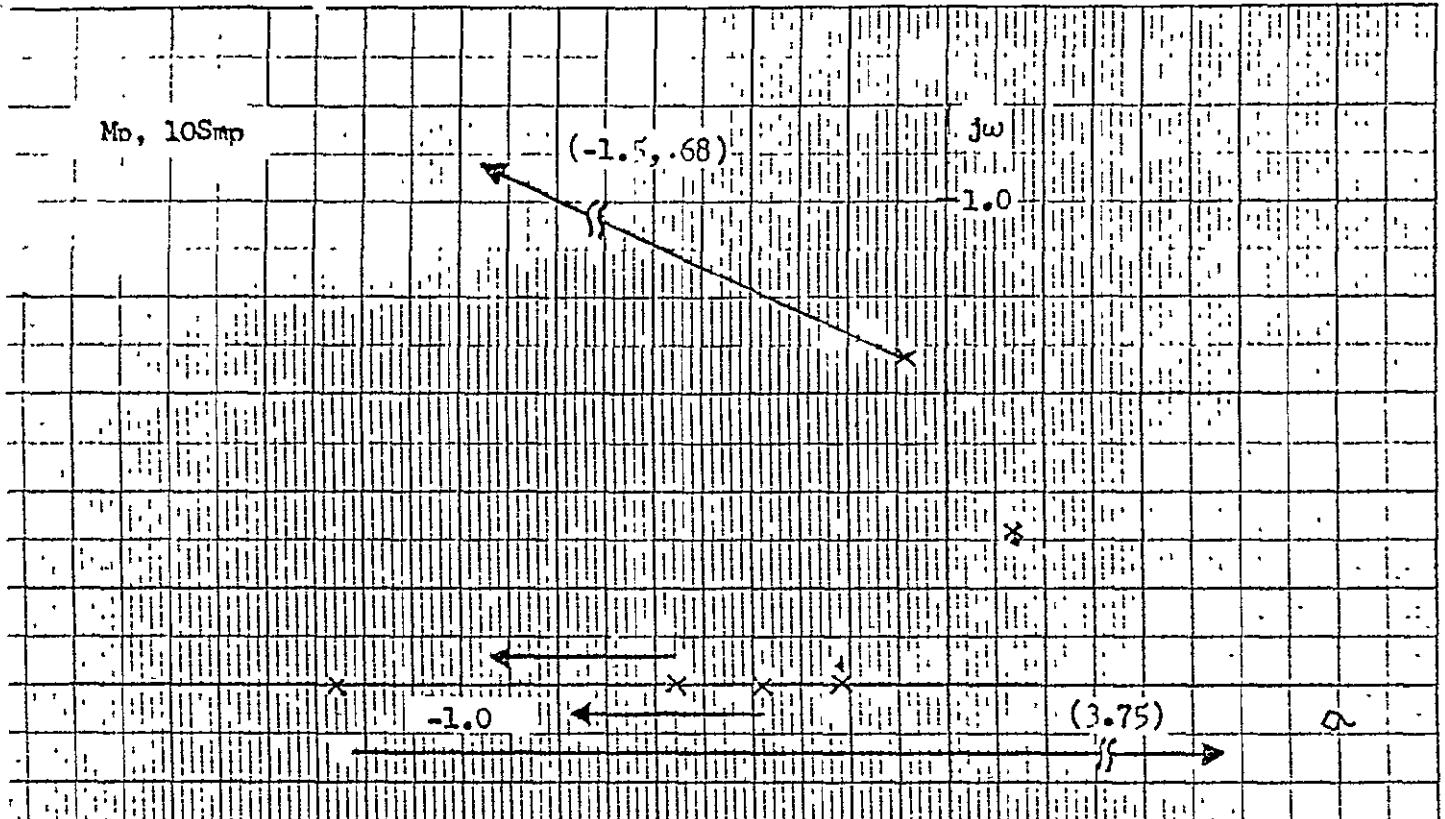


Fig. C-11 Sensitivity to M_p

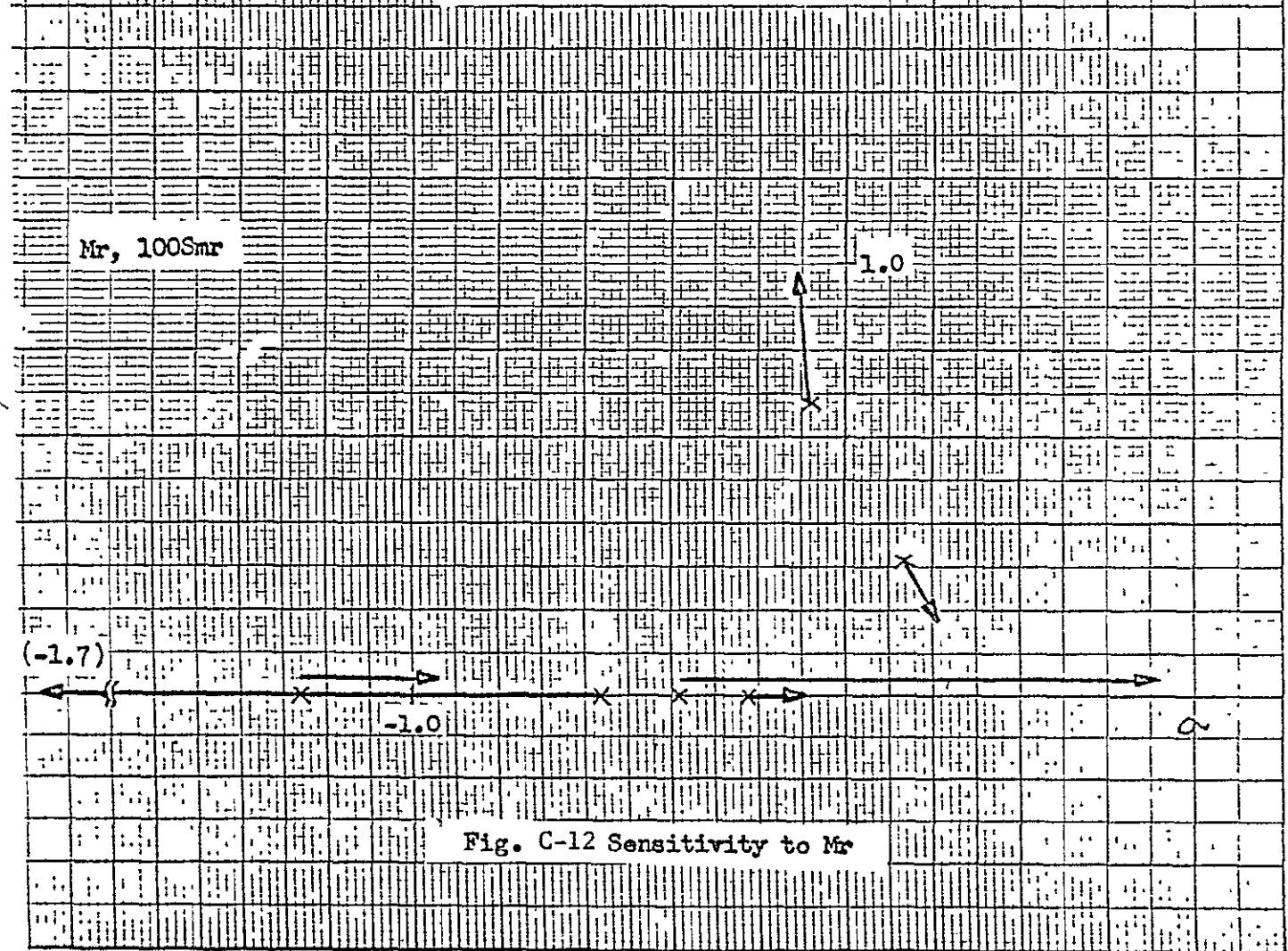


Fig. C-12 Sensitivity to M_r

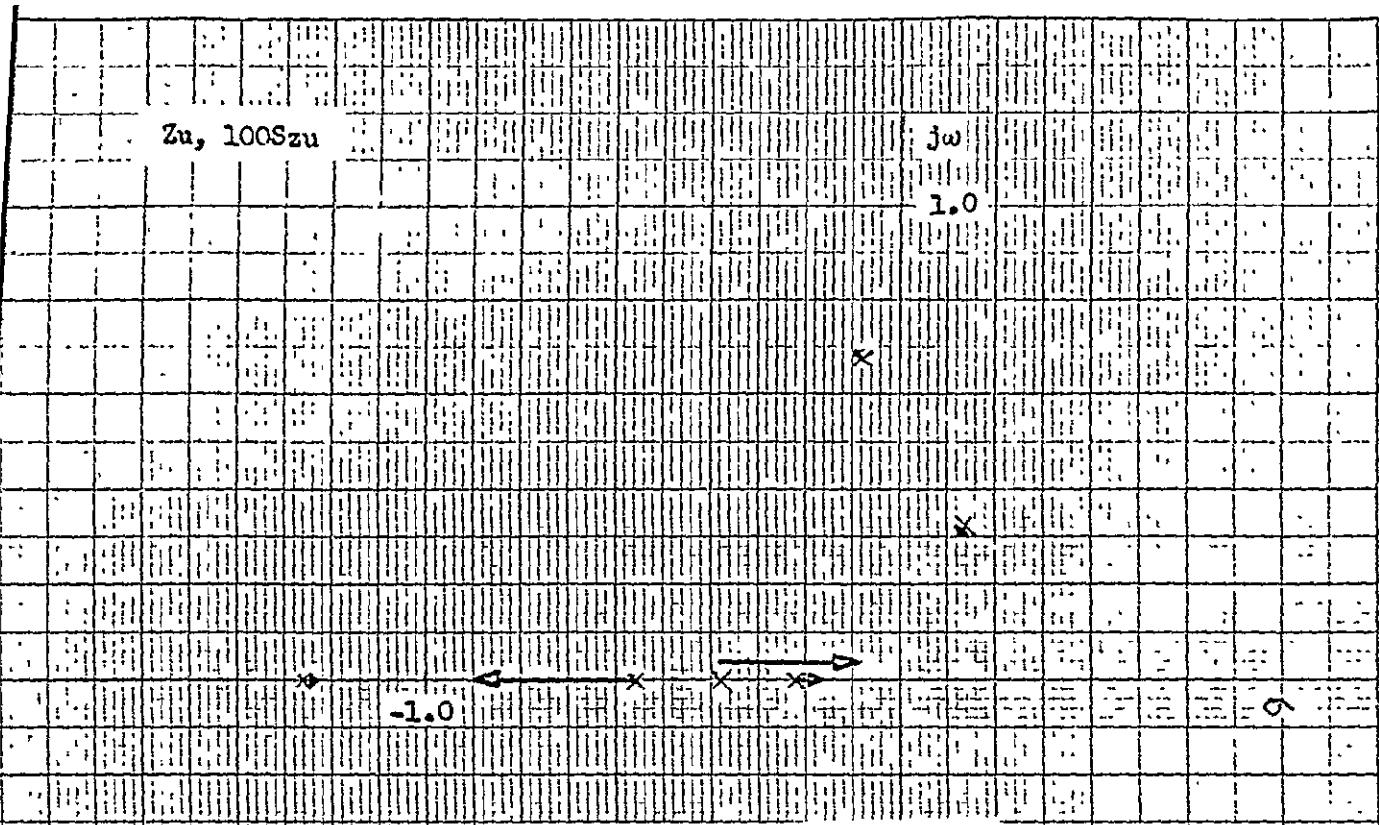


Fig.C-13 Sensitivity to Zu

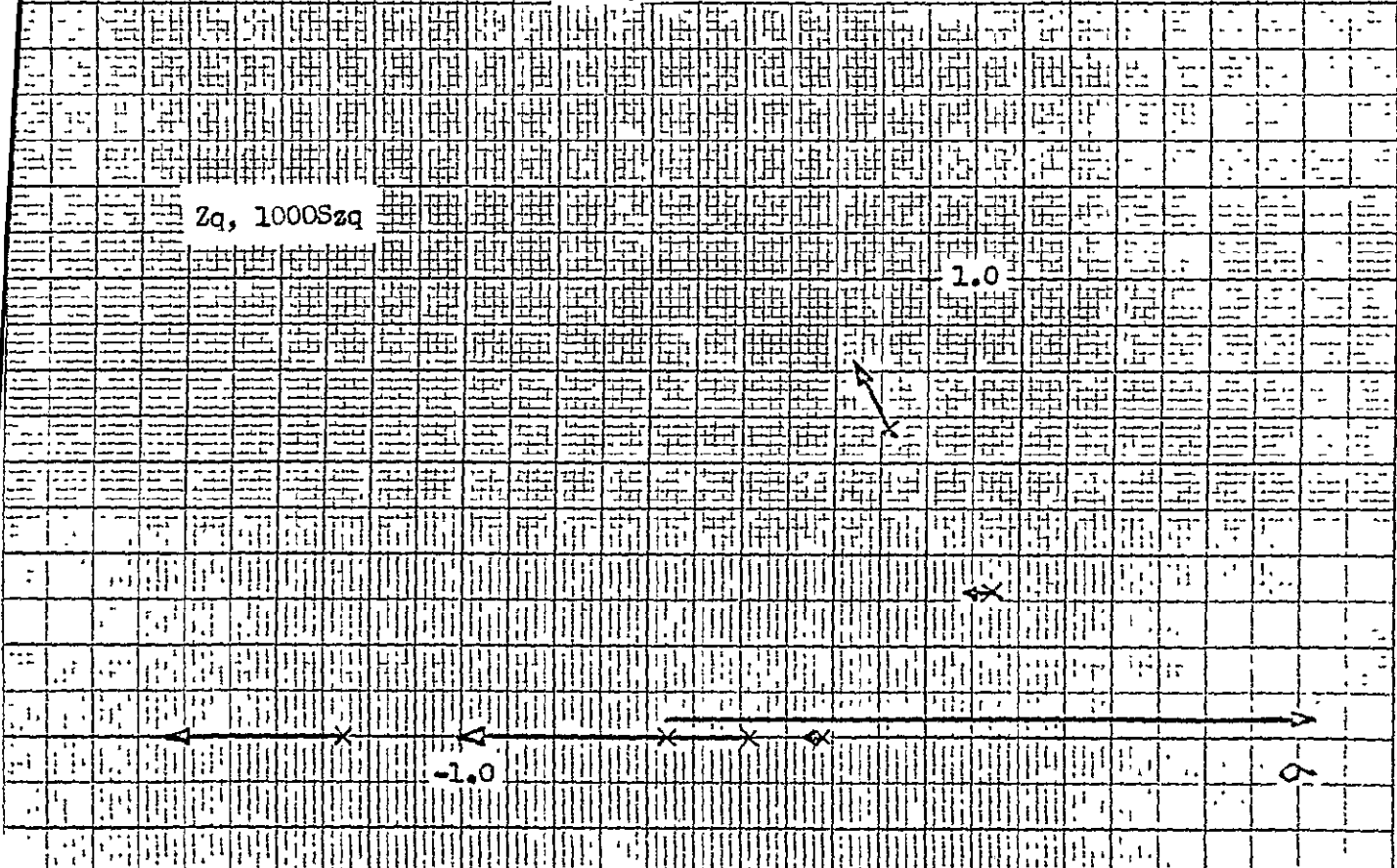


Fig. C-14 Sensitivity to Zq

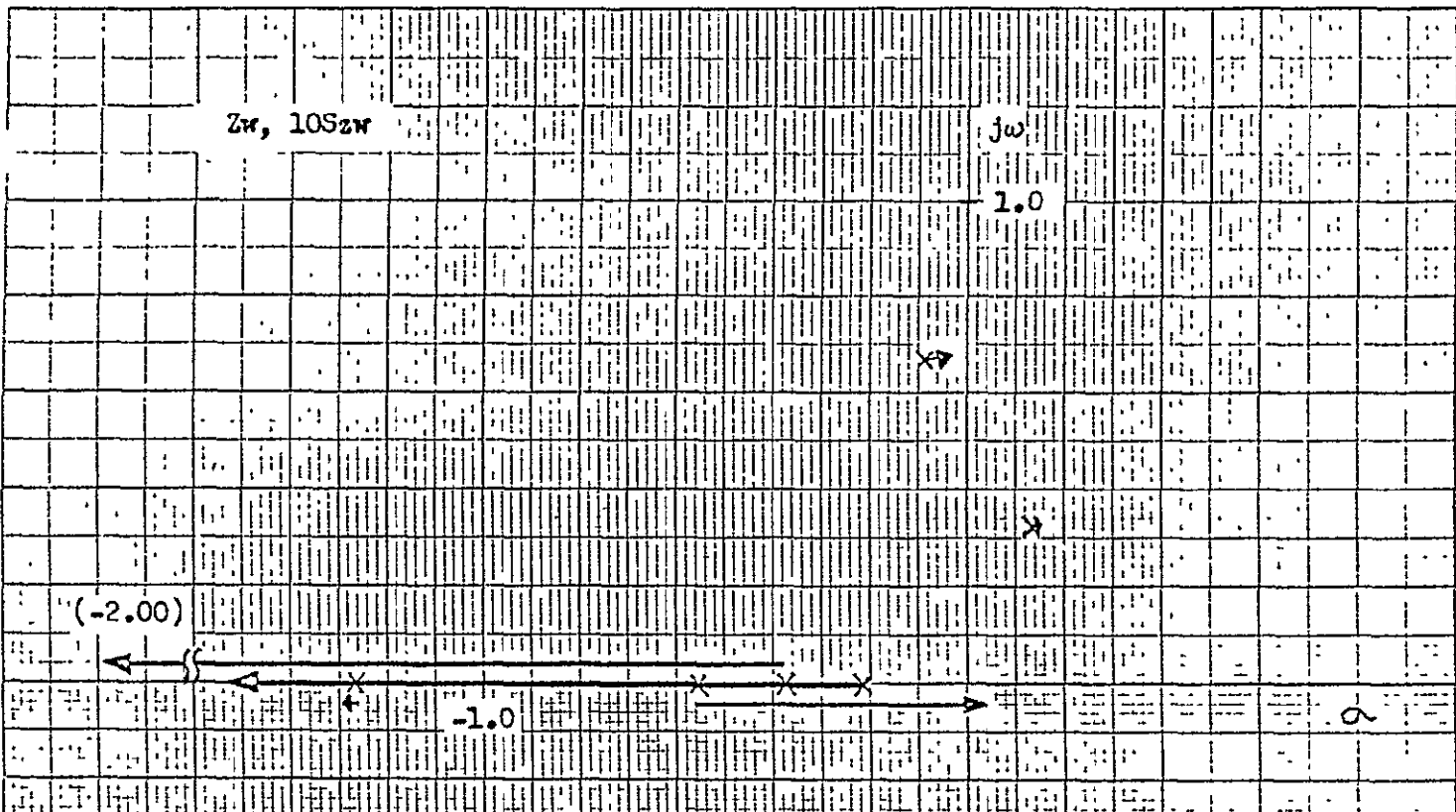


Fig.C-15 Sensitivity to Zw

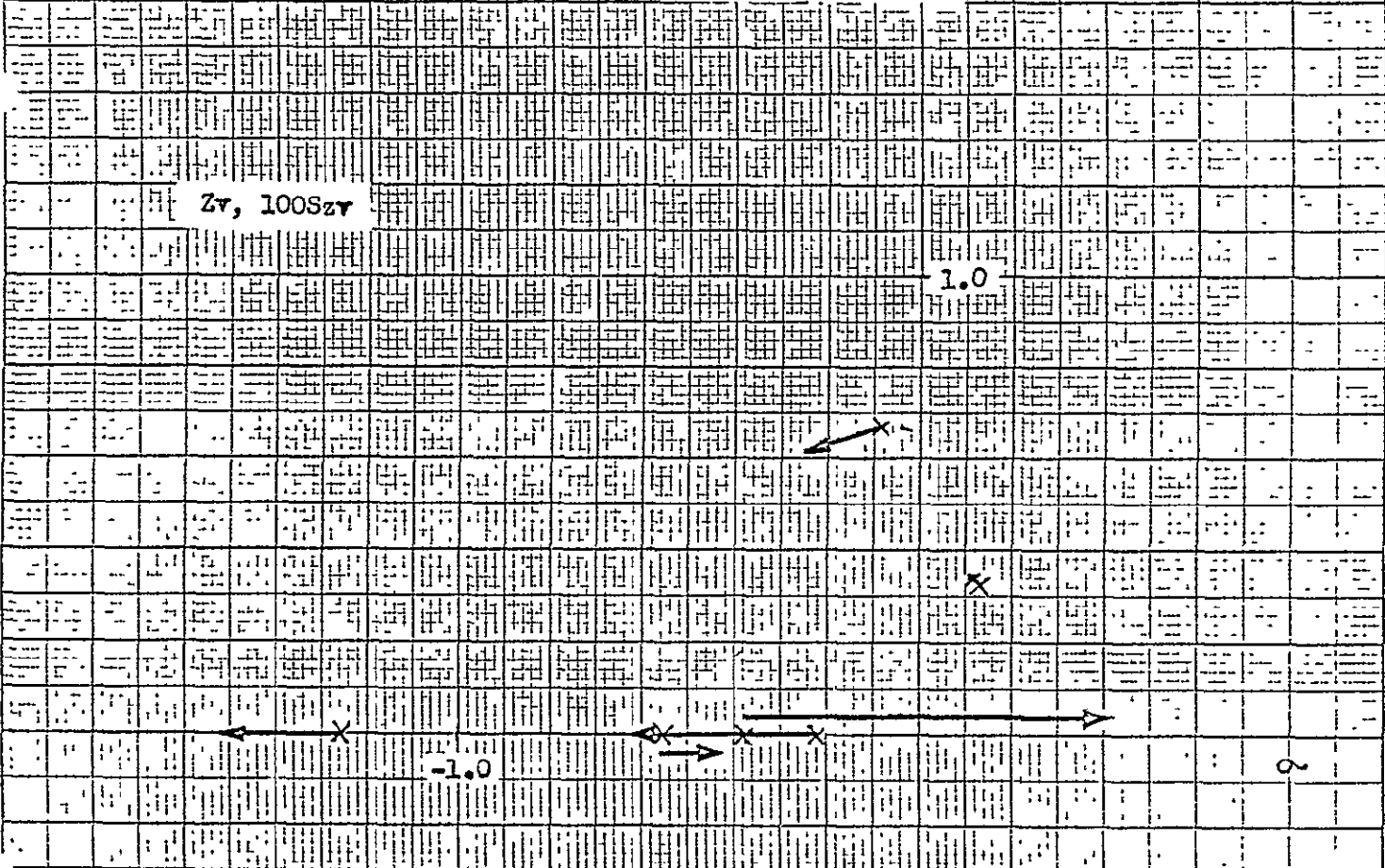


Fig. C-16 Sensitivity to Zv

MADE IN U.S.A.
 KEUFFNER & ESSER CO.

$Y_u, 1000S_{yu}$

$j\omega$



Fig. C-19 Sensitivity to Y_u

$Y_q, 100S_{yq}$

1.0

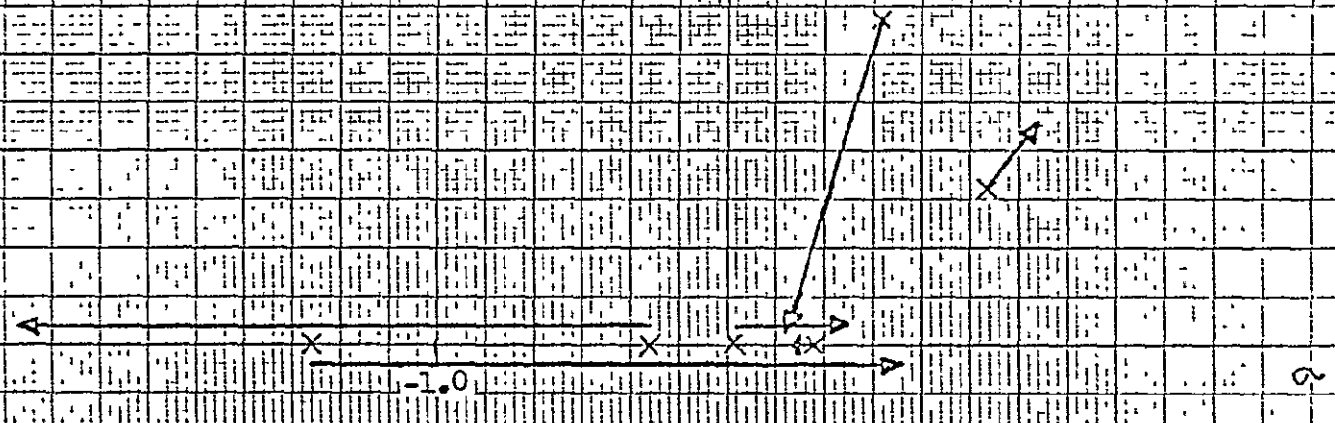


Fig. C-20 Sensitivity to Y_q

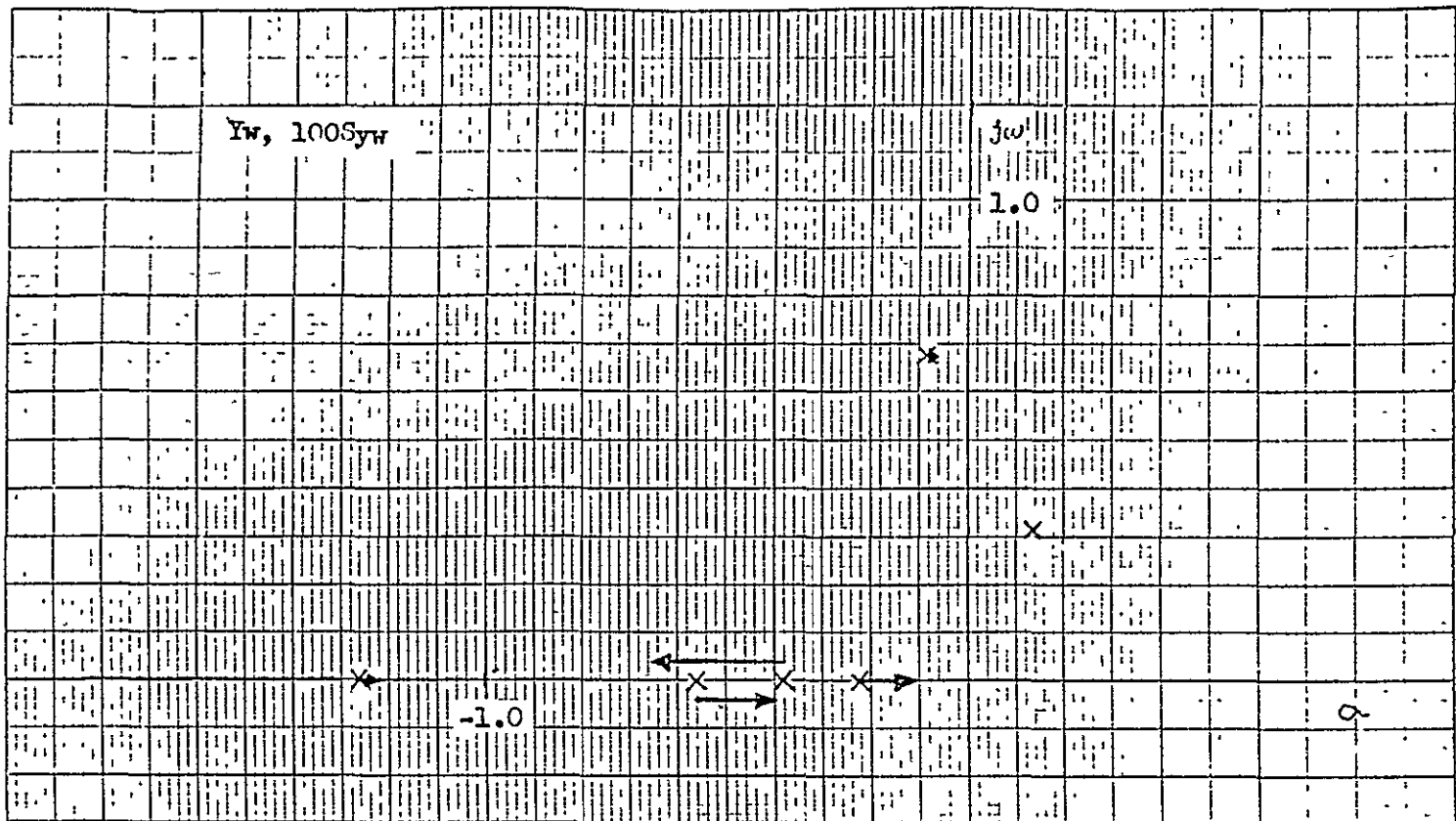


Fig. C-21 Sensitivity to Y_w

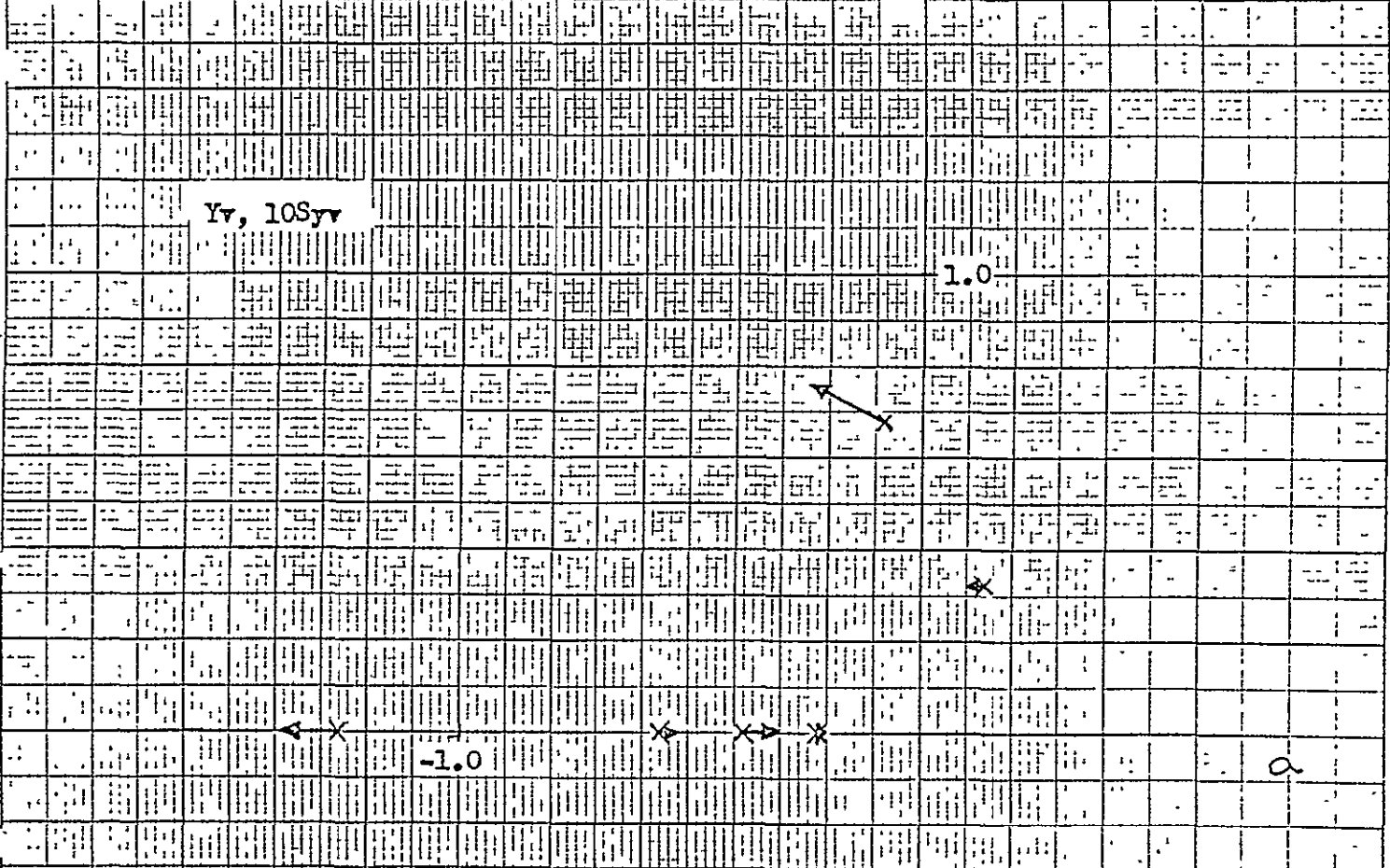


Fig. C-22 Sensitivity to Y_v

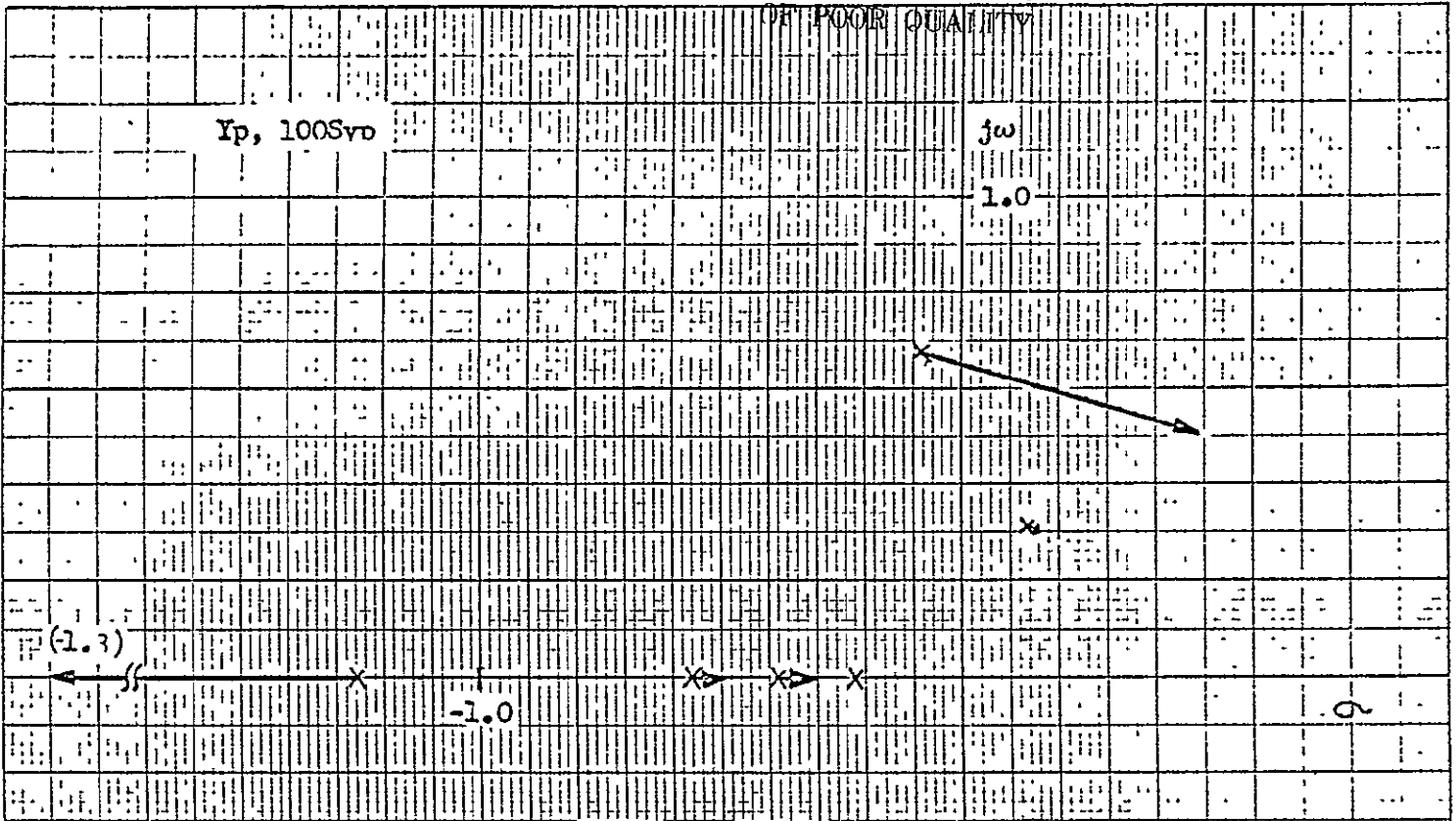


Fig. C-23 Sensitivity to Y_p

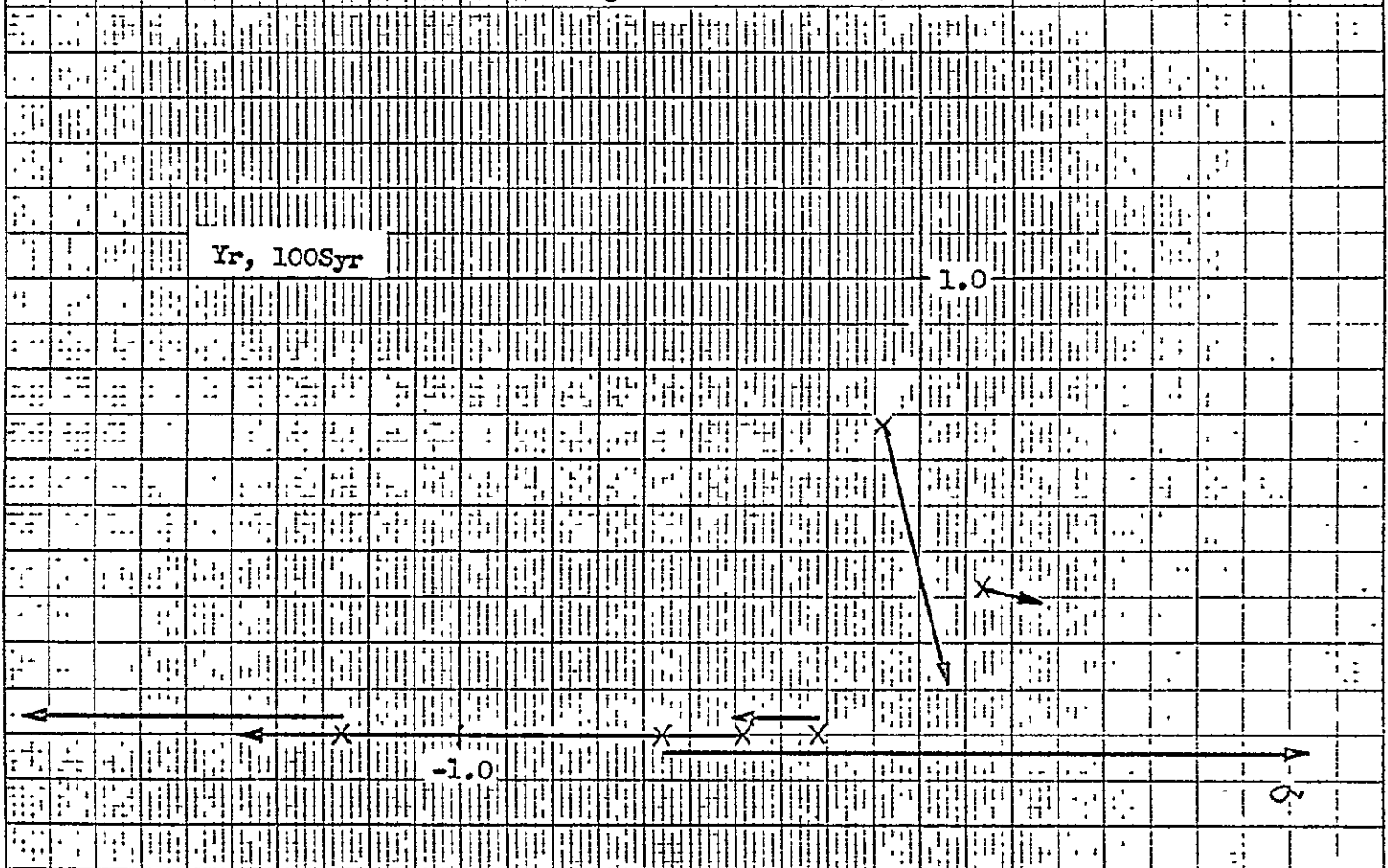


Fig. C-24 Sensitivity to Y_r

50-1479
 MADE IN U.S.A.
 KEUFFEL & ESSER CO.

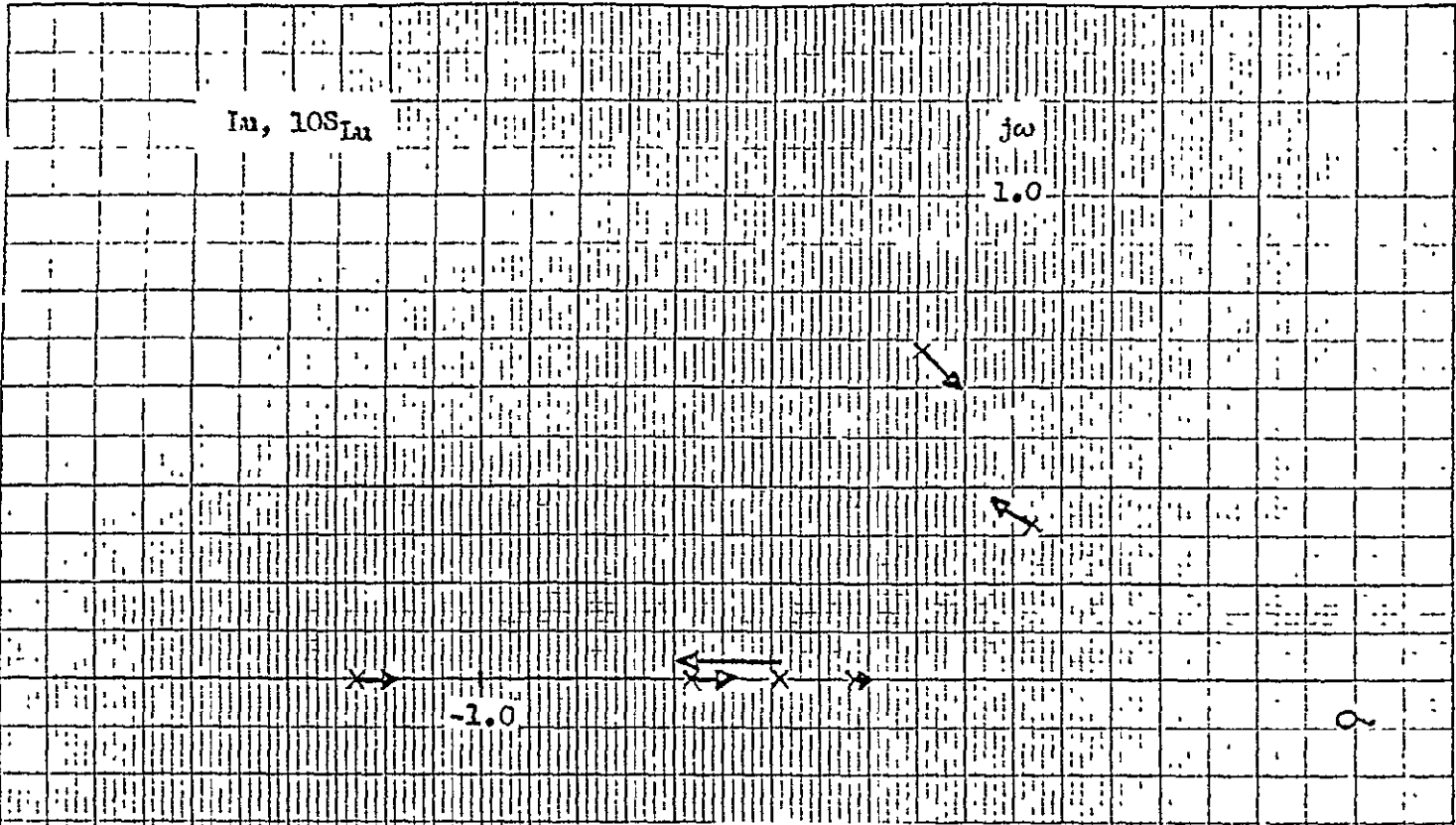


Fig. C-25 Sensitivity to I_u

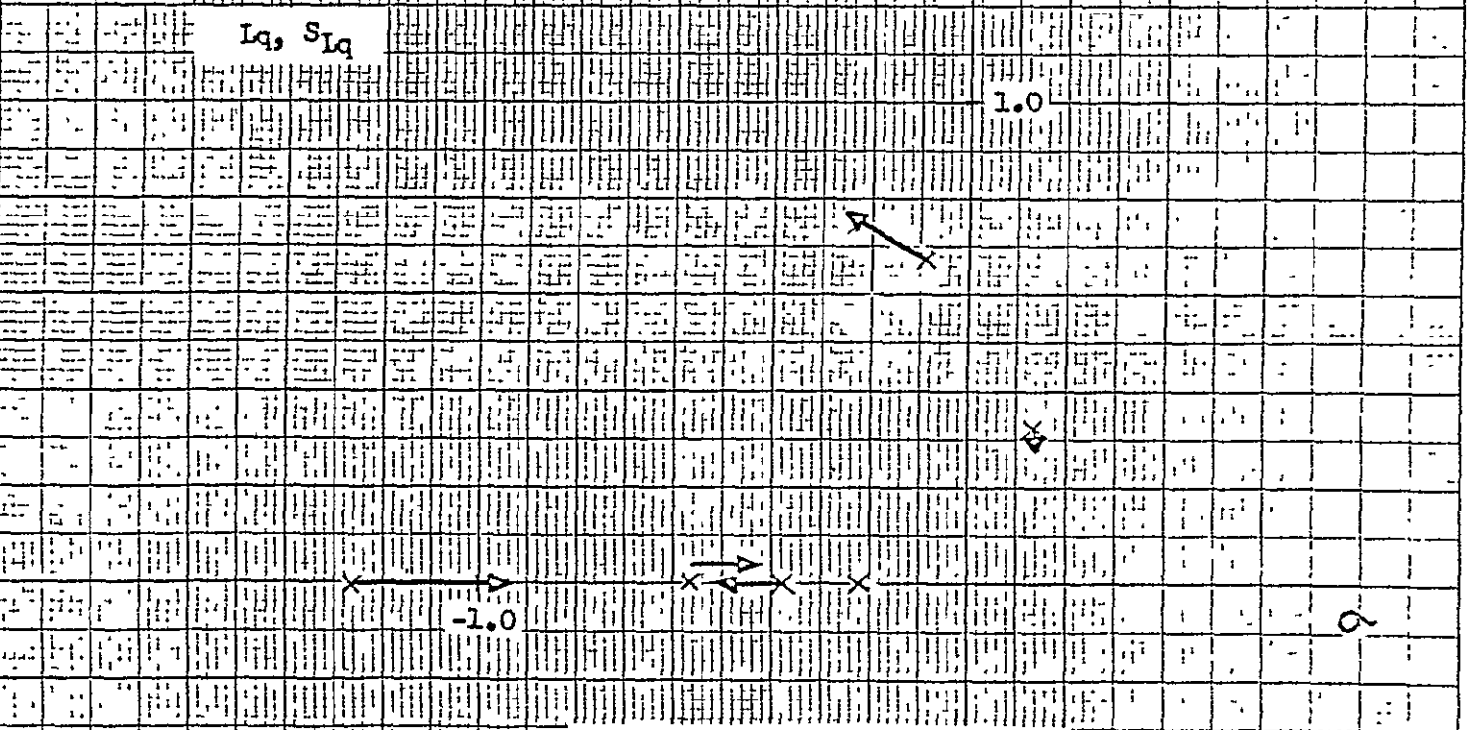


Fig. C-26 Sensitivity to L_q

P. V. 7/71 & 10/10/71
 KEUFFEL & ESSER CO.

$LW, 10SLW$

$j\omega$

1.0

-1.0

ρ

Fig. C-27 Sensitivity to LW

Lv, SLv

1.0

-1.0

ρ

Fig. C-28 Sensitivity to Lv

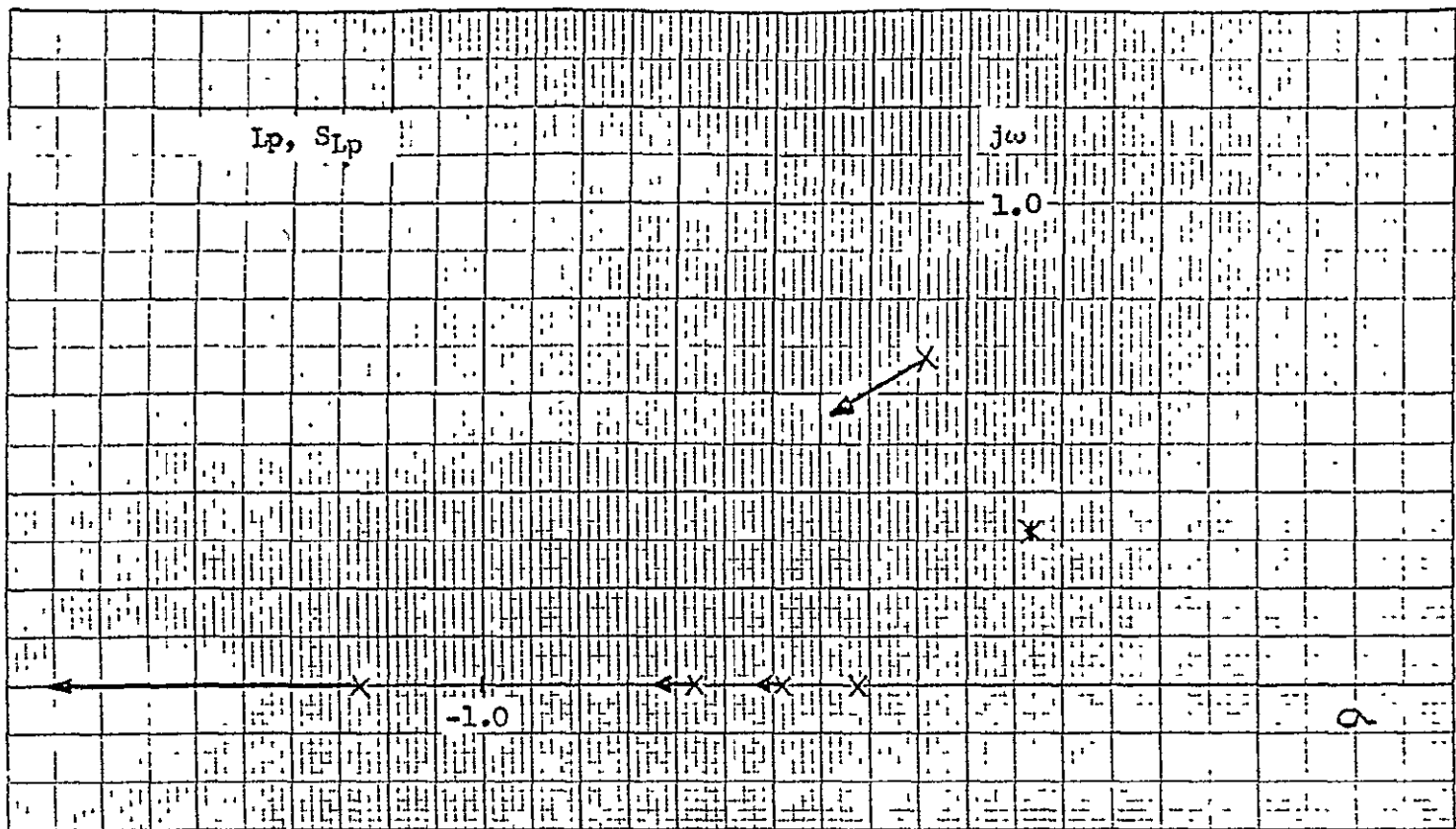


Fig. C-29 Sensitivity to L_p

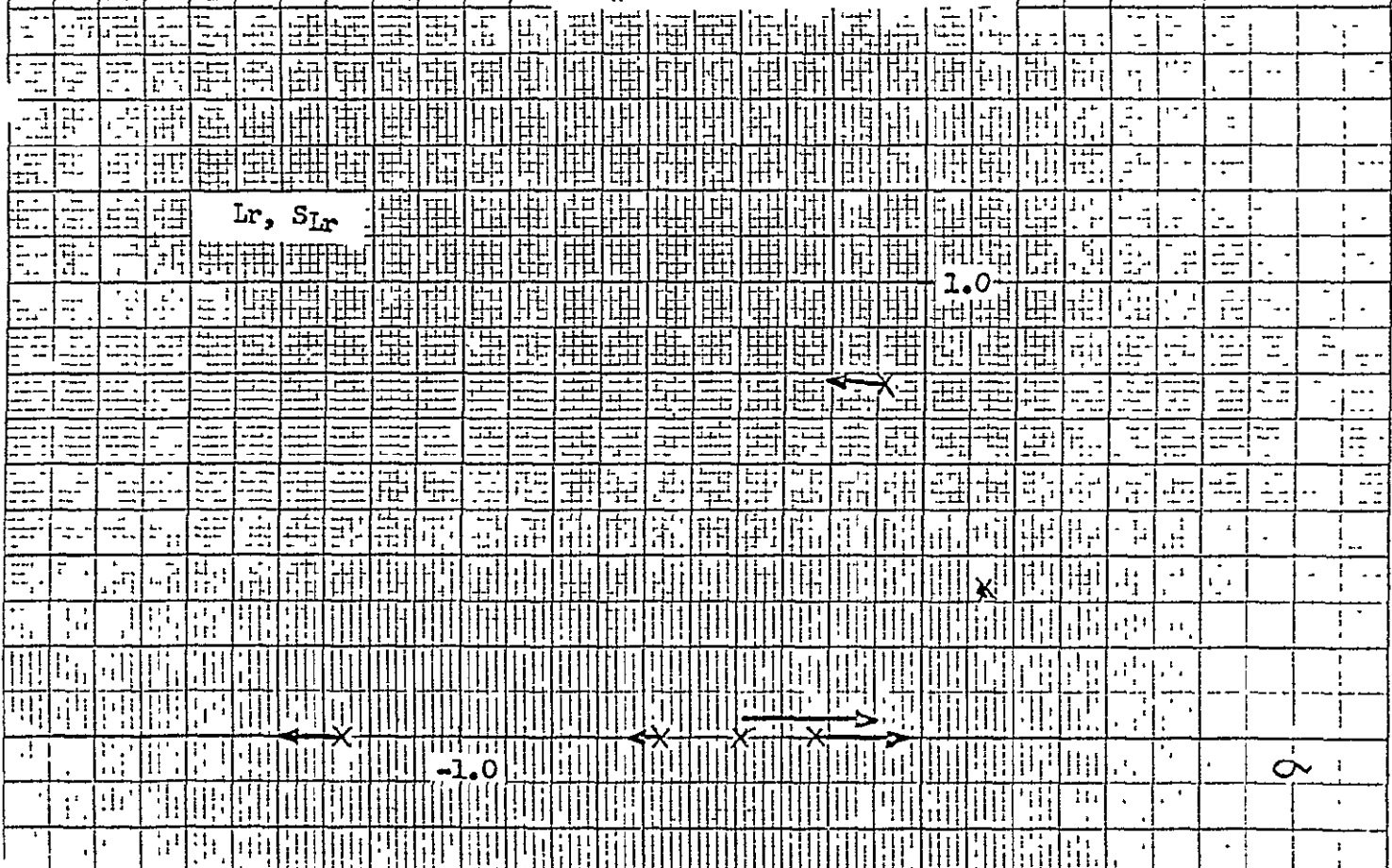


Fig. C-30 Sensitivity to L_r

INCHES 7/16 X 10 INCHES
KEUFFNER & ESSER CO.

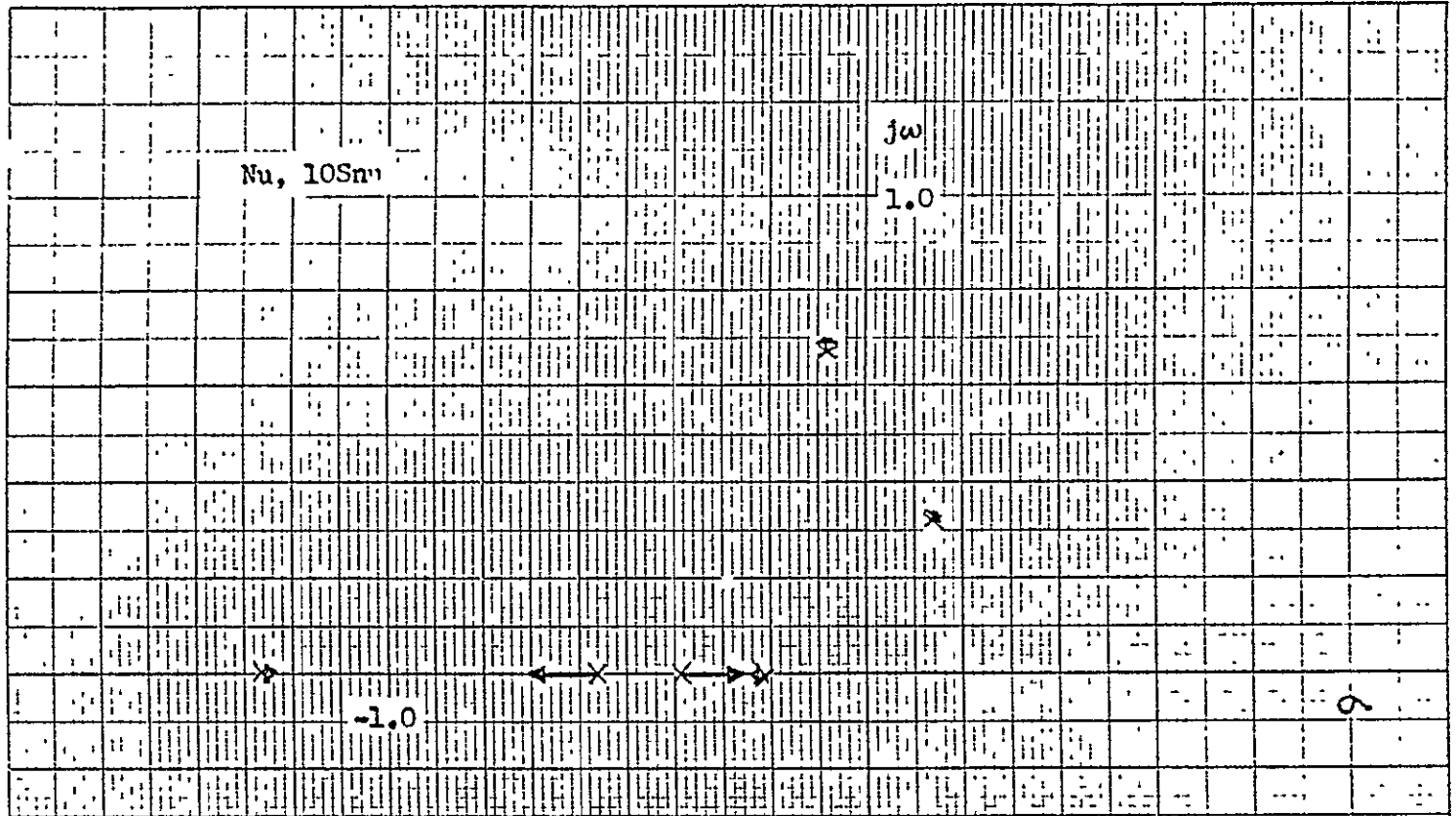


Fig. C-31 Sensitivity to Nu

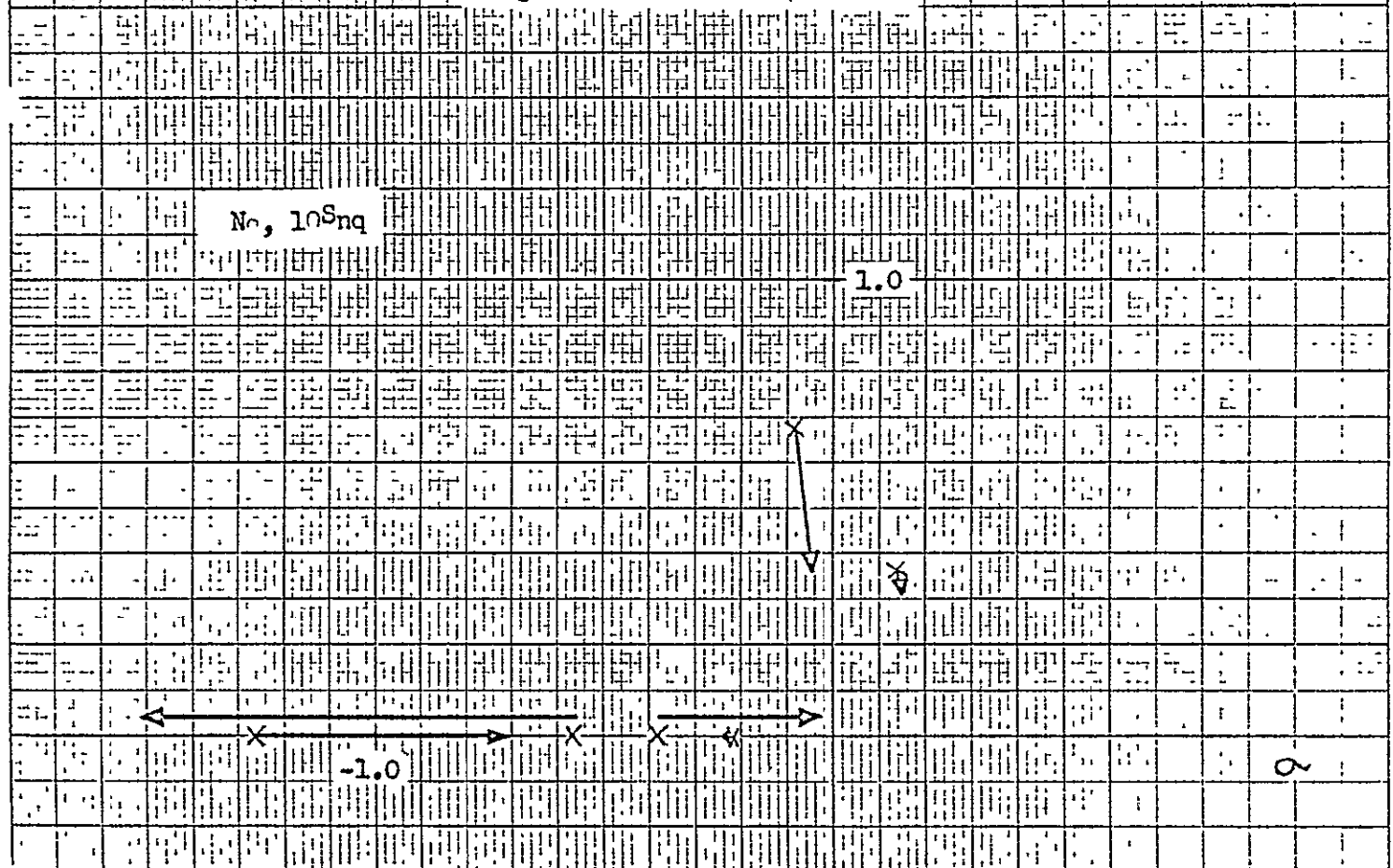


Fig. C-32 Sensitivity to Ng

$N_p, 10S_{np}$

$j\omega$

1.0

-1.0

Fig. C-35 Sensitivity to N_p

N_r, S_{nr}

1.0

-1.0

Fig. C-36 Sensitivity to N_r

APPENDIX D1
REVIEW OF LINEAR OPTIMAL REGULATOR

Optimal Time-Invariant Linear Regulator (Deterministic)

The general results of optimal time-invariant linear regulator problems are summarized in this section.

System Dynamics

Given is a deterministic, time-invariant, linear dynamical system with n -dimensional state vector (or variable) $x(t)$ and m -dimensional control vector (or variable) $u(t)$.

$$\dot{x}(t) = Ax(t) + Bu(t) \quad (D1-1)$$

$$x(t_0) = x_0 \quad (D1-2)$$

where A and B are $n \times n$ and $n \times m$ constant coefficient matrices, and x_0 is the initial state vector at time t_0 . Usually, the dimensional of state vector is larger than that of control vector ($n \geq m$).

The p -dimensional output vector $y(t)$ consists of a linear combination of the components of state vector $x(t)$:

$$y(t) = Hx(t) \quad (D1-3)$$

Without loss of generality, the $p \times n$ output matrix H has its maximum rank p ($p \leq n$). The output vector $y(t)$ can be regarded as p independent

measurements of the system state $x(t)$. Note that, in many or most of the practical cases, the output matrix H can be an $n \times n$ identity matrix. In Illustration (D1-1) is shown the block diagram of the system.

Throughout this work, the lower case character usually stands for a column vector and the upper case for a matrix. The argument "t" usually means time and $(\dot{\cdot})$ represents the time derivative of the argument.

Cost Function

By properly chosen output weighting matrix Q and control weighting matrix R , the quadratic cost function without cross coupled term of the output vector and the control vector is expressed as follows

$$J(x_0, u(t)) = \int_{t_0}^{\infty} [y^T(t)Qy(t) + u^T(t)Ru(t)]dt \quad (D1-4)$$

where the matrices Q and R are $p \times p$ and $m \times m$ constant symmetric matrices, and throughout this report, the superscript T $((\cdot)^T)$ stands for the transpose of vector or matrix.

The $p \times p$ symmetric output weighting matrix Q and the $m \times m$ symmetric control weighting matrix R are both assumed to be positive definite, or

$$\left. \begin{array}{l} Q > 0 \\ R > 0 \end{array} \right\} \quad (D1-5)$$

Hence, the integrand of quadratic cost function $J(x_0, u(t))$ in Eq. (D1-4) is non-negative for any output $y(t)$ and any control $u(t)$ during the process interval $[t_0, \infty)$.

Controllability

An optimal control law $u^*(t)$ has to be determined, that minimizes the quadratic cost function $J(x_0, u(t))$ subject to the system dynamics represented by Eqs. (D1-1), (D1-2) and (D1-3).

The assumption of the positive definiteness for Q and R weighting matrices guarantees the convexity of quadratic cost function $J_{\min}(x_0, u(t))$, but it does not imply that the minimum of cost function $J_{\min}(x_0)$ is finite. The cost function is finite by the "complete controllability condition".

The condition of "Complete Controllability" for stationary system (Eqs. (D1-1) and (D1-2) considered here is that the following n rows by nxnm composite matrix has the maximum rank (=n):

$$\text{Rank } \begin{bmatrix} B \\ \vdots \\ AB \\ \vdots \\ A^2B \\ \vdots \\ \dots\dots\dots \\ \vdots \\ A^{n-1}B \end{bmatrix} = n \quad \text{(D1-6)}$$

A matrix pair of A and B satisfying Eq. (D1-6) is usually said as "Completely Controllable pair [A, B]".

Complete controllability guarantees the finiteness of the minimum cost function $J_{\min}(t_0, u(t))$. Also, since the quadratic cost function Eq. (D1-4) is a convex function, the $J_{\min}(x_0, u(t))$ exists and is unique.

Optimal Control Law

The optimal control problem can be solved by the aid of calculus of variations, or Pontryagin's maximum principle and/or Bellman's dynamic programming. Since there is no active constraint involved except the dynamical equation, the simplest straightforward way may be to use the calculus of variations. The result of this calculation is that matrix K must

satisfy the "Algebraic Matrix Riccati Equation".

$$KA + A^T K - KDK + H^T QH = 0 \quad (D1-7)$$

(note $H^T QH \geq 0$)

where D is a n x n constant, symmetric, positive semidefinite matrix defined by

$$D \equiv BR^{-1}B^T \quad (\geq 0) \quad (D1-8)$$

Let the matrix K be a proper solution of Eq. (D1-7). Then the optimal control law is expressed in the linear feedback form. Using Eq. (D1-15) and (D1-17),

$$\begin{aligned} u^*(t) &= -R^{-1}B^T Kx^*(t) \\ &= -Gx^*(t) \end{aligned} \quad (D1-9)$$

where G is the feedback gain matrix (m x n) defined by

$$G \equiv R^{-1}B^T K \quad (D1-10)$$

By using the optimal feedback control law to the plant dynamics Eq. (D1-1), the optimal closed loop system dynamics become

$$\dot{x}(t) \equiv (A - BR^{-1}B^T K) x(t) = Fx(t) \quad (D1-11)$$

where the asterisks on $x(t)$ have been dropped off, and the $n \times n$ matrix F is the closed loop system matrix defined by

$$F \equiv A - BR^{-1}B^TK \equiv A - DK \equiv A - BG \quad (D1-12)$$

The eigenvalues of matrix F indicate the poles of the optimal closed loop system. The stability of the system depends on the signs of the real parts of the eigenvalues. There exist many real symmetric solution matrices (K 's) of the algebraic matrix Riccati equation (Eq. D1-7) for given positive definite matrices Q and R . It has been shown by R.E. Kalman in Ref. (A1) that if $[A, B]$ is a completely controllable pair, there exists a unique solution matrix K of Eq. (D1-19), which is a $n \times n$ positive definite symmetric matrix and makes the real parts of all the eigenvalues of F be negative (it means a stable system); namely,

$$K > 0, \text{ unique and symmetric}$$

$$\text{for } Q > 0 \text{ and } R > 0$$

and

$\text{Re}\{\lambda_i[\cdot]\}$ means the real part of the i -th eigenvalue of a matrix. Therefore, the closed loop system expressed by Eq. (D1-11) is asymptotically stable. Thus, the optimal control law $u^*(t)$ in Eq. (D1-9) exists and is unique for given weighting matrices Q and R .

It is important to note that the matrix Riccati equation (Eq. (D1-7)) is independent of the system state and time, and so is the optimal feedback gain matrix G in Eq. (D1-10).

observed vector) $y(t)$, despite the attempt to use the output $y(t)$ as the feedback signal. Hence, the optimal controller requires all the information about the system state $x(t)$, which has to be computable out of the observed vector $y(t)$. If the output vector $y(t)$ could not generate the (unique) state vector $x(t)$ or if the state vector $x(t)$ could not be directly observed (or measured), then the obtained optimal system would not be realizable.

A "state x_0 is observable at t_0 " if, given any control $u(t)$, there is a time $t_1 > t_0$ such that knowledge of $u(t)$ and the output $y(t)$ over $[t_0, t_1]$ is sufficient to determine x_0 . If the argument is true for every state x_0 at time t_0 , then the system is said to be "observable at t_0 ". If every x_0 is observable at every time t_0 in the interval of definition of the system, then the system is said to be "completely observable". Since the system under consideration here is stationary (constant coefficient), the system (Eqs. (D1-1), (D1-2), (D1-3)) is assumed to be completely observable.

The condition of complete observability for time-invariant linear system is that the following n -rows by np -columns composite matrix has the maximum rank ($=n$)

$$\text{Rank} \begin{bmatrix} H^T \\ A^T H^T \\ (A^T)^2 H^T \\ \vdots \\ (A^T)^{n-1} H^T \end{bmatrix} = n \quad (D1-12)$$

A matrix pair of A and H satisfying Eq. (D1-30) is said "Completely Observable pair $[A, H]$ ".

Minimum of Quadratic Cost Function

By using the unique optimal feedback control law (Eq. (D1-9)), the minimum of quadratic cost function $J_{\min}(x_0)$ can be uniquely evaluated in terms of K matrix and the initial state x_0 ; and equals:

$$J_{\min}(x_0 ; Q, R) = x_0^T K x_0 \quad (D1-13)$$

Block Diagram Optimal Regulator

The block diagram of the optimal system described above is shown as Illustration D1-1.

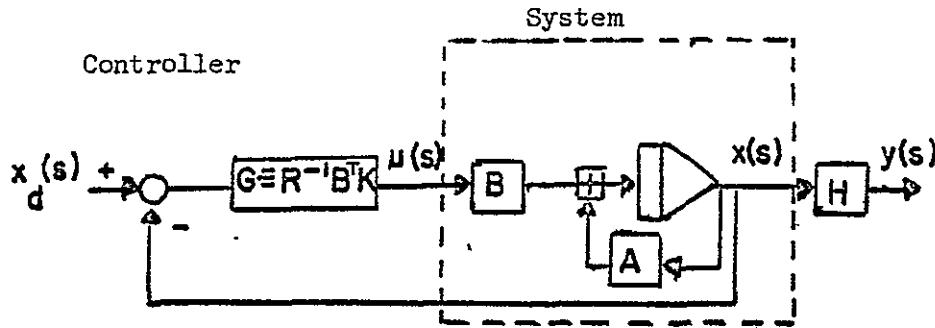


Illustration D1-1. Block Diagram of Linear Optimal Control System

Observability

Eq. (D1-21) and the block diagram shows that the optimal control $u^*(t)$ is a function of the state vector $x(t)$ rather than a function of the state vector $x(t)$ rather than a function of the output vector (or the

Note that, combining Eq. (D1-6) with Eq. (D1-12), the system is assumed to be both completely controllable and completely observable.

The observability condition Eq. (D1-12) guarantees that one can compute the unique state $x(t)$ from knowledge of the output $y(t)$ and the control $u(t)$ over $[t_0, t]$. When the output matrix H is the $n \times n$ identity matrix ($\equiv I_n$), the problem is called "State-Regulator Problem", whereas the problem with a nonidentity H matrix is called "Output-Regulator Problem".

Summary of the Deterministic Optimal Regulator

The deterministic optimal regulator for a completely controllable and observable system can be summarized as follows

System dynamics: $x(t) = Ax(t) + Bu(t); x(t_0) = x_0$
 $y(t) = Hx(t)$

where $x(t)$: n dimensional state vector

$u(t)$: m dimensional control vector ($m \geq n$)

$y(t)$: p dimensional output vector ($p \geq n$)

A, B and H : $n \times n$, $n \times m$ and $p \times n$ constant matrices

Cost function: $J_{\min}(x_0, Q, R) = \min_{u(t)} \int_{t_0}^{\infty} [y^T(t)Qy(t) + u^T(t)Ru(t)] dt \quad (3)$
 $= x_0^T K x_0 \quad (4 \text{ and } 11)$

where Q and R : positive definite symmetric constant matrices

Variables and equations:

Number of Variables	Number of Equations
$x(t) : n$	(1) : n
$u(t) : m$	(1) : p
$y(t) : p$	(3) : 1
$J(\cdot) : 1$	(11) or (4) : m
$Q : p^2$	(5) : n^2
$R : m^2$	
$K : n^2$	

Total: $(n+m+p+1+p^2+m^2+n^2)$ unknowns. Total: $(n+p+1+m+n^2)$ eqs.

- Conclusion:
1. If Q, R are given, then number of variables = number of equations.
 2. If Q and R are not given, then the number of equations is $n^2 + m^2$ less than the number of unknowns.

APPENDIX D2

OPTIMAL LINEAR CONTROLLER DESIGN APPLIED TO A SECOND ORDER SYSTEM

The system equation is represented by the following differential equation

$$\ddot{x}(t) = a\dot{x}(t) + bu(t) \quad (D2-1)$$

where

$x(t)$ = position

$\dot{x}(t)$ = rate of position

$u(t)$ = control input

a = rate damping

b = control derivatives

In the state variable form

$$\dot{x}(t) = Ax(t) + Bu(t) \quad (D2-2)$$

where

$$x(t) = \begin{bmatrix} x_1(t) \\ x_2(t) \end{bmatrix} = \begin{bmatrix} x(t) \\ \dot{x}(t) \end{bmatrix} \quad (D2-3)$$

$$A = \begin{bmatrix} 0 & 1 \\ 0 & a \end{bmatrix} \quad (D2-4)$$

$$B = \begin{bmatrix} 0 \\ b \end{bmatrix} \quad (D2-5)$$

$$u(t) = \delta \quad (D2-6)$$

The Optimal Linear Regulator Approach

The quadratic performance index be minimized is:

$$J = \frac{1}{2} \int_0^{\infty} (x(t)^T Q x(t) + r u(t)^2) dt \quad (D2-7)$$

where

Q : 2 by 2 non-negative, symmetric weighting matrix for

$q_{11}, q_{12}, q_{12}, q_{21} > 0$ states

r : a scalar weighting factor for control

The optimal control which minimize (D2-7) is

$$\begin{aligned} u &= -Gx(t) \\ &= -\frac{1}{r} B^T Kx(t) \end{aligned} \quad (D2-8)$$

where G is a feedback gain matrix and K is a solution matrix of the following Riccati matrix equation.

$$KA + A^T k - \frac{1}{r} KBB^T + Q = 0 \quad (D2-9)$$

Expanding the latter equation gives:

$$\frac{b^2}{r} k_{12} k_{21} - q_{11} = 0$$

$$\frac{b^2}{r} k_{12} k_{22} - (ak_{12} + k_{11}) - q_{12} = 0 \quad (D2-10)$$

$$\frac{b^2}{r} k_{12} k_{22} - (ak_{21} + k_{11}) - q_{21} = 0$$

$$\frac{b}{r} k_{22}^2 - 2ak_{22} - (k_{12} + k_{21}) - q_{22} = 0$$

From the symmetric property of weighting matrix Q follows $q_{12} = q_{21}$. The solution of Eq. D2-10 becomes

$$k_{11} = \sqrt{q_{11} r \left\{ \left(\frac{a}{b}\right)^2 + \frac{2}{b} \sqrt{\frac{q_{11}}{r}} + \frac{q_{22}}{r} \right\}}$$

$$k_{12} = k_{21} = \sqrt{\frac{q_{11} r}{b^2}} \quad (D2-11)$$

$$k_{22} = \frac{r}{b^2} \left(a + \sqrt{a^2 + 2b \sqrt{\frac{q_{11}}{r}} + \frac{b^2}{r} q_{22}} \right)$$

Substitution into (D2-8) gives the optimal control

$$u = - \frac{b}{r} [G_x x_1 + G_{\dot{x}} x_2] \quad (D2-12)$$

where G_x is a position feedback gain and $G_{\dot{x}}$ is its rate feedback gain given as follows:

$$G_x = - \sqrt{\frac{q_{11}}{r}} \quad (D2-13)$$

$$G_x^* = -\frac{a}{b} + \sqrt{\left(\frac{a}{b}\right)^2 + \frac{2}{b} \sqrt{\frac{q_{11}}{r}} + \frac{q_{22}}{r}} \quad (D2-14)$$

Note that the weighting factors q_{12} or q_{21} are irrelevant to the optimal feedback gains.

From (D2-2), (D2-12), (D2-13) and (D2-14), the equation for the closed loop system becomes:

$$\dot{x}(t) + \sqrt{a^2 + 2b\sqrt{\frac{q_{11}}{r}} + b^2 \frac{q_{22}}{r}} \dot{x} + b\sqrt{\frac{q_{11}}{r}} x(t) = 0 \quad (D2-15)$$

When this closed loop system is described by

$$\ddot{x}(t) + 2\zeta\omega_n \dot{x}(t) + \omega_n^2 x(t) = 0 \quad (D2-16)$$

then

$$\omega_n = \sqrt{b\sqrt{\frac{q_{11}}{r}}}$$

$$\zeta = \frac{1}{2} \sqrt{2 + \frac{a^2}{b} \sqrt{\frac{r}{q_{11}}} + bq_{22} \sqrt{\frac{1}{rq_{11}}}} \quad (q_{11} \neq 0) \quad (D2-17)$$

Closed Loop System Properties as a Function of Control Weighting

When the control weighting R approaches infinity, ($R \rightarrow \infty$)

$$G_x = 0 \quad (D2-18)$$

$$G_x^* = 0 \quad (a < 0)$$

$$= -\frac{2a}{b} \quad (a > 0) \quad (D2-19)$$

The feedback gains do not all go to zero; therefore the closed loop system

approaches the stable original system or the adjoint system in the case of an unstable original system because:

$$\ddot{x}(t) + |a| \dot{x}(t) = 0 \quad (D2-20)$$

always guarantees a stable system.

When the weighting for control approaches zero, ($r = 0$), which means there is no limitation on the control, the closed loop system approaches (D2-21) which is called model control equation in (D2-1).

$$\sqrt{\frac{q_{22}}{q_{11}}} \dot{x}(t) + x(t) = 0 \quad (D2-21)$$

when the weighting factor $q_{22} = 0$, the undamped natural frequency and damping become, from (D2-7):

$$\begin{aligned} \omega_n &= \infty \\ \zeta &= .707 \end{aligned} \quad (D2-22)$$

which are the second order Butterworth poles.

The Minimum Value of the Performance Index

The minimum value of the performance index, in general, is obtained by substitution of the optimal control (D2-8) into (D2-7). This yields:

$$J_{\min} = \frac{1}{2} x_0^T K x_0 \quad (D2-23)$$

This is obtained by substituting D2-11 into the latter equation:

$$\begin{aligned}
 J_{\min} = \frac{1}{2} x_{10}^2 & \left[\sqrt{\frac{q_{11}r}{b^2} (a^2 + 2b \sqrt{\frac{q_{11}}{r}} + \frac{b^2 q_{22}}{r})} \right. \\
 & + 2\sqrt{\frac{q_{11}r}{b^2}} \frac{x_{20}}{x_{10}} \quad (D2-24) \\
 & \left. + \frac{r}{b^2} (a + \sqrt{a^2 + 2b \sqrt{\frac{q_{11}}{r}} + \frac{b^2 q_{22}}{r}}) \left(\frac{x_{20}}{x_{10}} \right)^2 \right] \\
 & (x_{10} \neq 0)
 \end{aligned}$$

The formula, in general, is given as a function of initial states and solution of the Riccati equation. Minimizing this value is done by decreasing r and also by decreasing q_{11} and q_{22} . Therefore, without any constraints, minimizing J itself is meaningless. Hence, constraints are necessary, which leads to the discussion of the OWEM method. (Appendix E).

REFERENCE

- D2-1 Schultz, D.G. and Mersa, J.L., "State Functions and Linear Control Systems", McGraw Hill Inc., New York, 1967.

REVIEW OF OWEM DESIGN METHOD

The Optimal Weighting Matrices Controller Design Method (OWEM)

This appendix is a summary of the OWEM design method as presented in Refs. (E1) and (E2). The results of the method are given without proofs; for the details of mathematical derivations and proofs, see Ref. (E1).

The goal of the linear optimal control theory is to find a linear control law such that the following quadratic cost function is minimized

$$J(u(t); Q, R) = \lim_{T \rightarrow \infty} \frac{1}{2T} \int_{-T}^{+T} [y^T(t)Qy(t) + u^T(t)Ru(t)] dt \quad (E1-1)$$

subject to $\dot{x}(t) = Ax(t) + Bu(t) + Cn(t)$

$$y(t) = Hx(t)$$

$$\mathcal{E}\{n(t)\} = 0, \mathcal{E}\{n(t) n^T(\tau)\} = N\delta(t-\tau)$$

where $x(t)$: n dimensional state vector

$u(t)$: m dimensional control vector

$y(t)$: p dimensional output vector

$n(t)$: l dimensional stationary, Gaussian, white noise vector

Q : p x p output weighting matrix, weightings for the output errors, (positive definite, symmetric, constant matrix)

N : n x n noise intensity matrix

$\delta(\cdot)$: Dirac's delta function

- R : mxm control weighting matrix (positive definite, symmetric, constant matrix)
 $(\cdot)^T$: transpose of (\cdot)
 $\mathcal{E}\{\cdot\}$: expectation or average of $\{\cdot\}$

The optimal control law $u^*(t)$ is obtained in the state feedback form (a linear function of $x(t)$) as follows

$$u^*(t) = -R^{-1}B^TKx(t) \equiv -Gx(t) \quad (E1-2)$$

where $(\cdot)^{-1}$ represents the inverse of (\cdot) , and nxn matrix K is the unique positive definite solution of the following so-called "Algebraic Matrix Riccati (AMR)" equation:

$$KA + A^TK - KBR^{-1}B^TK + H^TQH = 0 \quad (E1-3)$$

Thus, if the matrices A , B , H , Q , and R are given, the controller can be designed by solving Eq. (E1-3) for K and using it in Eq. (E1-2).

Note that the optimal controller can be designed independently of the noise intensity (covariance) and the matrix C as long as the noise $n(t)$ is stationary, gaussian, white and of zero-mean.

Denote the corresponding state and output vectors to the optimal control $u^*(t)$ as $x^*(t)$ and $y^*(t)$ respectively. Namely,

$$\dot{x}^*(t) = Ax^*(t) + Bu^*(t) + Cn(t) \quad (E1-4)$$

$$y^*(t) = Hx^*(t) \quad (E1-5)$$

The equation should minimize $J(u(t);Q,R)$.

Assuming the stationarity of the system and the ergodic property, the minimum cost $J(u^*(t), Q, R)$ is obtained as follows (Ref. E1)

$$\begin{aligned} J_{\min}(Q, R) &\equiv J(u^*(t); Q, R) = \mathcal{E}\{y^*(t)Qy^*(t) + u^{*T}(t)Ru^*(t)\} \\ &= \text{Tr}[QY^*] + \text{Tr}[RU^*] \end{aligned} \quad (\text{E1-6})$$

$$= \text{Tr}[CNC^TK] \quad (\text{E1-7})$$

where $\text{Tr}[\cdot] = \text{Trace of } [\cdot]$

= the sum of the diagonals of $[\cdot]$

$Y^*(t) = \mathcal{E}\{y^*(t)y^{*T}(t)\}$: output covariance matrix

$U^*(t) = \mathcal{E}\{u^*(t)u^{*T}(t)\}$: control covariance matrix

The matrices A, B, C and H are inherent to the given controlled system and normally available a priori. In order to design the controller, the immediate question to be asked is how to choose Q and R matrices. They affect the solution matrix K in AMR equation and thereby the feedback gain matrix $G(=R^{-1}B^TK)$. Hence, the closed loop characteristics and the minimum quadratic cost $J_{\min}(Q, R)$ have considerable effects of Q and R.

First will be investigated how the minimum quadratic cost $J_{\min}(N; Q, R)$ behaves with respect to Q and R:

Suppose there is an ordered sequence of trial weighting matrices Q's.

$$[Q_i] = Q_1, Q_2, Q_3, \dots, Q_i, Q_{i+1}, \dots$$

If $Q_{i+1} - Q_i \geq 0$ or positive semidefinite, then $[Q_i]$ is called a monotonically increasing definite sequence (MIDS). For an example, consider one $Q_0 > 0$ and a scalar sequence $[k_i] = 1, 2, 3, \dots, i, i+1, \dots$. Then

$$Q_i = k_i Q_0$$

$$\begin{aligned} [Q_i] &= Q_1, Q_2, Q_3, \dots, Q_i, Q_{i+1}, \dots \\ &= Q_0, 2Q_0, 3Q_0, \dots, iQ_0, (i+1)Q_0, \dots \end{aligned}$$

is MIDS. Because

$$Q_{i+1} - Q_i = (i+1)Q_0 - iQ_0 = Q_0 \geq 0 \text{ for all } i = 1, 2, 3, \dots.$$

Likewise, $[R_i]$ and $[K_i]$ are defined.

Using these special sequences, the parametric behavior of the minimum quadratic cost $J_{\min}(N; Q, R)$ is summarized below (Ref. [E1]).

A solution sequence $\{K_i\}$ of AMR equation corresponds to the above defined sequences $[Q_i]$ and $[R_i]$.

Corresponding to the above defined sequence $[Q_i]$, and $[R_i]$ respectively, one obtains solution sequences $\{K_i\}$'s of AMR equation. The solution sequences $\{K_i\}$'s can be shown to be also monotonically increasing definite sequences $[K_i]$'s. This is shown in Illustration E-1.

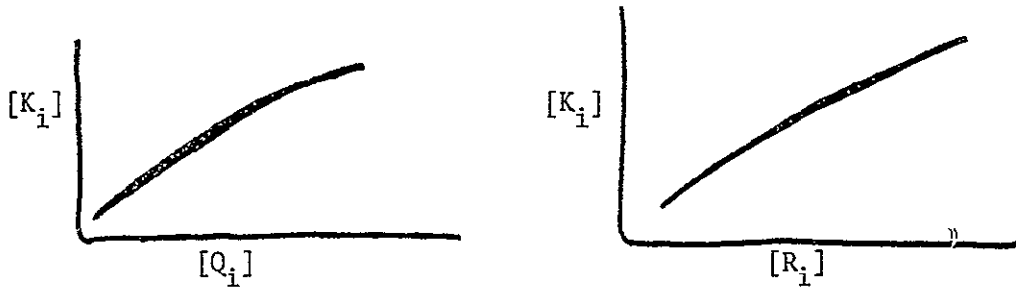


Illustration E-1. Behavior of $[K_i]$ with respect to $[Q_i]$ and $[R_i]$

The $J_{\min}(N;Q,R)$ with respect to a monotonically increasing definite sequence $[K_i]$ also increases monotonically.

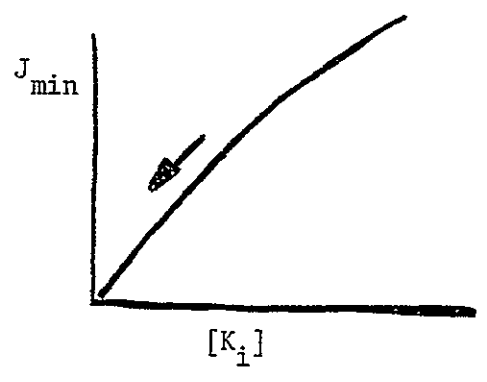


Illustration E-2. Behavior of $J_{\min} [K_i] (N;Q,R)$ with respect to $[K_i]$

The arrow in the illustration indicates the direction that is desirable for a design.

$$\text{Define } J_{\min}(K_i) \triangleq \text{Tr}[CNC^T K_i] \equiv \begin{cases} J_{\min}(N;Q_i,R) \\ \text{or} \\ J_{\min}(N;Q,R_i) \end{cases} \quad (\text{E1-8})$$

$$\text{Then if } K_{i+1} - K_i \geq 0, \text{ then } J_{\min}(K_{i+1}) \geq J_{\min}(K_i) \quad (\text{E1-9})$$

The behavior of $J_{\min}(N;Q,R)$ with respect to $[Q_i]$ and $[R_i]$ is shown in Illustration E-3. The sequences $[Q_i]$ and $[R_i]$ are monotonically increasing definite sequences.

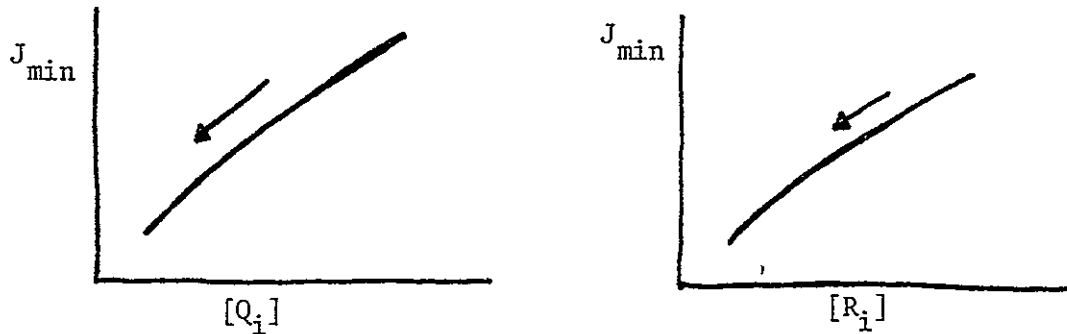


Illustration E-3. J_{\min} with Respect to $[Q_i]$ and $[R_i]$

The arrows in the illustration indicate the direction that is desirable in a design.

The monotonic property of $J(N;Q,R)$ indicates that J_{\min} will not remain finite unless the weighting matrices Q and R are limited within some finite allowable sets during their selection. When the elemental matrices of the allowable sets for choosing the Q and R matrices can be ordered and a definite differential matrix among any two of them is obtained; then the smallest weighting matrix yields the smallest $J_{\min}(N;Q,R)$. Hence, the

allowable sets for the weighting matrices Q and R should not contain any matrices which can be ordered in the sense of definite differential matrix.

To bound $J_{\min}(N;Q,R)$ from both below and above, consider Eq. (E1-6)

$$J_{\min}(N;Q,R) = \text{Tr}[QY^*] + \text{Tr}[RU^*].$$

The general form to be bounded is

$$\text{Tr}[\tilde{A}^T \tilde{B}] \quad \text{where} \quad \tilde{A}^T \text{ corresponds to } Q \text{ or } R$$

$$\tilde{B} \text{ corresponds to } Y^* \text{ or } U^*.$$

This trace indicates a sum of the products:

$$\text{Tr}[\tilde{A}^T \tilde{B}] = \sum_i \sum_j \tilde{a}_{ij} \tilde{b}_{ij} \quad (\text{E1-10})$$

where $\tilde{A} = \{\tilde{a}_{ij}\}$, $\tilde{B} = \{\tilde{b}_{ij}\}$.

For a sum of products of finite values, the lower bound is given by the arithmetic geometric average, the upperbound by the Cauchy-Schwarz theorem.

For an example,

$$2\sqrt{a_1 a_2 b_1 b_2} \leq a_1 b_1 + a_2 b_2 \leq \sqrt{a_1^2 + a_2^2} \sqrt{b_1^2 + b_2^2} \quad (\text{E1-11})$$

where $a, b, > 0$ and $a_2 b_2 > 0$ for the left hand side inequality.

In matrix form this becomes [Ref.E1-3]:

When \tilde{A} and \tilde{B} are non singular (nxn) matrices then

$$n |\tilde{A}|^{1/n} \cdot |\tilde{B}|^{1/n} \leq \text{Tr}[\tilde{A}\tilde{B}] \leq ||\tilde{A}|| \cdot ||\tilde{B}|| \quad (\text{E1-12})$$

where

$$|\cdot| : \text{Determinant}$$

$$||\cdot|| : \text{Matrix norm, } ||\tilde{A}|| = \sqrt{\text{Tr}[\tilde{A}^T \tilde{A}]}$$

The equalities occur at

$$\begin{aligned} \text{the left hand side when } \tilde{A}^T &= k_1 \tilde{B}^{-1} & k_1 \geq 0 \\ \text{the right hand side when } \tilde{A}^T &= k_2 \tilde{B} & k_2 > 0. \end{aligned}$$

Hence $J_{\min}(N;Q,R)$ is bounded by

$$\begin{aligned} p|Q|^{1/p} |Y^*|^{1/p} + m|R|^{1/m} |U|^{1/m} &\leq J_{\min}(N;Q,R) \leq \\ &\leq ||Q|| \cdot ||Y^*|| + ||R|| \cdot ||U^*|| \end{aligned} \quad (E1-13)$$

Eq. E-12 indicates that:

1. When $|Q|$ and $|R|$ are prescribed, the minimum of $J_{\min}(N;Q,R)$ with respect to Q and R can be obtained with $Q = k_3 Y^{*-1}$ and $R = k_4 U^{*-1}$.
2. When $||Q||$ and $||R||$ are prescribed, the maximum of $J_{\min}(N;Q,R)$ with respect to Q and R can be obtained with $Q = k_5 Y^*$ and $R = k_6 U^*$. where k_3, k_4, k_5 and k_6 are appropriate positive scalars for Q and r to satisfy the prescribed determinants and norms.

The minimum and maximum values of $J_{\min}(N;Q,R)$ occur when:

$$\begin{aligned} \text{Min } J_{\min}(N;Q,R) &\text{ when } Q = k_3 Y^{*-1} \text{ and } R = k_4 U^{*-1} \\ \text{Max } J_{\min}(N;Q,R) &\text{ when } Q = k_5 Y^* \text{ and } R = k_6 U^* \end{aligned}$$

The design method with Optimal Weighting Matrices (OWEM) is basically a linear optimal quadratic control system design method with calculated weighting factors such that the effect of disturbances on the performance index is minimized.

The OWEM design method can be summarized as follows:

The system is assumed to be completely controllable and observable and is shown in Illustration (E1-1).

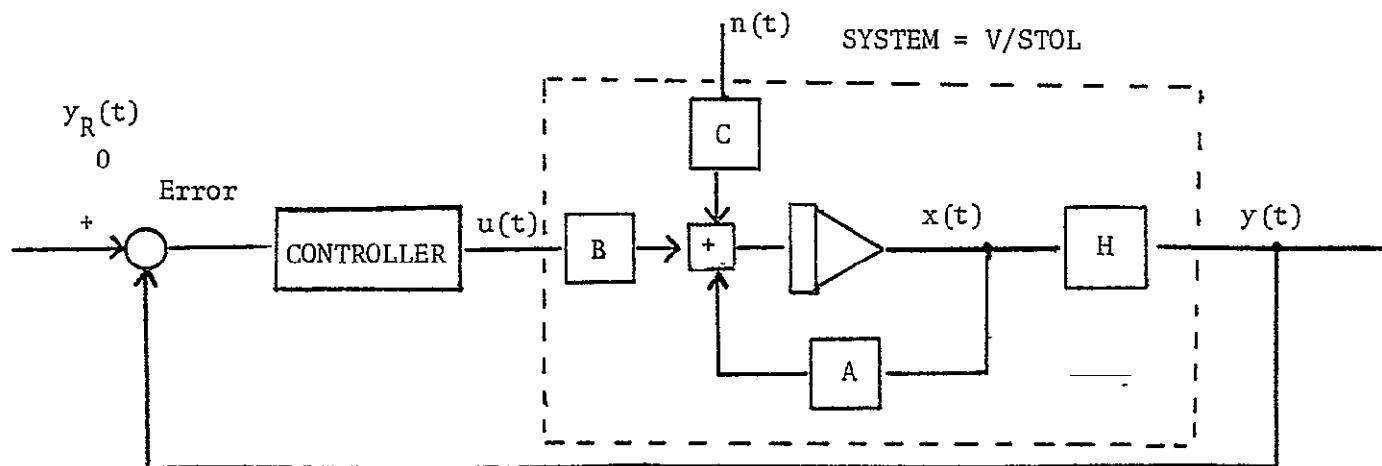


Illustration E1-1. Block Diagram of an Optimal Linear Regulator

System dynamics: $\dot{x}(t) = Ax(t) + Bu(t) + Cn(t)$ (E1-14)

$y(t) = Hx(t)$ (E1-15)

where $x(t)$: n dimensional state vector

$u(t)$: m dimensional control vector ($m < n$)

$y(t)$: p dimensional output vector ($p < n$)

$n(t)$: l dimensional noise vector ($l < n$)

$$\mathcal{E}\{n(t)\} = 0, \text{Cov}\{n(\tau)\} = N\delta(t-\tau)$$

A, B, C and H: nxn, nxm, nxℓ and pxn constant

given matrices.

(E1-16)

Cost function: $J_{\min}(N; Q, R) = \text{Min}_{u(t)} \left\{ \text{Lim}_{T \rightarrow \infty} \frac{1}{2T} \int_{-T}^T [y^T(t)Qy(t) + u^T(t)Ru(t)] dt \right\}$

(E1-17)

$$= \text{Tr}[CNC^T K]$$

(E1-18)

where Q and R: positive definite symmetric matrices.

Optimal control law: $u^*(t) = -R^{-1}B^TKx(t)$

(E1-19)

where K: nxn unique positive definite solution of (E1-20)

$$KA + A^TK - KBR^{-1}B^TK + H^TQH = 0$$

(E1-20)

Covariance matrices: $FX + XF^T + CNC^T = 0$ (Ref. E2)

(E1-21)

where $X = \mathcal{E}\{x(t)x^T(t)\}$, $F = A - BR^{-1}B^TK$

$$Y = \mathcal{E}\{y(t)y^T(t)\} = HXH^T$$

(E1-22)

$$U = \mathcal{E}\{u(t)u^T(t)\} = R^{-1}B^TKXBKBR^{-1}$$

(E1-23)

In the above equations, the number of equations is $p^2 + m^2$ less than the number of unknowns if Q and R are not given. To augment the lacking number of equations, an auxiliary performance index is minimized with respect to Q and R.

Auxiliary performance index:

$$\text{Min}_{Q, R} J_{\min}(N; Q, R) \equiv \text{Min}_{Q, R} \text{Tr}[CNC^TK]$$

(E1-24)

subject to $KA + A^TK - KBR^{-1}B^TK + H^TQH = 0$

(E1-25)

$$|R|$$

Constraints on Q and R: $|Q| = 1, |Q| = |R| = \rho^2$ (E1-26)

Optimal weighting matrices Q and R:

$$Q = \frac{P}{\sqrt{|HPH^T|}} \cdot (HPH^T)^{-1} \propto Y^{-1}$$
 (E1-27)

$$R = \rho^2/m \frac{B^T K P K B}{\sqrt{|B^T K P K B|}} \propto U^{-1}$$
 (E1-28)

where $FP + PF^T + CNC^T = 0 \rightarrow P \equiv X$ in this case. (E1-29)

$$F = A - BR^{-1} B^T K$$

Conclusion:

If ρ^2 is given, then Q and R can be determined provided the noise intensity matrix N is known. If the noise intensity matrix (or covariance matrix) N cannot be estimated, then the approach in this summary cannot be used.

It has been shown in Ref. (E1) that the introduction of a new performance index independent of N can remove this deficiency. This performance index extremizes the total system damping. It has been shown in Ref. [E1] that if one assumes that the disturbance is white noise entering the system at the controls with a magnitude $N = R^{-1}$ and $C = B$ then the results of both approaches yield the same result for the optimal calculation of the weighting matrix Q, however the optimal weighting matrix R is different. Using the same system dynamics as above, with $Cov\{n(t); n(\tau)\} = N\delta(t-\tau)$ unknown, one can summarize this approach as follows:

Cost function: $J_{\min}(N; Q, R) = \text{Min}_{u(t)} \left\{ \lim_{T \rightarrow \infty} \frac{1}{2T} \int_{-T}^T [y^T(t) Q y(t) + u^T(t) R u(t)] dt \right\}$ (E1-30)

$$= \text{Tr}[CNC^T K]. \quad (N: \text{unknown}) \quad (E1-31)$$

If $N_e = kC^+BR^{-1}B^T(C^+)^T$, then (E1-32)

$$J_{\min}(N_e; Q, R) = k\text{Tr}[BR^{-1}B^T K] \quad (E1-33)$$

where C^+ : $l \times n$ pseudo-inverse matrix of C , i.e.,

$$(=(C^T C)^{-1} C^T)$$

Optimal control law: $u(t) = -R^{-1}B^T Kx(t)$ (E1-34)

where K : $n \times n$ unique positive definite solution of (E1-21)

$$KA + A^T K - KBR^{-1}B^T K + H^T Q H = 0 \quad (E1-35)$$

This optimal control law (22) can be computed without knowing N if Q and R are given.

Covariance matrices (unknown):

$$FX + XF^T + CNC^T = 0 \quad (E1-36)$$

where $X = \{x(t)x^T(t)\}$, $F = A - BR^{-1}B^T K$ (E1-37)

$$Y = \{y(t)y^T(t)\}, \quad HXH^T$$

$$U = \{u(t)u^T(t)\} = R^{-1}B^T K X K B R^{-1} \quad (E1-38)$$

Note: These covariances are all unknown since N is unknown

Auxiliary performance index:

Total System Damping = TSD: the negative sum of the closed loop roots

$$\hat{L}^* = \text{Min}_Q \text{Max}_R \{TSD\} = \text{Min}_Q \text{Max}_R \{\text{Tr}[-(A - BR^{-1}B^T K)]\} \quad (E1-39)$$

or equivalently

$$L^* = \text{Min}_Q \text{Max}_R \{\text{Tr}[BR^{-1}B^T K]\} \quad (\because A = \text{constant matrix}) \quad (E1-40)$$

subject to $KA + A^T K - KBR^{-1}B^T K + H^T QH = 0$

Note: (1) TSD is equivalent to the Relative Rate of Change of Error Sets (RERACES, see Ref. [1], Chapter IV), and is generalized system response speed.

(2) The extremum (minimax) of TSD does not exist unless Q and R are appropriately constrained.

Constraints on Q and R: $|Q| = 1, |R| = \rho^2$ (E1-41)

where $|(\cdot)|$: the determinant of (\cdot)

Optimal weighting matrices:

$$Q = P \sqrt{|HPH^T|} \cdot (HPH^T)^{-1} \quad (E1-42)$$

$$R = \rho^{2/m} \cdot \frac{B^T KB - B^T KPB}{\sqrt[m]{|B^T KB - B^T KPB|}} \quad (E1-43)$$

where $FP + PF^T + BR^{-1}B^T = 0$ (E1-44)

$$F = A - BR^{-1}B^T K$$

Conclusions:

(1) When N is unknown, Q and R can be computed by the minimaximization of TSD with respect to Q and R under prescribed determinant constraints.

(2) The optimal Q matrix slows down the entire system response or error convergence speed by minimizing TSD. However, for an equivalent white noise disturbance with a magnitude N_e inversely proportional to the control weighting R, the minimization of TSD is equivalent to the minimization of $J_{\min}(N_e; Q, R)$.

Note: a faster system response can be obtained only at the expense of the entire system accuracy, i.e., a larger TSD accompanies a larger $J_{\min}(\cdot)$.

- (3) The optimal R is chosen such that the system response speed (with a given Q selection) is maximized.
- (4) The optimal Q matrix equalizes the closed loop poles in frequency-wise, while the optimal R matrix tries to separate them. The trade-off between these two effects is controlled by ρ^2 .
- (5) ρ^2 is the only scalar parameter to be determined by designers.
- (6) The approach summarized here can be directly applied for the deterministic case in Summary 1 since Q and R can be determined independently of N and C matrices.

Properties of the optimal weighting matrix determined by the OWEM design method (under determinant constraint), which can be of large significance in engineering applications, are the "Normalization and the Group-Wise Equalization".

Normalization

The state variables can be dimensionally different, and the weighted state and control variables are compared in the performance index. Hence, for a meaningful comparison, the weighted state and control variables should have the same dimensions. The resulting weighting matrices from the OWEM

design are inversely proportional to the output covariance matrix Y and the optimal control covariance.

Group-Wise Equalization

In the development of the OWEM design the following expression was obtained:

$$\begin{aligned} Q^* &= \sqrt[P]{ |Y| } Y^{-1} \\ &= k_5 Y^{-1} \quad \text{where } k_5 = \sqrt[P]{ |Y| } (>0) \end{aligned}$$

Hence the Q is inversely proportional to the covariance matrix Y .

The effect of the group-wise equalization constant k_5 can be evaluated as follows:

$$\xi_x \{ y^{*T} Q^* y^* \} = T_r [Q^* \mathcal{E}_x \{ y^* y^{*T} \}] = \sum_{i=1}^P \left(\sum_{j=1}^P q_{ij}^* \overline{y_j^* y_i^*} \right)$$

$$Q^* \equiv \{ q_{ij}^* \} = k_5 Y^{*-1} = k_5 \frac{ \{ Y_{ji}^* \} }{ |Y^*| }$$

$$Y_{ij}^* : (i-j)\text{th Cofactor of } Y^* \equiv \overline{ \{ y_i^* y_j^* \} }$$

$$\sum_{j=1}^P q_{ij}^* \overline{y_j^* y_i^*} = k_5 \sum_{j=1}^P \frac{ Y_{ji}^* }{ |Y^*| } \overline{y_j^* y_i^*} = k_5; \quad i=1, 2, \dots, p$$

$$\left. \begin{aligned}
i = 1 : & \quad q_{11}^* \overline{y_1^* y_1^*} + q_{12}^* \overline{y_2^* y_1^*} + \dots + q_{1p}^* \overline{y_p^* y_1^*} = k_3 \\
i = 2 : & \quad q_{21}^* \overline{y_1^* y_2^*} + q_{22}^* \overline{y_2^* y_2^*} + \dots + q_{2p}^* \overline{y_p^* y_2^*} = k_3 \\
i = p : & \quad q_{p1}^* \overline{y_1^* y_p^*} + q_{p2}^* \overline{y_2^* y_p^*} + \dots + q_{pp}^* \overline{y_p^* y_p^*} = k_3
\end{aligned} \right\} \text{p-groups}$$

Similarly

$$\sum_{i=1}^p q_{ij}^* \overline{(y_j^* y_i^*)} = k_3 \sum_{j=1}^p \frac{Y_{ji}^*}{|Y^*|} \overline{y_j^* y_i^*} = k_3 \quad j=1,2, \dots, p.$$

This evaluation shows a group-wise equalization of the terms of $\{y^{*T} Q y^*\}$.

In the initial approach all the constants k_3 are chosen to be equal. This corresponds to an Error Scaling Matrix (ESM) = 1. Making the ESM matrix not equal to the identity matrix corresponds to an error scaling factor (ESF) of the diagonal elements of the weighting matrix q_{1j} .

The elements of the ESM matrix are diagonal, hence, an easier interpretation is often possible. In general, the elements corresponding to the quantities to be controlled determine the error weighting, while the elements corresponding to the derivatives of the quantities to be controlled influence the damping of that mode. In practical application, one should first use a ESM matrix with only elements that affect the quantity to be controlled. If mode damping increase is desirable, then elements of the ESM matrix that affect the mode damping can be introduced. This method, using a step by step approach, is preferable as the effects of the ESM matrix and Q matrix are not yet fully investigated.

REFERENCES

- E1-1. Born, Gerard J. and Kawahata, Nagakatsu, "Control System Design with Optimal Weighting Matrices (OWEM)", Princeton University Report No. 1145, January 1974.
- E1-2. Kai, Tadao, "Optimal Control Theory Applied to Helicopter in Hover", Princeton University M.S.E. Thesis No. 1242-T, AMS Department, 1975.
- E1-3. Kawahata, N., "Linear Control System Optimization by Optimal Selection of the Weighting Matrices in Quadratic Cost Functions", Ph.D. Thesis, Princeton University, Dept. of Aerospace & Mechanical Sciences, Princeton, N.J., September 1972.
- E1-4. Kawahata, N., "Linear Control System Design by Maximizing Error Convergence", M.S.E. Thesis, Department of Aerospace & Mechanical Sciences, Princeton University, Princeton, N.J., May 1971.
- E1-5. Anderson, B.D.O. and Moore, J.B., "Linear Optimal Control", Prentice Hall, Inc., Englewood Cliffs, New Jersey, 1971.
- E1-6. Athans, M. and Falb, P.L., "Optimal Control", McGraw-Hill Book Company, New York, 1966.
- E1-7. Bryson, A.E. and Ho, Y.C., "Applied Optimal Control", Blaisdell Publishing Company, Waltham, Massachusetts, 1969.

APPENDIX E2

THE OWEM METHOD APPLIED TO A SECOND ORDER SYSTEM

A second order system equation is represented by the following differential equation

$$\ddot{x}(t) = a\dot{x}(t) + bu(t) \quad (E2-1)$$

where

$x(t)$ = position

$\dot{x}(t)$ = rate of position

$u(t)$ = control input

a = rate damping

b = control derivatives

In the state variable form

$$\dot{x}(t) = Ax(t) + Bu(t) \quad (E2-2)$$

where

$$x(t) = \begin{bmatrix} x_1(t) \\ x_2(t) \end{bmatrix} = \begin{bmatrix} x(t) \\ \dot{x}(t) \end{bmatrix} \quad (E2-3)$$

$$A = \begin{bmatrix} 0 & 1 \\ 0 & a \end{bmatrix} \quad (E2-4)$$

$$B = \begin{bmatrix} 0 \\ b \end{bmatrix} \quad (E2-5)$$

$$u(t) = \delta \quad (E2-6)$$

An analytical approach using the example clarifies the method and yields a solution for the choices of the Q matrix. The closed loop system obtained by conventional optimal design method assigning values for q_{11} , q_{22} and r yields:

$$\ddot{x}(t) + \sqrt{a^2 + 2b \sqrt{\frac{q_{11}}{r}} + b^2 \frac{q_{22}}{r}} \dot{x}(t) + b \sqrt{\frac{q_{11}}{r}} x(t) = 0 \quad (E2-7)$$

The total system damping is (Ref. E1-1).

$$\text{TSD} = \sqrt{a^2 + 2b \sqrt{\frac{q_{11}}{r}} + b^2 \frac{q_{22}}{r}} \quad (E2-8)$$

The determinant constraint on weighting matrix Q becomes:

$$|Q| = 1 = q_{11} q_{22} \quad \text{---(E2-9)}$$

This determinant constraint only specifies the lower limit of the minimized performance index value. Note that for decreasing q_{11} , q_{22} and r , the value of the performance index decreases and the minimized value becomes meaningless. The determinant constraint is used to avoid this.

Substituting Eq.(E2-3) into Eq. (E2-2) reduces the TSD to

$$\text{TSD} = \sqrt{a^2 + 2b \sqrt{\frac{q_{11}}{r}} + b^2 \frac{1}{rq_{11}}} \quad (E2-10)$$

The TSD value with respect to q_{11} is illustrated in Illustration (2-1).

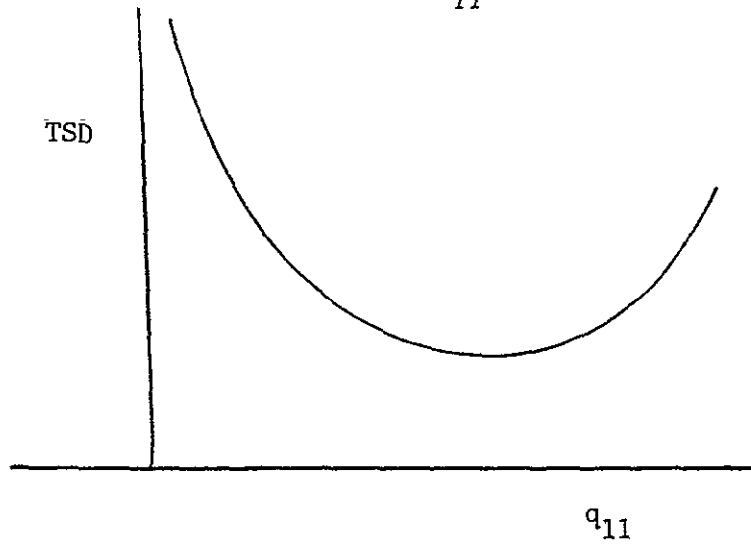


Illustration 2-1. TSD as a Function of the Weighting q_{11}

The minimization of TSD with respect to q_{11} elements leads to minimization of the performance index with determinant constraint. The minimization of TSD is obtained by differentiating (E2-10) with respect to q_{11} .

And TSD, q_{11} and q_{22} are:

$$\text{TSD} = \sqrt{a^2 + \frac{3b \frac{4}{3}}{r \frac{2}{3}}} \quad (\text{E2-11})$$

$$q_{11} = \frac{b \frac{2}{3}}{r \frac{1}{3}} \quad (\text{E2-12})$$

$$q_{22} = \frac{r \frac{1}{3}}{b \frac{2}{3}} \quad (\text{E2-13})$$

Note that when the weighting factor Q is obtained, the OWEM method minimizes the performance index.

$$J_{\min} = \frac{1}{2} \int_0^{\infty} \left(\frac{b \frac{2}{3}}{r \frac{1}{3}} x_1^2(t) + \frac{r \frac{1}{3}}{b \frac{2}{3}} x_2^2(t) + r u^2(t) \right) dt \quad (\text{E2-14})$$

Substituting the optimal weighting factors into (E2-1) gives the optimal closed loop system

$$\ddot{x}(t) + \sqrt{a^2 + \frac{3b}{r} \frac{4}{3}} \dot{x} + \frac{b}{r} \frac{4}{3} x(t) = 0 \quad (\text{E2-15})$$

And the undamped natural frequency ω_n and the damping ratio ζ are respectively

$$\zeta = \frac{1}{2} \sqrt{3 + \frac{a^2}{b} \frac{2}{4} \frac{2}{3}} \quad (\text{E2-16})$$

$$\omega_n = \frac{b}{r} \frac{2}{3} \quad (\text{E2-17})$$

The optimal control is given by substituting (E2-12) and (E2-15) into (D2-13), (D2-14), and from (D2-12).

$$u(t) = - \frac{b}{r} \frac{1}{2} \frac{3}{3} x(t) - \left(- \frac{a}{b} + \sqrt{\left(\frac{a}{b} \right)^2 + \frac{3}{br} \frac{2}{3}} \right) \dot{x}(t) \quad (\text{E2-18})$$

The solution of the Riccati equation is as follows:

$$\begin{aligned} k_{11} &= \sqrt{3 + a^2 \frac{r}{b} \frac{2}{4} \frac{2}{3}} \\ k_{12} = k_{21} &= \frac{r}{b} \frac{2}{3} \\ k_{22} &= \frac{r}{b^2} \left(a + \sqrt{a^2 + \frac{3b}{r} \frac{4}{3}} \right) \end{aligned} \quad (\text{E2-19})$$

Closed Loop System Properties as a Function of Control Weighting

When the control weighting r goes to infinity, the closed loop system reduces the original basic one or its adjoint one

$$\ddot{x}(t) + |a| \dot{x}(t) = 0 \tag{E2-20}$$

When the control weighting r goes to zero, then

$$\omega_n = \infty \tag{E2-21}$$

$$\zeta = 0.866 \tag{E2-22}$$

which is more damped than that of the Butterworth poles for the second order system.

Minimized Value of the Performance Index

The minimized value of the performance index is:

$$\begin{aligned} \frac{1}{2} J_{\min} &= \frac{1}{2} [k_{11} x_{10}^2 + 2k_{12} k_{21} x_{10} x_{10} + k_{20}^2] \\ &= \frac{1}{2} x_{10}^2 \left[\sqrt{3 + a \frac{r}{b} \frac{2}{3}} + \frac{r}{b^2} \left(a + \sqrt{a^2 + \frac{3b^2}{r} \frac{4}{3}} \right) \frac{x_{20}^2}{x_{10}^2} \right. \\ &\quad \left. + \frac{2r^{\frac{2}{3}}}{b \frac{2}{3}} \frac{x_{10}}{x_{10}} \right] \tag{E2-23} \end{aligned}$$

when $r = 0$,

$$\frac{1}{2} J_{\min} = \frac{\sqrt{3}}{2} x_{10}^2 \quad (\text{E2-24})$$

Note that its value for conventional selection is given by

$$\frac{1}{2} J_{\min} = \frac{1}{2} \sqrt{q_{11} q_{22}} x_{10}^2$$

which becomes zero when $q_{22} = 0$.

REFERENCES

- E2-1. Bryson, A.E. and Ho, Y.C., "Applied Optimal Control", Blaisdell Publishing Company, Waltham, Massachusetts, 1969.

APPENDIX F 1
THE ROOT SQUARE LOCUS

The Root Square Locus Method

In the optimal control problem is minimized

$$J = \frac{1}{2} \int_0^{\infty} (y^T Q y + u^T R u) dt \quad (F1-1)$$

subject to

$$\dot{x}(t) = Ax(t) + Bu \quad (F1-2)$$

$$Y = Hx, \quad H = I \quad (F1-3)$$

where $x(t)$: n dimensional state vector

$u(t)$: m dimensional control vector ($m < n$)

$y(t)$: p dimensional output vector ($p < n$)

A, B and H : $n \times n$, $n \times m$ and $p \times n$ constant matrices

The solution of this problem yields the optimal control

$$u^* = -R^{-1} B^T Kx(t) \quad (F1-4)$$

where K is a solution of the Riccati matrix equation

$$KA + A^T K - KBR^{-1} B^T K + Q = 0 \quad (F1-5)$$

The optimal closed loop system is given by

$$\begin{aligned}\dot{x}(t) &= Ax(t) + Bu^*(t) \\ &= Ax(t) + B(-R^{-1}B^TK)x(t)\end{aligned}\tag{F1-6}$$

$$= (A-GK)x(t)\tag{F1-7}$$

where

$$G = BR^{-1}B^T\tag{F1-8}$$

The characteristic equation is:

$$|sI - A + BK| = 0\tag{F1-9}$$

The roots of the characteristic equation can be obtained by solving (Eq. F1-9) with a priori-known K. The relationship between K, Q and R is given by (Eq. F1-5), and is non-linear.

The spectral form product of the characteristic Eq. F1-9

$$|sI - A + BK| \quad | -sI - (A-BK)^T | = 0\tag{F1-10}$$

The characteristic equations of the optimal system and its adjoint

$$\dot{x} - Ax + BR^{-1}B^T\lambda = 0\tag{F1-11}$$

$$H^TQHx + \dot{\lambda} + A^T\lambda = 0$$

$$\begin{vmatrix} sI - A & BR^{-1}B^T \\ -H^TQH & -sI - A^T \end{vmatrix} = 0 \quad (F1-12)$$

and the following relationship is satisfied.

$$\begin{vmatrix} sI - A + BK & \\ & -sI - (A-BK)^T \end{vmatrix} = \begin{vmatrix} sI - A & BR^{-1}B^T \\ -H^TQH & -sI - A^T \end{vmatrix} \quad (F1-13)$$

The roots can be obtained by solving (Eq. F1-12) with respect to Q and R or graphically by making the "root square locus". Equation F1-13 yields expressions relating the feedback gains K with A, B, H, and Q.

Adding the control equation to (F1-11) one obtains:

$$\begin{aligned} \dot{x} - Ax + BR^{-1}B^T\lambda &= 0 \\ H^TQH + \dot{\lambda} + A^T\lambda &= 0 \\ Ru + B^T\lambda &= 0 \end{aligned} \quad (F1-14)$$

and substituting $u = -R^{-1}B^T\lambda$ into the top equation of (F1-14), we can obtain the characteristic equation,

$$\begin{vmatrix} -sI - A^T & -H^TQH & 0 \\ 0 & sI - A & -B \\ B^T & 0 & R \end{vmatrix} = 0 \quad (F1-15)$$

In the transfer function form, this becomes:

$$\left| I + R^{-1} \left[\frac{Y}{u}(-s) \right]^T Q \left[\frac{Y}{u}(s) \right] \right| = 0 \quad (\text{F1-16})$$

where

$$\begin{aligned} \frac{Y}{u}(s) &= H(Is-A)^{-1}B \\ &= \begin{bmatrix} \frac{y_1}{u_1}(s) & \frac{y_1}{u_2}(s) & \dots & \frac{y_1}{u_m}(s) \\ \frac{y_p}{u_1}(s) & \frac{y_p}{u_2}(s) & \dots & \frac{y_p}{u_m}(s) \end{bmatrix} \end{aligned} \quad (\text{F1-17})$$

For single input system with R equal to a scalar ρ , the characteristic equation becomes:

$$1 + \rho^{-2} \left[\frac{Y}{u}(-s) \right]^T Q \left[\frac{Y}{u}(s) \right] = 0$$

where

$$\frac{Y}{u}(s) = \begin{bmatrix} \frac{y_1}{u} \\ \frac{y_2}{u} \\ \frac{y_p}{u} \end{bmatrix} \quad (\text{F1-18})$$

The root square locus can be made by using similar rules as used for the root locus method, e.g.:

N number of poles of $\frac{Y}{u}(s)$
 p number of zeroes of $\frac{Y}{u}(s)$

Angle condition:

(N-p) = odd number 0 degree condition

(N-p) = even number 180° degree condition

Asymptotes:

$\frac{2n\pi}{2(N-p)}$ N-p = odd n=0, ±1, ±2, ... 2(N-p)-1

$\frac{2n\pi}{2(N-p)}$ N-p = even n=0, ±1, ±2, ... 2(N-p)

Center of asymptotes: always at origin

2(N-p) poles go to infinity along asymptotes, as $p^2 \rightarrow 0$

2(p) poles to zero, as $p^2 \rightarrow 0$

APPENDIX F2

ROOT SQUARE LOCUS METHOD APPLIED TO A HELICOPTER (HOVER)

The following is a summary from [Ref. F1]. Consider a single input, dynamic system of the form:

$$\dot{y}(t) = Ay(t) + Bu(t) \quad (F2-1)$$

where $y(t)$ = n-dimensional state vector

$u(t)$ = m-dimensional control vector

A, B = nxn and nxm constant matrices

For an optimal control law, we seek to minimize the cost function.

$$J(Q,R) = \int_{t_0}^{\infty} [x^T(t)Qy(t) + u^T(t)Ru(t)] dt \quad (F2-2).$$

where Q,R = positive definite symmetric constant weighting matrices.

For this analysis, Q is chosen to be:

$$Q = \begin{bmatrix} q_{11} & 0 & 0 & 0 \\ 0 & q_{22} & 0 & 0 \\ 0 & 0 & q_{33} & 0 \\ 0 & 0 & 0 & q_{44} \end{bmatrix} \quad (F2-3)$$

and $R = \rho^2$, a scalar (F2-4)

The performance index (cost function) then becomes

$$J = \frac{1}{2} \int_0^{\infty} (y^T Q y + u^T \rho^2 u) dt \quad (\text{F2-5})$$

The characteristic equation of the single input system is shown

to be (Appendix F1).

$$I + \rho^{-2} \left[\frac{y}{u} (-s) \right]^T Q \left[\frac{y}{u} (s) \right] = 0 \quad (\text{F2-6})$$

The characteristic equation then becomes:

$$1 + \frac{1}{\rho^2} \left[\frac{y_1}{u} (-s), \frac{y_2}{u} (-s), \frac{y_3}{u} (-s), \frac{y_4}{u} (-s) \right] \begin{bmatrix} q_{11} & 0 & 0 & 0 \\ 0 & q_{22} & 0 & 0 \\ 0 & 0 & q_{33} & 0 \\ 0 & 0 & 0 & q_{44} \end{bmatrix} \begin{bmatrix} \frac{y_1}{u} (s) \\ \frac{y_2}{u} (s) \\ \frac{y_3}{u} (s) \\ \frac{y_4}{u} (s) \end{bmatrix} = 0 \quad (\text{F2-7})$$

The change in roots of this equation, resulting from varying a given parameter may be described by a root-square locus. The root-square locus technique is described in (Appendix F1).

A simplified longitudinal model for a helicopter is:

$$(s - X_u)u + g\theta = X_{B_1} B_1 s \quad (\text{F2-8})$$

$$-M_u u + s(s - M_q)\theta = M_{B_1} B_1 s \quad (\text{F2-9})$$

and may be expressed in state variable form as:

$$\frac{d}{dt} \begin{bmatrix} y_1 \\ y_2 \\ y_3 \\ y_4 \end{bmatrix} = \begin{bmatrix} 0 & 1 & 0 & 0 \\ 0 & X_u & -g & 0 \\ 0 & 0 & 0 & 1 \\ 0 & M_u & 0 & M_q \end{bmatrix} \begin{bmatrix} y_1 \\ y_2 \\ y_3 \\ y_4 \end{bmatrix} + \begin{bmatrix} 0 \\ X_{B_1} \\ 0 \\ M_{B_1} \end{bmatrix} u \quad (\text{F2-10})$$

where

$$\begin{bmatrix} y_1 \\ y_2 \\ y_3 \\ y_4 \end{bmatrix} = \begin{bmatrix} X \\ \dot{X} \\ \theta \\ \dot{\theta} \end{bmatrix}, \quad u = B_1 s \quad (\text{F2-11})$$

From Eq. (F2-7), the characteristic equation is

$$1 + \frac{1}{\rho^2} \left[(q_{11} \frac{y_1}{u} (-s) \frac{y_1}{u} (s) + q_{22} \frac{y_2}{u} (-s) \frac{y_2}{u} (s) + q_{33} \frac{y_3}{u} (-s) \frac{y_3}{u} (s) + q_{44} \frac{y_4}{u} (-s) \frac{y_4}{u} (s)) \right] = 0 \quad (\text{F2-12})$$

where $\frac{y_1}{u}$, $\frac{y_2}{u}$, $\frac{y_3}{u}$, and $\frac{y_4}{u}$ are given by:

$$\frac{y_1}{u} = \frac{x}{u} = \frac{X_{B_1} s \left[s^2 - M_q s - \left(\frac{M_{B_1} s}{X_{B_1} s} \right) g \right]}{s \left[s^3 + (X_u + M_q) s^2 + X_u M_q s + g M_u \right]} \quad (\text{F2-13})$$

$$\frac{y_2}{u} = \frac{\dot{x}}{u} = \frac{X_{B_1} s \left[s^2 - M_q s - \left(\frac{M_{B_1} s}{X_{B_1} s} \right) g \right]}{s \left[s^3 + (X_u + M_q) s^2 + X_u M_q s + g M_u \right]} \quad (\text{F2-14})$$

$$\frac{y_3}{u} = \frac{\theta}{u} = \frac{M_{B_1s} \left[s - X_u + \left(\frac{X_{B_1s}}{M_{B_1s}} \right) g \right]}{\left[s^3 - (X_u + M_q) s^2 + X_u M_q s + g M_u \right]} \quad (F2-15)$$

$$\frac{y_4}{u} = \frac{\dot{\theta}}{u} = \frac{M_{B_1s} s \left[s - X_u + \left(\frac{X_{B_1s}}{M_{B_1s}} \right) g \right]}{\left[s^3 - (X_u + M_q) s^2 + X_u M_q s + g M_u \right]} \quad (F2-16)$$

In order to determine the effect of q_{ii} on the roots of Equation F2-12, we apply the root-square locus technique. These cases will be examined. First, weighting in the performance index will be applied only to y_1 , position. Next, the performance index will weight position and velocity. Weighting will then be applied to position, velocity and attitude. Then all four state variables will be weighted.

Finally, is given a weighting for position and attitude.

Case I

$$\text{Characteristic equation: } 1 + \frac{q_{11}}{\rho} \frac{y_1}{u} (-s) \frac{y_1}{u} (s) = 0$$

$$J = \frac{1}{2} \int_0^{\infty} (q_{11} y_1^2 + \rho^2 u^2) dt \quad (F2-17)$$

$$(F2-18)$$

The root-square locus is shown in Illustration F2-1.

or

Case II

$$\text{Characteristic equation: } 1 + \frac{q_{11}}{\rho^2} \frac{y}{u} (-s) \frac{y}{u} (s) + \frac{q_{22}}{\rho^2} \frac{y_2}{u} (-s) \frac{y_2}{u} (s) \quad (\text{F2-19})$$

or:

$$\therefore 1 + \frac{q_{11}}{\rho^2} \frac{y(s)}{u} = \frac{y}{u} (-s) (1 - s^2 \frac{q_{22}}{q_{11}}) = 0 \quad (\text{F2-20})$$

$$J = \frac{1}{2} \int_0^\infty (q_{11} y_1^2 + q_{22} y_2^2 + \rho^2 u^2) dt \quad (\text{F2-21})$$

The root-square locus is shown in Illustration F2-2.

Case IIIa

Characteristic equation:

$$1 + \frac{q_{11}}{\rho^2} \frac{y_1}{u} (s) \frac{y_1}{u} (-s) + \frac{q_{33}}{\rho^2} \frac{y_3}{u} (s) \frac{y_3}{u} (-s) = 0 \quad (\text{F2-22})$$

$$1 + \frac{q_{11}}{\rho^2} \frac{y_1}{u} (s) \frac{y_1}{u} (-s) \cdot$$

$$\left[1 + \frac{q_{33}(-s^2)}{q_{11}} \frac{M_{B1s}^2}{X_{B1s}^2} \frac{(s - X_u + \frac{X_{B1s}}{M_{B1s}} M_u) (-s - X_u + \frac{X_{B1s}}{M_{B1s}} M_u)}{M_{B1s} (s^2 - M_q s - \frac{X_{B1s}}{X_{B1s}} g) (s^2 + M_q s - \frac{X_{B1s}}{X_{B1s}} g)} \right] = 0 \quad (\text{F2-23})$$

$$J = \frac{1}{2} \int_0^\infty (q_{11} y_1^2 + q_{33} y_3^2 + \rho^2 u^2) dt \quad (\text{F2-24})$$

The root square locus is shown in Illustration F2-3.

Case IIIb

Characteristic equation:

$$1 + \frac{q_{11}}{\rho^2} \frac{y_1}{u} (-s) \frac{y_1}{u} (s) + \frac{q_{22}}{\rho^2} \frac{y_2}{u} (-s) \frac{y_2}{u} (s) + \frac{q_{33}}{\rho^2} \frac{y_3}{u} (-s) \frac{y_3}{u} (s) = 0$$

or

$$1 + \frac{q_{11}}{\rho^2} \frac{y_1}{u} (s) \cdot \frac{y_1}{u} (-s) \left(1 + \frac{q_{22}}{q_{11}} (-s^2)\right)$$

$$\left[1 + \frac{q_{33}}{q_{11}} (-s^2) \frac{M_{B1s}^2 (s - X_u + \frac{X_{B1s}}{M_{B1s}} M_u) (-s - X_u + \frac{X_{B1s}}{M_{B1s}} M_u)}{X_{B1s}^2 (s^2 - M_q s - \frac{M_{B1s}}{X_{B1s}} q) (s^2 + M_q s - \frac{M_{B1s}}{X_{B1s}} q) \left(1 + \frac{q_{22}}{q_{11}} (-s^2)\right)} \right]$$

= 0

(F2-25)

The root-square locus is shown in Illustrations F2-4.

Case IV

Characteristic equation:

$$1 + \frac{q_{11}}{\rho^2} \frac{y_1}{u} (-s) \frac{y_1}{u} (s) + \frac{q_{22}}{\rho^2} \frac{y_2}{u} (-s) \frac{y_2}{u} (s) + \frac{q_{33}}{\rho^2} \frac{y_3}{u} (-s) \frac{y_3}{u} (s)$$

$$+ \frac{q_{44}}{\rho^2} \frac{y_4}{u} (-s) \frac{y_4}{u} (s) = 0 \quad (F2-26)$$

or:

$$1 + \frac{q_{11}}{\rho^2} \frac{y_1}{u} (s) \frac{y_1}{u} (-s) \left(1 + \frac{q_{22}}{q_{11}} (-s^2)\right)$$

$$\left[1 + \frac{q_{33}}{q_{11}} (-s^2) \frac{M_{B1s}^2 (s - X_u + \frac{X_{B1s}}{M_{B1s}} M_u) (-s - X_u + \frac{X_{B1s}}{M_{B1s}} M_u) (1 + \frac{q_{44}}{q_{33}} (-s))}{X_{1s}^2 (s^2 - M_q s - \frac{M_{B1s}}{X_{B1s}} q) (s^2 + M_q s - \frac{M_{B1s}}{X_{B1s}} g) (1 + \frac{q_{22}}{q_{11}} (-s^2))} \right]$$

$$= 0$$

(F2-27)

The root square locus is shown in Illustrations (F2-5).

Conclusions

1. In Case I, called position error control, where weighting is applied only to position in the performance criterion, the short period mode is not highly damped and the best possible phugoid damping is .707.
2. In Case II, called velocity error control, where weighting is applied to both position and velocity, the damping of the attitude mode is still not high, but the position mode can be more damped than in Case I.
3. In Case III, called acceleration error control, where weighting is applied to position, velocity and attitude, the damping of the attitude mode can be made greater than either of the two preceding cases.
4. In Case IV, called accurate rate control, where weighting is applied to position, velocity, attitude, and attitude rate, the attitude mode is further damped.
5. For precision flight path control with minimum (position) error, the velocity error control is minimum desirable.
6. Acceleration and acceleration rate error control do not have a large effect upon the position error, but yield a reduction in control effort.
7. In conclusion, for precision flight path control, only the short term dynamics for velocity, acceleration and accurate rate are important, hence one needs to consider only the "dynamic error control" for precision in flight path control.

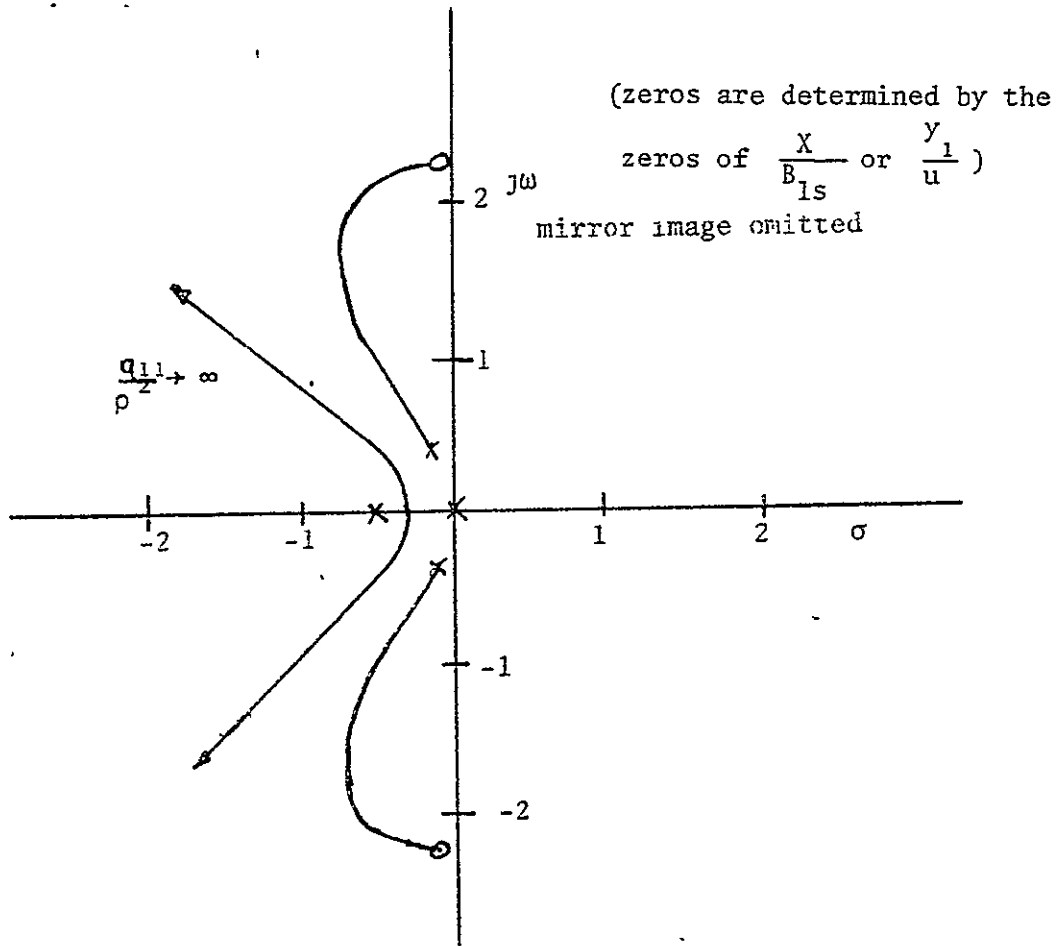


Illustration F2-1. Root-Square Locus - Weighting Applied to q_{11} , Position

with varying $\frac{q_{11}}{\rho^2}$

(the zeros are determined by the zeros of $\frac{Y_1}{u}$ or $\frac{X}{B_{1s}}$)

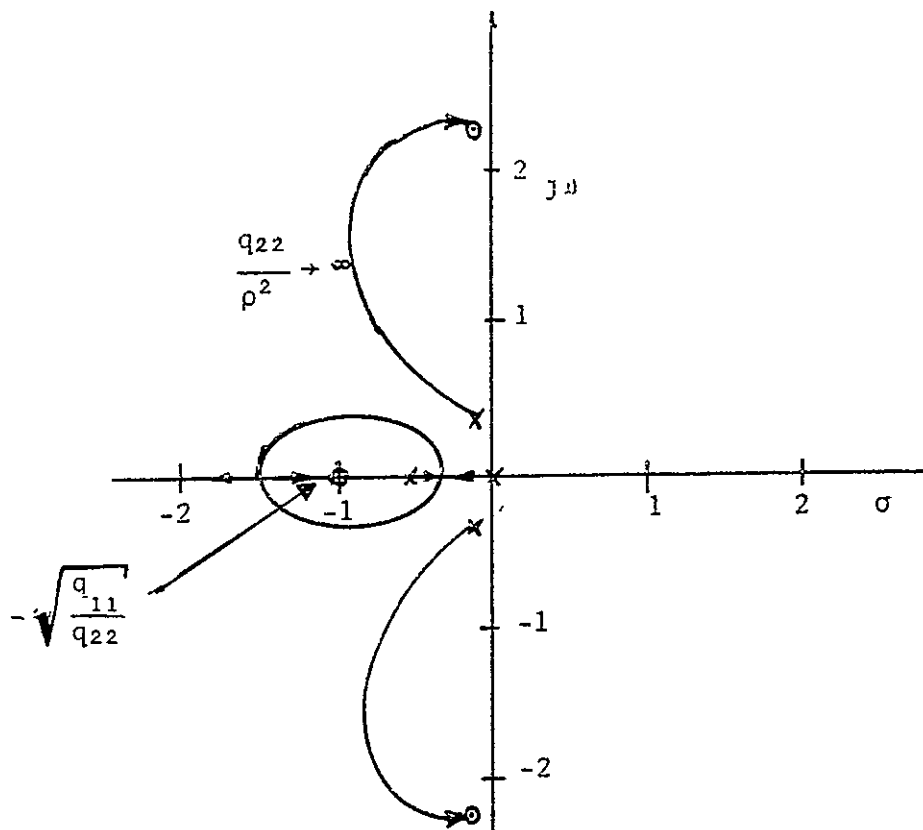


Illustration F2-2. Root Square Locus - Weighting Applied to q_{11} (Position) and q_{22} (Velocity) with varying q_{22}

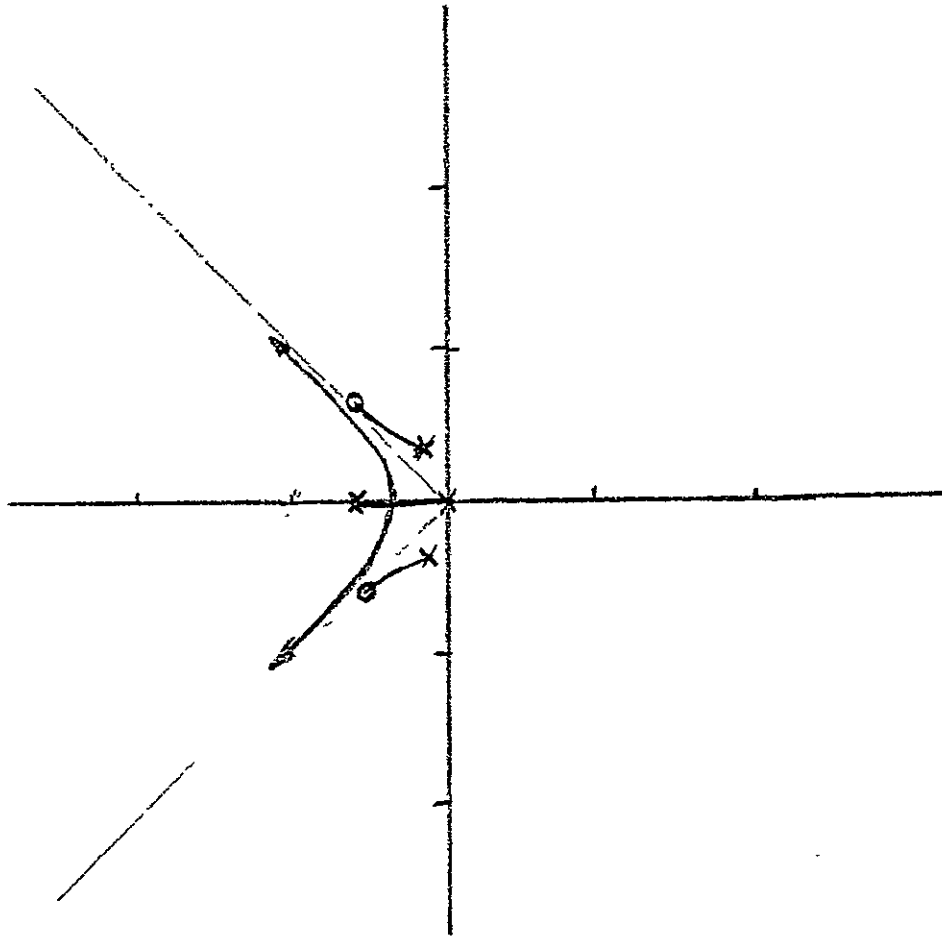


Illustration F2-3. Root Square Locus Weighting Applied to q_{11} (position) and q_{33} (attitude) with Varying q_{33}

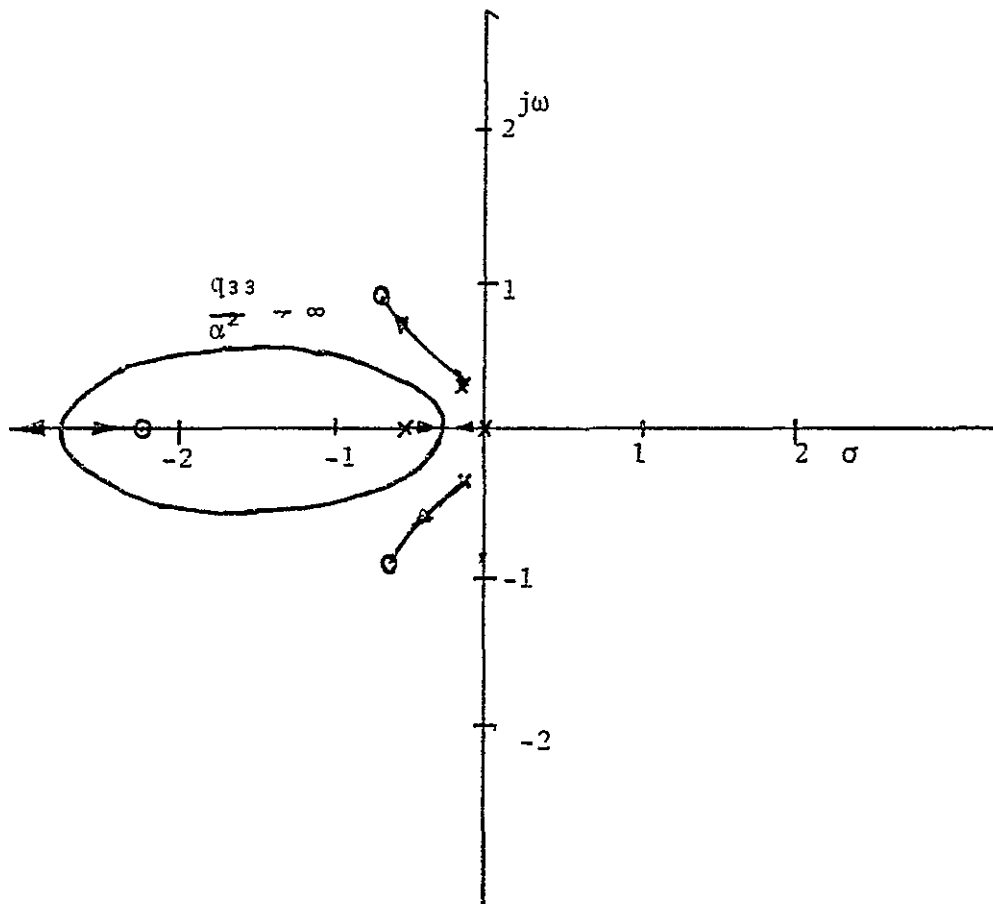


Illustration F2-4. Root Square Locus Weighting Applied to q_{11} (Position), q_{22} (Velocity), and q_{33} (Attitude) with varying $\frac{q_{33}}{\rho^2}$

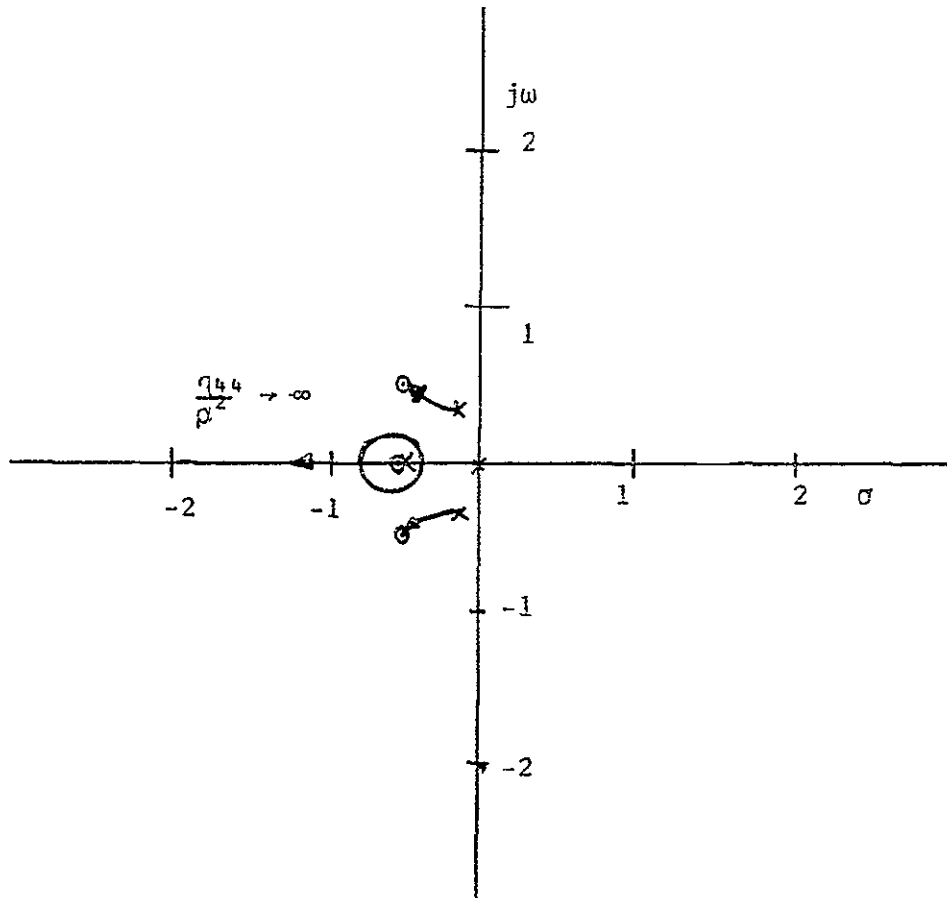


Illustration F2-5. Root Square Locus Weighting Applied to q_{11} (Position), q_{22} (Velocity), q_{33} (Attitude), and q_{44} (Attitude Rate)

APPENDIX G1

REVIEW OF MODEL FOLLOWING BY LINEAR OPTIMAL CONTROL

Introduction

Given the system:

$$\dot{x}(t) = Ax(t) + Bu(t) \quad (G1-1)$$

where: $x(t)$: n dimensional state vector, and output vector

$u(t)$: m dimensional control vector (m_n)

A, B : nxn, nxm and pxn constant matrices

The "ideal" model is given by:

$$y(t) = A_m y(t) \quad (G1-2)$$

where:

A_m is nxn constant matrix of the model

There are in principle two methods to provide a good match between the dynamic of the system and the dynamic of the "ideal model". Namely, 1. model in the performance index and 2. model in the system.

Model in the Performance Index

This approach is shown in Illustration G1 and uses the minimization of the norm:

$$||\dot{x} - A_m x(t) || \quad (G1-3)$$

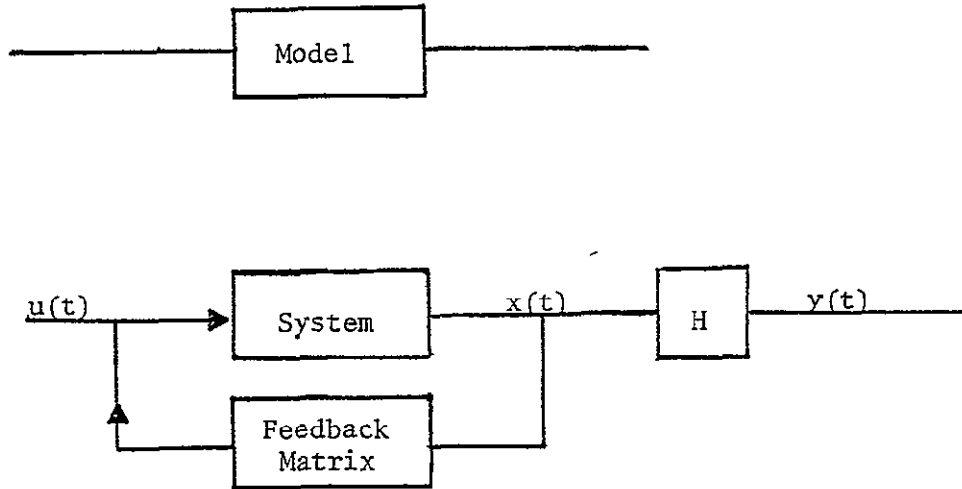


Illustration G1-1. Model Following (Model in the Performance Index)

Hence, the following performance index is defined.

$$2V = \lim_{T \rightarrow \infty} \int_0^T (\dot{x}(t) - A_m x(t))^T Q (\dot{x}(t) - A_m x(t)) + u^T(t) R u(t) dt \quad (G1-4)$$

Using the Hamiltonian and maximum principle of Pontryagin (Ref. [G1-2], [G1-9]), one obtains the optimal control law:

$$u(t) = - (\hat{R}^{-1} \hat{B}^T P + \hat{R}^{-1} \hat{B}^T Q (A - A_m)) x(t) \quad (G1-5)$$

where P is the nxn steady state solution to the Riccati equation:

$$-P \hat{B} \hat{R}^{-1} \hat{B}^T P + A^T P + (A - A_m) P = 0 \quad (G1-6)$$

and

$$\begin{aligned}\hat{R} &= B^TQB+R \\ \hat{A} &= A-BR^{-1}B^TQ(A-A_m) \\ \hat{B} &= B\end{aligned}\tag{G1-7}$$

When the dimensions of the model matrix are the same as that of system matrix and when the system and model are exactly matchable (Ref. G2 and G9), the optimal control is of the following form:

$$u^*(t) = -(A-A_m) x(t)\tag{G1-8}$$

Substituting Eq. (G1-6) into (G1-1) the optimal closed loop becomes:

$$\dot{x}(t) = A_m x(t)\tag{G1-9}$$

which has the dynamic of the model. This exact matching is achieved (in general) as $|Q|/|R|$ becomes large. (Ref. [G1-2]).

When the model and system are exactly matchable, there is no need in using optimal control and the optimal control $u^*(t)$ can be derived from algebraic considerations (Ref. [G1-6]). The algebraic conditions for "perfect" following are derived in Ref.[G1-6]. In order that the dynamics of the model and system be the same, it is required that:

$$\dot{x}(t) = A_m x(t)\tag{G1-10}$$

Substituting (G1-8) into G1-1),

$$A_m x(t) = Ax(t) + Bu(t) \quad (G1-11)$$

hence

$$Bu(t) = (A_m - A) x(t) \quad (G1-12)$$

Multiplying both sides of (G1-10) by B^+ (where B^+ is the pseudoinverse of B) one obtains

$$u(t) = B^+ [A_m - A] x(t) \quad (G1-13)$$

It has been shown in Ref. [G1-6] that necessary and sufficient conditions for perfect matches between the dynamics of the plant and that of the model are:

$$[B B^+ - I][A_m - A] = 0 \quad (G1-14)$$

This equation indicates that for $u(t)$ (given by G1-13) to exist, there must be a great structural similarity between the system matrix A and the model matrix L. Moreover, B must have sufficient rank. However, it is clear that for this limited class of problems, this approach involves much less computation than the quadratic cost integral approach.

Model in the System

This approach is shown in Illustration G2 and is based on the minimization of the square error between the output of the given plant and the output of the

desired plant model; thus forcing the output of the given system to follow the model.

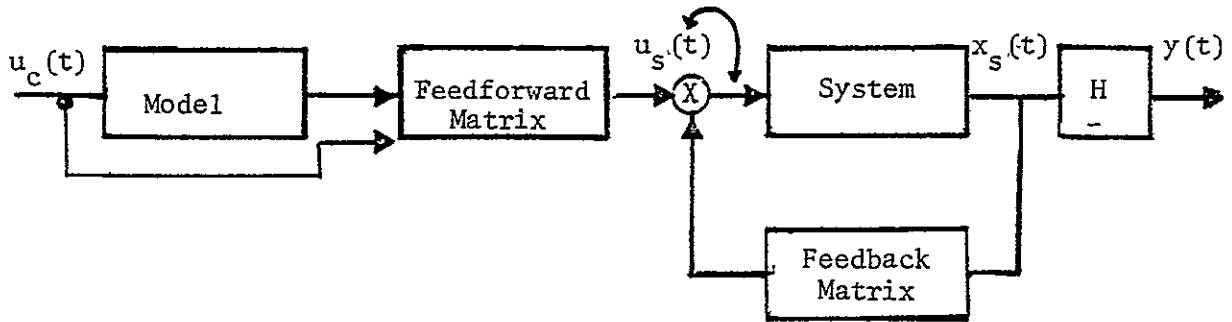


Illustration G1-2. Model Following (Model in the System)

Given the system:

$$\dot{x}_s(t) = A_s x_s(t) + B_s u_s(t) \quad (G1-15)$$

where:

$x_s(t)$: n dimensional state vector, and output vector

$u_s(t)$: m dimensional control vector ($m \leq n$)

A_s, B_s : $n \times n$, $n \times m$ and $p \times n$ constant matrices

The model is given by:

$$\dot{x}_m(t) = A_m x_m(t) + B_m u_m(t) \quad (G1-16)$$

where:

$x_m(t)$: n dimensional state vector, and output vector

$u_m(t)$: m dimensional control vector ($m \leq n$)

A_m, B_m : nxn, nxm and pxn constant matrices

In general, the dimension of the system's output may be different from that of the model (Ref. [G1-10], G1-7] and [G1-2]). The appropriate performance index is defined as:

$$J = \int_0^T [x_m(t) - x_s(t)]^T Q [x_m(t) - x_s(t) + u^T(t) R u(t)] dt \quad (G1-17)$$

where:

Q : nxn positive-semi definite matrix

R : vxv positive-definite matrix

The performance index J is to be minimized with respect to the control $u(t)$. This problem can be treated as tracking problems or servo-problems. (Ref.[G1-8], G1-3], [G1-10]). There are basically two different approaches to the problem. One is established by Ref. [G1-6]; in that work algebraic conditions for perfect following are derived. The second is developed by Ref. [G1-1], and[G1-9] and others. The development in[Ref. G1-1] is basically the same as in Ref. G1-9] with the exception that the input to the model is a zero input.

When given the system (G1-15) and the model (G1-16), and suppose that u_m can be produced by ordinary differential equations such that:

$$\dot{u}_m = D u_m \quad (G1-18)$$

then one can define the enlarged state vector $x(t)$:

$$x(t) = \begin{bmatrix} x_p(t) \\ \text{---} \\ x_m(t) \\ \text{---} \end{bmatrix} \quad (G1-19)$$

$$u_m(t)$$

The dynamic of the new system is given by:

$$\dot{x}(t) + Bu(t) \quad (G1-20)$$

where:

$$A = \begin{bmatrix} A'_s & 0 & 0 \\ 0 & F_m & B_m \\ 0 & 0 & 0 \end{bmatrix}$$

$$B = \begin{bmatrix} B_s \\ 0 \\ 0 \end{bmatrix}$$

where:

A is a $(2n+m) \times (2n+m)$ matrix

B is a $(2n+m) \times v$ matrix

Considering the new system a regulator problem (Ref. [G1-1],[G1-10]), one can define the following performance index:

$$J = \int_0^T [x^T(t) \hat{Q} x(t) + u^T(t) R u(t)] dt \quad (G1-21)$$

where R is a constant positive definite matrix, and J is to be minimized with respect to u(t). In order that J is meaning full, Q must be defined in appropriate ways. Since the error between the system and the model is to be minimized, the weighting matrix \hat{Q} is defined as follows:

$$\hat{Q} = \begin{bmatrix} Q & -Q & 0 \\ -Q & Q & 0 \\ 0 & 0 & 0 \end{bmatrix} \quad (G1-22)$$

It is easy to verify that with the definition Eq. (G1-22) substituted into Eq. (G1-21), the performance index in Eq. (G1-3) is identical to that in Eq. (G1-9). Hence, the model following is formulated by defining the performance index. Using the Hamiltonian for the system, Eq. (G1-6) and the performance index Eq. (G1-9) and applying Pontryagin's maximum principle, one obtains the following optimal control (Ref.[G1-1],[G1-7] and others).

$$u^*(t) = -R^{-1} B_s^T [P_{11} x_s(t) + P_{12} x_m(t) + P_{13} u_m(t)] \quad (G1-23)$$

or

$$u^*(t) = -K_s x_s(t) + K_m x_m(t) + K_v u_m(t) \quad (G1-24)$$

where

$$\begin{aligned} K_s &= R^{-1} B_s^T P_{11} \\ K_m &= -R^{-1} B_s^T P_{12} \\ K_v &= -R^{-1} B_s^T P_{13} \end{aligned} \quad (G1-25)$$

P_{11} is the solution to ricatti equation, and is nxn symmetric matrix.

$$P_{11} + P_{11} A_s + A_s^T P_{11} + Q - P_{11} \Lambda P_{11} = 0 \quad (G1-26)$$

The solution P_{11} of Eq. (G1-26) is independent of the other two gain-matrices : P_{12} , P_{13} . These two matrices (Eq. G1-25) are the solutions to the following algebraic equations:

$$P_{12} + (A_s - \Lambda P_{11})^T P_{12} + P_{12} A_m = Q \quad (G1-27)$$

$$P_{13} + (A_s - \Lambda P_{11})^T P_{13} + P_{13} D = P_{12} B_m \quad (G1-28)$$

where

$$\Lambda = B_s R^{-1} B_s^T$$

The solution of Equation (G1-28) depends on D which is undesirable. Therefore, it usually makes D equal to zero which means designing the system to step input (see for example, Ref. [G1-9]).

For linear systems with time-invariant parameters, it is very desirable to find a solution (P_{ij} matrices) which is time-invariant which means constant gains. The question which arises is if there exists the limit of the performance index J as T approaches infinity. It is well known that sufficient condition for this limit to exist is that the system (Eq. G1-1) is completely controllable. Unfortunately the system (Eq. G1-1) is uncontrollable by definition, so that the existence of the limit of (Eq. G1-3) is not guaranteed.

In Ref. G1-5 is shown that partially controlled systems can be divided into two parts, the part being independent of each other. Hence, the Ricatti equation has the well known steady state solution. Similarly as in the development of the model in the performance index in Ref. G1-1 and G1-3.

Conditions are established for perfect model following. In Ref. G1-3 is taken the difference between the system and the model equations (G1-15, G1-16) and substituted to that the optimal control given by Eq. (G1-25), we have

$$\begin{aligned} \dot{x}_s(t) - \dot{x}_m(t) &= (A_s - B_s K_s) x_s(t) + (B_m K_m - A_m) x_m(t) \\ &+ (B_s K_v - B_m) u_m(t) \end{aligned} \quad (G1-29)$$

If one equates:

$$A_s - B_s K_s = -B_p K_m + A_m \quad (G1-30)$$

$$B_s K_v = B_m$$

Then from Eq. (G1-29)

$$(\dot{x}_s(t) - \dot{x}_m(t)) = (A_s - B_s K_s)(x_s(t) - x_m(t)) \quad (G1-31)$$

and K_s may be chosen to make the system less sensitive to variations of parameters. Up to this point, this condition (Eq. G1-30) for perfect following seems to be equivalent in both approaches. Conditions require that B_s is invertible, which often is not the case.

In the case where B_s is not invertible, Ref. [G1-7] canonical forms (for derivation, see Ref. G1-12) in order to solve (Eq. G1-30).

It has been said that for any pair (A_s, B_s) there exists a transformation T such that:

$$T^{-1}A_s T = \begin{bmatrix} 0 & | & T \\ - & | & - \\ A & | & B \end{bmatrix} \begin{array}{l} \} \text{ n-m} \\ \\ \} \text{ m} \end{array} \quad (G1-31)$$

$$T^{-1}B = \begin{bmatrix} 0 \\ - \\ T \end{bmatrix} \begin{array}{l} \} \text{ n-m} \\ \\ \} \text{ m} \end{array}$$

where 0 is null matrix. However, such transformation does not exist in general (see Ref. G1-13). Hence, Eq. (G1-30) does not have a solution for every system and model, and this reduces the number of cases which can be solved.

In Ref. (G1-3) is derived the algebraic solution for model following; following that derivation for model following a command input and using the previous notation, one obtains:

$$x_m(t) = A_m x(t) + \hat{B} u_c(t)$$

Where $u_c(t)$ is command input and \hat{B} as a constant command control matrix. For perfect matching:

$$x_s(t) = x_m(t)$$

and also its first derivatives should be equal. This yields the control law:

$$u(t) = (B^+) (A_m - A_s) x(t) + B^+ \hat{B} u_c(t)$$

The first derivatives of $x_s(t)$ and $x_m(t)$ will be equal for all $x(t)$ and $u_c(t)$ if

$$[BB^+ - I][A_m - A_s] x(t) = [BB^+ - I] \hat{B} u_c(t)$$

which yields the conditions

$$[B_S B_S^+ - I] (A_m - A_S) = 0$$

$$[B_S B_S^+ - I] \hat{B} = 0$$

(G1-32)

REFERENCES

- G1-1. Asseo, S.J., "Application of Optimal Control to 'Perfect' Model Following", Reprints of 1968 TACC, pp. 1056-1070.
- G1-2. Tyler, J.S., "The Characteristic of Model-Following Systems as Synthesized by Optimal Control", IEEE Trans. on A.C., Vol. AC-9, October 1964.
- G1-3. Eliezer, Kreindler, "On the Linear Optimal Servo Problem", Int. J. Control, 1969, Vol. 9, No. 4, pp. 465-472.
- G1-4. Tyler, J.S., Tuteur, R.B., "The Use of Quadratic Performance Index to Design Multivariable Control Systems", IEEE Trans. on A.C., Vol. AC-11, No. 1, January 1966.
- G1-5. Larson, Robert E. and Pressler, Robert M., "Optimal Control of Close of Partially Controlled Systems", Stanford Research Institute, Menlo Park, California.
- G1-6. Erzberger, H., "On the Use of Algebraic Methods in the Analysis and Design of Model-Following Control Systems", NASA TN D-4663, July 1968.
- G1-7. Gossett, T.D. and Corliss, L.D., "A Quadratic Performance Index for a VTOL Aircraft Prefilter Model Reference Attitude Control System", NASA TN D-6731, March 1971.
- G1-8. Altrane, M. and Falk, P.L., "Optimal Control", McGraw-Hill, 1966.
- G1-9. Rynoski, E.G. and Whitbeck, R.F., "The Theory and Application of Linear Optimal Control", Wright-Patterson AFB, Tech. Report, AFFDL-TR-65-28.
- G1-10. Anderson, B.D.O. and Moore, J.B., "Linear Optimal Control", Prentice-Hall, 1971.

REFERENCES (continued)

- G1-11. Winsor, C.A. and Roy, R.J., "The Application of Specific Optimal Control to the Design of Desensitized Model - Following Control Systems", IEEE Trans. on A.C., Vol. AC-15, No. 3, June 1970.
- G1-12. Luenberger, D.G., "Canonical Forms for Linear Multivariable System", IEEE Trans. on A.C., June 1961.
- G1-13. Curran, R.T., "Equicontrollability and the Model-Following Problem", NASA NGL-05-020-007, July 1971.